

**APPLICATION OF ROCK HARDNESS AND ABRASIVE INDEXING TO  
ROCK EXCAVATING EQUIPMENT SELECTION.**

**BY**

**V.B.Cassapi. M Phil.**

**Thesis submitted to the University of Nottingham  
for the degree of Doctor of Philosophy.**

**October 1987.**

**AFFIRMATION.**

The work submitted in this thesis is entirely my own work and has not been submitted for any other degree.

The following publications have been presented based on this research:

- 1) Atkinson, T. and Cassapi, V.B.

The prediction and Reduction of Abrasive Wear in  
Mine Excavation Machinery.

Int. Nat. Conf. on Tribology in Mineral Extraction.

War on Wear. Instn. of Mech. Eng. 1984.

- 2) Cassapi, V.B. and Wright, D.N.

Factors Influencing the Sawability of Stone.

Le Mousolee. Paris.

Sept 1984, No 173, pp 31-42.

- 3) Atkinson, T. Cassapi, V.B. and Denby, B.

Problems Associated with Rock Material Properties  
in Surface Mining Equipment Selection. 1985.

Trans. Instn. Min. Metall. (Section A. Min. Industry)

- 4) Cassapi, V.B. Waller, M.D. and Ambrose, D.

Performance and Wear Characteristics in Diamond Core  
Drilling.

Drillex 87. Conf. Trans. Instn. Mining and Metallurgy.

- 5) Cassapi, V.B. Singh, R.N. and Unver, B.

Statistical Assessment of Sawability of Rocks.

(Awaiting Publication)

- 6) Cassapi, V.B. and Singh, R.N.

The Development of New Tests and Procedures for the  
Determination of Hardness and Abrasiveness of Rocks.

(Awaiting Publication)

**ABSTRACT.**

The work carried out in this thesis outlines some of the problems associated with abrasive wear in machines and other mechanical equipment used to excavate or process natural rock material. It has been stated that if the problems associated with abrasion are to be better understood, then a sound knowledge of the abrasive potential of rocks is essential. A number of common wear mechanisms are described together with existing hardness and abrasive tests

The author has investigated rock hardness and abrasiveness by the use of existing methods and subsequently, developed new tests which can be correlated with the well established methods of determining physical and mechanical properties of rock. A project on hard rock drilling has been conducted to determine the rate of wear on expensive diamond impregnated coring drill bits. A detailed investigation which involved the design and manufacture of special measuring equipment to accurately measure and record changes in the profile shape of the bit during its life span. This has permitted a study of the wear characteristics related to the various drilling parameters employed.



A collaborative project was carried out with DeBeers, UK, to attempt to discover methods of predicting the rate of specific wear on diamond impregnated saw blades and the cutting forces required with the sawing of hard stone materials. This project has led to a new statistical approach to the analysis of the acquired test data for this purpose.

A number of case histories have been discussed and recommendations made. As a result of these investigations together with the work covered in this thesis, the author has developed two new abrasive tests. These tests can be used to test materials such as unconsolidated rocks which otherwise, could not be satisfactorily tested by the established tests already in existence. The new tests have been tried and proved by correlating the test data by combining multiple regression analysis with the results obtained from physical and petrological rock property tests with actual rock cutting data.

Conclusions have been drawn and recommendations for future work suggested.

.

## CONTENTS.

AFFIRMATION.

ABSTRACT

LIST OF FIGURES.

LIST OF TABLES.

SUMMARY OF TERMS.

### CHAPTER .1

#### ABRASIVE WEAR IN MINE EXCAVATION MACHINERY.

1.1. Introduction.	Page 1.
1.2. Identification of Abrasive Wear.	3.
1.2.1. Wear in Rock Cutting Tools.	4.
1.2.2. Wear of Bucket and Digger Teeth.	7.
1.2.3. Gouging Abrasion.	7.
1.2.4. High and Low Stress abrasion.	8.
1.2.5. Third Body Abrasion.	8.
1.3. The Effects of Rock Properties on Abrasion.	10.
1.4. Hardness and Abrasive Testing.	12.
1.5. Hardness Testing.	14.
1.5.1. The Cerchar Durette Test.	14.
1.5.2. The Brinell Hardness Test.	15.
1.5.3. The Vickers Hardness Test.	15.
1.5.4. The Rockwell Hardness Test.	16.
1.6. Abrasive Measurements.	19.
1.6.1. The Hacksaw Test.	20.
1.6.2. Tool Wear Test.	21.
1.6.3. The Modified Taber Abrasion Test.	22.
1.6.4. The Steel Cube Test.	22.
1.7. Conclusions.	24.

### CHAPTER 2.

#### DETERMINATION OF HARDNESS AND ABRASIVENESS OF ROCK.

2.1. Introduction.	26.
2.2. Determination of Rock Hardness and Abrasiveness.	27.
2.2.1. Petrological Methods.	28.
2.2.2. The Moh's Scale of Mineral Hardness.	29.
2.2.3. Rosiwal's Scale of Mineral Hardness.	32.
2.2.4. Silica Content.	34.
2.2.5. X-Ray Diffraction. (XRD).	35.
2.2.6. X-Ray Fluorescence. (XRF).	36.
2.2.7. Cementation Coefficient.	37.
2.2.8. Relationship between Rock Properties.	38.

2.2.9.	Competency, Grain Size and Angularity.	41.
2.3.	Petrographic Examination of Thin Sections.	45.
2.3.1.	Thin Section Preparation.	46.
2.3.2.	Thin Section Laboratory Equipment.	46.
2.3.3.	Systemised Thin Section Production.	49.
2.4.	Mechanical Methods.	56.
2.4.1.	Introduction.	56.
2.4.2.	Hardness Tests.	58.
2.4.3.	The Shore Scleroscope.	59.
2.4.4.	The National Coal Board Cone Indenter.	64.
2.4.5.	The Schmidt Hammer.	67.
2.5.	The Cerchar Abrasive Test.	72.
2.5.1.	Test Procedure.	73.
2.6.	Conclusions.	75.

### CHAPTER 3.

#### CORRELATION BETWEEN LABORATORY TEST RESULTS.

3.1.	Introduction.	77.
3.2.	The Shore Scleroscope.	78.
3.2.1.	Method of Operation.	80.
3.2.2.	Specimen Preparation.	81.
3.2.3.	Interpretation of Results.	82.
3.2.4.	Correlation of Shore Hardness with Strength.	85.
3.3.	The NCB Cone Indenter.	88.
3.3.1.	Inspection of the Cone Indenter.	88.
3.3.2.	Specimen Preparation.	91.
3.3.3.	Use of the NCB Cone Indenter.	92.
3.3.4.	Uniaxial Compressive Strength versus Cone Indenter Index.	94.
3.4.	The Modified Cone Indenter.	99.
3.4.1.	Specimen Preparation.	100.
3.4.2.	Use of the Modified Cone Indenter.	101.
3.5.	The Cerchar Abrasive Test.	102.
3.5.1.	Test Procedure.	103.
3.6.	Conclusions.	105.

### CHAPTER 4.

#### DIAMOND CORE BIT WEAR CHARACTERISTICS.

4.1.	Introduction.	108.
4.2.	The Core Drilling Machine.	112.
4.2.1.	Resume of Previous Work.	113.
4.3.	The Monitoring System.	114.
4.3.1.	Flush Rate.	115.
4.3.2.	Rotational Speed.	116.
4.3.3.	Torque.	116.
4.3.4.	Load on the Bit.	118.
4.3.5.	Penetration	118.
4.4.	The Drill Bit Wear Jig.	120.
4.5.	Electronic Hardware.	122.

4.6.	Interface Hardware.	123.
4.7.	Software.	124.
4.8.	Core Bits and Bit Wear Measurements.	126.
4.9.	Drilling Test Programme.	127.
4.10.	Physical Properties of the Rock Material.	133.
4.11.	Applied Drilling Parameters and Bit Performance.	134.
4.12.	Test Procedure.	137.
4.13.	Physical Property Tests.	137.
4.14.	Petrographic Analysis. (Swedish Granite)	138.
4.15.	Petrographic Analysis. (Sandstone)	138.
4.16.	Drilling Test Results. (Core Bit "A")	139.
4.17.	Core Bit "B". (Granite)	150.
4.17.1.	Core Bit "B". (Sandstone)	151.
4.18.	Discussion of Results.	152.
4.18.1	Core Bit "A".	152.
4.18.2.	Core Bit "B".	153.
4.19.	Conclusions.	158.

## CHAPTER 5.

### FACTORS INFLUENCING THE SAWABILITY OF STONE.

5.1.	Introduction.	166.
5.2.	Sample Material mineralogy and their Proportions.	167.
5.3.	Mechanical Tests.	169.
5.4.	Sawing Trials.	172.
5.5.	Force Table.	174.
5.6.	Preliminary Investigations.	175.
5.7.	Blade Specifications.	178.
5.8.	Presentation and Discussion of Results.	179.
5.8.1.	Statistical Analysis of the Data Base.	179.
5.8.2.	Factor Analysis to Evaluate Specific Wear.	181.
5.8.3.	Specific Wear Rates and Mineralogical Factors.	183.
5.8.4.	Specific Wear and Physical Properties of Rock.	190.
5.8.5.	Specific Wear and Abrasiveness.	191.
5.8.6.	Factors Affecting Cutting Forces for Sawing.	198.
5.9.	Analysis of Diamond Particles after Sawing.	198.
5.10.	Multiple Regression Analysis and Prediction of Sawability of Rocks.	199.
5.10.1.	Prediction of Specific Wear.	199.
5.10.2.	Prediction of Cutting Force Requirements.	202.
5.11.	Analysis of Important Variables and their Interrelation with Sawability of Rocks.	209.
5.11.1.	Method of Analysis.	209.

5.11.2. Factors Affecting Specific Wear Rates.	209.
5.11.3. Factors Affecting Cutting Force Requirements.	212.
5.12. Discussion of Results.	212.
5.12.1. The Need for Multiple Tests.	212.
5.12.2. Statistical Analysis.	214.
5.12.3. Rationalisation of Tests.	215.
5.12.4. Further Scope for Development.	215.
5.13. Conclusions.	216.

## CHAPTER 6.

### CASE STUDIES.

6.1. Introduction.	219.
6.2. Undersea Trenching operation.	222.
6.2.1. Introduction.	222.
6.2.2. Rock Sample Material.	222.
6.2.3. Petrographic Analysis.	223.
6.2.4. Summary of Petrographic Analysis	225.
6.2.5. Mechanical Pyhysical Property Tests.	226.
6.2.6. Discussion of Results.	227.
6.2.7. Conclusions.	229.
6.3. Bucket Wheel Operation in Weathered Sandstone.	231.
6.3.1. Introduction.	231.
6.3.2. Core Sample Material.	232.
6.3.3. Initial Inspection of Core Samples.	233.
6.3.4. Mineralogical Examination.	236.
6.3.5. Conclusions.	238.
6.4. Bucket Wheel Operation in Fine Grain Sandstone.	241.
6.4.1. Introduction.	241.
6.4.2. Rock Sample Material.	242.
6.4.3. Test Procedure.	243.
6.4.4. Summary of Test Results.	244.
6.4.5. NCB Cone Indenter Hardness Test.	245.
✓ 6.4.6. The Shore Scleroscope Hardness Test.	245.
✓ 6.4.7. The Cerchar Abrasive Test.	246.
✓ 6.4.8. Dynamic Impact Abrasive Test.	247.
6.4.9. Petrological Analysis.	248.
6.4.9. Conclusions.	251.
6.5. Uranium Mining Operation.	256.
6.5.1. Introduction.	256.
6.5.2. Rock Sample Material.	257.
6.5.3. Rock Description.	259.
6.5.4. Conclusions.	262.
6.6. Bucket Wheel Operation in Weak Unconsolidated Sandstone.	268.
6.6.1. Introduction.	268.
6.6.2. Sample Material.	271.
6.6.3. Test Results.	274.
6.6.4. Soak Tests.	277.
6.6.5. Conclusions.	278.

6.7.	Core Drilling in Banded Ironstone.	280.
6.7.1.	Introduction.	280.
6.7.2.	Rock Sample Material.	281.
6.7.3.	Specimen Preparation.	281.
6.7.4.	Discussion of Results.	282.
6.7.5.	Conclusions.	286.

## CHAPTER 7.

### DEVELOPMENT OF DYNAMIC TESTS FOR THE EVALUATION OF ABRASIVITY AND HARDNESS OF ROCKS.

7.1.	Introduction.	289.
7.2.	Research Objectives.	290.
7.3.	Dynamic Particle Impact Abrasive Test.	291.
7.3.1.	Description of Test Equipment.	292.
7.3.2.	Test Concepts.	294.
7.3.3.	Impact Tests on Unconsolidated Rock Material.	296.
7.4.	Abrasive Wear Tests on Consolidated Rock Material.	297.
7.4.1.	Continuous Abrasive Test.	297.
7.4.2.	Description of Test Equipment.	297.
7.4.3.	Test Concepts.	299.
7.5.	Characteristics of Unconsolidated Rock Rock,	301.
7.5.1.	Rock Sample Description.	301.
7.5.2.	Difficulties Encountered With Conventional Tests.	302.
7.5.3.	Dynamic Impact Abrasive Results.	306.
7.6.	Assessment of Abrasiveness of Unconsolidated Rocks.	307.
7.6.1.	Preliminary Tests.	307.
7.7.	Discussion of Preliminary Test Results.	313.
7.7.1.	The Effects of Strength and Deformation Properties of Rock on Various Abrasivity Indices.	313.
7.7.2.	The Effects of Hardness and Petrological Properties on the Abrasivity of Rocks.	313.
7.7.3.	Interaction of Impact Abrasivity, Cerchar Index and Continuous Abrasive Index.	316.
7.7.4.	Toughness Index of Rock and its Interrelation to Rock Abrasiveness.	318.
7.8.	Presentation and Analysis of Results.	327.
7.8.1.	Factors Affecting Abrasivity of Rocks.	327.
7.8.2.	Multiple Regression Analysis and Prediction of Various Abrasive Properties.	328.
✓7.8.3.	Prediction of Cerchar Abrasivity.	328.
7.8.4.	Prediction of Impact Abrasivity.	330.
7.8.4.1.	Using Hardness and Grain Size.	332.
7.8.4.2.	Using Other Abrasive Indices.	332.
7.8.4.3.	Prediction of Impact Abrasiveness by Cone Indenter and Other Abrasive Indices.	333.

7.8.4.4.	Impact Abrasiveness in Relation to Shore Hardness and Other Abrasive Indices.	335.
7.8.4.5.	Prediction of Impact Abrasivity Using Shore and NCB Cone Indenter Hardness and Cerchar Abrasive Indices.	335.
7.8.4.6.	Prediction of Impact Abrasivity From Continuous Abrasivity and Rock Hardness.	337.
7.8.4.7.	Prediction Equation for Impact Abrasivity Based on Measured Values for Grain Size and other Abrasive Indices.	337.
7.8.5.	Prediction of Continuous Abrasive Indices.	338.
7.8.5.1.	Continuous Abrasivity and Internal Angle of Friction With Measured Shore Hardness Indices.	338.
7.8.5.2.	Relationship Between Continuous Abrasivity, Cerchar and Impact Abrasive Indices.	338.
7.9.	Discussion of Results.	339.
7.10.	Conclusions.	340.
7.10.1.	Limitations of the Cerchar Abrasive Test.	340.

## CHAPTER 8.

### GENERAL CONCLUSIONS AND RECOMMENDATIONS FOR FURTHER STUDY.

8.1.	General Conclusions.	344.
8.2.	Recommendations for Further Study.	350.

## LIST OF FIGURES.

FIGURE.	PAGE.
1.1. Cerchar Hardness Test.	13.
2.1. Powers Roundness Chart.	40.
2.2. Cuddalore Sandstone Microphotograph.	42.
2.3. Ultraphot petrological Microscope.	44.
2.4. Conditioning Ring.	48.
2.5. Setting Fixture and Hot Plate.	50.
2.6. Rock Slicing Machine.	51.
2.7. Lapping Jig.	52.
2.8. Twin Gauge Setting Block.	54.
2.9. Shore Scleroscope.	60.
2.10. NCB Cone Indenter.	63.
2.11. Dead Weight Penetrometer.	65.
2.12. "N" Type Schmidt Hammer.	71.
2.13. Cerchar Abrasive Test Equipment.	74.
3.1. Shore Scleroscope.	79.
3.2. Shore Scleroscope versus UCS.	84.
3.3. Cone Indenter Calibration.	90.
3.4. Specimen Setting Position.	92.
3.5. NCB Cone Indenter versus UCS.	97.
3.6. Modified Cone Indenter.	99.
4.1. Core Bits "A" and "B" With Technical Specifications.	109.
4.2. Rock Drilling Machine with Micro-Computer	111.
4.3. Bit Profile Measuring Device.	121.
4.4. Photomicrograph of Swedish Granite.	131.
4.5. Photomicrograph of Sandstone.	132.
4.6. Core Bits "A" and "B" After Test the Program.	135.



4.7.	Wear Characteristics of Outside Section of Core Bit "A".	143.
4.8.	Wear Characteristics of Middle Section of Core Bit "A".	144.
4.9.	Wear Characteristics of Inside Section of Core Bit "A".	145.
4.10.	Graph of Cumulative Wear Against Distance Drilled for Three Positions on the Kerf.	147.
4.11.	Performance Characteristics for Core Bit "B" in Swedish Granite.	149.
4.12.	Performance Characteristics for Core Bit "B" in Sandstone at a Constant Speed.	154.
4.13.	Performance Characteristics for Core Bit "B" in Sandstone at a Constant Load.	155.
4.14.	Variation in Bit Profile With Distance Drilled.	161.
4.15.	Computer Printout of Test Data.	162.
4.16.	Computer Printout of Bit Profiles.	163.
4.17.	Computer Printout of Superimposed Profiles.	164.
5.1.	Gregori Bridge Saw.	170.
5.2.	Force Table.	173.
5.3.	Specification of Blade Parameters.	177.
5.4.	Scatter Plot Between Specific Wear and Quartz Grain Size.	184.
5.5.	Scatter Plot Between Specific Wear and Plagioclase Grain Size.	184.
5.6.	Scatter Plot Between Specific Wear and Moh's Hardness.	185.
5.7.	Vertical Cutting Forces.	187.
5.8.	Scatter Plot Between Specific Wear and Cone Indenter Hardness.	189.
5.9.	Scatter Plot Between Specific Wear and Shore Hardness.	189.
5.10.	Relationship Between Cutting Force and Shore Hardness.	194.

5.11. Relationship Between Cutting Force and Cone Indenter Hardness.	194.
5.12. Relationship Between Cutting Force and Plagioclase Grain Size.	195.
5.13. Relationship Between Cutting Force and Quartz Grain Size.	195.
5.14. Relationship Between Cutting Force and Uniaxial Compressive Strength.	196.
5.15. Relationship Between Cutting Force and Cerchar Abrasive Index.	196.
5.16. Relationship Between Measured and Predicted Wear using Equation 5.3.	201.
5.17. Relationship Between Measured and Predicted Wear using Equation 5.4.	201.
5.18. Correlation Between Predicted and Measured Cutting Forces.	203.
5.19. Correlation Between Measured and Predicted Cutting Forces.	203.
5.20. Effect of Grain Size on Specific Wear.	205.
5.21. Effect of Rock Hardness on Specific Wear Rates.	205.
5.22. Effect of Grain Size on Cutting Force.	210.
5.23. Effect of Shore Hardness on Cutting Force.	210.
5.24. Effect of Cone Indenter Hardness on Cutting Force.	212.
6.1. Worn and Damaged Picks.	221.
6.2. Sample Material Set in Concrete.	269.
6.3. Specimen Material.	270.
6.4. Australian Banded Ironstone.	285.
7.1. Schematic View of Impact Abrasive Test Equipment.	293.
7.2. Continuous Abrasive Test Equipment.	298.
7.3A. Correlation Between Impact Abrasivity and Silica Percentage.	304.

7.3B.	Correlation Between Impact Abrasivity and Kaolinite Percentage.	304.
7.4.	Correlation Between Internal Angle of Friction and Continuous Abrasive Index.	312.
7.5.	Cerchar Abrasivity and Cone Indenter Hardness.	312.
7.6.	Cerchar Abrasivity and Shore Hardness.	314.
7.7.	Effect of Grain Size on Shore Scleroscope Hardness Number.	314.
7.8.	Correlation of Toughness Index and Youngs Modulus.	322.
7.9.	Correlation of Toughness Index and Tensile Strength.	322.
7.10.	Correlation Between Toughness Index and Cone Indenter Hardness Number.	323.
7.11.	Correlation Between Toughness Index and Cohesive Strength.	323.
7.12.	Correlation Between Toughness Index and Shore Scleroscope Hardness Number.	324.
7.13.	Correlation Between Toughness Index and Uniaxial Compressive Strength.	324.
7.14.	Correlation Between Predicted and Measured Cerchar Abrasivity.	329.
7.15.	Correlation Between Measured and Predicted Cerchar Indices.	329.
7.16.	Correlation Between Predicted and Measured Impact Abrasivity.	331.
7.17.	Correlation Between Predicted and Measured Impact Abrasivity.	331.
7.18.	Predicted and Measured Impact Abrasivity Based on C10, C11 and C13.	334.
7.19.	Predicted and Measured Impact Abrasivity Based on C9, C12 and C13.	334.
7.20.	Measured and Predicted Impact Abrasivity Based on C9, C10 and C13.	336.
7.21.	Predicted and Measured Impact Abrasivity	

Based on C12, C13 and C14.	336.
7.22. Correlation Between Cerchar and Impact Abrasiveity.	341.
7.23. Correlation Between Imact and Continuous Abrasiveity.	341.

## LIST OF TABLES.

TABLE.		PAGE.
1.1.	Comparison of Hardness Values for SAE Carbon and Alloy Constructional Steels.	17-18.
1.2.	The Steel Cube Test.	23.
2.1.	The Moh's Hardness Scale of Mineral Hardness.	30.
2.2.	Moh's Hardness Classification of Mean Abrasiveness.	31.
2.3.	Rosival's Scale of Mineral Hardness.	33.
2.4.	Quartz versus Silica Content.	39.
2.5.	Cementation Coefficient.	39.
2.6.	Table of Rebound Values.	69.
3.1.	Shore Scleroscope.	79.
3.2.	Shore Hardness versus UCS.	84.
3.3.	Callibration Setting Position for the NCB Cone Indenter.	90.
3.4.	Recommended Positioning of Specimen.	92.
3.5.	NCB Cone Indenter Hardness Index versus UCS.	97.
4.1.	Summary of Physical Properties.	128.
4.2.	Percentage Mineral Proportions. (Swedish Granite)	129.
4.3.	Percentage Mineral Proportions. (Course Grained Sandstone)	130.
4.4.	Wear Characteristics of Outside Section of Core Bit "B".	140.
4.5.	Wear Characteristics of Middle Section of Core Bit "B".	141.

4.6.	Wear Characteristics of Inside Section of Core Bit "B".	142.
4.7.	Wear Characteristics of Core Bit "A".	146.
4.8.	Performance Characteristics for Core Bit "B" in Swedish Granite.	148.
5.1.	Mineralogy and Proportions.	168.
5.2.	Summary of Mechanical Properties.	171.
5.3.	Dependent and Independent Variables Used in Statistical Analysis.	179.
5.4.	Correlation Coefficients Between Wear and Various Parameters.	182.
5.5.	Linear Relationship Between Specific Wear rate and Independent Variables.	188.
5.6.	Correlation Coefficients Between Cutting Forces and Various Parameters.	192.
5.7.	Linear Relationship Between Cutting Force and Index Properties of Rock.	193.
5.8.	Analysis of Diamond Particles After Sawing.	197.
5.9.	Assessment of Factors Affecting the Sawability of Rocks.	206.
5.10.	Assessment of Factors Affecting Wear Rates.	206.
5.11.	Assessment of Factors Affecting Cutting Force Requirements. (Eq 5.3.)	207.
5.12.	Assessment of Factors Affecting Cutting Force Requirements. (Eq 5.4.)	208.
6.1.	Percentage Mineral Proportions.	224.
6.2.	Summary of Physical Properties.	226a.
6.3.	Summary of Mineral Proportions.	226a.
6.4.	Percentage Mineral Proportions.	234.
6.5.	Grain Size. (Bowen Basin Overburden)	235.
6.6.	Mineral Proportions. (Oaklands)	250.
6.7.	Summary of Physical Properties.	258.

6.8.	Mineral Proportions. (Uranium Mine)	265.
6.9.	Mineral Grain Size.	266.
6.10.	Shore Scleroscope Hardness Index.	272.
6.11.	Shore Scleroscope Hardness Index.	273.
6.12.	NCB Cone Indenter Hardness Index.	275.
6.13.	Percentage Mineral Proportions.	283.
6.14.	Laboratory Index Tests.	284.
7.1.	Impact Abrasive Wear Index and Petrological Properties of Unconsolidated Rock Material.	305.
7.2.	Laboratory Index Properties and Petrological Analysis and Abrasivity Indices of Rocks.	308.
7.3A.	Correlation Between Mechanical Properties, Petrological Parameters, Index Tests and Abrasive Tests.	310.
7.3B.	Correlation Between Mechanical Properties, Petrological Parameters, Index Tests and Abrasive Tests.	311.
7.4.	The Influence of the Cerchar Abrasive Index, Continuous Abrasive Index and Hardness Indices on Impact Abrasivity.	316.
7.5.	Toughness Index and its Relationship Strength Classifications.	319.
7.6.	Correlation Coefficients Between various Independent Variables.	320.
7.7.	Abrasivity Results on 15 Rock Types Together with Hardness and Petrological Properties.	325.
7.8.	Correlation Between Abrasivity Indices, Hardness Numbers and Petrological Properties of Rocks.	326.
7.9.	Classification of Abrasiveness.	343.

## SUMMARY OF TERMS

A-D	Analogue to Digital.
BWE	Bucket Wheel Excavator.
C	Correlation.
dc	Direct Current.
GS	Geological Society.
H <sub>b</sub>	Brinell Hardness.
H <sub>v</sub>	Vickers Hardness.
H <sub>c</sub>	Cerchar Hardness.
Kerf	Cross Section of Core Bit Profile.
MCI	Modified Cone Indenter.
NCB	National Coal Board. (British Coal)
R	Relationship.
SAE	Society of Automobile Engineers.
T <sub>1</sub>	Toughness Index.
UCS	Uniaxial Compressive Strength.
UTS	Uniaxial Tensile Strength.
XRD	X Ray Diffraction.
XRF	X Ray Fluorescence.



## **CHAPTER 1.**

### **ABRASIVE WEAR IN MINE EXCAVATION MACHINERY.**

## CHAPTER 1.

### ABRASIVE WEAR IN MINE EXCAVATION MACHINERY.

#### 1.1. Introduction.

Mining operations, whether carried out underground or on surface mining sites, consist essentially of the excavation and processing of rock material. The increasing trends towards modern mechanised methods of mining have almost completely replaced the older traditional methods of mining operations and consequently, the new mechanical systems, while contributing much to increased productivity and improved working conditions, generate within their applications, a series of new problems which hitherto, were of no serious economic or environmental consequence.

The performance of mine excavation or mineral processing machinery is dependent upon a number of factors, some of which may be outside the control of the operator or contractor, such as the state of the weather, severe and prolonged inclemency or long periods of freezing conditions for instance, can result in massive losses in production leading to major economic consequences.

In addition to these uncontrollable and sometimes, unpredictable environmental conditions, problems associated with the rock mass properties may also present some major set-backs in the anticipated production rates of mechanical mining equipment. These may be characterised by the following:

- a) Strength and deformation properties of intact rock and their discontinuities.
- b) Degree of prior ground preparation by blasting or ripping.
- c) The weight, power and type of machine together with the shape, size and the geometry of cutting tools.
- d) The number, type and configuration of the picks in the cutting head.
- e) The hardness and abrasiveness of the rock material in-situ.
- f) Mineral constituent grains e.g. grain size and shape, particularly their angularity, the hardness and percentage of the mineral particles together with the degree of cementation.
- g) The mode of excavation, transport, and processing, together with the resistance of machines, tools and other auxiliary equipment to abrasive wear and damage.
- h) Excavation characteristics, e.g. (gradients)

size, shape and the presence of water.

- i) Operational characteristics, e.g. mode of cutting, slewing speed, advance rates and cutting speeds.

## 1.2. Identification of Abrasive Wear.

Abrasive wear in mining operations occurs as a result of some dynamic interaction between tools and machinery with natural rock material. All rock material is, to some degree, an abrasive material which inevitably leads to abrasive wear of mechanical equipment and the control of this abrasive wear is of major importance to the economic viability of the mining operation.

The identification of the type of abrasive wear is essential to the design of tools and other mechanical equipment so that material scientists, machine tool designers and the many other interrelated disciplines can work towards the reduction of this important phenomenon.

Therefore, the identification of the mode of abrasive wear is essential to assist in the selection of the most advantageous wear resistant materials used for the manufacture and construction of mining machinery and other equipment.

### 1.2.1. Wear in Rock Cutting Tools.

There are four basic mechanisms of tool degradation which can be associated with tungsten carbide, the most common material used for inserts in rock cutting tools and these may be identified as follows:

- 1) Abrasive wear.
- 2) Micro-chipping.
- 3) Impact failure.
- 4) Thermal cracking.

Unfortunately, most of these characteristics have an interactive effect and steps taken to advantageously alter any one of these parameters may only result in an adverse effect on the others.

These forms of wear or damage are however, readily identified in tools in service and may take the form of frictional wear, attrition, erosion and thermal shock and it is only necessary to identify these in order to take some remedial action.

A common example of this, is to attempt to optimise the percentage cobalt content within the tungsten carbide composites to achieve a compromise between hardness to resist wear and toughness to resist impact damage.

Abrasive wear has been compared to a process of micro-machining of surfaces and has been the subject of extensive study by Harle (1977), Atinoluk (1981), and

Kenny and Johnson (1976) et al. and it was agreed that abrasive wear was a function of the distance travelled in contact with rock.

Micro-chipping may result from two causes, impact and impact failure. Impact fatigue is the mechanism proposed by Montgomery and Stjernberg (1964) as a wear mechanism associated with percussive tools such as percussive drills, it has also been related to the wear mechanism involved with roadheader cutting tools. Thus, the occurrence of this type wear is related to the number of stress reversals the tool undergoes and is not so dependent on the maximum stress the tool tip is subjected to.

On impacting against hard rock, compressive stress waves are generated, which, on meeting an interface, are only partly transmitted, the remainder being reflected as a highly destructive tensile wave, which may result in catastrophic failure of the tungsten carbide insert. The resistance to this impact failure may be found in the composition of the tungsten carbide or the geometry of the tool or a combination of these, together with the avoidance of porosity and low traverse rupture strengths in the tungsten carbide specifications.

Although tungsten carbide is considered to possess good thermal fatigue resistance, Osbourne, H.J. (1969), there are many examples in practice where tungsten

carbide composites have failed by this mechanism. Thermal fatigue is most noticeable when cutting relatively non-abrasive rocks and is manifest by the characteristic snake-skin crazing pattern on the surface of the carbide. Water has an important influence on this phenomenon. If sufficient water is used, a grinding medium may be formed where tools are alternatively heated and quenched with water which leads to thermal cracking.

In practice, several wear mechanisms may be in operation and one mechanism may well initiate another, thus producing a fracture zone leading to gross failure.

Cutting tools generate very high spot face temperatures at the interface between the cutting tool and the rock. Temperatures in excess of 1200° C have been registered when tungsten carbide sliders have been run dry against sandstone wheels, Rae, (1966), although these temperatures are not the actual temperatures at the interface, 'these will be higher'. Osbourne, (1969), indicated that the hardness of tungsten carbide drops rapidly with increased temperature and at about 400° C quartz grains at ambient temperature are harder than that of tungsten carbide, thus leading to rapid abrasive wear.

### 1.2.2. Wear of Bucket and Digger Teeth.

Bucket and digger teeth attached to the front, corners and sides of the buckets are subject to various compressive and tensile stresses as a direct result of scraping, ploughing, slewing and breakout mechanisms. These teeth have to handle material of a wide variety of shape and size of rock and of equally differing physical rock properties. Their life is dependent upon a number of factors and may be as short as 2 to 3 hours or as long as several months of continuous use. Digger teeth therefore, are subjected to both sliding abrasive wear and impact abrasive damage, most digger teeth can however, be repaired or reinforced by hard faced metal welding techniques. In other cases it has been found that the use of tungsten carbide inserts can greatly reduce downtime caused by the time taken to replace worn and damaged teeth. Kasturi (1984).

### 1.2.3. Gouging Abrasion.

Gouging abrasion occurs when the product shears or tears sizable particles from the wearing surface of the confining media, this involves heavy impact and local stresses, e.g. handling large lumps as in loading and dumping, or middling sized lumps at a higher velocity such as conveyor discharge points and impact crushers.



#### **1.2.4. High and Low Stress abrasion.**

High stress abrasion occurs particularly in those crushers that employ direct compression mechanisms, i.e. jaw crushers or milling and grinding machines.

Low stress abrasive wear can be related to a continual scratching or the erosion of surfaces on equipment such as chutes and hoppers or as material is conveyed, pumped or processed in air or liquid under relatively high velocities.

#### **1.2.5. Third Body Abrasion.**

Wear of moving or sliding components of machines and bearings cause major problems and many lost hours of production. There are some 1.6 million sets of conveyor belt idlers currently in use within the British coal industry alone. Each set consists of three idlers, one in the centre and two wing idlers and each of these idlers are supported on two bearings. In addition to these, the returning empty belt is supported on full width horizontal idlers and these also are supported on two bearings. In total therefore, there are about 5.6 million idlers and thus, about 11 million bearings in use.

The bearings are single row radial ball bearings with a 52 mm outside diameter and a 25 mm inside diameter. The dynamic capacity of these bearings, C, is 11.74 kN

and the design loading  $P$ , varies with size and type of conveyor, the ratio  $C/P$  ranges from 13.8 to 41.9. These values are relatively large and indicate that the bearings are not heavily loaded. The bearings are prepacked with grease during assembly and do not require further attention during their life span.

Normal failure of these bearings eventually takes place as a result of fatigue and this can be scheduled within the normal maintenance routine. If the bearing grease is inadequate due to losses caused by overheating or purging, the bearing can fail because of wear at areas of sliding contact. This occurs between the balls and the cage and because of slip or skidding between the balls and the ball races.

Another common reason for the deterioration and eventual total breakdown of ball bearings, may result from contamination. This contamination may be either liquid, resulting in the purging of grease from the bearings, thus leading to failure due to corrosion or solid intrusions of highly abrasive dust particles which contaminate the balls and tracks after passing through the grease barrier. This will result in accelerated deterioration of bearing surfaces, leading to eventual catastrophic failure.

### 1.3. The Effects of Rock Properties on Abrasion.

It is apparent therefore, that there are a great many variables which determine the performance of mining machines and associated equipment. This can range from the ability of the operator to choose the most advantageous equipment or method of operation down to the size, shape and proportion of the hard mineral constituents grains within the rock mass.

The most significant of these variables however, must be those factors that directly affect the wear resistance of those elements in direct contact with the rock material. These include cutting tools, digger teeth, jaw and gyratory crushers, etc. which can directly affect production rates in the following manner:

- a) Worn and damaged tools cause higher than normal cutting forces with consequent increased energy costs. Worn tools also increase the volume of respirable dust, thus increasing possible health hazards in addition to any effects caused by contamination to mining machines and equipment.
- b) Frequent tool replacements leads to unscheduled machine down time with consequential production losses.

Thus, the control of tool wear is essential and must be kept within practical economic limits. The wear of these cutting tools in practice, occurs as a result of two principal mechanisms.

- 1) Wear and/or damage due to impact loading of the tool or tool tip material in contact with the rock.

- 2) Wear of the tool or tool tip material caused by gradual erosion of the tool material due to the hardness and abrasiveness of the rock mass.

Both of these types of wear mechanisms can be directly associated with the interaction of the rock material properties and their condition.

Impact wear for instance, can be related to the physical strength properties of the rock and its discontinuities. Research has shown that under the action of a pick cutting tool, most rocks fail under the influence of tensile stresses due to the propagation of stress fractures within the rock and the sudden release of these stresses can cause tool tip failure.

The toughness of rock can also affect cuttability and can be defined as the ability of rock to resist residual penetration by a cutting element and consequently the ability of rock to absorb energy without failure.

The hardness of rock material is also an important

area of concern and can significantly affect the power and weight requirements of rock cutting machines in situ.

Abrasive wear can be directly related to the proportion of hard mineral constituents of the rock mass and in particular, their sizes, shapes and angularity.

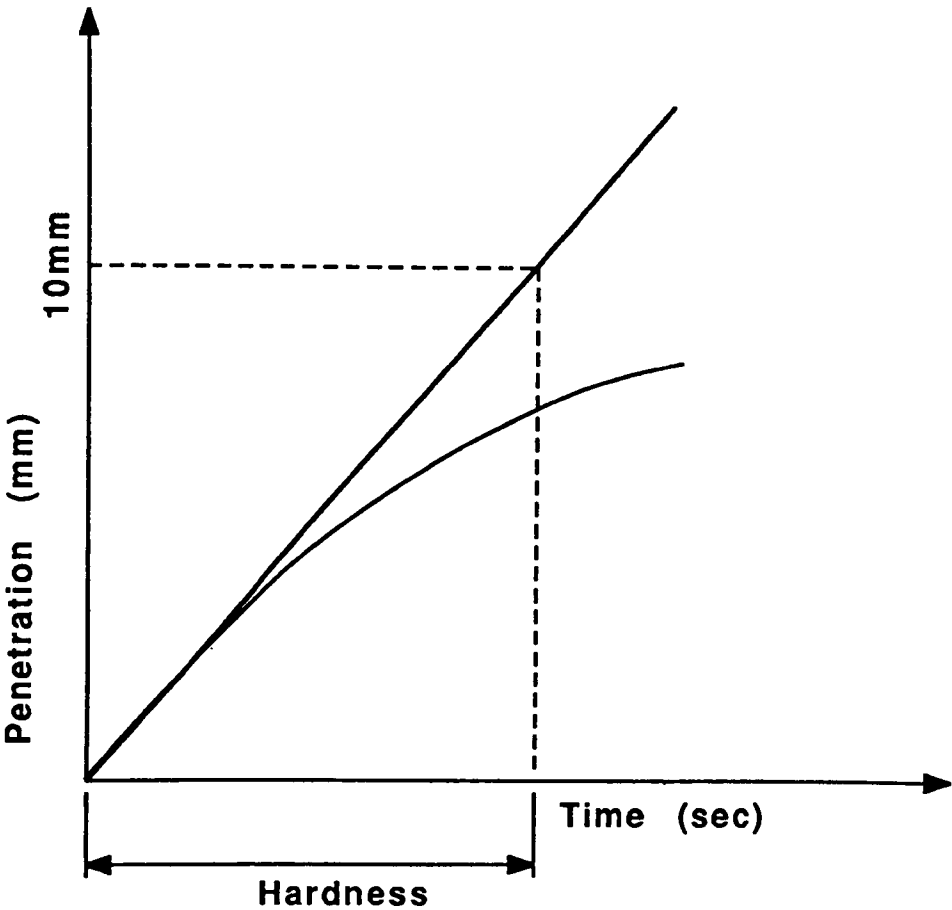
It must be concluded therefore, that a knowledge of these rock property parameters are of vital importance to the mode of excavation or process and the choice of mining equipment installed.

#### **1.4. Hardness and Abrasive Testing.**

Hardness tests performed on homogeneous man made materials seldom present problems. Unfortunately, some confusion exists as to what is meant by the term hardness and abrasiveness when applied to rock material. Most of this confusion stems from the numerous test methods that have been adopted.

For example, petrological analysis of thin sections of sedimentary rocks, in which hardness and abrasiveness is determined as a function of the percentage of hard mineral constituents, fails to take account of the competency of the cementing material with hardness and ignores grain size and angularity with abrasiveness

Figure 1.1      Cerchar Hardness Test



**Bit Penetration as a Function of Time**

and yet, gives equal weight to both hardness and abrasiveness.

### 1.5. Hardness Testing.

#### 1.5.1. The Cerchar Durete Test.

The Cerchar durete, combined hardness and toughness test, is widely used throughout the French coal mining industry to predict the forces experienced by picks under known working conditions. Hardness is determined by applying a new 8 mm diameter tungsten carbide drill bit, terminating in a 90° dihedron, to the rock surface while being rotated at 190 rev/min under a load (dead weight) of 20 kg. The penetration of the bit is monitored with time, penetration progressively decreasing as cominuted debris impairs the cutting action of the bit.

The durete index is defined as the initial penetration rate as determined from the gradient of the curve at the origin of a bit penetration versus time plot. To establish an index which increases proportionally with hardness, the time required to advance 10 mm has been designated. (assuming a constant initial penetration rate). This relationship is illustrated in Figure 1.1. The index has shown to correlate linearly with the normal forces developed by new rock cutting picks

under controlled cutting conditions.

Typical values for the index are 0 - 4 units for coal, 4 - 10 units for shales and some sandstones and up to 200 units for strong rocks.

#### 1.5.2. The Brinell Hardness Test.

A very well known metallurgical hardness test which has been adopted for the determination of rock hardness, is the Brinell indentation test. This test employs a metal ball which is forced onto and into the specially prepared surface of the specimen being examined. The Brinell hardness number is calculated from the following equation:

$$H = \frac{L}{\pi D/2 (D - \sqrt{D^2 - d^2})}$$

Where L = Load (kg)

(Eq.11)

D = Ball diameter (mm)

d = Indentation diameter (mm)

The hardness index number is derived from a load of 3000 kg on a 10 mm diameter ball.

#### 1.5.3. The Vickers Hardness Test.

The Vickers hardness test is yet another indentation test originally designed to determine the hardness of metals. However, this test has been adopted by geologists to determine the hardness of individual



mineral grains. The test employs a four sided diamond pyramid having an apical angle of 136°. The diamond pyramid is forced into the surface of the specimen and the ratio of the applied load divided by the pyramidal area of the indentation determines the Vickers hardness (VHN).

$$VHN = \frac{1.845p}{D^2} \quad (Eq\ 1.2)$$

Where p = Applied load (kg)

D = Length of the diagonals of  
the permanent impression

#### 1.5.4. The Rockwell Hardness Test.

The Rockwell hardness test is also an indentation hardness test originally designed for the determination of metal materials. This test employs a 1.6 mm diameter steel ball for the designated "B" test, or a pointed conical diamond for the "C" test. The test consists of minor loading for either the steel ball or the diamond cone against the face of the specimen under a normal load of 10 kg. Subsequently, a major load of 100 kg for the "B" test or 150 kg for the "C" test is applied. The major load is removed while the minor load is maintained and the depth of penetration caused by the major load is determined from a dial gauge indicator using the scale appropriate for either the "B" or "C" tests.

TABLE 1.1

Comparison of Hardness Values for SAE Carbon  
and Alloy Constructional Steel

Brinell			Rockwell		Shore Scleroscope No.
Diam. in mm, 3000 kg Load 10 mm Ball	Hardness No.	Vickers or Firth Diam. Hardness No.	C 150 kg load 120° Diamond Cone	B 100 kg load 1/16 in. diam. ball	
2.60	555	633	55	120	75
2.65	534	598	53	119	72
2.70	514	567	52	119	70
2.75	495	540	50	117	67
2.80	477	515	49	117	65
2.85	461	494	48	116	63
2.90	444	472	46	115	61
2.95	429	454	45	115	59
3.00	415	437	44	114	57
3.05	401	420	42	113	55
3.10	388	404	41	112	54
3.15	375	389	40	112	52
3.20	363	375	38	110	51
3.25	352	363	37	110	49
3.30	341	350	36	109	48
3.35	331	339	35	109	46
3.40	321	327	34	108	45
3.45	311	316	33	107	44
3.50	302	305	32	107	43
3.55	293	296	31	106	42
3.60	285	287	30	105	40
3.65	277	279	29	104	38
3.70	269	270	28	104	38
3.75	262	263	26	103	37
3.80	255	256	25	102	37
3.85	248	248	24	102	36
3.90	241	241	23	100	35
3.95	235	235	22	99	34
4.00	220	229	21	98	33
4.05	223	223	20	97	32
4.10	217	217	18	96	31
4.15	212	212	17	96	31
4.20	207	207	16	95	30
4.25	202	202	15	94	30
4.30	197	197	13	93	29
4.35	192	192	12	92	28
4.40	187	187	10	91	28
4.45	183	183	9	90	27
4.50	179	179	8	89	27
4.55	174	174	7	88	26

cont,

4.60	170	170	6	87	26
4.65	166	166	4	86	25
4.70	163	163	3	85	25
4.75	159	159	2	84	24
4.80	156	156	1	83	24
4.85	153	153		82	23
4.90	149	149		81	23
4.95	146	146		80	22
5.00	143	143		79	22
5.05	140	140		78	21
5.10	137	137		77	21
5.15	134	134		76	21
5.20	131	131		74	20
5.25	128	128		73	20
5.30	126	126		72	
5.35	124	124		71	
5.40	121	121		70	
5.45	118	118		69	
5.50	116	116		68	
5.55	114	114		67	
5.60	112	112		66	
5.65	109	109		65	
5.70	107	107		64	
5.75	105	105		62	
5.80	103	103		61	
5.85	101	101		60	
5.90	99	99		59	
5.95	97	97		57	
6.00	95	95		56	

Table 1.1. Illustrates a table of comparative hardnesses.

Note. The Shore Scleroscope is discussed later in Chapter 2.

#### **1.6. Abrasive Measurements.**

Like the mechanical methods of determining hardness, there are equally as many mechanical tests designed to measure the abrasiveness of rocks. Indeed, each of the workers in this field of study appears to have designed tests of their own for some specific purpose. The many tests available have been adequately reviewed by Barr (1977) and by Brown and Phillips (1977) and it is not the author's intention to dwell on these, except to give some typical examples of tests that deal with both intact rock and rock aggregates. It should be noted however, that some of these tests also reflect a measure of the rocks resistance to abrasion at the same time.

#### 1.6.1. The Hacksaw Test.

The Hacksaw test is carried out on a cored specimen of rock and uses a standard workshop, reciprocating hack saw machine. The machine is fitted with a new high speed steel hacksaw blade and a rock core clamped in the machine's vice at right angles to the blade. The blade is lowered onto the rock core specimen and subjected to 10 strokes of the reciprocating arm. The rock core is then moved along the vice and this procedure is repeated 10 times. A new blade being used for each test which is weighed before and after the test and the weight loss experienced by the blade expressed in mg, is given as a measure of abrasiveness. The advantages claimed by Fowell (1977) are that the tests can be carried out on site investigation rock core samples and uses commonly available workshop machinery rather than specially manufactured proprietary apparatus.

The test results range up to 350 mg for abrasive sandstones.

An attempt was made by Fowell to correlate the test results with quartz content, but no relationship was established, this being attributed to the fact that the abrasiveness of rocks depended on texture, grain size and the bonding of the mineral grains in addition to percentage quartz content.

#### 1.6.2. Tool Wear Test.

A cylindrical rock specimen 200mm long by 75mm in diameter is mounted in a centre lathe three jaw chuck and turned down using a cutting tool held in a specially constructed toolholder. The abrasiveness of the rock is assessed after 30m cutting distance by measuring the resultant weight loss, to 0.1mg, of the detachable tip of the tool. The result of the test is expressed as the weight loss per metre. The width of the wear flat produced on each tip is also measured using a vernier microscope. Further details of this test are given by Potts (1972).

The advantages of this test are that it can be conducted on a standard workshop machine using field core samples and with tools of similar shape, made from the same insert material as tools used on tunnelling machines.

While this test gives good results with hard abrasive rock. with non-abrasive, weak and friable material, the resultant weight loss is often too small to be of a significant value or any resultant wear flat, too small to measure. Thus a classification using this system would be difficult to establish.

#### 1.6.3. The Modified Taber Abrasion Test.

A modified Taber abraser machine was used for this test. The test specimen is a 6mm disc of rock, normally cut from a 50mm diameter rock core sample. The disc of rock is subjected to 800 revolutions (400 revolutions on each face) under the action of an abraser wheel loaded with a 250g weight. The abrasiveness of the rock is obtained by measuring the weight loss of the abraser wheel and is defined as the reciprocal of this weight loss in grammes.

Values given by Tarkoy and Hendron (1975) range from 0.3 for some sandstones to 57 for dolomitic limestones.

The main disadvantages with this test lies in the fact that, after each test the abraser wheel is required to be resurfaced and proprietary apparatus and equipment are necessary.

#### 1.6.4. The Steel Cube Test.

The steel cube test employs a one-inch, bright mild steel cube which is tumbled for three hours in a tumble-polishing machine together with a 900g sample of rock aggregate saturated with water. The loss in weight per hour of the steel cube, expressed as percentage of its original weight, is given as a measure of the abrasiveness of the rock. The test was

first developed to test the abrasiveness of rock debris produced from a full-face tunnelling machine, but was later used to assess the abrasiveness of aggregates used to manufacture concrete blocks for instrumented drilling trials. West, McCaul and Horning 1977.

Good correlation between the test results and the rate of disc cutter replacement on the full-face tunnelling machine was claimed and some typical results are presented in Table 1.2.

TABLE 1.2

The steel Cube Test.

Rock type	Abrasiveness (%/Hour) $\times 10^{-4}$
Mudstone	99
Sandstone	156
Limestone	99
Granite	111

Although the test requires some proprietary equipment, an advantage is gained by conducting the test on aggregate material, which implies that specially cored rock samples (which can often present problems) are not necessary. The test is however, time consuming and



and the author found, that the resultant percentage weight loss experienced by the relatively heavy steel cube, when testing some non-abrasive rocks was insignificant, and consequently, the determination of abrasiveness was considered unreliable. Furthermore, subsequent analysis of the aggregate material after the test, show a significant change in the shape of the rock particles.

#### 1.7. Conclusions.

It can be seen that wear caused to mining machinery and other equipment takes place through a variety of reasons. Therefore, the definition of the mode of wear and damage must be regarded as of importance when attempting to devise some predictive test.

A disadvantage with most of the mechanical tests derived to determine rock hardness and abrasiveness, whether or not a rock aggregate or specially prepared specimen is used, is that, being empirical, the results need to be correlated with operational results obtained from reliable field data. It can be seen that some of the tests described have been related to some specific application and consequently, some credibility can be placed with these tests when related to their intended application. However, it

should be clear that no single test can be used for every occasion where an abrasive potential assessment of a rock type is required.

The subsequent chapters in this thesis are devoted to the determination of hardness and abrasiveness of rocks together with a test programme devised to provide a predictability guide to the abrasive wear potential of rocks when being machined or excavated.

## **CHAPTER 2.**

**DETERMINATION OF HARDNESS AND ABRASIVENESS OF ROCK.**

variety of test equipment involving the testing of large numbers of rock specimens. Rock strength parameters such as uniaxial compressive strength, tensile strength, deformation properties together with various intrinsic properties have been well established and are commonly assessed by universally accepted standard test procedures. Unfortunately however, these properties alone cannot be used to predict the consequential interactive wear and subsequent damage to mining machines and their associated tools and equipment.

\* A study of rock hardness and abrasiveness together with their effects on the wear rates of machines, machine tools and other mechanical equipment must be regarded as vitally important. This is especially true in view of the very high costs incurred with the replacement of tools, repair and maintenance to machinery together with their consequential detrimental effects on production.

## **2.2. Determination of Rock Hardness and Abrasiveness.**

The determination of hardness and abrasiveness of natural rock material may be assessed by the use of the two methods described as follows:

- 1) Petrological Methods.
- 2) Mechanical Methods.

### 2.2.1. Petrological Methods.

The petrological methods used by geologist and mineralogists to determine hardness and abrasiveness of rocks involve the analysis of thin sections or polished mounts of rock material under a standard petrographic microscope.

This is conducted to determine the mineral constituents contained within the rock and their proportions, by the use of spot counting techniques, together with the mineral hardnesses, grain sizes, shape and angularity. The mean hardness of the rock is derived simply by accurately quantifying the proportions of each of the individual mineral groups present, to which a hardness number is ascribed. The proportion of each mineral is then multiplied by its ascribed hardness number and summed to give a mean hardness value for the whole rock. This is given as a measure of abrasiveness also.

Two well known geological scales of rock mineral hardnesses are as follows:

- 1) The Mohs' Scale of Mineral Hardness
- 2) The Rosiwals Scale Mineral Hardness.

### 2.2.2. The Moh's Scale of Mineral Hardness

The Moh's scale of mineral hardness is preferred by geologists because it is relatively easy to perform in the field.

This scale of rock mineral hardness was proposed by Professor F. Moh's who was appointed to the chair of Mineralogy in Vienna in 1826 and is basically a scale of relative hardness, such that rock minerals of high Moh's hardness numbers are able to scratch minerals of lower Moh's hardness numbers. The system is based on the ability of a hard mineral to scratch another mineral of lesser hardness, and is basically a "one rank only order of hardness" in which diamond, the hardest mineral known to man, is ascribed a hardness value of 10. and talc the lowest value of 1. The relative hardness of a given mineral can therefore, be assessed by attempting to scratch the given mineral with a hardness pencil tipped with one of the standard minerals. This scale however, is imprecise, mistakes are easily made and the standard minerals do not advance in any definite or regular ratio of hardness. Furthermore, this method ignores the strength of the bond of the matrix material binding the minerals

The following table gives an example of some typical standard minerals and their Moh's hardness numbers.

Table 2.1 .

THE MOH'S SCALE OF MINERAL HARDNESS.

Mineral	Mohs' Hardness
Talc.	1
Rocksalt or Gypsum	2
Calcite	3
Fluorspar	4
Apatite	5
Orthoclase Feldspar	6
Quartz	7
Topaz	8
Corundum	9
Diamond	10

Window glass could be used for apatite and flint for quartz. Hardness can be determined by attempting to scratch the mineral under examination with the standard minerals, e.g. a mineral that scratches quartz but does not scratch topaz will have a hardness of about 7.5. A penknife will scratch minerals up to 6.5 and a fingernail up to 2.5 "although fingernails vary in hardness". A definite scratch must be produced, which should be carefully examined by blowing away the powder produced and then inspected with the aid of a magnifying lens to avoid mistaking

Table 2.2.

Rock	Mineral	Proportion	Moh's Hardness	Abrasiveness Mean Hardnes
Mudstone	Quartz	0.65	7	5.24
	Calcite	0.11	3	
	Mica's )			
	Clay Minerals )			
	Plagioclase )	0.24	1.5	
	Amphibole )			
	Siderite )			
Sandstone	Quartz )	0.97	7	6.87
	Mica )			
	Clay Minerals )	0.03	2.5	
	Iron Hydroxide)			
Limestone	Calcite	0.98	3	3.08
	Quartz	0.02	7	
Granite	Feldspar	0.60	6-6.5	6.25
	Quartz	0.30	7	
	Biotite	0.05	2.5-3	
	Hornblende	0.03	5-6	
	Magnetite	0.01	5.5-6.5	



a whitish strip, sometimes produced on a harder mineral by a soft mineral. Similarly, a penknife can produce a steel mark on a hard mineral, also, granular materials may appear to be scratched if mineral grains are broken from the surface. A fresh surface is essential to avoid decomposed materials giving erroneous results. Table 2.2. illustrates some typical results obtained from the use of the Moh's scale of hardness.

#### **2.2.3. Rosiwal's Scale of Mineral Hardnesses.**

A further scale of mineral hardness has been proposed by Rosiwal. This scale is relatively a more quantitative scale than the Moh's scale of hardness in that it is based on a minerals treatment by an abrasive powder in which corundum is given a value of 1000. All other minerals are expressed relative to corundum.

An example of the Rosiwal's scale of mineral hardnesses is given in the following Table 2.3.

Table 2.3.

ROSIWALS SCALE OF MINERAL HARDNESSES

Mineral	Rosiwal's Hardness Number
Diamond.	140,000
Corundum.	1000
Topaz.	175
Quartz.	120
Orthoclase Feldspar.	37
Apatite.	6.5
Fluorspar.	5
Calcite.	4.5
Gypsum.	0.25
Talc.	0.03

The mean hardness of the whole rock however, is calculated in the same way as for the Mohs' scale of hardness.

An example of this is given as follows:

Mineral.	Percentage	Rosiwal's Hardness
Quartz.	77	120
Feldspar	10	37
Carbonates	13	4

The composite Rosiwals mean hardness number =  $(0.77 \times 120) + (0.1 \times 37) + (0.13 \times 4) = 96.2$  and as with the Moh's scale of hardness, this is given as a measure of abrasiveness also. Further details of both the Moh's and Rosiwal's scales of hardness are given by Borner. (1962)

#### 2.2.4. Silica Content.

Silicon (Si) does not occur in a natural free state but it's compounds are present in great abundance within the earth's crust. The oxide quartz and a large group of silicates are the most important rock forming minerals. Silica ( $SiO_2$ ) one of the oxides of silicon occurs as quartz, chalcedony, agate and flint etc. Sand is usually made up of small grains of quartz, and possibly flint, and consolidated sands (cemented) form the sedimentary rock, sandstone.

Silica is a hard mineral, 'Moh's Hardness 7. Other forms of silica include chert, hornblende and jasper. There are also a large number of silicon derivations, (which include the garnet family) essentially silicates of various divalent and trivalent minerals, their shapes are rhombodecahedral or trapezohedral or these two forms in combination, e.g. relatively spheroidal, but with sharp cornered crystals. They range in hardness from 6.5-7.5 on the Moh's scale.

Topaz,  $\text{Al}_2\text{F}_2\text{SiO}_6$  occurs in acid igneous rocks such as granites or rhyololites, it can also be present in tin bearing pegmatites and in tin veins associated with cassiterite, fluorspar and tourmaline. Topaz have prismatic crystals made up from brachypinacoid, basal pinacoid, brachydone, macradome and pyramid crystals, without sharp corners, but very hard. 'Moh's hardness 8.

Corundum  $\text{Al}_2\text{O}_3$  is, with the exception of diamond, the hardest mineral known and has a Moh's hardness of 9. It is produced from contact metamorphism of shales and limestones as an original constituent of various igneous rocks and from residual deposits derived from gniess. One variety containing admixed magnetite and haematite is crushed and powdered to produce the material more commonly known as 'Emery'.

#### **2.2.5. X-Ray Diffraction. (XRD)**

When the mineral grain sizes are too small to accurately define under a standard petrographic microscope. e.g.  $<0.01\text{mm}$ , this can lead to a serious underestimation of certain important hard mineral constituents, which could result in the underestimation of the whole rock hardness together with its abrasive potential also. Consequently, in these circumstances, XRD is to be recommended. Furthermore, it has been suggested by McFeat-Smith,

(1977) that quartz content alone, determined by XRD methods conducted on finely ground rock, (380BS.Mesh) may be used to define the abrasiveness of rocks. The advantage of this method being, that it is more rapid and simpler to measure quartz than to carry out a full mineralogical analysis.

#### 2.2.6. X-Ray Fluorescence. (XRF)

It has been further proposed, that the Silica content of rocks determined by XRF methods, may also be used to define abrasiveness. This method will not only reflect the proportion of quartz present but in addition, the amount of other silicate minerals such as feldspars, micas, and clay minerals also. As with XRD, this method is much quicker and easier to carry out than a full mineralogical analysis. It should be noted however, that while XRF can accurately quantify the proportion of the silicate materials present, this does not necessarily reflex the proportion of quartz and the following Table 2.4. gives an example of this:

Table 2.4.

Rock.	Quartz. %	Silica. %
Granite	31	72
Basalt	0	47
Sandstone	70	80
Shale	32	59

It would appear therefore, that if quartz is the dominant mineral, then XRD would be the better method to adopt in order to give a more accurate indication of abrasiveness. However, McFeat-Smith has warned, that quartz content alone is not sufficient to explain the the abrasive properties of rocks. It was found that for Bunter and Keuper Sandstones, the rate of road header tool consumption was related to the degree of cementation rather than the quartz content alone.

#### 2.2.7. Cementation Coefficient.

A study was conducted to determine the intensity of the cementation of various sedimentary rock types based on the following observations:

- (i) The type of cementation should be assessed according to the hardness of the cementing material.

(ii) The grain size of the quartz cements i.e. silt and clay, influence the strength of the bond and should be represented in that order.

(iii) The degree of cementation is significant in extreme cases and major variations in porosity of a rock provide a suitable measure of this.

Table 2.5. shows the classification of a cementation coefficient constructed according to these observations. The higher the coefficient number, the more the matrix material contributes to the overall hardness of the rock.

#### 2.2.8. Relationship Between Rock Properties.

It can be readily observed that the relationship between rock competency, hardness and abrasiveness are all of importance and it can be shown that even very weak rocks can cause severe abrasive wear problems. The two following examples given by McKenzie and Dodds, (1972). clearly illustrate this point:

Project	Rock	Com/Strength	SiO2
Mersey Tunnel	Bunter Sandstone	30-40Mpa	82%
Kielder Tunnel	Little Whin Sill (Dolerite)	300-400Mpa	1%

Table 2.5.

CEMENTATION COEFFICIENT.

Coefficient.	Cementing Material.
1,	Non-cemented rock's or those having greater than 20% voids.
2.	Ferruginous cement.
3.	Ferruginous and clay cement.
4.	Clay cement.
5.	Clay and calcite cement.
6.	Calcite (or Halite) cement.
7.	Silt, Clay or calcite with quartz overgrowths.
8.	Silt with quartz overgrowths.
9.	Quartz cement, quartz mozale cements.
10.	Quartz cement with less than 2% voids.

after McFeat-Smith.



POWERS ROUNDNESS CHART.

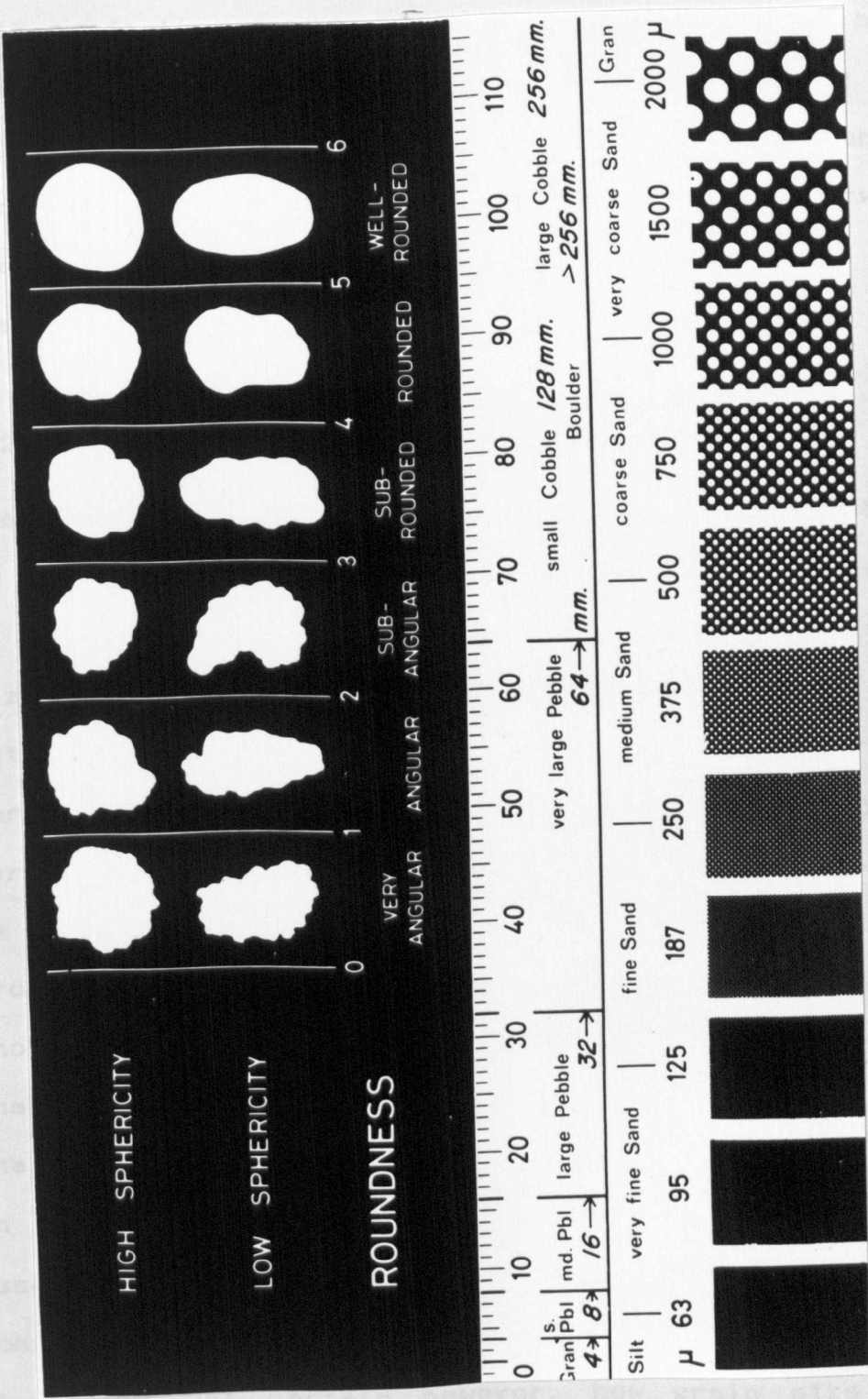


Figure 2.1.

Both projects experienced high cutter wear. The high compressive strength being the cause when cutting the dolerite and the high quartz content with the bunter sandstone. It is clear therefore, that some forward knowledge of the rock properties to be excavated are essential.

#### 2.2.9. Competency, Grain Size and Angularity.

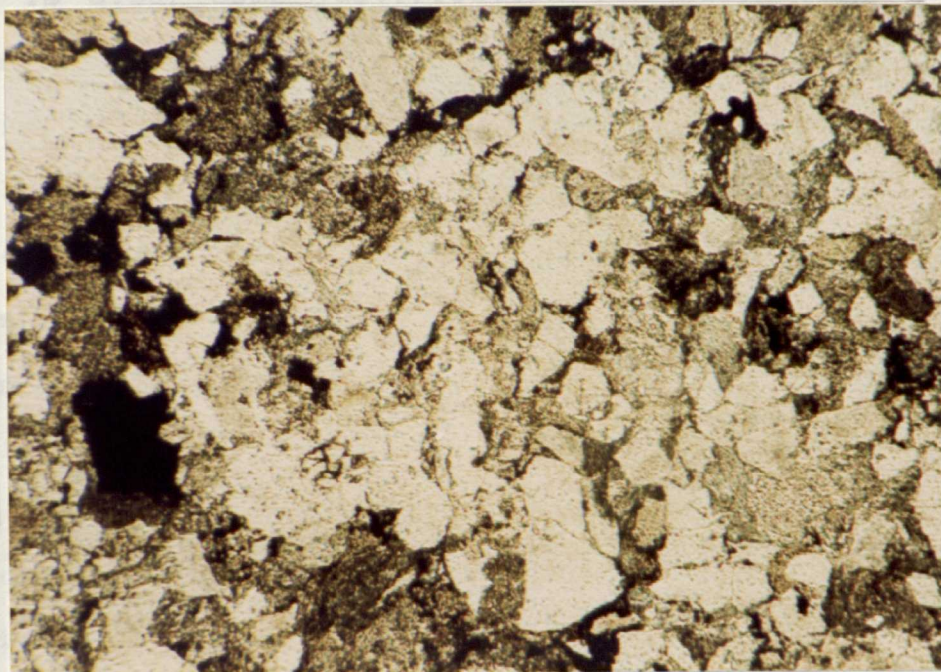
The main disadvantages with the petrological methods so far discussed are, that the 'mean hardness measure of abrasiveness' takes no account of mineral grain size, angularity or the degree of firmness of attachment of the mineral grains within the rock. Furthermore, while the mineral constituents may be hard and proportionally high, the whole rock mass may be much more yielding than one might be led to expect from the petrologically derived mean hardness.

Another area neglected by petrological analysis, is that of grain size and shape. A method of classifying shape has been proposed by Powers and is illustrated in Figure. 2.1. However, these factors are often assessed subjectively after a number of tests and in consideration of the processes involved.

It is not yet certain however, how grain size and shape affect abrasiveness, for example, although it might be thought obvious that coarse grained material

may be more abrasive than fine grain material. It has been suggested, West (1981) that fine grains, because of increased contact with cutting tools, transport systems machine equipment will be more abrasive than coarse grains. The mode of attack will of course, have some considerable effect.

# PHOTOMICROGRAPH.



Cuddalore Sandstone.

Quartz	Cryptic Silica	Clay minerals
31	21	13

Figure 2.2.

may be more abrasive than fine grain material, it has been asserted, West (1981) that fine grains, because of increased contact with cutting tools, transport systems and other mining machine equipment will be more abrasive than coarse grains. The mode of attack will of course, have some considerable effect. There is also, some justification for suspecting the adverse effects of hard mineral grain angularity on abrasive wear. Considering the Cuddalore sandstone of Neyveli in India. This rock is a very weak sandstone with a uniaxial compressive strength of 1.585 MPa. It consists of very angular grains of quartz, less than 0.5 mm, with practically no sub-angular or rounded material.

The quartz is set in a ground mass of cryptocrystalline silica (chalcedony) and some geotite is also present. The main mineral proportions are given as follows:

#### Mineral Proportions.

Quartz.	Crypto Silica.	Clay minerals.
31	31	11

XRD tests were considered unnecessary in view of the simple nature of the rock which is illustrated by a thin section microphotograph in Figure 2.2.



**PHOTOPHOT PETROLOGICAL MICROSCOPE.**

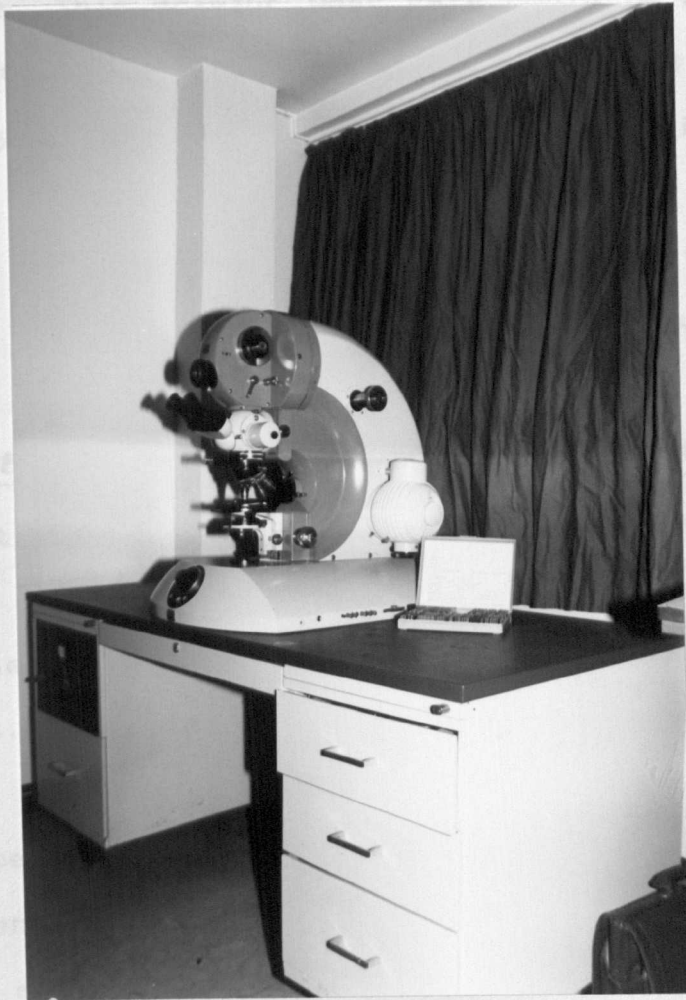


Figure 2.3.

The material which formed part of the overburden to be excavated by BWE caused severe abrasive wear problems. Kasturi (1984) reported BWE teeth wear rates of alarming proportions, resulting in the rapid erosion of the normal hard metal bucket wheel teeth within 2.5 to 3 hours. This dramatic wear rate could be attributed directly to the high proportions of hard and very high angularity of the mineral constituents. Atkinson and Cassapi, (1984)

It should be noted that it takes between 6 to 8 hours to change all the teeth on a bucket wheel excavator.

### 2.3. Petrographic Examination of Thin Sections.

Thin section microscopy is the method most commonly used by geologists to determine hardness and abrasiveness of rocks and requires special laboratory equipment. However, the detailed examination of thin sections of rock specimens under a petrographic microscope can be used to identify the mineral constituents present, their proportions, by employing standard spot counting techniques, grain size, shape and angularity. The "Leitz Photophot" petrographic microscope illustrated in Figure 2.3. has a facility which allows excellent quality colour photography of the various mineral constituents being examined.

### **2.3.1. Thin Section Preparation.**

The quality of thin section preparation of sample material is of importance to the integrity of the microscopic analysis and therefore, a step by step system of specimen production has been devised to standardise both consistency and quality alike.

Thin section specimens should be of uniform thickness over all of the rock slice to precise geological requirements in the range. ie. quartz, grey to very pale yellow. The rock surface exposed and bonded should be scratch free, smooth and free from plucking to the best standards normally required.

The rock should be bonded to the glass slide with an epoxy resin adhesive of acceptable refractive index such that the thickness is effectively zero. The glass slide of original commercial polished face on the bonded side should be reduced to a machine controlled standard thickness by precise smooth lapping.

### **2.3.2. Thin Section Laboratory Equipment.**

The need to analyse large numbers of specimen material required to carry out a study into the abrasive potential of rocks, led to the setting up of a departmental thin section laboratory. The laboratory equipment required to produce a thin section of

acceptable quality is composed of certain standard items of equipment plus a number of consumables and these are listed as follows:

- a) A precision lapping machine with reciprocating arm oscillation to ensure perfectly flat specimen production.
- b) Abrasive cylinders with automatic drip feed to the lapping table. (two or more required for differing grades of abrasives).
- c) A test block to true and check the accuracy of the lapping table by means of twin-dial gauge and master flat block.
- d) A diamond wheel saw with vice and vacuum chuck for first and second sample slicing.
- e) A conditioning ring and pressure block for first lap operations.
- f) Spring loaded holding fixture and hot plate for setting and curing resin bonded thin sections.
- g) A precision lapping jig for lapping slides before mounting specimen material and for final lapping of thin section specimens.
- h) High vacuum impregnation unit for resin impregnation of friable and porous rock sample material.
- i) Vacuum pumps for the lapping jig and rock slicing chuck.



CONDITIONING RING.



Figure 2.4.

### 2.3.3. Systemised Thin Section Production.

A system [LOGITECH] has been adopted for the production of thin sections of rock material which allows relatively inexperienced personnel to prepare thin section specimens of consistently good quality, although some subjective judgement will always be required when deciding whether or not to resin impregnate the rock sample before preparation.

This routine system begins by selecting a small piece of sample material to be roughly cut to a size that will fit onto a standard glass slide, e.g. a piece 18mm wide by 40mm long by about 6mm thick would be suitable to fit onto a standard 25mm x 50mm commercial glass slide. At least four rock sample slices are cut at the same time in order to completely fill the lapping jig to full capacity

The four samples are then placed in the conditioning ring and positioned on the lapping table by a fork on the reciprocating arm of the lapping machine. The samples are lapped to a precise surface finish while being firmly held in place by the pressure block.

The conditioning ring is illustrated in Figure 2.4

The next stage in the system involves lapping one side of the glass slide, although most experienced operators will have done this as a batch operation and

SETTING FIXTURE AND HOT PLATE.

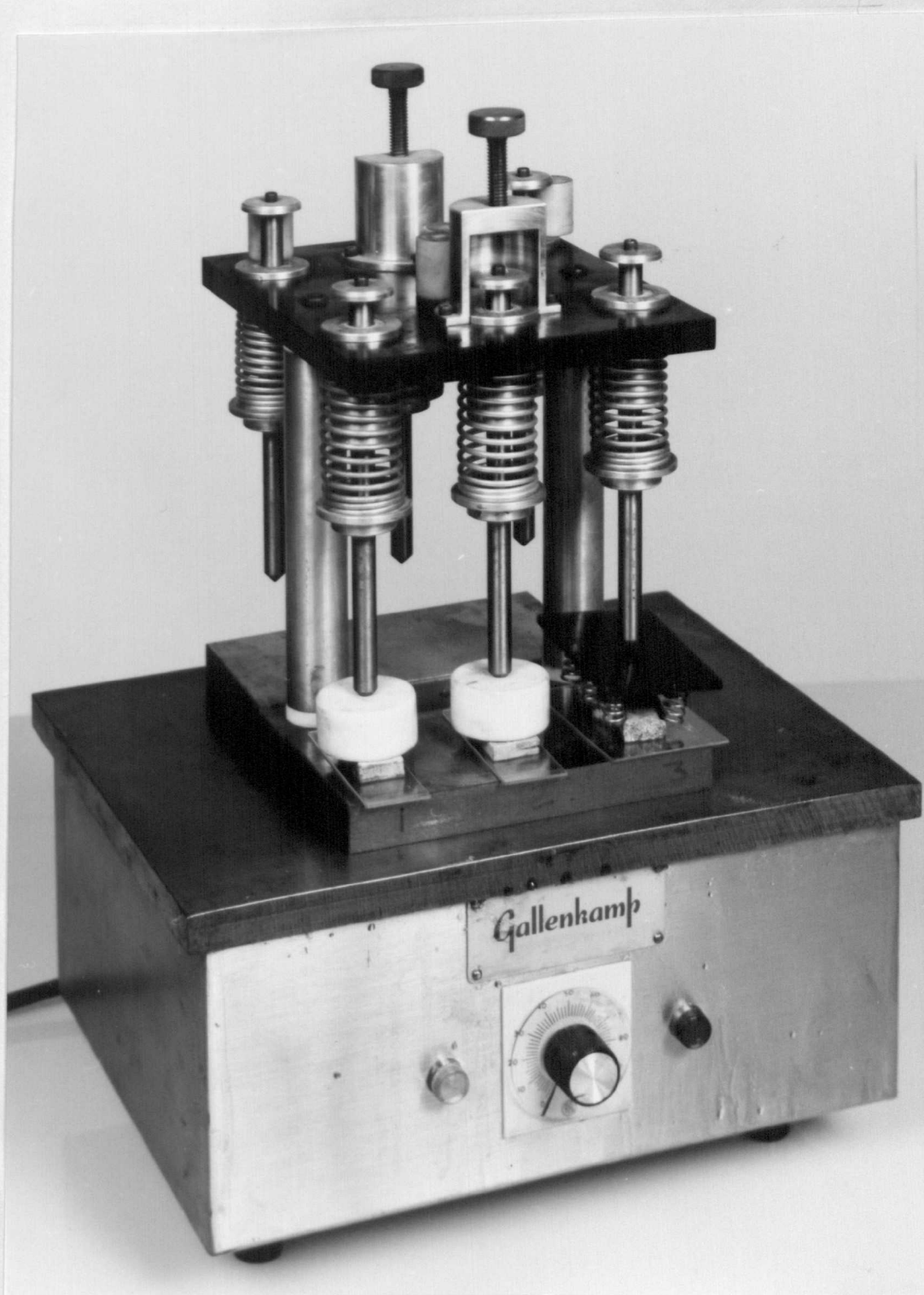


Figure 2.5.

ROCK SLICING MACHINE.

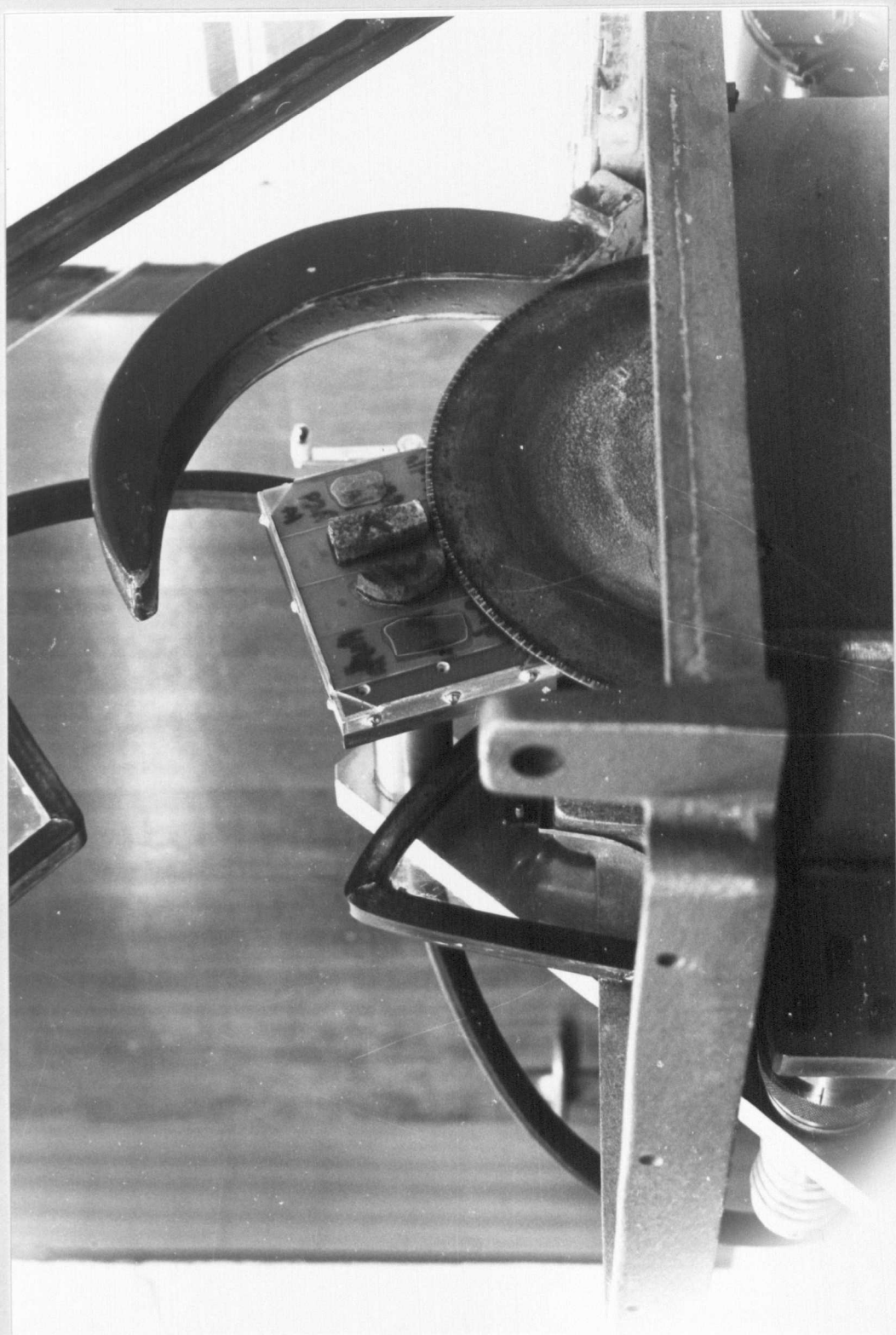


Figure 2.6.



LAPPING JIG.



Figure 2.7.

will have a number of glass slides ready lapped and prepared for use when required.

After the first lap operation, the specimens are thoroughly cleaned using a ultra-sonic bath and dried before bonding to the glass slide. Bonding is carried out with a two part epoxy resin of acceptable refractive index, the rock specimen being held in place and under pressure provided by a spring loaded setting fixture. The setting fixture and slide is placed on a temperature controlled hot plate for one hour at a temperature of 60°C and then allowed to cool to ambient room temperature. The setting fixture and hot plate are shown in Figure 2.5.

The next operation involves setting the rock bonded slides on the rock slicing machine shown in Figure 2.6. These are held in place by an integral vacuum chuck and can then be trimmed off to about 1 mm. thickness in preparation for final lapping.

Final lapping is carried out with the aid of the precision lapping jig illustrated in Figure 2.7. This jig has a diamond impregnated outer ring which resists abrasive wear so that the finished specimen thickness of approximately 30 $\mu$ m "depending on the refractive index of the material" can be preset by the twin-dial setting gauge before lapping commences.

The twin gauge setting block is shown in position on

TWIN GAUGE SETTING BLOCK.

the lapping jig in Figure 2.7.

The thin section spectrometer is used to measure the thickness of the thin section.

placed by an integral component of the spectrometer.

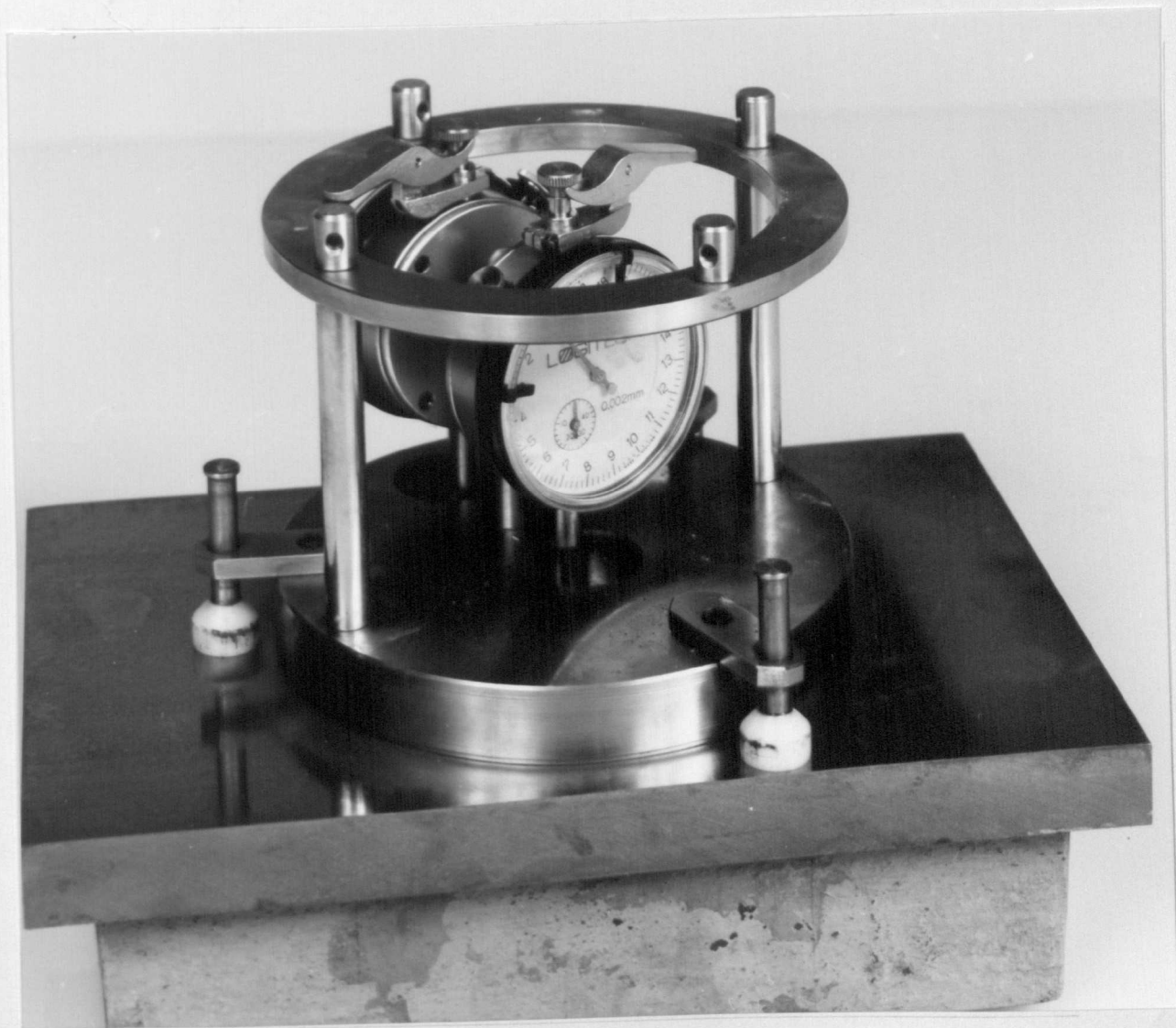


Figure 2.8.

the lapping jig in Figure 2.8.

The thin section specimens (4 off) are firmly held in place by an integral vacuum chuck situated inside the diamond impregnated ring of the lapping jig. The abrasive grit size used for this operation is usually 600 $\mu$ m for the initial lapping stage, which reduces the thickness to about 35  $\mu$ m. The remaining 5 $\mu$ m of the rock specimen thickness being finished off with 1000 $\mu$ m grit size to ensure a scratch free surface finish. After final lapping stage has been completed and checked on a petrographic microscope for thickness and surface finish, the specimen is covered with a thin slip of transparent material (cover slip) to both improve the refractive index quality and to provide some protection against possible surface damage to the thin section specimen.



## 2.4. MECHANICAL METHODS.

### 2.4.1. Introduction.

It has been stated and is generally conceded by many researchers concerned with the performance of drill rigs, tunnel excavation machinery and other methods of rock excavation and mining equipment, that rock hardness and abrasiveness together with the mineralogy of rock materials are among the fundamental parameters requiring investigation if the problems associated with abrasion are to be better understood.

However, mechanical tests devised to determine the hardness and abrasiveness of rocks appear to suffer from a lack of standardisation and while there are many tests which have been employed for this purpose, they tend to have been designed for some specific purpose or geographical area, furthermore, there appears to be little or no correlation between the different tests being exploited.

It is doubtful therefore, that any single test could provide an accurate prediction of likely tool wear with certain mining operations or indeed, where any interaction between rock material and mechanical mining equipment may occur.

Therefore, a minimum number of tests are proposed to determine these parameters. These should be assessed both qualitatively and subjectively in order to provide a more accurate prediction of the abrasive potential of the rock mass, together with the consequential wear rate of tools and other mechanical equipment

The proposed tests to determine the hardness and abrasiveness of rock material are outlined as follows:

- 1) Uniaxial compressive strength.
- 2) Tensile strength. (indirect).
- 3) Toughness Index Tests.
- 4) Hardness Index Tests
- 5) Abrasive Index Tests
- 6) Petrological Analysis.
- 7) Point Load Index.
- 8) Schmidt Hammer.
- 9) Rock quality description. (RQD)

The first three parameters (1,2,3) are all well established rock mechanics, laboratory tests and it is not the intention of the author to dwell on these techniques further, except to emphasise the importance of these parameters in the final analysis.

The Point Load Index and Schmidt Hammer tests (7&8) are also well documented and have proven to be very useful field tests and these will be discussed later.

#### 2.4.2. Hardness Tests.

There are many tests designed to determine the hardness of rocks and a number of these have been based on the standard metallurgical hardness testers, such as the Vickers, Brinel or Rockwell tests. Most of these metallurgical tests rely on the homogeneous nature of man made materials such as metals and various alloys etc, for integrity and accuracy. The Vickers test can be adapted to standard petrographic microscopes and used to determine the micro-hardness of individual rock mineral grains. The Knoop test having a facility to determine the directional hardness of individual mineral crystals.

Natural rock however, is seldom even remotely similar in nature to the consistent homogeneous man made metal materials and consequently, when using these tests for the determination of rock hardnesses, a modified procedure must be adopted in order to compensate for the scattered values usually obtained. This scatter normally results from the variation in the hardness of the mineral constituents present, and with sedimentary rocks, the degree of firmness by which these minerals are cemented by the matrix material. The adaptation used therefore, attempts to obtain a representative value of hardness by making a large number of tests over a comparatively large area.

The results obtained, have been statistically resolved to give a mean value of hardness for the whole rock mass.

Clearly therefore, any test to be of value with a wear potential index, should be one that measures the hardness of the whole rock, which includes the cementing material and not just the hardness of its individual mineral constituents.

#### 2.4.3. The Shore Scleroscope.

The Shore Scleroscope was invented by Albert F Shore in 1907. and was the first commercially built metallurgical hardness tester. This instrument has been adapted by many geotechnical engineers for the determination of rock hardnesses. Muftuoglu, Y,V. 1983. et al.

The instrument consists of a vertically disposed steel tube containing a diamond tipped hammer. The hammer is dropped from a predetermined fixed height onto the surface of a specially prepared rock specimen which strikes the specimen a blow and then rebounds. The rebound height however, falls short of its original height since some of the energy in the falling hammer is dissipated in the production of a minute indentation. The height of rebound is proportional to the hardness of the face of the rock specimen and is

THE SHORE SCLEROSCOPE.

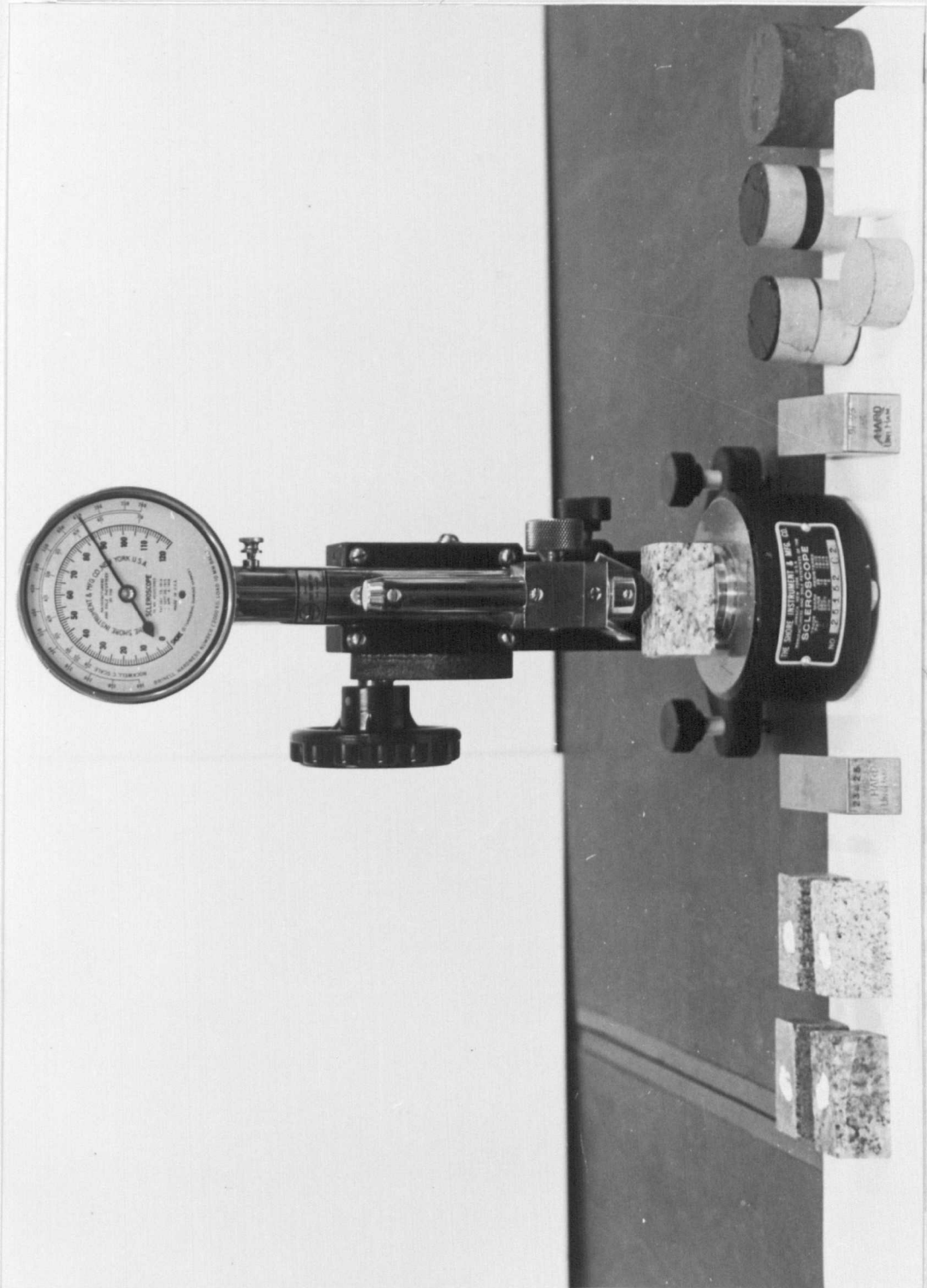


Figure 2.9.

recorded on a integral dial gauge mounted on top of the tube. The dial gauge is indexed in Shore Scleroscope hardness numbers 0 - 120. and equivalent Rockwell and Brinel hardness numbers are also displayed.

Figure 2.9 illustrates the Shore Scleroscope with two steel calibration blocks, (one hard 91-93 and one soft 23-25) together with a selection of prepared specimen sample material for hardness testing.

Because of the small contact area of the diamond tipped hammer between the surface of the rock specimen, the results obtained are subject to varying degrees of scatter and consequently it is necessary to to use statistical analysis to determine the minimum number of tests to achieve an acceptable degree of confidence with the results obtained.

Surface finish of the prepared face of the rock specimen can significantly affect the integrity of the test results and a standard specimen specification has been proposed by "The International Society of Rock Mechanics" (ISRM). The ISRM also recommend at least 20 determinations should be made on each specimen with no two readings made on the same spot. The author has found that this is in many cases insufficient and at least 100 determinations are more often necessary and these should be made orthogonally on rectangular shaped specimens. Good correlation between uniaxial

compressive strength and Shore Scleroscope hardness have been found by a number of authors, Muftuoglu, (1983) et al and are discussed later in Chapter 3.

#### 2.4.4. The National Coal Board Cone Indenter.

The National Coal Board Cone Indenter was designed and developed at the NCB, Research and Development Establishment at Bretby in the UK, for the determination of rock hardness.

The instrument is of the penetrometer type and consists of a steel frame portal with a spring steel leaf fixed along it's horizontal axis. A dial gauge is mounted mid way along one side of the frame with its probe in contact with the spring leaf, so that any deflection of the spring leaf can easily be detected and accurately measured. On the opposite side of the frame, a micrometer with a tungsten carbide cone inserted in its spindle is mounted. This measures the depth of penetration of the cone plus the deflection of the spring steel leaf.

The deflection of the spring steel leaf is calibrated to represent a known force, e.g. a deflection of 0.635 mm equals a force of 40 Newtons, this being the force applied to determine the standard cone indenter hardness number. The actual depth of penetration into the rock is simply calculated by subtracting the

# THE NCB CONE INDENTER..

spring deflection distance indicated on the dial gauge. e.g. 0.535 mm from the total distance indicated by the micrometer.

The standard cone indenter used is



Figure 2.10.



spring deflection distance indicated on the dial gauge, e.g. 0.635 mm from the total distance indicated by the micrometer.

The standard cone indenter index is derived from the following equation:

$$I = \frac{D}{P} \quad (\text{Eq 2.1})$$

where I = Cone indenter number.

D = Deflection of spring leaf, mm.

P = Penetration of cone, mm.

Two other loads are recommended according to the descriptive strength of the rock material being tested.

For weak rocks; a load of 12 Newtons, which equals a spring deflection of 0.23 mm is recommended and for strong rocks; a load of 110 Newtons is used which requires a spring deflection of 1.27 mm.

NCB cone indenter specimens are produced from standard rock cored material of about 38 mm diameter by 6-8 mm thick, although any shape of specimen may be used providing its thickness does not exceed the maximum thickness of 6-8 mm allowed between the cone and spring leaf.

When testing both sides of the specimen, approximately 20 determinations can be made on each side of any specimen material of a competent nature.

Figure 2.10. illustrates the NCB Cone Indenter with

THE DEAD WEIGHT PENETROMETER.

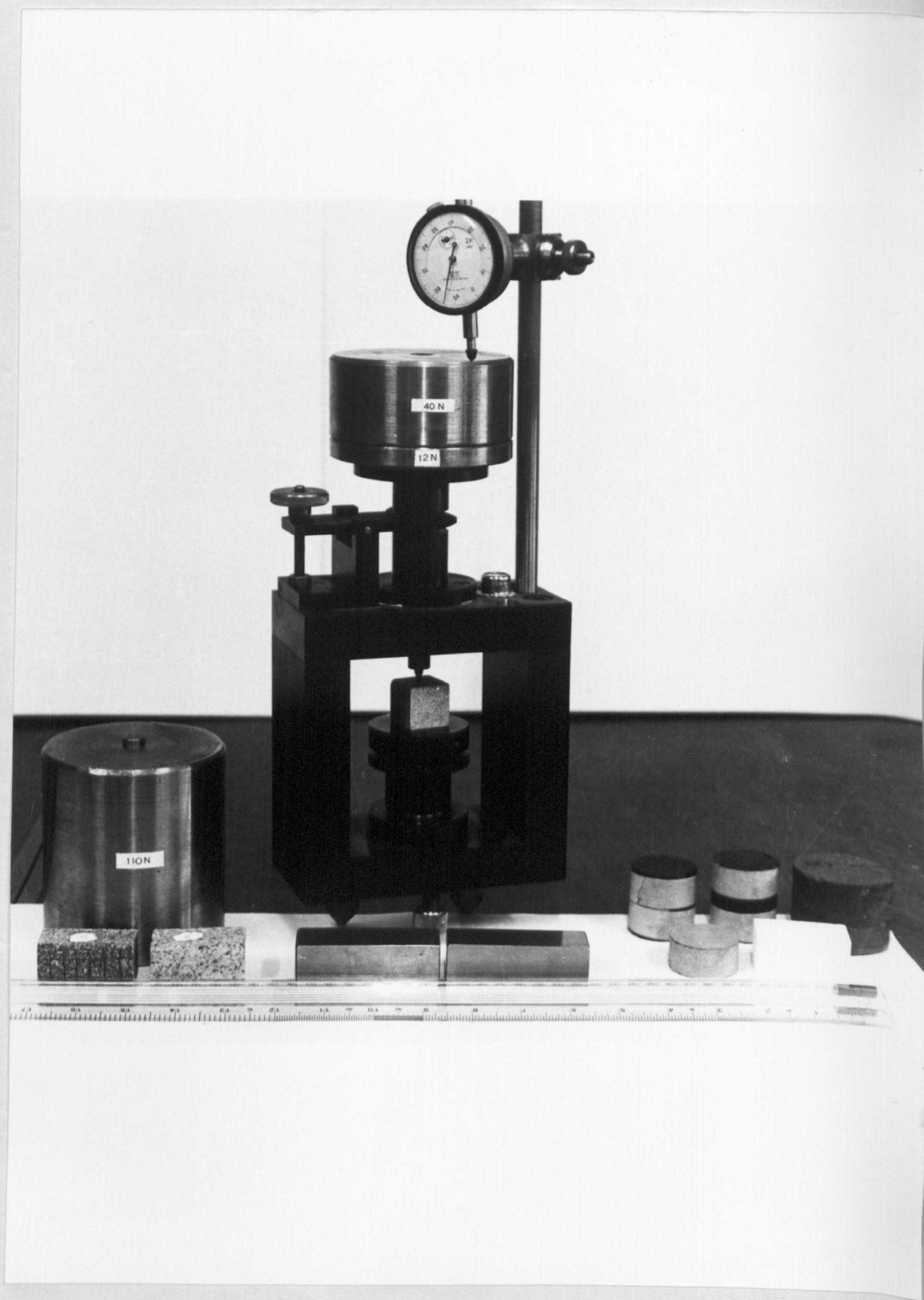


Figure 2.11.

specimen material and calibration weights. These calibration weights are used at regular intervals to check the accuracy of the spring deflection.

Problems were encountered however, with some very weak and friable rock materials in the C4. (cemented soil) - R1. (weak rocks) range of the GS scale, where even under the lowest recommended load of 12 Newtons the cone penetration was so deep that failure of the rock specimen often took place at the point of contact.

Consequently, the number of tests per specimen was effectively reduced to no more than 5. This being a marked disadvantage, particularly where specimen material was limited.

These problems indicated the need to increase the thickness of the specimen to improve integrity with the results obtained from this type of material. Subsequently, a dead weight penetrometer was designed with a daylight opening suitable for specimens up to 50 mm in thickness.

The Dead Weight Penetrometer is illustrated in Figure 2.11.

A correlation between uniaxial compressive strength and the NCB cone indenter index of certain rock types has been established by a number of workers in this

field and these will be discussed later. Szlavín, (1973). West, (1981) et al.

#### 2.4.5. The Schmidt Hammer.

The Schmidt Hammer rebound hardness tester was originally designed for non-destructive, in-situ testing of the quality of concrete through empirical relations to estimate the strength of 28 day old concrete cube specimens. Koblek (1958). The device is a lightweight hand held tool and has been widely used in a similar way to estimate the uniaxial compressive strength of natural rock material.

The Schmidt Hammer consists of a coil spring loaded, impact plunger contained in a housing. The plunger is placed horizontally against the rock mass and by pushing on the housing the impact spring is tensioned. When the plunger reaches a trip screw in the housing, the hammer is released and strikes the impact plunger with a prescribed energy. After impact, the hammer rebounds by an amount proportional to the hardness of the rock material, e.g. the harder the rock material under test, the higher the rebound value.

Schmidt Hammers, are available in basic models with differing impact energies.

The type 'M' model is intended for testing road concrete; type 'P' for concrete of low strength and type 'L' for testing small and impact sensitive parts of concrete. The 'N' type has been utilised to measure the compressive strength of coal measures rocks. Poole and Farmer, (1980)

The Schmidt Hammer is normally calibrated for horizontal impact testing on vertical faces. However, when using the device on horizontal or inclined faces, the rebound values must be corrected according to the following Table 2.6.

Frequent checks of rebound values against a testing anvil are recommended, during which the hammer is tested vertically downwards on a 16kg cylinder of hardened steel (Brinell hardness 500) and should give a reading of  $80 \pm 2$ .

The Schmidt Hammer is user sensitive and consequently, a number of techniques have been investigated with its use. Local experience has indicated the best results were obtained from the repeated rebound technique as recommended by Poole and Farmer. They studied both single and repeated impact techniques on data obtained from tunnel side walls. Considerable statistical analysis of the rebound data showed the results obtained from the repeated impact technique to be more consistent and repeatable when compared with the

Schmidt Hammer Model.

Hammer Type.	Impact Energy. (Nm)
M.	43
N	2.207
P	0.883
L	0.735

Table 2.6.

Rebound Value	Correction For Inclination Angle.			
	Upwards		Downwards	
	+90°	-45°	-45°	+90°
10	-	-	+2.4	+3.2
20	-5.4	-3.5	+2.5	+3.4
30	-4.7	-3.1	+2.3	+3.1
40	-3.9	-2.6	+2.0	+2.7
50	-3.1	-2.1	+1.6	+2.2
60	-2.3	-1.6	+1.3	+1.7

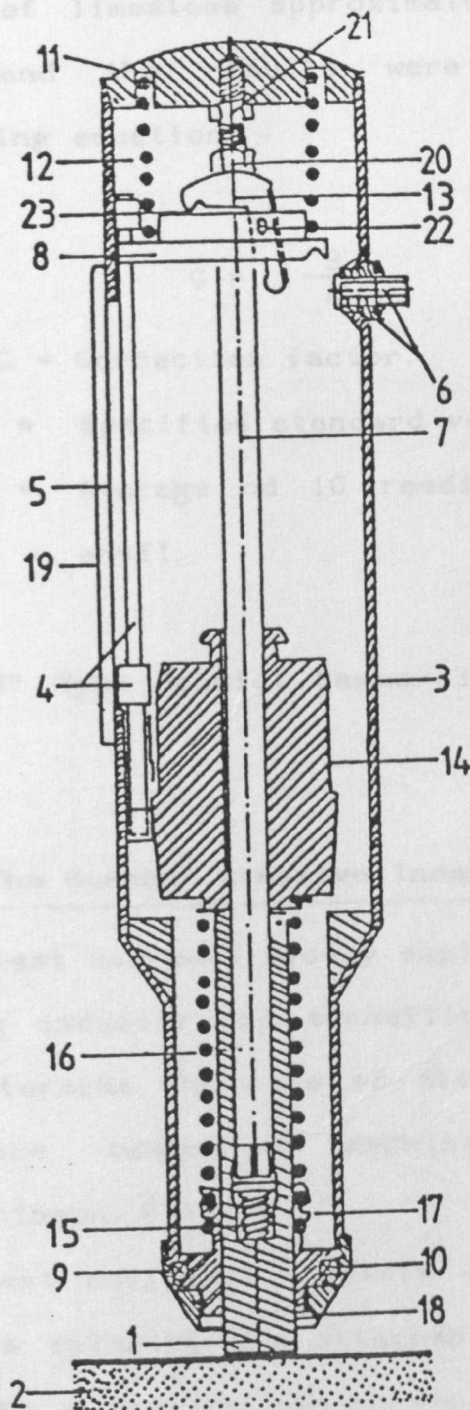
single impact technique. It is also recommended that 5 continuous impact readings be taken on the same spot prior to selecting the peak rebound value.

Schmidt Hammer rebound values have been correlated with uniaxial compressive strength by a number of workers, including Deere, (1965). Poole, and Farmer, (1980) et al.

Muftuoglu conducted a series of investigations carried out in ten coal mining tunnels on coal measures rocks representing various mining depths, geology and lithology during which the following conclusions were determined.

- a) The Schmidt Hammer tests gave an acceptably accurate assessment of rock strength range.
- b) Some difficulty was experienced in comparing the same rock type at different field sites.
- c) Schmidt Hammer tests conducted in the laboratory on rectangular specimens and bore-hole cores yielded much lower derived compressive strength values when compared with the conventional UCS values obtained from compression test machines by Singh, Hassani and Elkington (1982).

The Schmidt Hammer laboratory tests were conducted on a specially designed clamping arrangement with a vertical slide to ensure accurate alignment of the hammer. The device was securely bolted to a large



1. Impact plunger
2. Rock sample
3. Housing
4. Rider with rod guide
5. Scale
6. Push-button
7. Hammer guide bar
8. Disc
9. Cap
10. Two-part ring
11. Rear cover
12. Compression spring
13. Pawl
14. Hammer mass
15. Retaining spring
16. Impact spring
17. Guide sleeve
18. Felt washer
19. Plexiglass window
20. Trip screw
21. Lock nut
22. Pin
23. Pawl spring

Longitudinal Section of the Type N Concrete Test Hammer



block of limestone approximately one cubic metre in size and the results were calculated from the following equation:

$$C = \frac{S}{A} \quad (\text{Eq 2.2})$$

where C = Correction factor.

S = Specified standard value of the anvil.

A = Average of 10 readings on the calibration anvil.

The "N" Type Schmidt Hammer is illustrated in Figure 2.12.

#### 2.5 . The Cerchar Abrasive Index.

This test has been widely exploited by the French coal mining industry and tunnelling machine manufacturers to determine the rate of disc cutter replacement in fullface tunnelling machines, Des Lauriers and Broennimann. (1979).

The test equipment consists of a steel frame fixture with a swinging arm attached to a sliding bar which permits a precise and controlled lateral movement of 10.0 mm. At the extreme end of the swinging arm, a dead weight of 7.0 kg mass is attached and directly under this mass, a sharp pointed steel stylus is fixed in a holder. The stylus is manufactured from EN25 or

EN24 steel and is accurately heat treated to a precise hardness value of 610 Vickers hardness  $\pm 5.0$  Hv. The cone angle is  $90^\circ$  and is ground to an infinite point. The test specimen is prepared from rock sample material to sizes of about 25 mm x 25 mm x 50 mm. and the faces are accurately ground to a good surface finish. During the test, the specimens are firmly held in place under the stylus in an integral vice attached to the fixture and at least 5 tests are conducted on each specimen.

#### 2.5.1. Test Procedure.

The test procedure is simply conducted by positioning the specimen in the vice under the point of the stylus. The point of the stylus should always be examined under a microscope before each test to ascertain that there are no defects or existing flats. With the stylus held in place in its holder, the swinging arm is then carefully lowered until the point of the stylus comes into contact with the rock specimen. The test is carried out by the operation of a lever which moves the stylus over the surface of the rock specimen a controlled 10.0 mm under the normal load of 7 kgf. The abrasive index is derived from the diameter of the resultant wear flat.

The wear flat diameter is accurately measured on a

CERCHAR ABRASIVE TEST EQUIPMENT.

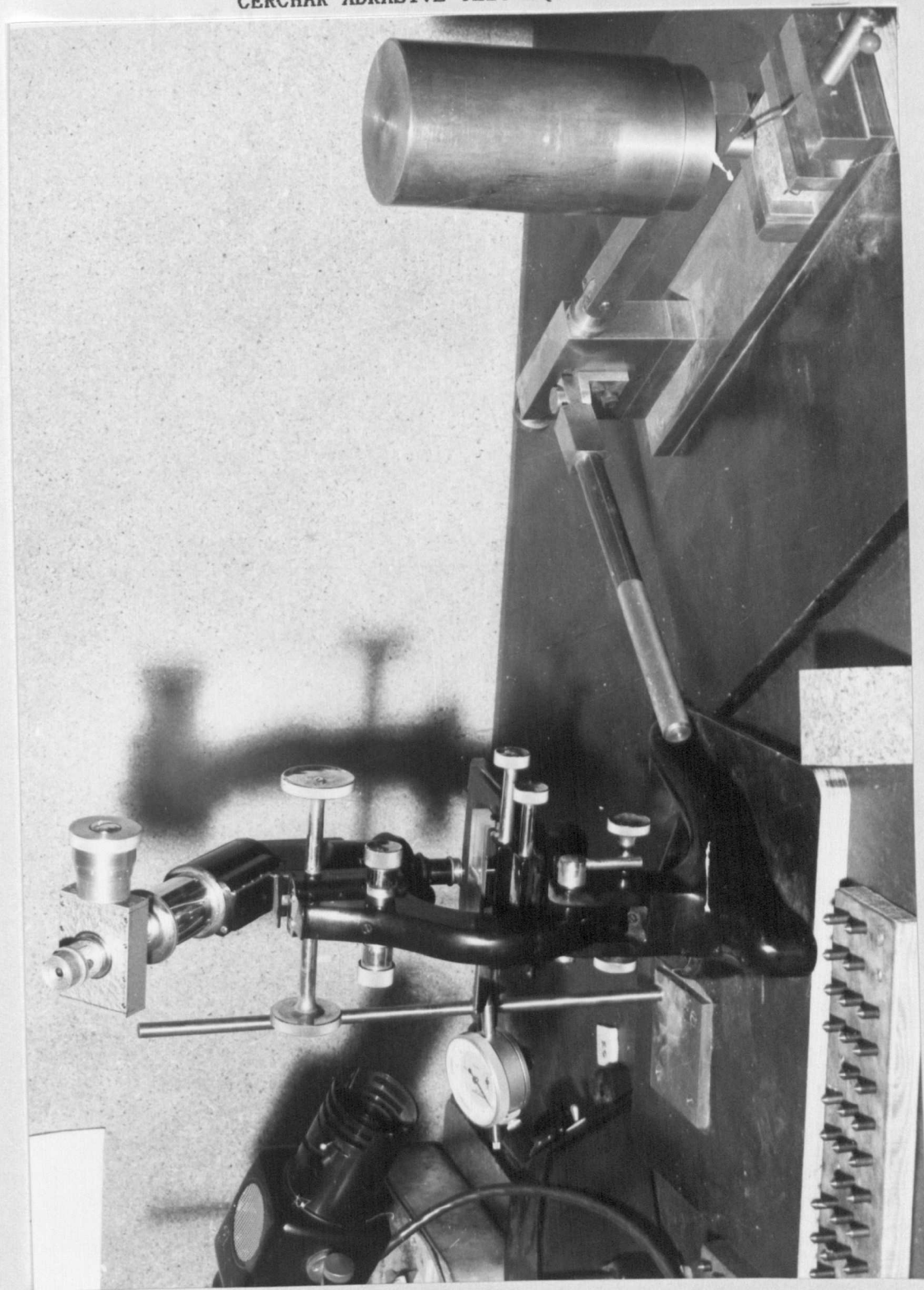


Figure 2.13.

travelling microscope to within 0.01 mm. A wear flat diameter of 0.1 mm is given as an index value of 1.0. Current classifications would suggest that a wear flat diameter of 0.4 mm equals an abrasive index of 4 and would be regarded as highly abrasive.

The accuracy of the test however, depends largely upon the accuracy of the heat treatment of the stylus in the initial stage and furthermore, the ability of the technician to maintain this hardness during the regrinding of the stylus.

Figure 2.13. illustrates the Cerchar abrasive measuring equipment together with the microscope and specimen material.

## 2.8. Conclusions.

It can be seen that though there are a great number of tests designed to determine the hardness and abrasiveness of rocks. Each of these tests have their own advantages and disadvantages depending on the rock type and condition and the mechanical processes involved. However, no single test can be used exclusively for this purpose. Each of the tests described can be used to give some indication to the degree of hardness or abrasiveness of rock. But their relationship to potential rates of wear or damage due to the interaction by some mechanical process, still

requires special purpose built test equipment, designed to simulate the actual processes involved, or ideally, a full scale test program. Alternatively, a multi-test system combined with some subjective judgement based on prior knowledge and experience should be employed. This latter method will be discussed later in this work.

## **CHAPTER 3.**

### **CORRELATION BETWEEN INDEX AND LABORATORY TEST RESULTS.**

## CHAPTER 3.

### CORRELATIONS BETWEEN INDEX AND LABORATORY TEST RESULTS.

#### 3.1. Introduction.

Laboratory tests were conducted to determine those physical properties which may be used to assess the interactive abrasive wear potential of rock material with mechanical mining processes and to attempt to find some useful correlations between the different tests carried out.

Many of these tests have previously been described in Chapters 1 and 2. The test procedures and specimen preparation must therefore, play an important role with the integrity of the results obtained and will require more detailed description.

It must be clear however, that sample material from which these rock specimens are produced, should be as closely representative to the rock mass in-situ as possible.

Rock sample material used for the production of laboratory test specimens are usually prepared from either, carefully selected cores from field drilling operations or from sample material collected from

underground or surface mining sites. In either case, this requires experienced and careful selection with regard to the test concepts and those problems associated with the economics and integrity of laboratory specimen preparation.

In many cases, the author has experienced the delivery of sample material for investigatory laboratory tests, which may have travelled many thousands of miles involving long periods of freight time. These include samples from India, Australia, America, South Africa and many other locations. In each case, the significance of careful sample selection and the preservation of sample condition must be regarded as of paramount importance to the test results obtained. Cassapi, (1983) and Atkinson and Cassapi (1983).

### **3.2. The Shore Scleroscope Hardness Test.**

Although the Shore scleroscope test was originally designed for the determination of the hardness of metals, it has been widely accepted as a reliable laboratory tool for the determination of rock hardnesses. (ISRM).

Figure 3.1. illustrates the essential components of the Shore Scleroscope.



SHORE SCLEROSCOPE.

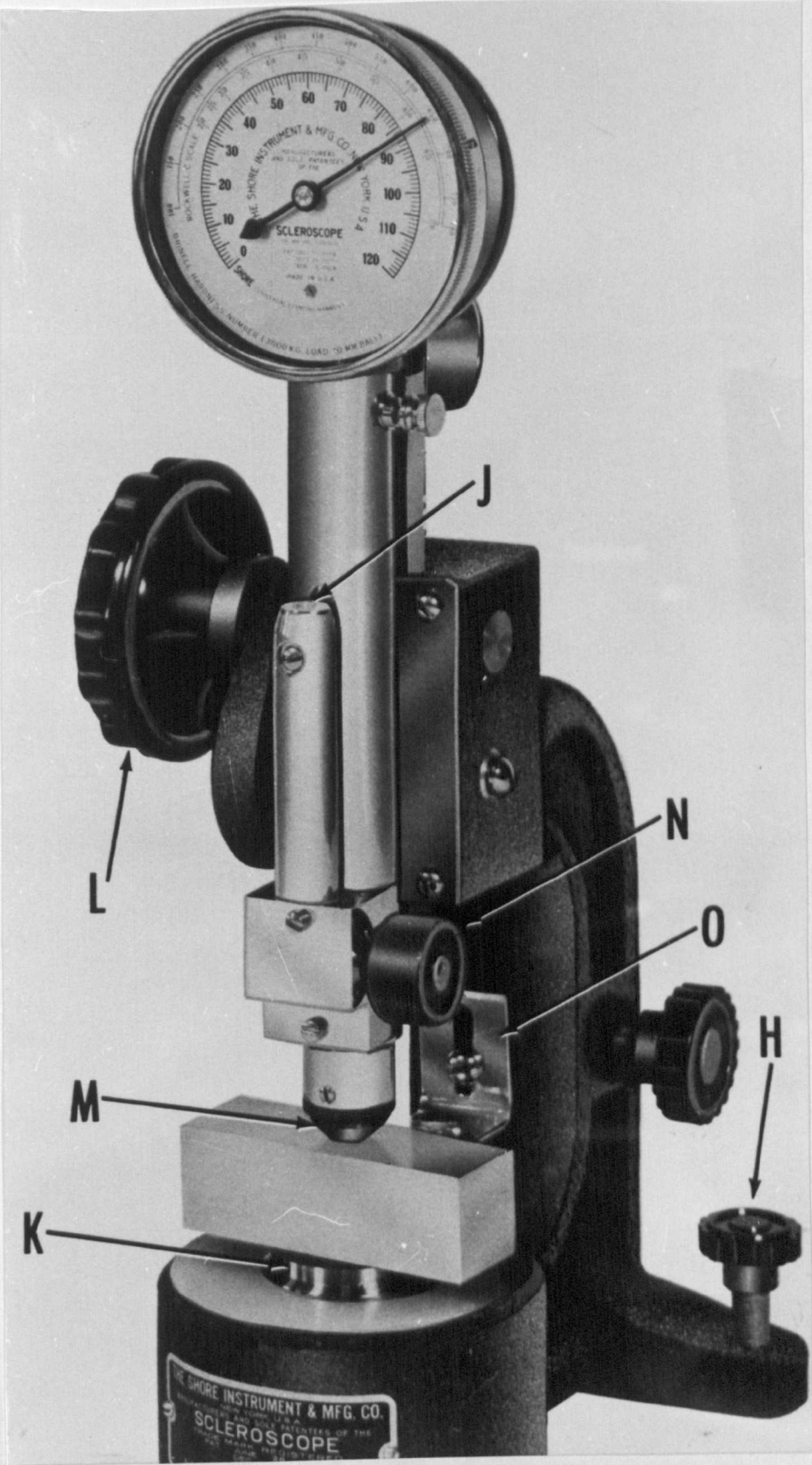


Figure 3.1.

### 3.2.1. Method of Operation.

The following procedures are recommended with its use when testing sample rock material:

- a) The instrument should be used on a sturdy bench to reduce vibration. It is also essential to ensure the instrument is set perpendicular by adjusting the two levelling screws (H) to coincide with the bubble spirit level (J) in order to minimise friction
- b) The scleroscope should always be checked before use to determine its accuracy. This is carried out with the aid of the two steel test blocks of known Shore hardnesses, one hard at 91-93 and one soft at 23-25 Shore hardness and one of these is shown in position. (see Figure 3.1.) Any deviation from the prescribed hardness indicated on the test block may result from incorrect setting up of the instrument, dirt or dust in the tube containing the hammer, user inexperience or possible damage to the instrument. If the readings correspond to those indicated on the test blocks e.g. 23-25 and 91-93 respectively, the instrument is ready for use.
- c) The operation of the instrument is carried out by the following method:

The specimen is placed between the anvil (K) and the tube (M) the tube can then be lowered onto the specimen by rotating the clamping knob (L). A steady pressure should be maintained throughout the test. The hammer is set and released by the control knob (N), and the resultant rebound height is automatically recorded on the dial gauge.

This latter part of the operation often requires the acquisition of some elementary skills in operation, it is therefore, advisable to practice in the first instance with the test blocks or similar reference pieces before resorting to actual tests on rock specimens.

### **3.2.2. Specimen Preparation.**

The standard of preparation of rock specimens for Shore Scleroscope hardness tests can significantly affect the integrity of the test results. The ISRM recommend that specimens should be at least 12 mm thick with a ground surface finish of not greater than 125 microns. The surface area of the specimen should be at least sufficient to make a minimum of 20 measurements and the numerical mean of these are then given as a measure of the whole rock hardness.

Test readings therefore, should be made at a spacing distance of not less than 6 mm from the preceding test

point. Tests made on the same point will result in higher than normal readings due to a work hardening effect directly beneath the hammer.

From practical experience , the author has found that the best results have been obtained from specimens with a rectangular shape of 25 x 25 x 50 mm so that measurements can be made orthogonally and at least 100 points can be measured. Further, a consistently good surface finish can easily be obtained by lapping the relevant surfaces on a lapping machine normally employed with thin section preparation of rock.

### **3.2.3. Interpretation of results.**

Because the Shore Scleroscope is basically a dynamic rebound test and as such, measures the elastic properties of the material, the results obtained therefore, may be affected by surface finish. This implies that a coarse surface finish with specimen preparation will give rise to erratic and generally lower readings than expected. The provision of this quality of surface finish sometimes presents problems with weakly cemented rocks. This could be because the bonding of the cementing material is not sufficiently strong enough to contain the constituent minerals during the preparation process. This may result in the plucking of individual mineral grains, thus producing,

consequential voids. Furthermore, because in practice a truly homogeneous rock does not exist, the results obtained may be affected by grain size, hardness and the degree of which the cementing material binds the mineral constituents.

The Shore scleroscope hardness numbers reflect the hardness of all the constituents within the rock specimen, thus, if sufficient tests are made on each specimen, a mean hardness for the whole rock can be obtained. It can be shown that fine grained rocks are much more amenable to this type of hardness test. This is made manifestly clear by the level of scatter with the test results obtained. However, certain rock types such as some igneous granites often possess large grains of minerals of varying size, shape and hardness. These may reach up to >15mm in size and the Shore hardness results obtained from these rocks, more often reflect this phenomenon. However, these properties of hardness, elasticity, mineralogy and the degree of cementation are of importance when considering the prediction of the abrasiveness of rocks and their subsequent wear potential on machine tools and other equipment associated with the cutting, processing or excavation of rock materials.

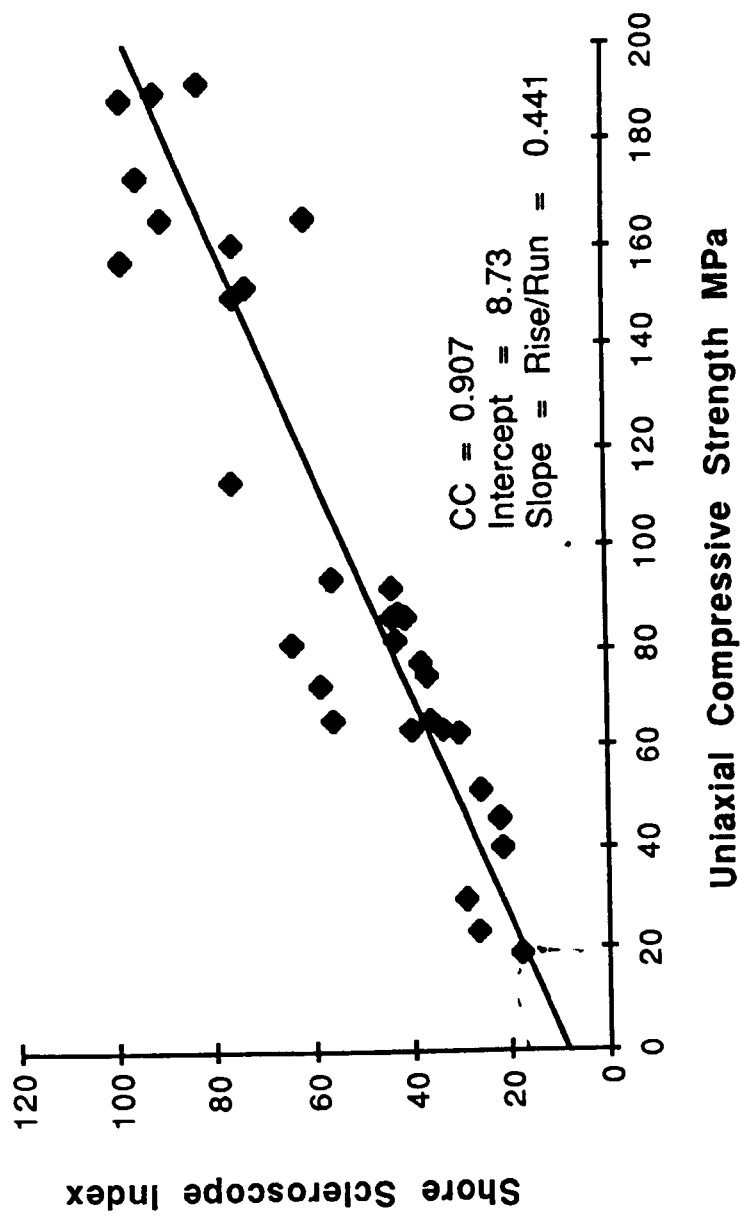


**Fig. 3.2**

#### 3.2.4. Correlation of Shore Hardness with Strength.

A correlation between Shore hardnesses and unconfined compressive strength has been established with a number of different rock types and in many cases, "especially those rocks of a fine grain competent nature", this means of determining rock hardness can be used to derive an adequate assessment of the physical strength properties of rocks also. This is especially significant where the available amount of specimen material will not provide sufficient cores for conventional compressive strength tests. Furthermore, because the Shore scleroscope is a non-destructive test, this permits other tests to be carried out on the same sample material, thus enabling maximum data to be extracted from limited supplies of sample material.

The correlation graph illustrated in Figure 3.2. shows the results obtained from a range of rock types which vary from standard British coal measures to hard granites. These rocks are all relatively of a competent nature with a grain size ranging from  $<0.05\text{mm}$  with the UK coal measures rocks to  $>15\text{mm}$  with some of the granites from Italy. At least 100 determinations were made with each rock type and the statistical numerical mean of these are determined to constitute a single point on the graph. A correlation

Table 3.1.

Rock Type	Specific Wear mm/m <sup>2</sup>	Shore Hardness
Red Granite	0.204	99.5
Grey Granite	0.129	93.9
Red Granite	0.124	94.1
Gabbro	0.085	84.3
Pink Granite	0.064	88.2
Larvakite	0.055	82.6
Diorite	0.030	81.1
Sandstone	- 0.019	52.8

After Cassapi, V.B. and Wright, D.N. (1985)



coefficient of 0.907 was found and assumed to be useful for general geotechnical engineering purposes. This usefulness was highlighted with wear tests on diamond saw blades cutting the hard granites. These tests were conducted at DeBeers R&D laboratories at Ascot England, (see Chapter 5.) and indicated that the high wear rate of diamond saws could be associated with hardness determined by the Shore scleroscope. Thus a useful prediction of tool wear could be made and subsequent alteration to diamond type, concentration and matrix material hardness could be adopted to improve cutting performance and reduce the wear rate of expensive diamond saws.

Table 3.1. Illustrates the relationship of Shore hardness values with specific wear.

### 3.3. The NCB Cone Indenter.

The NCB cone indenter is described in detail in Chapter 2. and was specifically designed by the National Coal Board's Research Establishment at Bretby as a rock hardness tester. It is however, a derivation of the Vickers or Brinel hardness testers and measures hardness as a function of residual penetration by a cone under a predetermined load.

The cone indenter hardness values for any particular test is obtained by dividing the applied force (i.e. the spring deflection) by the amount of residual penetration that has occurred. Thus, the cone indenter hardness number can be calculated from the following equation.

$$(3.1) \quad I = \frac{D}{P}$$

Where D = Nominal deflection of the steel strip.

P = Penetration of the cone. (mm).

#### 3.3.1. Inspection of the Cone Indenter.

Before use, the tungsten carbide cone should be inspected and checked under a microscope for damage or wear to the point. The point of the cone should be free of damage and the radius at its tip should measure 0.10 mm, plus or minus 0.025 mm and it should be free to rotate in its housing on a suitable single

ball bearing pivot.

The deflection of the spring leaf should be checked against a dead weight calibration for each of the three prescribed forces i.e. 0.23 mm deflection for 12 N, 0.635 mm for 40 N and 1.27 mm for 110 N.

The procedures for this calibration are as follows:

- 1) Remove the cone and micrometer thimble from the frame.
- 2) Set the frame in the vertical position and insert the spindle of the carrier for the calibration weights through the micrometer barrel so that the spherical end of the spindle comes into contact with the spring leaf.
- 3) Place the appropriate weights on the carrier and check the deflection indicated on the dial gauge coincides with the prescribed deflection.
- 4) If the deflection does not closely match the suggested values, the mounting of the steel strip should be examined and minor adjustments can be made by adjusting the tightening tension of the mounting screws. If this is not possible, the spring leaf should be dismantled and replaced with a new spring.

If the instrument is in constant use, these checks should be carried out at regular intervals, or at any time after a series of spurious results have been recorded. This is of importance with the detection of

possible degradation of the cone point specifications; otherwise, this procedure should be carried out each time before use.

Figure 3.3 illustrates the calibration setting position of the NCB Cone Indenter.

### 3.3.2. Specimen Preparation.

The NCB Cone Indenter was developed as a portable rock hardness tester and is used for giving a measure of rock hardness or for accurately shaped tapered specimens. However, the better engineering practice is to use a test that does not require the use of a portable hardness tester. The author has used a portable hardness tester for the purpose of quality control of rock specimens and has found that the results are not reliable. The author has also used a portable hardness tester for the purpose of quality control of rock specimens and has found that the results are not reliable. The author has also used a portable hardness tester for the purpose of quality control of rock specimens and has found that the results are not reliable.

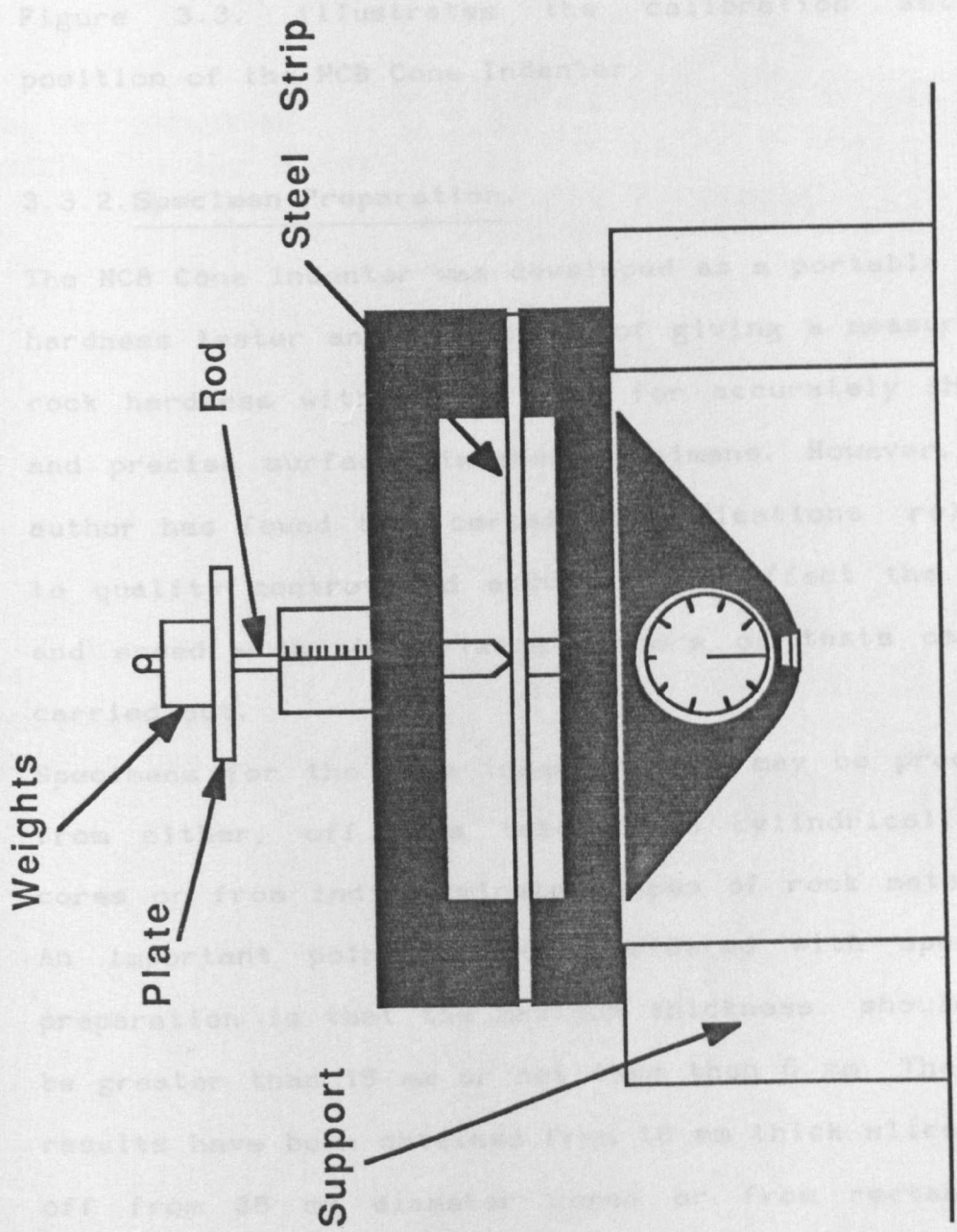


**Fig 3.3**

possible degradation of the cone point specifications, otherwise, this procedure should be carried out each time before use.

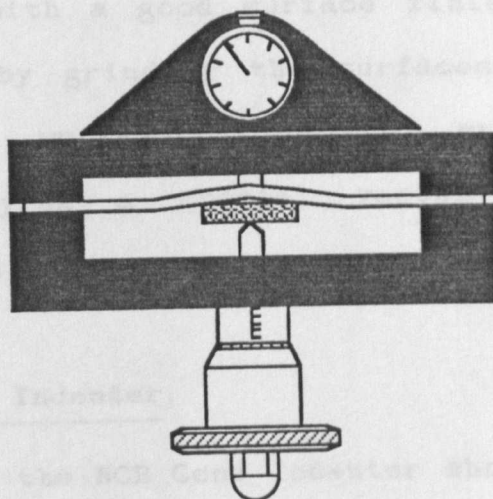
Figure 3.3. illustrates the calibration setting position of the NCB Cone Indenter.

### 3.3.2. Specimen Preparation.

The NCB Cone Indenter was developed as a portable rock hardness tester and is capable of giving a measure of rock hardness without the need for accurately shaped and precise surface finished specimens. However, the author has found that certain specifications related to quality control and accuracy can affect the ease and speed with which large numbers of tests can be carried out.

Specimens for the cone indenter test may be produced from either, off cuts taken from cylindrical rock cores or from indiscriminate shapes of rock material. An important point to be considered with specimen preparation is that the maximum thickness should not be greater than 15 mm or not less than 6 mm. The best results have been obtained from 10 mm thick slices cut off from 38 mm diameter cores or from rectangular pieces of about 25 mm x 25 mm x 10 mm. Although parallelism is not essential to the integrity of the test results,

**Not recommended  
(loading in the middle)**



**Recommended  
(loading near the edge)**

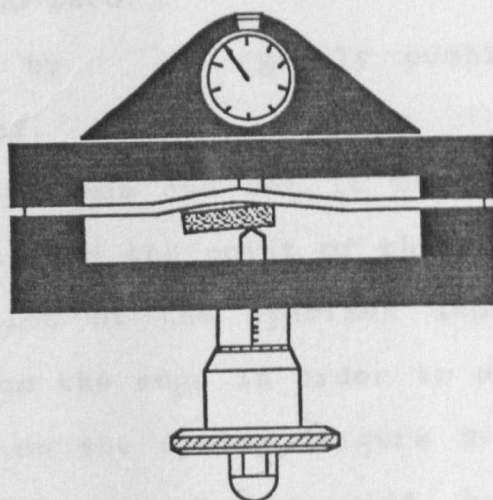


**Fig 3.4**

measurements can be made significantly faster when the specimen thickness is uniform and parallel. Parallelism together with a good surface finish can easily be achieved by grinding the surfaces on a standard engineering workshop, surface grinding machine, while employing a special vacuum chuck mounted on a magnetic table.

### 3.3.3. Use of the Cone Indenter.

The test procedure for the NCB Cone Indenter should be carried out in the following manner:

- 1) Set the dial gauge to zero.
- 2) Check the movement by gently pushing on the spring steel leaf.
- 3) Select a rock specimen and set it between the spring steel leaf and the point of the indenter cone. The position of the specimen should be about 4-5 mm from the edge in order to avoid a bridging effect on the spring. Figure 3.4. The micrometer is then screwed down until the cone indenter point just supports the specimen. Reset the dial gauge to zero if necessary.
- 4) Note the micrometer reading  $M_0$ .
- 5) Rotate the micrometer clockwise until the spring deflection indicated on the dial gauge is 0.635mm,

equivalent to a load of 40N for the standard cone hardness indenter number.

6) Note the second micrometer reading  $M_1$ ,

The penetration of the cone (P) can then be calculated from:

$$(3.2) \quad P = (M_1 - M_0) - D_1$$

The standard cone indenter hardness number is calculated from:

$$(3.3) \quad I_s = \frac{0.635}{P}$$

In the case of some strong and hard rocks, the penetration of the cone may be less than 0.13 mm and consequently, the recommended load should be increased to 110N, which is equivalent to a spring deflection of 1.27 mm. The author has found that measurements taken with both 40N and 110N loads can be recorded at the same time with little extra effort and the results compared. This can be a useful exercise when the penetration of the cone under a 40N load is marginal. Conversely, with weak and friable rocks, the cone penetration at 40N may be so deep as to cause fracture at the point of contact, therefore, in these circumstances it is recommended that the normal load of 40N be reduced to 12N, equivalent to a spring deflection of 0.23 mm.

Because the spring deflection for the instrument represents the force required to produce sufficient



residual penetration into the rock, three different deflections may be used to determine rock hardness and any one or more of these may be chosen, depending upon the descriptive strength or hardness of the rock specimen.

The cone indenter hardness numbers are derived from the following equations:

$$(3.4) \quad I = \frac{D}{\text{Penetration}}$$

Where D = Spring deflection (= applied force)

For weak rocks:

$$(3.5) \quad I_w = \frac{0.23}{\text{Penetration.}}$$

$$D = 0.23 \text{ mm.}$$

For average strength rocks:

$$(3.6) \quad I_s = \frac{0.635}{\text{Penetration}}$$

$$D = 0.635 \text{ mm.}$$

For high strength rocks:

$$(3.7) \quad I_m = \frac{1.27}{\text{Penetration}}$$

$$D = 1.27 \text{ mm.}$$

#### 3.3.4. Uniaxial Compressive Strength v Cone Indenter.

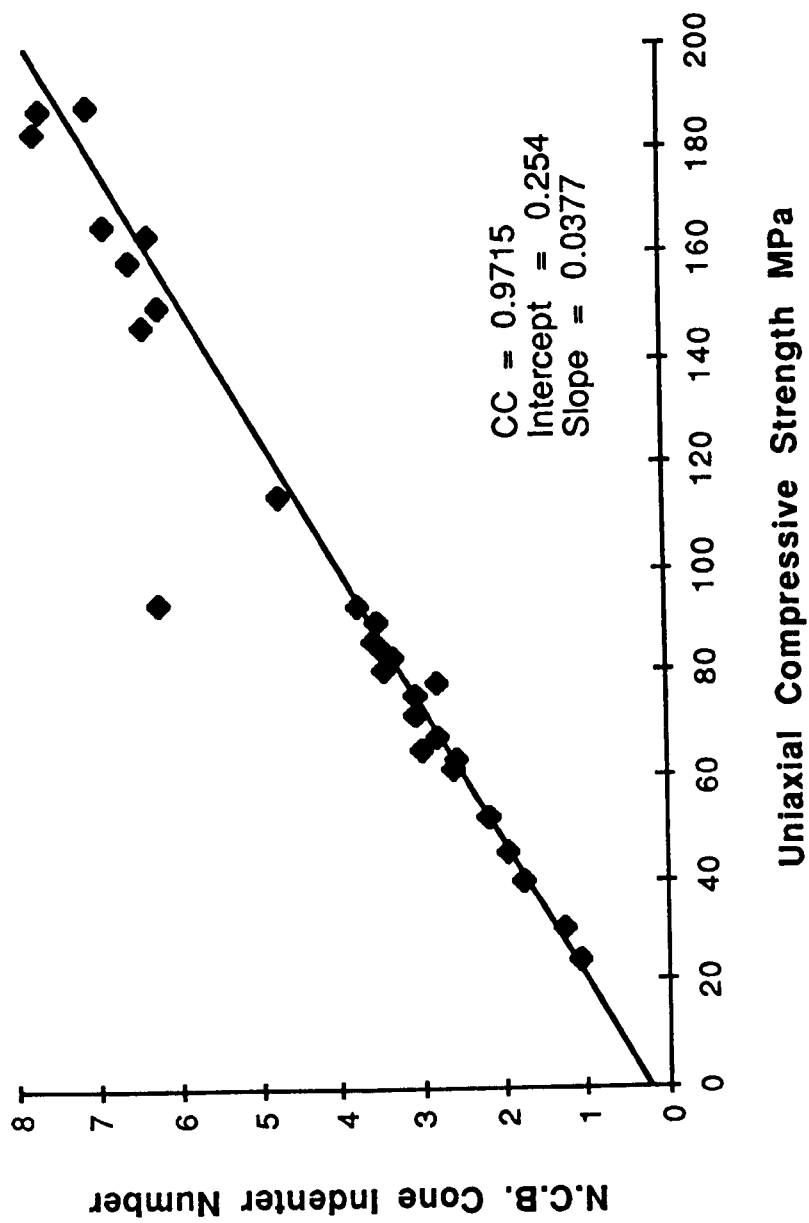
A good correlation between the NCB Cone Indenter hardness index and uniaxial compressive strength has been established by a number of workers already mentioned in Chapter 2. The author has conducted cone

Table 3.2.

Cone Indenter Index vs UCS

C. I.,	UCS MPa	Derived UCS	% Deviation [ (Y'-Y)/Y ] x100
2.52	65.26	62.58	-4.1
3.35	82.59	84.37	2.2
2.91	66.64	72.82	9.3
3.49	89.85	88.05	-2.0
2.93	76.21	73.35	-3.8
1.73	40.77	41.84	2.6
2.55	63.58	63.67	-0.3
1.93	45.32	47.09	3.9
2.74	79.41	68.36	-13.9
2.95	65.99	73.87	11.9
(x)	(Y)	(Y')	

$$Y' = 26.25 x - 3.57$$



**Fig. 3.5**

indenter hardness tests on more than 1700 different rock specimens, representing 25 different rock types from many different locations throughout the world. (These are referred to in a later Chapter).

The test programme has shown the NCB Cone Indenter to be a reliable laboratory tool for the determination of rock hardnesses in addition to the derivation of other strength parameters.

The resulting correlation coefficient of 0.941 for this relationship is significant and details of this are presented in the following Table 3.2. Szlavín (1974) studied the same relationship for a number of U.K Coal Measures rocks, found an equation with a correlation coefficient of 0.880. his equation ( $Y' = 20 X + 12.4$ ) differs slightly from the authors.

The correlation graph presented in Figure 3.5. was compiled from 23 different U.K. Coal Measures rocks and 8 Italian granites. The correlation coefficient of 0.9715 is significant when consideration is given to the wide range of mineralogy and grain size. These sizes ranged from <0.5mm in the coal measures to >15mm in the granites.

**PAGE  
MISSING  
IN  
ORIGINAL**

### 3.4. The Modified Cone Indenter. (MCI).

The NCB cone indenter cannot be used with any degree of confidence when testing very weak and friable rocks, where the author encountered problems with certain rock types in the G4 (cemented soil) and R1 (weak rocks) range of the GS scale. This was evident when even under the lowest possible load of 12N, the penetration of the cone was so deep as to cause failure at the point of contact with the rock specimen. The main cause of this failure could be attributed to the limitations placed on specimen thickness due to the available space between the spring steel leaf and the point of the cone.

These problems indicated the need to increase the thickness of the specimens beyond the capacity of the standard cone indenter, e.g. 15 mm. Subsequently, a modified dead weight cone indenter was designed with a facility to accept specimens of up to 50 mm thick.

The modified cone indenter is illustrated in Figure 2.11.

The main features illustrated, show a sturdy steel framed fixture with a dead weight carrier mounted on a steel spindle. Stability and friction free movement of the spindle and carrier plate is provided by two linear ball bearings housed in the top bracket of the

frame and the cone is mounted in the lower end of carrier spindle. A thumb screw operated lever supports the cone and weights which can be precisely lowered onto the specimen. The specimen is supported on the platen of an adjustable screw jack and a spot level spirit bubble is fixed to the top bracket to enable the fixture to be accurately levelled before use.

Penetration of the cone is measured by the use of a standard dial gauge indicator of 0.02 mm increments. The dial gauge is mounted on a rigid steel post by an adjustable knuckle clamp. This provides for easy positional changes in height with any of the three dead weights of 12 N, 40 N or 110 N respectively.

#### 3.4.1. Specimen Preparation.

Because the Modified Cone Indenter (MCI) was designed specifically as a laboratory tool and cannot be regarded as a portable instrument in the same way as the NCB Cone Indenter, the specifications for the preparation of rock specimens demands a high degree of quality control with regard to surface finish and accuracy of parallelism. Therefore, the surfaces of the test specimen should be ground and lapped parallel to each other. The MCI however, can accept specimens of varying thicknesses ranging from 10 mm to 50 mm.

### 3.4.2. The Use of The Modified Cone Indenter.

The MCI rock hardness test is carried out in the following manner:

- 1) The instrument should be set vertical by use of adjustable feet screws and spot level.
- 2) Select the relevant weight, place and locate over the spigot on the top of the carrier plate.
- 3) Position the dial gauge indicator over the weight so that its probe is in contact with the ground face of the weight and secured by the knuckle clamp.
- 4) Place the specimen on top of the screw jack platen and adjust both position and height within close proximity to the point of the cone.
- 5) Adjust the thumb screw of the lever supporting the weight to lower the spindle and cone indenter point to lightly interfere with the rock specimen.
- 6) Set the dial gauge indicator to zero.
- 7) Lower the weight onto the specimen until the dial gauge has reached its limit of movement.
- 8) Read the dial gauge to within the limits indicated, e.g. 1.2 mm +/- 0.02 mm.

The index  $I_m$  is derived from:

$$1.2 - 0.635 = 0.565$$

$$\text{Then } I_m = 0.635 / 0.565 = 1.123$$



The MCI index is given as equivalent to the standard NCB Cone Indenter hardness number.

Providing the accuracy with parallelism is maintained during specimen preparation, large numbers of tests can easily and speedily be made without the need to reset the dial gauge indicator.

In addition to being able to test specimens of much greater thickness, the MCI index has the added advantage of being a true force/penetration ratio, furthermore, the results do not require the tedious processing associated with the NCB Cone Indenter, therefore, the method of testing is relatively easier, quicker and because measurements are made from a single dial gauge indicator, are generally more accurate.

### 3.5. The Cerchar Abrasive Index Test.

The Cerchar abrasive test has been extensively used by the French Coal Mining Industry and by tunnelling machine manufacturers. Des Lauriers and Broennimann (1979) reported good correlation with the rate of disc cutter replacements in full face tunnelling machines with the Cerchar abrasive index.

The equipment consists of a steel frame fixture with a hinged swinging arm attached to a sliding bar which permits a precise and controlled lateral movement of

10 mm. At the extreme end of the swinging arm, a dead weight of 7 kg mass is attached and directly below this mass, a sharp pointed steel stylus is fixed in a holder. The styli are manufactured from EN24 or EN 25 alloy steel and are heat treated to 610 VHN  $\pm$  5 VHN. The styli have a cone angle of 90° inclusive and are accurately ground to an infinite point.

The rock specimens are prepared from sample material by cutting to blocks of approximately 25 x 25 x 50 mm and are ground to a good surface finish. During the test, the specimens are firmly held in place directly under the stylus by means of an integral vice attached to the base plate of the fixture.

#### 3.5.1. Test Procedure.

Before a test takes place, the point of the stylus is closely inspected under a microscope to ensure that it meets the specifications required. e.g. an infinite point.

With the stylus installed and the specially prepared specimen held firmly in place below the stylus, the face of the rock specimen is scratched over the precisely controlled distance of 10 mm and under the normal load provided by the 7 kg mass. The abrasiveness of the rock is determined by the resultant wear flat generated at the point of the

stylus, measured on a travelling microscope. The unit of abrasiveness is defined as a wear flat of 0.1 mm = 1. A wear flat diameter of 0.4 mm equals a Cerchar abrasive index of 4.0 and would be regarded as a highly abrasive rock material.

The accuracy of the test depends largely on the accuracy of the heat treatment to the stylii and ability of the technical support services to maintain the hardness limitations when regrinding the stylii points after use. The Cerchar abrasive equipment together with stylii, microscope and specimen material are illustrated in Figure 2.13. of Chapter 2.

Some typical examples of abrasiveness of rocks determined by the Cerchar abrasive index test are given as follows:

**THE CERCHAR ABRASIVE INDEX OF ROCKS.**

ROCK MATERIAL.	CERCHAR INDEX.
Limestone	0.2 - 1.2
Conglomerates	1.0 - 1.8
Schists	1.4 - 2.0
Portland sandstone	1.5 - 2.5
Californian granite	3.0 - 3.5
Dolorite	3.0 - 3.5
Diabase and granites	3.0 - 4.2
Bio-cordierite gniess	4.0 - 4.6
Pennant sandstone	4.5 - 5.0

### 3.6. Conclusions.

The tests described in this chapter have all proven to give reliable results within certain limitations. In addition, good correlation between these tests and other physical properties have been found by a number of workers already mentioned. These correlations with uniaxial compressive strength have been very useful, especially when supplies of sample material have been limited.

The NCB cone indenter for instance, can provide important indications of hardness and strength parameters with very little specimen preparation and from relatively minute sample material. This makes it a very useful tool for field testing of site gathered material.

The Shore scleroscope is a more sophisticated laboratory test which requires precise specimen preparation. However, a great many tests can be made on each specimen and because the test is non-destructive, other tests can be carried out on the same specimens used for other tests.

The Cerchar abrasive test was specifically designed to predict the rate of disc cutter wear on full face tunnelling machines and has been widely accepted by a number of tunnelling machine manufacturers for this

purpose. Manufacturers of boom tunnelling machines using either forward attack or point attack picks in the cutting head, also appear to favour this test and although the author has had long associations with manufacturers of these types of tunnelling machines, it has been difficult to acquire corroborative evidence to justify the confidence which manufacturers place on this test.

The author has found that, results obtained from the Cerchar test often correlate well with the percentage of hard minerals present, but the results appear to be affected significantly with increased grain size. Grain size appears to be a factor of some significance with the other two tests also. The major difference being, that a greater number of test determinations can be made with both the NCB cone indenter and the Shore scleroscope with little extra effort or expense. This can be qualified by the costs involved with the manufacture and servicing charges for the Cerchar styli:

Current cost of manufacture: £350.00 per 100 styli.

Servicing e.g. resharpening: £125.00 per 100 styli.

Service life. approximately: 10 tests.

Thus, it can be seen that the cost per test for the styli alone could amount to £1.60, and with a minimum of 5 tests per specimen, this would amount to £8.00.

## **CHAPTER 4.**

### **DIAMOND CORE BIT WEAR CHARACTERISTICS.**

## CHAPTER 4.

### DIAMOND CORE BIT WEAR CHARACTERISTICS.

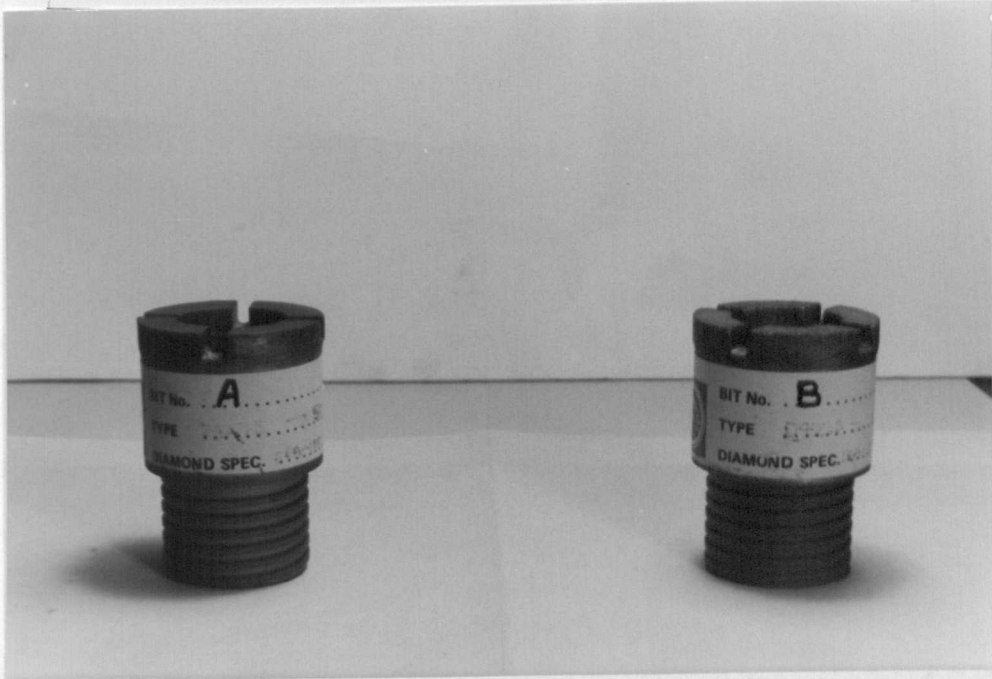
#### 4.1. Introduction.

Diamond core drilling is still one of the most reliable and accurate means of gaining information about the extent of valuable ore bodies and minerals underlying the earth's surface. For this reason, it is imperative that new and more economical drilling methods are devised and the tendency towards slim-hole diamond core drilling is now common practice.

While it is true to say, that slim-hole core drilling techniques using NX (52mm diameter core drills) are much faster than previously exploited 175mm diameter exploration core drills, the rate of wear is, in many cases, very high. This has led to greater efforts by the diamond core bit and drilling machine manufacturers to provide equipment that give better all-round improved performance.

The application of computers to drilling has already occurred with automatic rod handling and drill positioning which has led to dramatic reductions in production costs. However, the application of

**Diamond Impregnated Core Bits.**



**Core Bit "A"**

Diamond size:

D/427, 40/50 US Mesh

Diamond Type: SDA100

Concentration: 40

Matrix 70% Tungsten

30% Copper

**Core Bit "B"**

Diamond Size:

D/427, 40/50 US Mesh

Diamond Type: SDA100

Concentration: 45

Matrix 70% Tungsten

30% Copper

Figure 4.1.



computers to the study of wear problems associated with diamond core bits has not received proportional attention and consequently, the choice and style of core bit is still a matter of subjective judgment, often based on experience which may or may not be reliable.

This chapter outlines a series of drilling trials on diamond impregnated bits, to ascertain optimum drilling parameters in relation to penetration rates and total bit wear with distance drilled.

A computer monitoring system was designed to measure and record the relevant drilling parameters and to present an on-going and instantaneous VDU display of events as they occur during the actual drilling trials. In addition to these facilities, a computer controlled bit wear measuring jig was also designed to allow accurate wear measurements of the bit profile to be made with distance drilled. This scheme allowed a study of the effects of changing drilling parameters, the near optimisation of these parameters together with a study of the mode of bit wear taking place.

Two diamond impregnated core bits of a new design concept were supplied by a well known drill bit manufacturer and are designated core bit "A" and core bit "B", these together with their technical specifications are illustrated in Figure 4.1.

ROCK DRILLING MACHINE WITH MICRO-COMPUTER

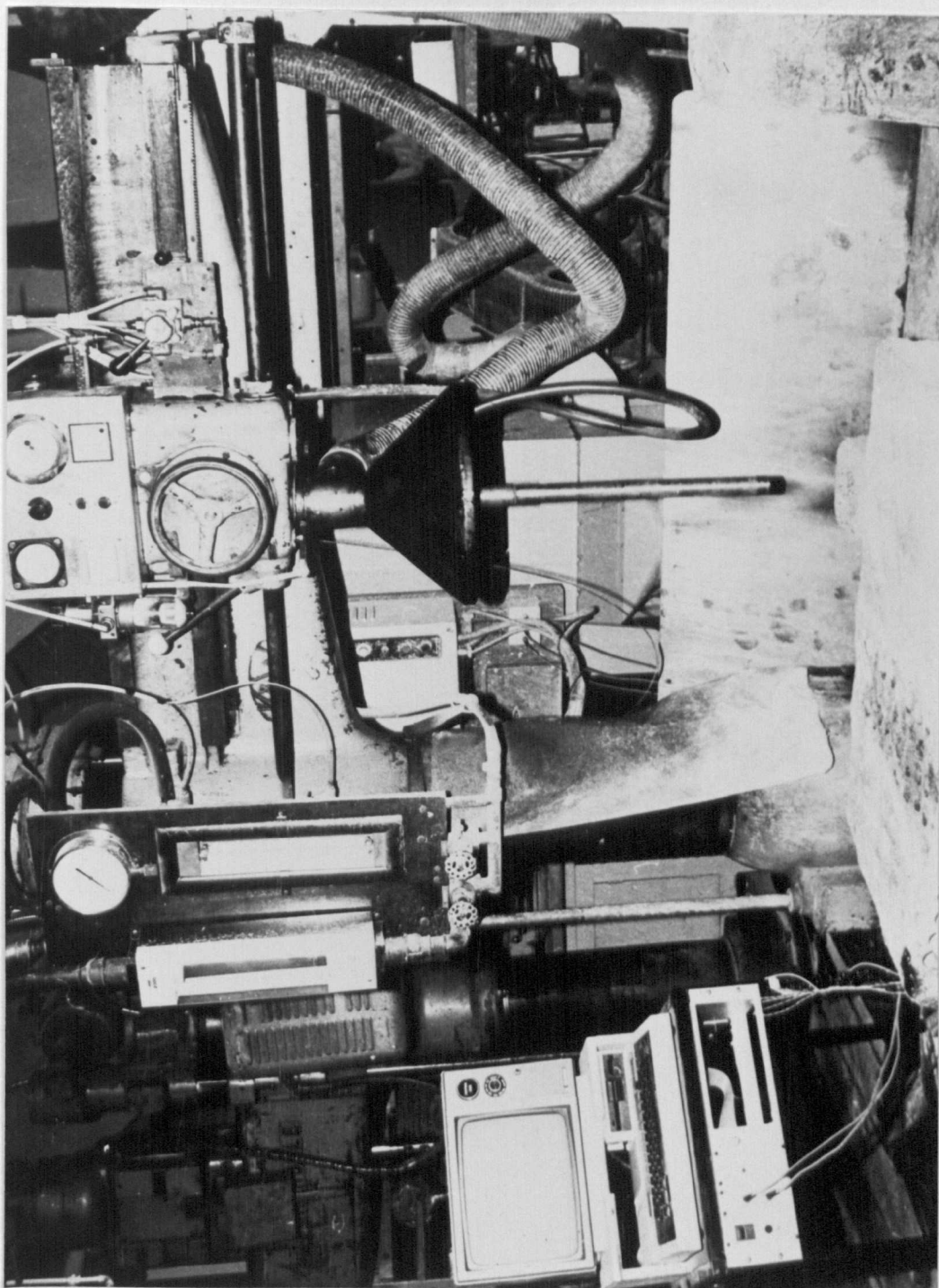


FIG 4. 2

In addition to the drilling test programme, a number of physical property tests together with a study of the petrological analysis of thin sections were conducted on the sample rock material and an attempt made to correlate the results with the bit wear characteristics.

#### 4.2. The Core Drilling Machine.

The machine used for these test trials is illustrated in Figure 4.2. together with the micro-computer used to monitor the output from the various facilities provided by the machine. The machine was a converted Kitchen & Wade radial arm, engineering workshop drill and had been specially modified for core drilling duties. The modifications consisted of the provision of a constant loading device to the drill spindle, which replaces the normal geared feed system. An infinitely variable speed system within the range 0-2000 rev/min was also provided together with a number of special modifications designed to reduce vibration within the machinery.

In addition to these modifications, adequate visual instrumentation was included to pre-set and maintain the principal drilling parameters:

- a) Load on the bit.

- b) Rotational speed,
- c) Flush rate. (water or air).
- d) Current.
- e) Voltage.
- f) Penetration indicator.

#### 4.2.1. Resume of Previous Work.

The original modifications to the drilling machine were carried out to improve the quality and production of cores extracted from sampled friable material. This type of material, such as coal, seat earth, mudstone etc. was always regarded as particularly difficult material from which to produce good quality test specimen cores. Futhermore, the production of cores from these rock materials was of great importance, since these represented the range of rocks requiring the most intensive investigation.

The monitoring of the drilling parameters was at that time, conducted by visual observation of the gauges provided to preset and control load on the bit and water or air flush flow rates. Penetration rates and subsequent bit performance was determined by use of a stop watch and tape measurements of distance cored.

Bit design was also considered important and a number of different core bits were investigated to determine the effects of diamond type, concentration and matrix

material on penetration rates, wear rates and core production. These modifications are described in greater detail elsewhere. Cassapi, (1983) and Atkinson and Cassapi (1984).

It became evident however, that if drill bit performance was to be investigated in greater detail, then a more sophisticated method of data acquisition and data analysis would have to be provided.

#### 4.3. The Monitoring System.

The principal parameters to be measured on the test rig may be summarised as follows:

- |                     |         |
|---------------------|---------|
| 1) Flush rate       | l/min   |
| 2) Torque           | Nm      |
| 3) Speed            | rev/min |
| 4) Load on the bit  | kN      |
| 5) Penetration      | mm      |
| 6) Penetration rate | mm/min  |
| 7) Bit wear         | mm      |

The monitoring system developed to enable these measurements to be made was based on a micro-computer linked via signal conditioning units with appropriate transducers. The following sections outline the measuring techniques used for the indicated parameters.

#### 4.3.1. Flush Rate.

The flow of either air or water to the swivel and subsequently the drill bit is regulated by standard gate valves. An in the line rotameter with a range of 0-30 l/min for the water flush system and a manometer in the range of 0/150 l/min of air for none aqueous flush media gave indications of flush flow rates. Turbine flow meters were considered for the monitoring system, but because of the required dual flush system, no single device of this kind could be identified, however, a single orifice plate and differential transducer was capable of covering the required ranges of both flush media. Therefore, a 12.5 mm orifice plate placed in a straight section of 25.4 mm diameter steel pipe and fed to the swivel via a flexible hose was employed. The pressure difference, in the range 0-500 pascals was measured using a semiconductor pressure transducer and mercury and oil snubbers were used to overcome the transducers incompatibility with water. The transducer was energised with 24 Vdc and produces an output in the range 0.7 to 10.7 volts which was fed to the logging system.

#### 4.3.2. Rotational Speed.

The drill rig motor was already equipped with a tachogenerator and readout as part of the original conversion to provide an accurate speed indicator. The principle of operation being, that the tachogenerator coupled to the the spindle drive motor generates a voltage proportional to the motor speed. This voltage is indicated on a moving coil voltmeter and converted to read rev/min. The instrument was calibrated by a potentiometer and accurately set with a photo-tachometer. The tachogenerator output was then tapped and scaled with a potential divider and the commutator noise removed with a low pass filter. The signal was then fed to the logging system.

#### 4.3.3. Torque.

A number of techniques were considered for direct and indirect measurments of torque, including measurments of the reaction on the workpiece, rotating load cells and measuring the separating force on the gears. The final choice however simply derives torque as a function of the electrical input power to the drive motor and its rotational speed. Therefore, torque (T) is given by the following equation (Eq 4.1.):

$$T = \frac{W_s}{2\pi n}$$

The rotational speed ( $n$ ) is a measured parameter and the shaft power ( $W_s$ ) is obtained from: (Eq 4.2.)

$$W_s = W_{in} - W_{loss}$$

$W_{in}$  is the electrical input power to the motor.

$W_{loss}$  are the motor losses and function of motor speed ( $n$ ) The armature current ( $I_a$ )

The motor speed and the current are both measured quantities. The losses are the computed from: (Eq 4.3.)

$$W_{loss} = K_1 \cdot I_a^2 + K_2 \cdot n^2$$

Where:  $K_1$  and  $K_2$  are machine constants.

The measurements of the motor electrical input power was complicated by the non-sinusoidal current and voltage waveforms produced by the single phase thyristor speed control unit. To enable power determination, the voltage and current waveforms were sampled, multiplied and integrated. The voltage was sampled through a resistive divider and differential input buffer. Current was sampled using a Hall effective device placed in a loop of the cable feeding the motor armature. The two signals were then scaled and multiplied in a four quadrant integrated circuit multiplier. The voltage and current waveforms were each converted to rms values and dc signals fed to the logger. The moving iron instrumentation was also used to give direct read out of current and voltage.



#### 4.3.4. Load on the Bit.

Bit axial load was provided by a pneumatic cylinder acting directly on the drill spindle. Constant and predetermined pressure being maintained through a pressure regulator and the cylinder was protected by an integral oil lubricator and water trap. Visual indication of load on the bit was presented by a standard capillary tube pressure gauge. To measure and record the applied pressure, a pressure transducer was fitted in the regulated air supply line to the cylinder and fed with a 24 Vdc supply. This developed an output signal in the range 0.7 to 10.7 volts. Knowing the cylinder area and applied pressure it was a simple task to compute the applied weight to the bit, which was then converted to read out as kilonewtons.

#### 4.3.5. Penetration.

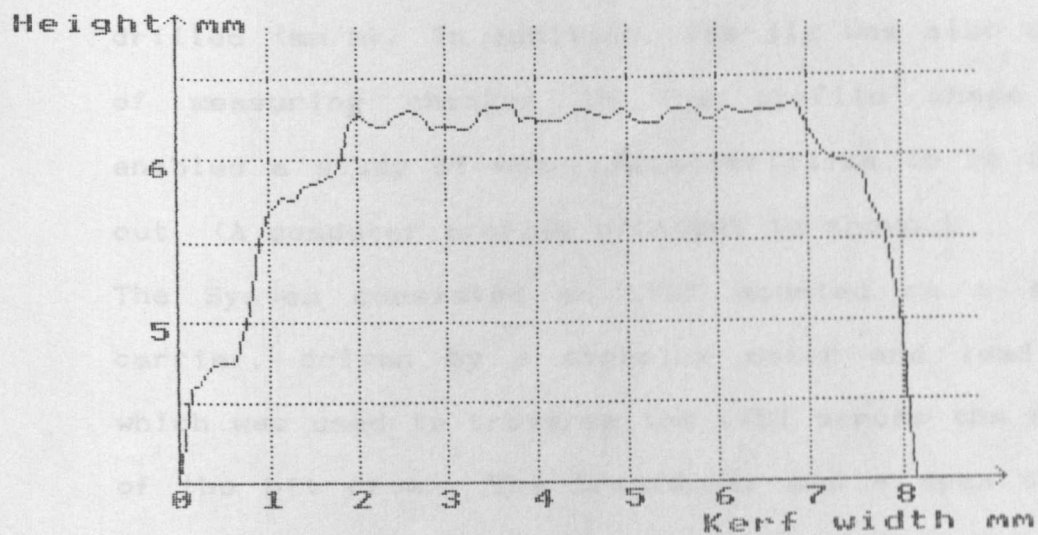
A range of techniques for the measurement of the linear penetration of the drill bit were evaluated and these included, linear potentiometers, linear gratings, linear induction capacitance transducers and rotary potentiometers and coders with motion converters. However, for the desired stroke length of 300mm minimum, the linear variable differential transformer (LVDT) gave the best value, in terms of

# UNIVERSITY OF NOTTINGHAM

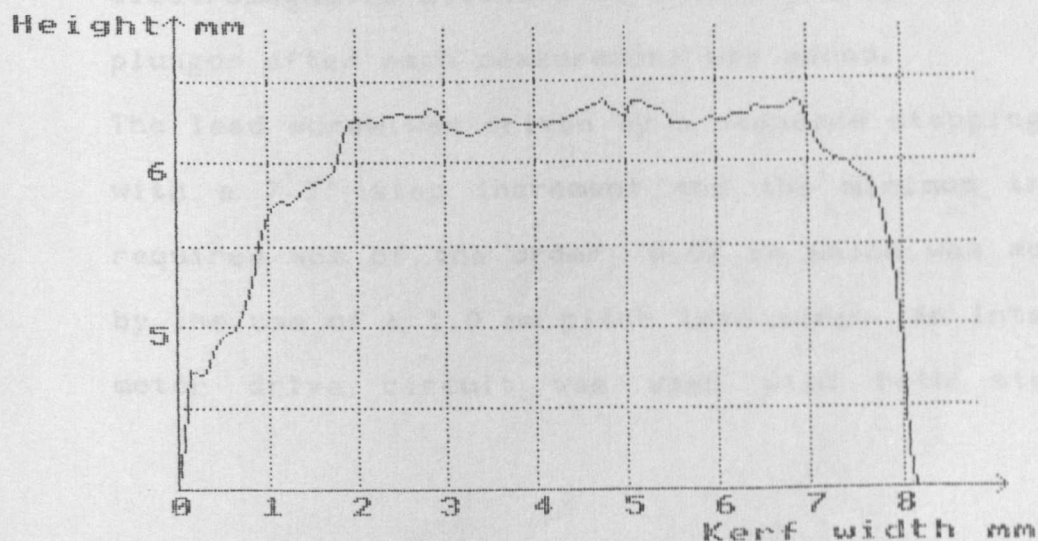
## DEPARTMENT OF MINING ENGINEERING

### PROFILE MEASUREMENT ANALYSIS CA1

DATE OF TEST.....5/2/87  
MANUFACTURER.....CRAELIUS  
BIT TYPE.....IMP  
BIT SIZE.....38/22  
DIAMOND.....SDA100  
CONCENTRATION.....45  
MATRIX.....X99  
FLUSH MEDIA.....WATER  
ROCK TYPE.....GNEISS



Test No 3



Test No 2

accuracy and resolution for money. This device was fitted along the length of the cylinder and connected to the actuator by specially manufactured brackets. The necessary circuitry was then added and linked to the logger.

#### 4.4. The Drill Bit Wear Jig.

The drill bit wear jig was designed to accurately measure the rate of bit wear with actual distance drilled (mm/m). In addition, the jig was also capable of measuring changes in the profile shape which enabled a study of wear characteristics to be carried out. (A computer profile printout is shown.)

The System consisted an LVDT mounted on a sliding carrier, driven by a stepping motor and lead screw which was used to traverse the LVDT across the surface of the bit crown. The transducer has a span of 10mm +/- 0.05mm resolution and to allow the spring loaded plunger to move freely across the surface of the bit a electromagnetic solenoid to incrementally withdraw the plunger after each measurement was added.

The lead screw was driven by a standard stepping motor with a 7.5° step increment and the minimum traverse required was of the order 0.02 mm which was achieved by the use of a 1.0 mm pitch lead screw. An integrated motor drive circuit was used with both step and

## BIT PROFILE MEASURING JIG..

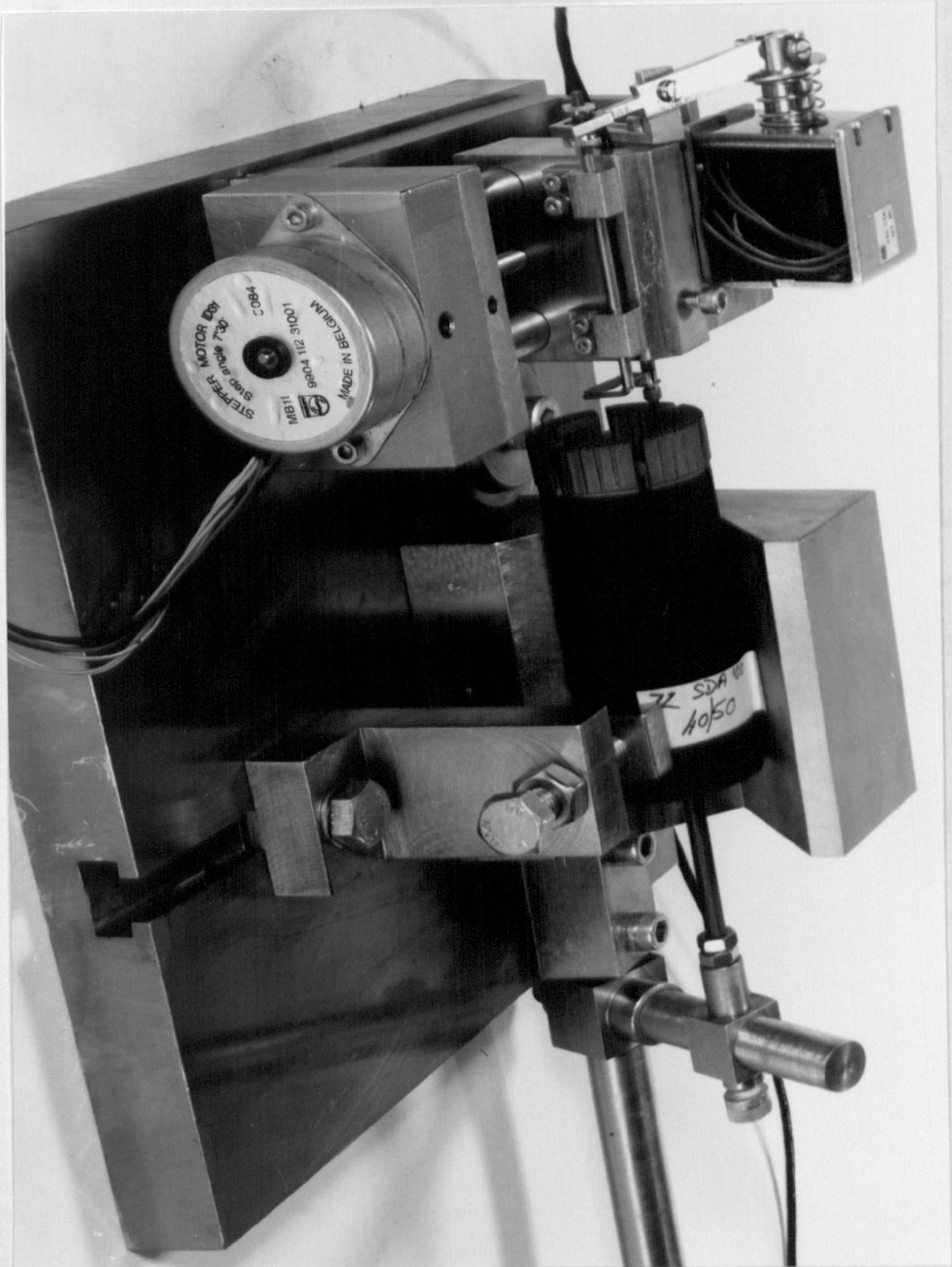


Figure 4.3.

direction signals taken from the logger microcomputer. The assembled measuring unit was mounted on a base plate with vee block and clamping facilities to secure and accurately locate and relocate the drill bit when required.

The drill bit profile measuring device is illustrated in Figure 4.3.

#### 4.5. Electronic Hardware.

When designing the drill monitoring system, the long term objectives lay in the future possibility of developing closed loop control systems for the independent drilling variables in order to optimise the rates of drill bit penetration and drill bit wear. It was therefore, most desirable that electronic hardware should be capable of extension to cover these requirements.

The monitoring system was required to accept inputs from the various drill rig transducers, to massage the data and provide on-line displays of critical parameters. In the case of the drill bit wear jig, control outputs were required for the indexing motor. The system was also required to continuously log all of the raw data for subsequent analysis.

At an early stage of the project development it was decided to use a microcomputer-based system to perform

the required functions. A number of other systems were considered but, mainly on the basis of technical specifications, costs and prior experience, the Acorn BBC. B. was chosen. This however, immediately placed constraints on processing speed and memory size. Even so, the machine proved to be, just adequate for the demands placed on it, although on occasions, it did tax the ingenuity of the software writer.

The BBC computer, around which the system was built, has a 32k memory, 400k disc and monochrome monitor. For field use, a much more rugged machine would be required, however, conversion to a different computer should not present any major technical difficulties.

#### 4.6. Interface Hardware.

To avoid using the notorious internal analogue input of the BBC micro, an external eight bit by eight channel analogue to digital ( A/D ) converter was coupled to the BBC 1MHz bus. The bus was also coupled to four 12 bit digital to analogue converters, thus providing outputs to an X-Y plotter and control outputs for later use in control of the drilling rig.

All signals from the transducers were scaled using purpose designed instrument amplifiers to match the 0 - 10 volt input requirements of the A/D converter.

The readings on this channel however, initially

suffered from noise interference, but this was eventually subdued by subsequent modifications to the hardware and software. Control outputs for the wear jig were taken from the BBC's parallel interface.

The interface circuitry was constructed on standard Eurocards on a modular basis. The cards, and power supplies, etc. were housed in a rack case.

#### 4.7. Software.

Programmes for the drill rig and bit wear measurement jig were produced separately but both shared the same data base. The programmes are highly structured to enable easy modification and updating. They are menu driven to allow the user to determine the way in which data is collected and which information is to be displayed on line.

At the start of a drill test programme, the operator is requested to input some basic information about the drill bit specifications, some of this information can then be used by the monitoring programme and included in the final test report.

Under menu control, the user selects which channels are to be displayed. A maximum of three channels may be simultaneously displayed in an updated graphical form and instantaneous values for all channels are displayed in digital form. All data is automatically

recorded on disc on an event or data change basis to economise on disc space. A visual and audible warning is given should the disc approach full capacity. The test can then be paused while a new disc is loaded. During the tests, the operator needs only to make single key strokes to mark the start and end of each test run.

The mode of operation of the drill bit wear jig software is configured at the start of the test.

During this phase the input data required are:

- 1) The number of segments to be measured.
- 2) The number of measurement points per segment.
- 3) The dimensions of the kerf width of the crown.
- 4) Additional gauge added.

Additional gauge is sometimes required to compensate for the limited reach of the wear measurement transducer.

Before testing, the operator is required to align the drill bit in the vee block before clamping in position. The transducer probe can then be positioned in close proximity to the inner edge of the bit kerf by use of the directional arrows on the key board. A single key stroke is all that is necessary to start the measurements and an audible signal is given when the measurement is completed. From the data recorded, the profile of the bit segments can be plotted and changes in profile resulting from wear can be plotted



at various stages throughout the life of the bit. The programme can also compute the volume loss due to wear at any stage.

#### **4.8. Coring Bits and Bit Wear Measurements.**

The two bits used for these trials are illustrated in Figure 4.1. together with the manufacturers specifications. Each bit was made up from four individual polycrystalline diamond impregnated segments which had been brazed onto a separately machined steel shank. The profiles of these segments were of a flat form and initial measurements made before the commencement of the test programme indicated minor irregularities in height (0 - 0.3 mm) and further irregularities in concentricity (0 - 0.4 mm). The method used to measure concentricity of the segments, was to accurately set the shank in the chuck of a standard workshop centre lathe and measure deflection by means of a dial gauge indicator while slowly rotating the chuck by hand. Thereafter, resultant changes in profile shape after discrete distances cored was plotted by taking measurements across each segment of the bit from the inside to the outside peripheries with the specially designed computer controlled profile measuring jig, which can then subtract these measurements from the preceding

reference measurements, calculate and record the volumetric loss due to wear, any consequential change in profile shape was plotted and logged on disc for future reference.

#### 4.9. Drilling Test Programme.

The drilling test programme consisted of core drilling in two different rock types:

- 1) Swedish Granite.
- 2) Coarse Grained Sandstone.

The tests were conducted under strictly controlled conditions and accurately monitored with the aid of the specially installed micro-computer.

The bits were prepared for use by first running them in sandstone to ensure sufficient diamond exposure before each actual test run in the Swedish granite. The initial drilling parameters were predetermined and based on recommendations included in a manufacturers handbook and those found by the authors own experiences, Van Moppes IDP LTD (1986) and Cassapi, (1983).

TABLE 4.1

Summary of rock physical properties

Rock Type	"Swedish" Granite	'Coarse Grained' Sandstone
Uniaxial Compressive Strength (MPa)	217.1	32.7
Indirect Tensile Strength (MPa)		2.5
Shore Scleroscope Test Index	91.4	39.0
N.C.B. Cone Indenter Test Index	8.6	3.6
Cerchar Test Index	3.9	3.6

TABLE 4.2.

Table of Mineral Proportions

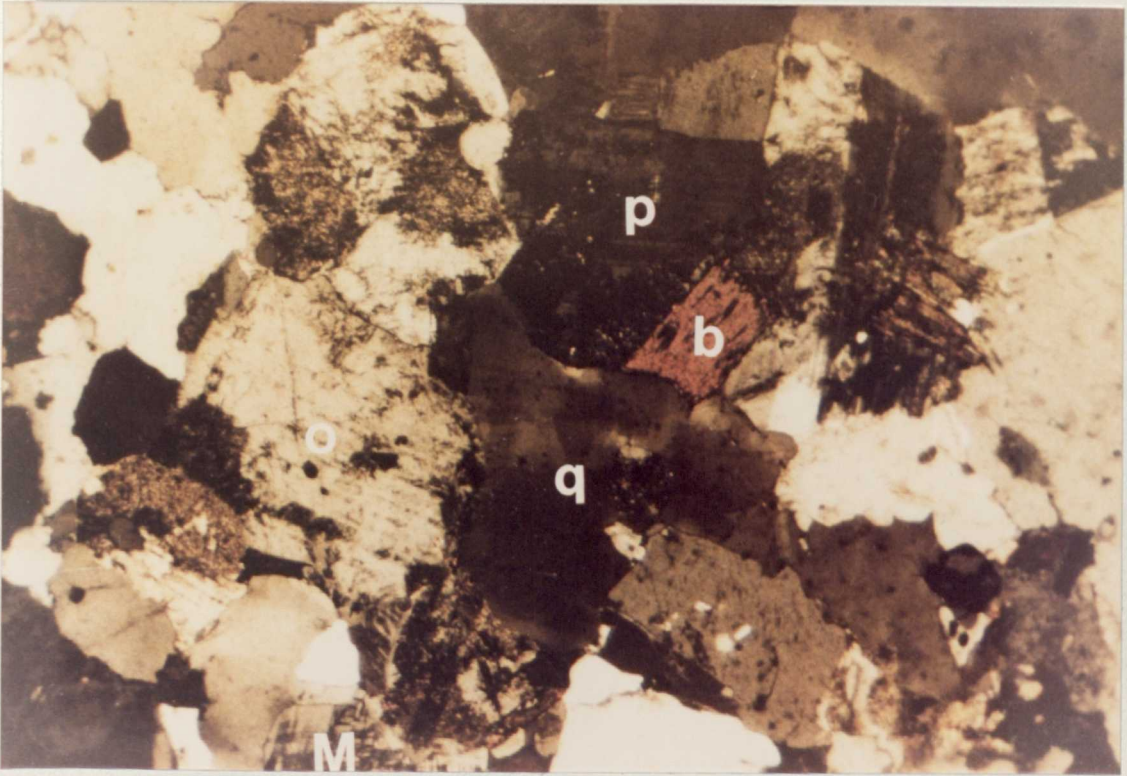
Rock Type: SWEDISH GRANITE

Mineral	Percentage	Mohs' Hardness
Quartz $\text{SiO}_2$	12%	7
Plagioclase $\text{Na}(\text{AlSi}_3\text{O}_8) - \text{Ca}(\text{Al}_2\text{Si}_2\text{O}_8)$	15%	6 - 6½
White Mica $\text{KA1}_2(\text{Si}_3\text{Al})\text{O}_{10}(\text{OH})_2$	1%	2 - 2½
Orthoclase $(\text{KgNa})\text{AlSi}_3\text{O}_8$	62%	6 - 6½
Microcline $\text{KA1Si}_3\text{O}_8$	6%	6 - 6½
Biotite $\text{K}(\text{MgFe})_3(\text{Si}_3\text{Al})\text{O}_{10}(\text{OH})_2$	3%	2½ - 3
Apatite $\text{Ca}_5\text{F}(\text{PO}_4)_3$	<1%	5
Sphene $\text{CaTiSiO}_5$	<1%	5
Zircon $\text{ZrSiO}_4$	<1%	7.5

TABLE 4.3  
Percentage Mineral Proportions  
 ROCK TYPE : COARSE GRAINED SANDSTONE

Mineral	Percentage	Moh's Hardness
Quartz $\text{SiO}_2$	60.0	7.00
Feldspars Plagioclase $\text{NaAlSi}_3\text{O}_8 - \text{CaAl}_2\text{Si}_2\text{O}_8$ Orthoclase $(\text{K Na}) \text{AlSi}_3\text{O}_8$ Microcline $(\text{K} \text{AlSi}_3\text{O}_8)$ Perthite and Micoperthite $(\text{K}_1\text{Na}) \text{AlSi}_3\text{O}_8$ Altered Feldspar	2.0 8.0 1.5 1.5 15.0	} 6.00 - 6.50
Mica $\text{KA1}_2(\text{OH})_2(\text{AlSi}_3\text{O}_{10})$	1.0	
Clay $(\text{Al}_2\text{O}_3 \cdot 2\text{Si}_2 \cdot 2\text{H}_2\text{O})$	10.0	
Rock Fragments	1.00	

SWEDISH GRANITE.



Thin Section Microphotograph.

P - Plagioclase

O - Orthoclase

B - Biotite

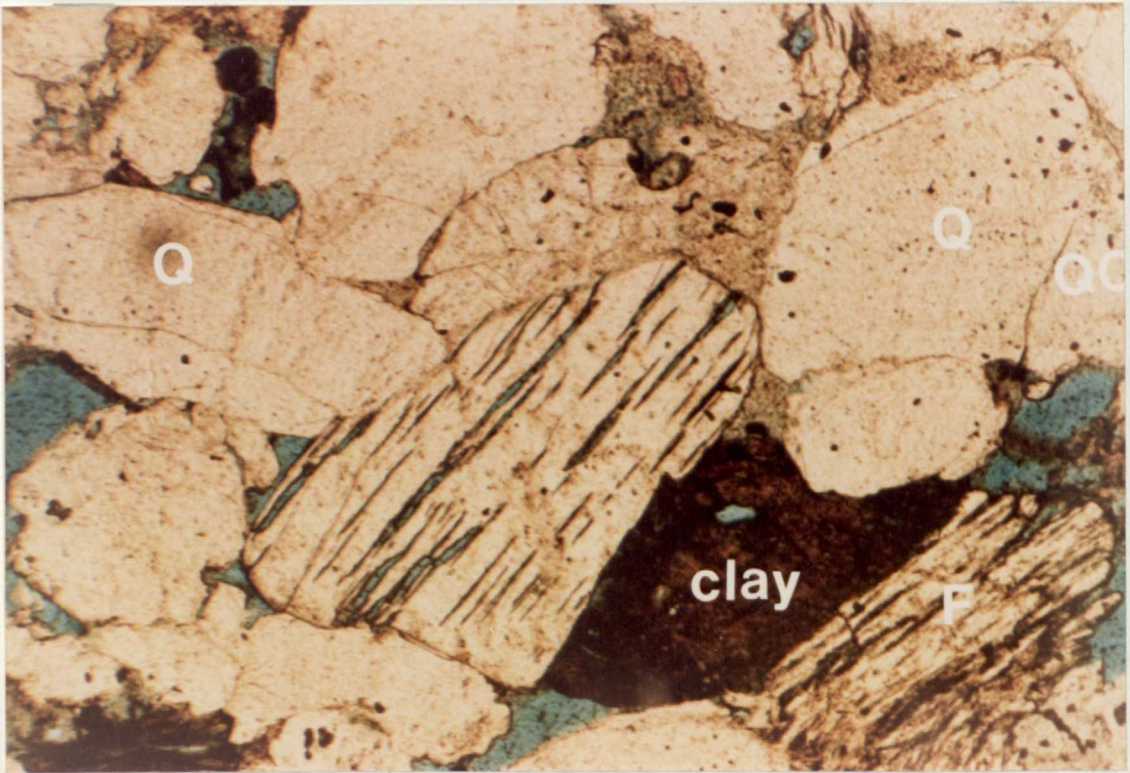
M - Microcline

Q - Quartz

Figure 4.4.



COARSE GRAINED SANDSTONE.



Microphotograph.

Figure 4.5.

The parameters monitored were:

- a) Load on Bit. kg.
- b) Rotational cutting speed. rev/min.
- c) Water Flush Rate. 1/min,
- d) Torque. Nm.
- e) Penetration rate. mm/min.
- f) distance drilled. mm.

#### 4.10. Physical Properties of the Rock Material.

Physical property tests were conducted on the rock sample material and are detailed as follows:

- a) Uniaxial compressive strength.
- b) Indirect tensile strength.
- c) Rock hardness index.
- d) Rock abrasiveness index.
- e) Petrographic analysis.

A summary of the physical properties of the rocks are given in Table 4.1. The mineral constituents and their proportions, analysed by thin section microscopy are given in Tables 4.2 and 4.3. Figures 4.4 and 4.5. illustrate photomicrographs of thin sections of the Swedish granite and coarse grained sandstone.

It should be noted that rock hardness was determined by two well known hardness tests, i.e. Shore Scleroscope and the NCB Cone Indenter, the



abrasiveness of the rock material was determined by the Cerchar rock abrasive index test. Physical strength properties were conducted on standard laboratory compression test machines.

#### 4.11. Applied Drilling Parameters and Bit Performance.

##### 4.11.1. Core Bit "A".

When used to core the Swedish granite the following drilling parameters were employed:

Linear cutting speed,        180 m/min

Load on Bit,                270 kg.

Water flush rate,            10 l/min

The mean wear rate obtained from this bit was 0.3 mm per metre cored and the total bit life was 17.03 metres of cored material.

The mean penetration rate was: 96mm/min.

##### 4.11.2. Core Bit "B".

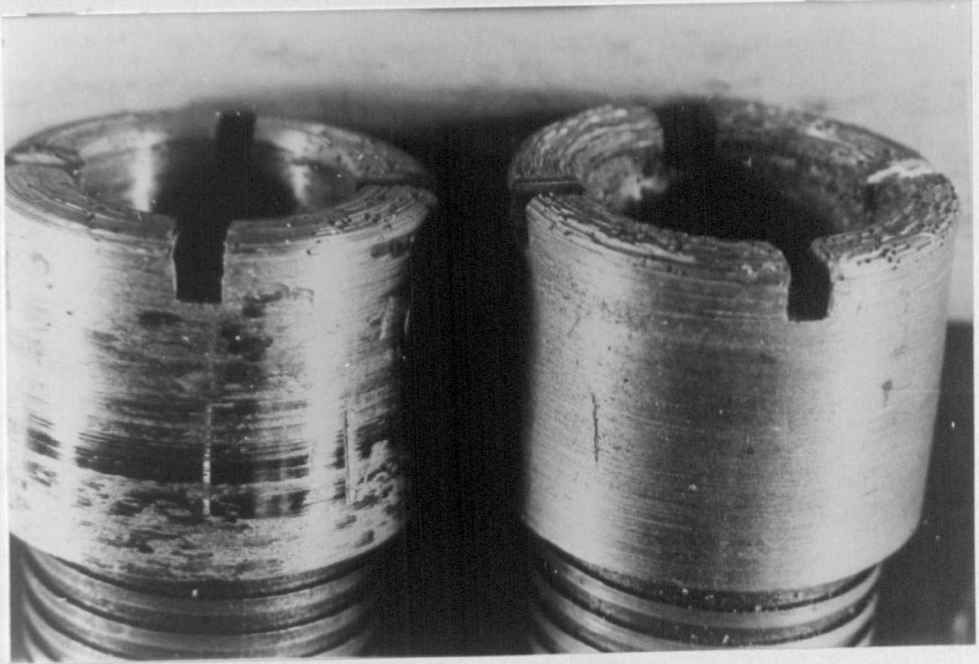
The best cutting parameters for this core bit in the Swedish granite were found to be as follows:

Linear cutting speed        1500 m/min

Load on bit                303 kg

Water flush rate            11 l/min

USED CORE BITS.



Core Bit "A"

Core Bit "B"

Figure 4.6.

Both bits were initially run in the coarse grained sandstone to ensure sufficient sharp diamond exposure before each test run. However, while drill bit "A" quickly established an acceptable cutting performance in the Swedish granite, this was not the case with drill bit "B". Here, the performance of this bit in the Swedish granite was found to be unsatisfactory and perturbing the drilling parameters did not significantly improve the results. Therefore, much of the initial test work was monitored in the coarse grained sandstone and the following drilling parameters were found to produce the best results.

Rotational speed	1500 rev/min
Load on bit	237 kg
Water flush rate	11 l/min

Subsequently, the best performance obtained with these parameters was found to be:

Petration Rate	260 mm/min
Wear Rate	0.090 mm/m drilled

Tests were continued with the coarse grained sandstone until a naturally developed, rounded bit profile had been established, at which time, tests were then continued in the Swedish granite. Figure 4.6. illustrates Core Bits "A" and "B" at the conclusion of

the test programme and shows the natural profile formed on each bit during the drilling tests.

#### 4.12. Test Procedure.

The test programme for each core bit comprised a series of individual drilling trials, during which, wear was accurately measured across the surface of each segment of the crown and at regular intervals of known distance drilled.

Drilling trials included tests during which the main parameters were kept constant, as with drill bit "A" and trials which involved perturbing the parameters as with core bit "B", thus by analysing the results obtained from these individual tests, wear with total distance drilled with the applied drilling parameters could be assessed.

#### 4.13. Physical Property Tests.

The physical properties of the rock material used with the drill test programme which deserve consideration, are those concerned with strength, hardness and abrasiveness. Although many other factors concerned with rock properties may have to be considered in a normal field operation.

The methods employed to determine the physical strength parameters of natural rocks are well

documented and need no further detailed description here,

#### **4.14. Petrographic Analysis. (Swedish Granite)**

Petrographic analyses of thin sections of the Swedish granite were conducted to determine the mineral constituents, their proportions, grain size and shape. The rock is described as a "Microline Granite" and showed partial alteration which include biotite to chlorite and orthoclase to mica. Along the cleavage planes all the plagioclase showed total alteration to white mica although about 1% of these crystals were fresh. Furthermore, the rock is well crystalline (interlaced), equiangular and some of the orthoclase crystals reach up to 8 mm and these are the largest.

In hand, the rock was solid and competent with no visible evidence of weathering, cracks or veins.

A summary of the mineral constituents and their proportions is given in Table 4.2. and the thin section photomicrograph is illustrated in Figure 4.4.

#### **4.15. Petrographic Analysis (Coarse Grained Sandstone)**

In hand specimen, the grains of quartz and feldspar reach up to 2 - 3 mm and can easily be seen by the naked eye

In thin section, some of the feldspar show alteration

to sericite or kaolinite. The grains are well sorted and sub-angular to sub-rounded in shape and the cementing material is a mixture of quartz and clay. The quartz grains however, appear to have two different origins, i.e. sedimentary and metamorphic.

A summary of the mineral constituents and their proportions are given in Table 4.3. and a photomicrograph of the thin section is presented in Figure 4.5.

#### 4.16. Drilling Tests Results (Core Bit "A")

The derived drilling parameters for this core bit when coring the Swedish granite were based on the recommendations in a manufacturers handbook, together with the practical experience gained from previous trials with impregnated core bits in various laboratory core drilling investigations.

The drilling parameters however, required only minor adjustments before an apparent acceptable cutting condition was achieved, e.g. water flush rate being reduced from 15 l/min to 11 l/min. drill speed from 1625 rev/min to 1500 rev/min with a bit loading of 270 kg.

These drilling parameters appeared to give the best sustained penetration rate commensurate with the unavoidable, but gradually continuous decline in

TABLE 4.4  
Wear characteristics of outside section of core bit 'A'

Test	Distance Drilled A (mm)	Average Wear B (mm)	Wear Rate $C = \frac{B}{A}$ (mm/m)	Cumulative Distance D (m)	Cumulative Wear E (mm)	Cumulative Wear Rate $F = \frac{E}{D}$ (mm/m)
A1	0.79977	0.099	0.124	0.80	0.099	0.124
A2	0.86461	0.165	0.191	1.66	0.264	0.159
A3	0.20016	0.056	0.280	1.87	0.320	0.171
A4	0.66276	0.026	0.039	2.53	0.346	0.137
A5	0.63273	0.154	0.243	3.16	0.500	0.158
A6	0.75981	0.194	0.255	3.92	0.694	0.177
A7	0.82893	0.456	0.551	4.75	1.151	0.242
A8	0.80413	0.254	0.316	5.55	1.405	0.253
A9	0.82876	0.432	0.521	6.38	1.837	0.288
A10	0.74419	0.737	0.990	7.12	2.574	0.362
A11	0.73526	0.025	0.034	7.86	2.599	0.331
A12	0.09997			7.99		
A13	0.83170	0.127	0.153	8.79	2.726	0.310
A14	0.85448	0.203	0.238	9.65	2.929	0.340
A15	0.61107	0.076	0.124	10.26	3.005	0.293
A16	0.41693	0.076	0.182	10.68	3.081	0.289
A17	0.40807	0.203	0.498	11.09	3.284	0.296
A18	0.40837	0.102	0.250	11.49	3.386	0.295
A19	0.39583	0.102	0.260	11.89	3.488	0.293
A20	0.67311	0.076	0.113	12.56	3.564	0.284
A21	0.27414	0.025	0.091	12.84	3.589	0.280
A22	0.38086	0.229	0.601	13.22	3.818	0.289
A23	0.80647	0.254	0.315	14.03	4.072	0.290
A24	0.85111	0.152	0.178	14.88	4.224	0.284
A25	0.76561	0.127	0.166	15.64	4.351	0.278
A26	0.69041	0.229	0.332	16.33	4.580	0.280
A27	0.69484	0.457	0.658	17.03	5.037	0.296



TABLE 4.5

Wear characteristic of middle section of core bit 'A'

Test	Distance Drilled A (mm)	Average Wear B (mm)	Wear Rate $C = \frac{B}{A}$ (mm/m)	Cumulative Distance D (m)	Cumulative Wear E (mm)	Cumulative Wear Rate $F = \frac{E}{D}$ (mm/m)
A1	0.79977	0.145	0.181	0.80	0.145	0.181
A2	0.86461	0.105	0.121	1.66	0.250	0.151
A3	0.20016	0.048	0.240	1.87	0.298	0.159
A4	0.66276	0.035	0.053	2.53	0.333	0.132
A5	0.63273	0.065	0.103	3.16	0.398	0.126
A6	0.75981	0.235	0.309	3.92	0.633	0.161
A7	0.82893	0.178	0.215	4.75	0.811	0.171
A8	0.80413	0.279	0.347	5.55	1.090	0.196
A9	0.82876	0.406	0.490	6.38	1.496	0.234
A10	0.74419	0.229	0.308	7.12	1.725	0.242
A11	0.03526	0.127	0.173	7.86	1.825	0.236
A12	0.09997			7.99		
A13	0.83170	0.127	0.153	8.79	1.979	0.225
A14	0.85448	0.178	0.208	9.65	2.157	0.224
A15	0.61107	0.051	0.083	10.26	2.208	0.215
A16	0.41693	0.152	0.365	10.68	2.360	0.221
A17	0.40807	0.102	0.250	11.09	2.460	0.222
A18	0.40837	0.102	0.250	11.49	2.564	0.223
A19	0.39583	0.127	0.321	11.89	2.691	0.226
A20	0.67311	0.076	0.113	12.56	2.767	0.220
A21	0.27414	0.102	0.372	12.84	2.869	0.223
A22	0.38086	0.254	0.667	13.22	3.123	0.236
A23	0.80647	0.152	0.189	14.03	3.275	0.233
A24	0.85111	0.051	0.060	14.88	3.326	0.244
A25	0.76561	0.102	0.133	15.64	3.428	0.219
A26	0.69041	0.203	0.294	16.33	3.631	0.222
A27	0.69484	0.279	0.402	17.03	3.910	0.230

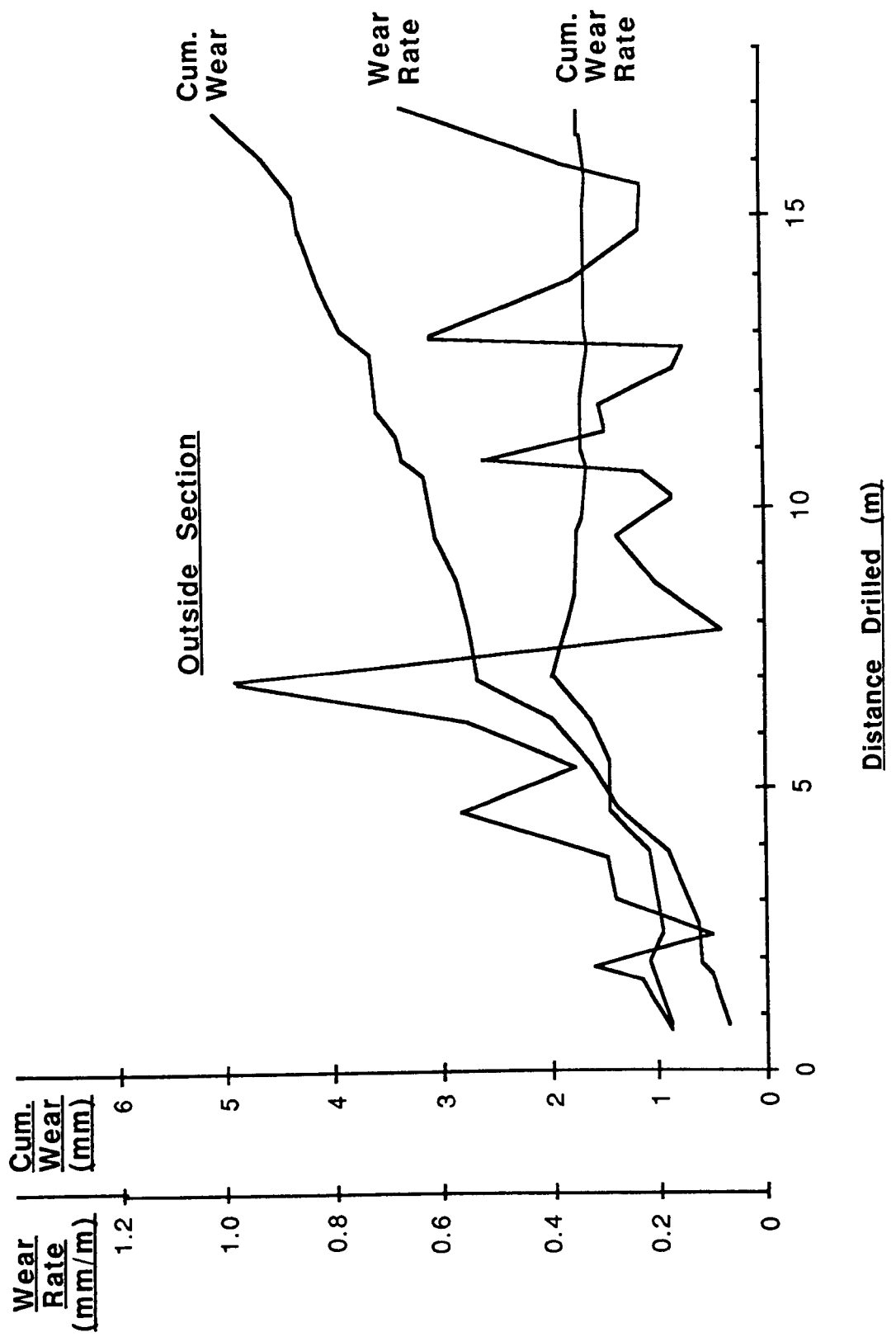


TABLE 4.6

Wear characteristic of inside section of core bit 'A'

Test	Distance Drilled A (mm)	Average Wear B (mm)	Wear Rate $C = \frac{B}{A}$ (mm/m)	Cumulative Distance D (m)	Cumulative Wear E (mm)	Cumulative Wear Rate $F = \frac{E}{D}$ (mm/m)
A1	0.79977	0.090	0.113	0.80	0.090	0.113
A2	0.86461	0.174	0.121	1.66	0.264	0.159
A3	0.20016	0.120	0.275	1.87	0.384	0.205
A4	0.66276	0.124	0.113	2.53	0.508	0.201
A5	0.63273	0.256	0.119	3.16	0.764	0.242
A6	0.75981	0.296	0.355	3.92	1.060	0.270
A7	0.82893	0.178	0.369	4.75	1.238	0.261
A8	0.80413	0.559	0.095	5.55	1.797	0.324
A9	0.82876	0.813	0.766	6.38	2.610	0.409
A10	0.74419	0.762	0.204	7.12	3.372	0.474
A11	0.73526	0.330	0.276	7.86	3.702	0.471
A12	0.09997			7.99		
A13	0.83170	0.178	0.123	8.79	3.880	0.441
A14	0.85448	0.413	0.297	9.65	4.293	0.441
A15	0.61107	0.051	0.167	10.26	4.344	0.423
A16	0.41693	0.076	0.609	10.68	4.420	0.414
A17	0.40807	0.050	0.187	11.09	4.470	0.403
A18	0.40837	0.050	0.322	11.49	4.520	0.393
A19	0.39583	0.050	0.258	11.89	4.570	0.384
A20	0.67311	0.050	0.226	12.56	4.620	0.368
A21	0.27414	0.050	0.091	12.84	4.670	0.364
A22	0.38086	0.229	0.601	13.22	4.899	0.371
A23	0.80647	0.076	0.315	14.03	4.975	0.355
A24	0.85111	0.178	0.089	14.88	5.153	0.346
A25	0.76561	0.051	0.133	15.64	5.204	0.333
A26	0.69041	0.127	0.258	16.33	5.331	0.326
A27	0.69484	0.381	0.366	17.03	5.712	0.335

**Fig. 4.7 Wear characteristics of outside section of core bit 'A'**



**Fig. 4.8 Wear characteristics of middle section of core bit 'A'**

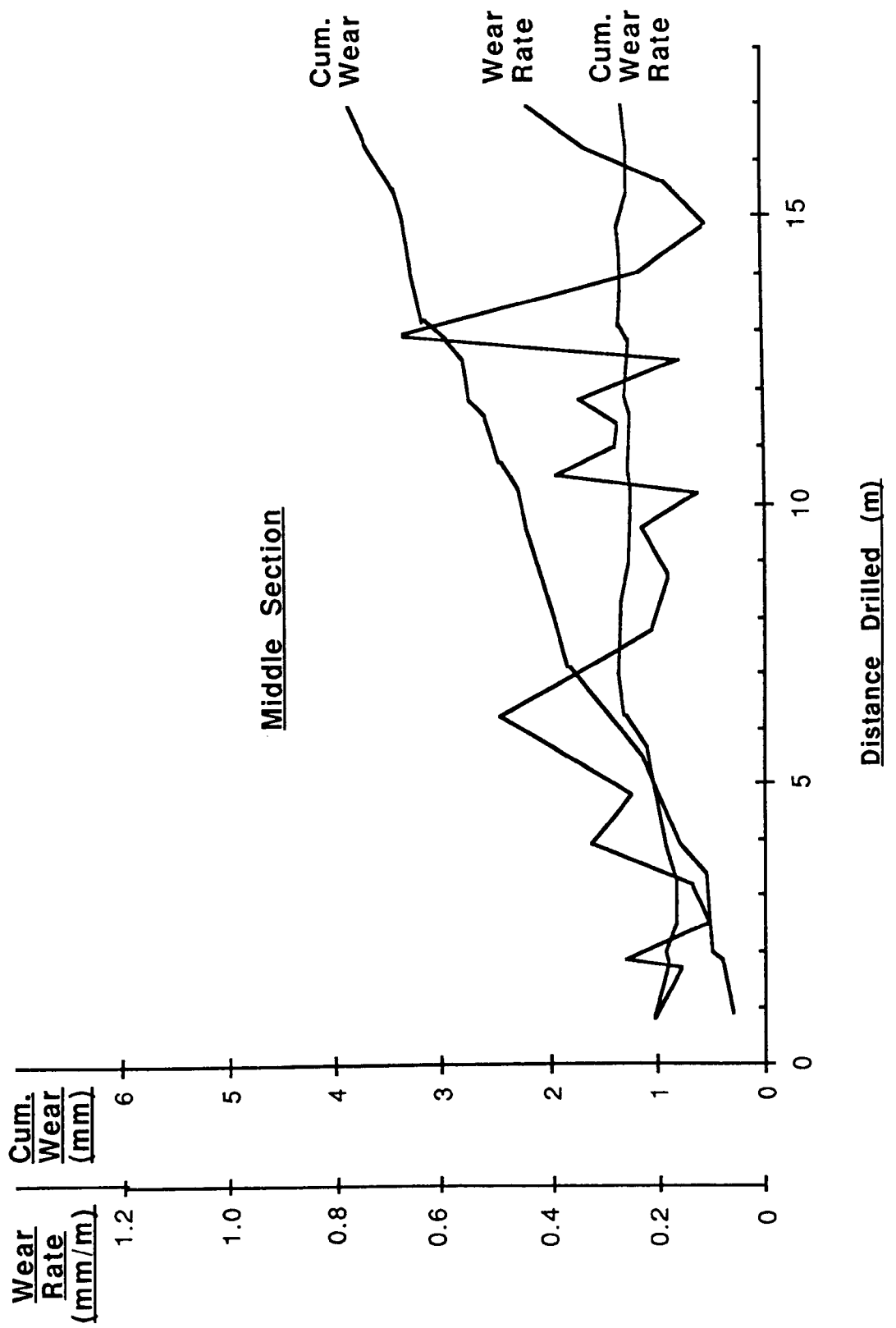


**Fig. 4.9 Wear characteristics of inside section of core bit 'A'**

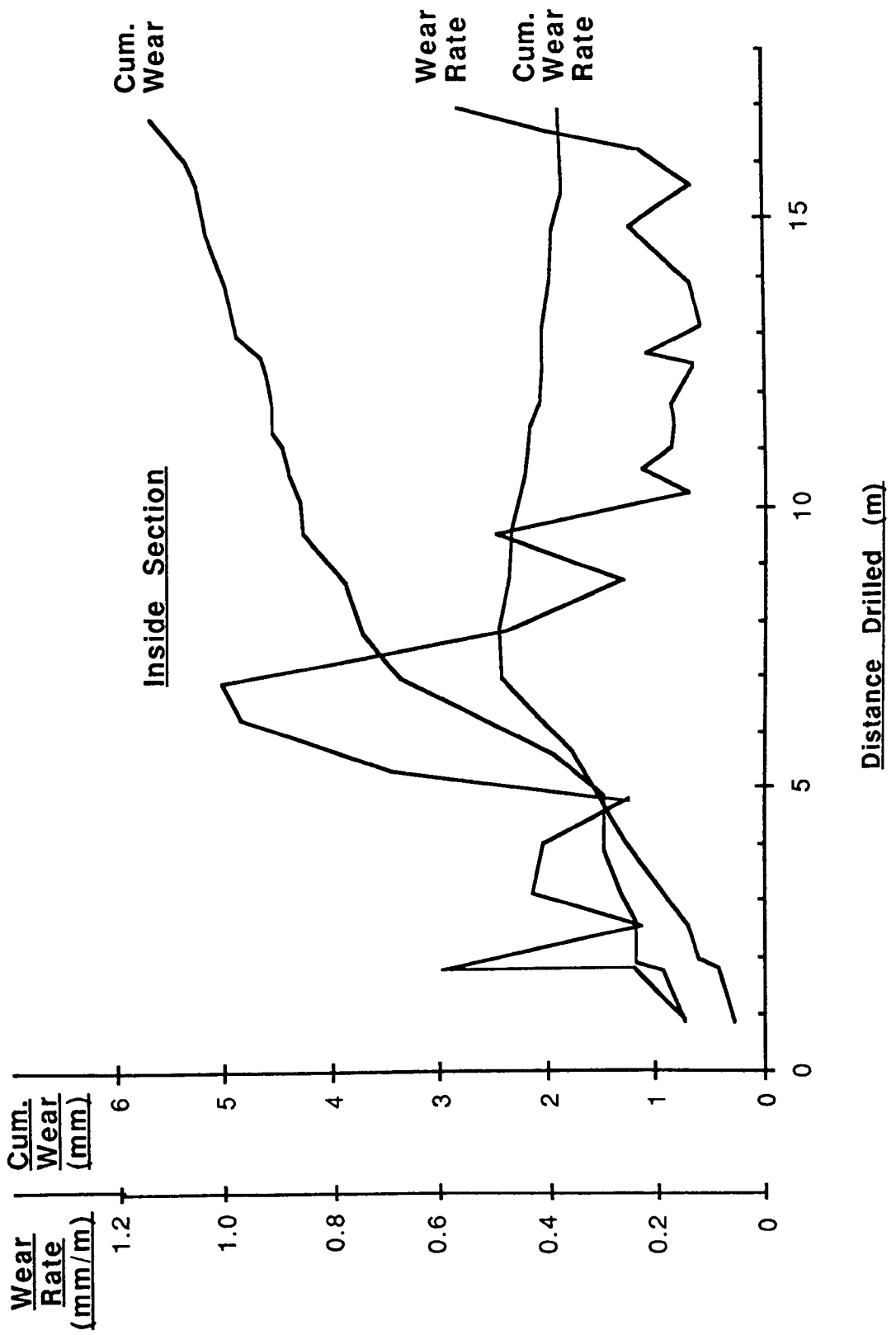


TABLE 4.7  
Wear characteristic of core bit 'A'

Test	Cumulative Distance Drilled (m)	Cumulative Wear Outside (mm)	Cumulative Wear Middle (mm)	Cumulative Wear Inside (mm)
A1	0.80	0.099	0.145	0.090
A2	1.66	0.264	0.250	0.264
A3	1.87	0.320	0.298	0.384
A4	2.53	0.346	0.333	0.508
A5	3.16	0.500	0.398	0.764
A6	3.92	0.694	0.633	1.060
A7	4.75	1.151	0.811	1.238
A8	5.55	1.405	1.090	1.797
A9	6.38	1.837	1.496	2.610
A10	7.12	2.574	1.725	3.372
A11	7.86	2.599	1.852	3.702
A12	7.96	2.599	1.852	3.702
A13	8.79	2.726	1.979	3.880
A14	9.65	2.929	2.157	4.293
A15	10.26	3.005	2.208	4.344
A16	10.68	3.081	2.360	4.420
A17	11.09	3.284	2.462	4.470
A18	11.49	3.386	2.564	4.520
A19	11.89	3.488	2.691	4.570
A20	12.56	3.564	2.767	4.620
A21	12.84	3.589	2.869	4.670
A22	13.22	3.818	3.123	4.899
A23	14.03	4.072	3.275	4.975
A24	14.88	4.224	3.326	5.153
A25	15.64	4.351	3.428	5.204
A26	16.33	4.580	3.631	5.331
A27	17.03	5.037	3.910	5.712

**Fig. 4.10** Graph of cumulative wear against distance drilled for the three positions on core bit 'A's kerf

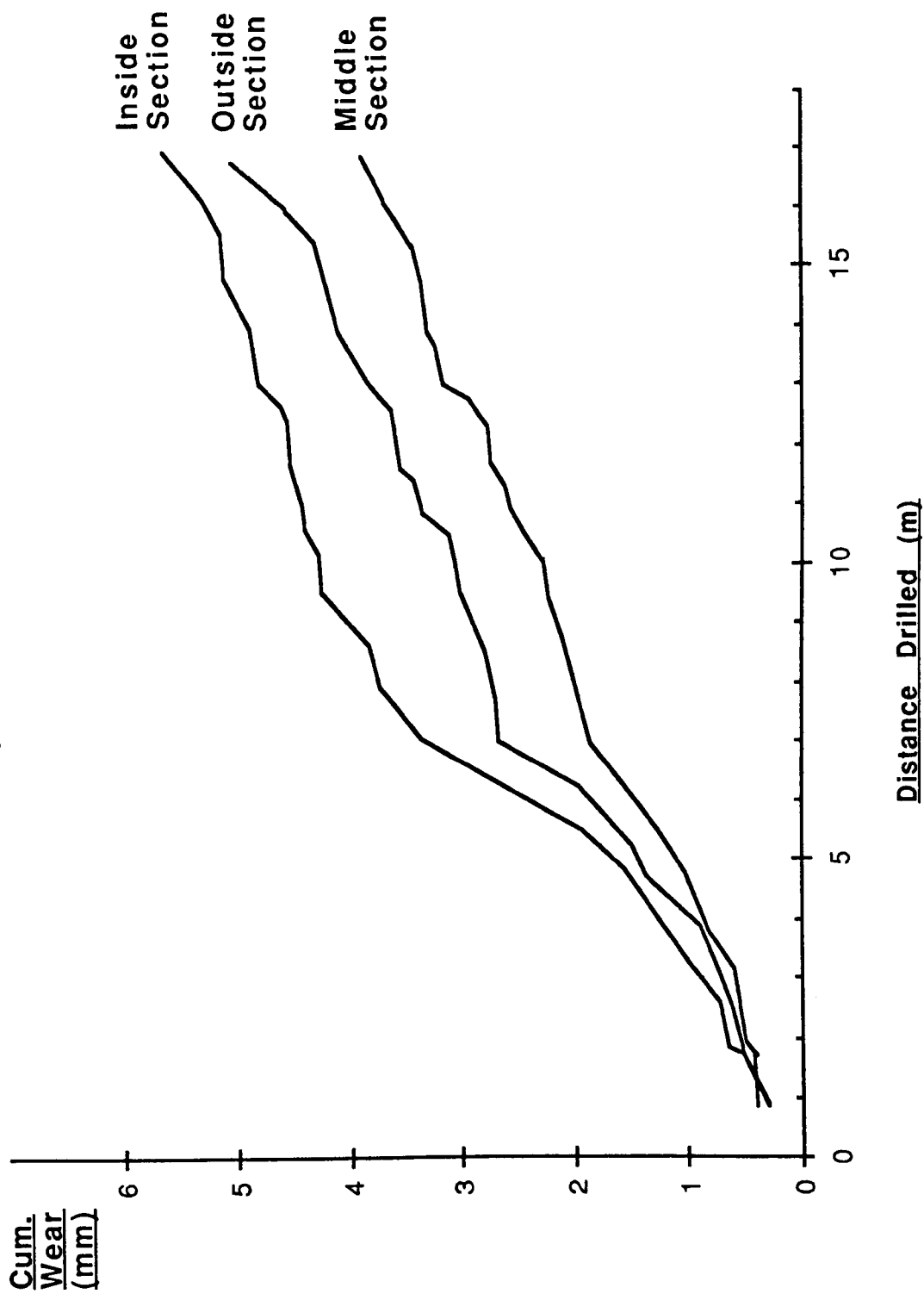
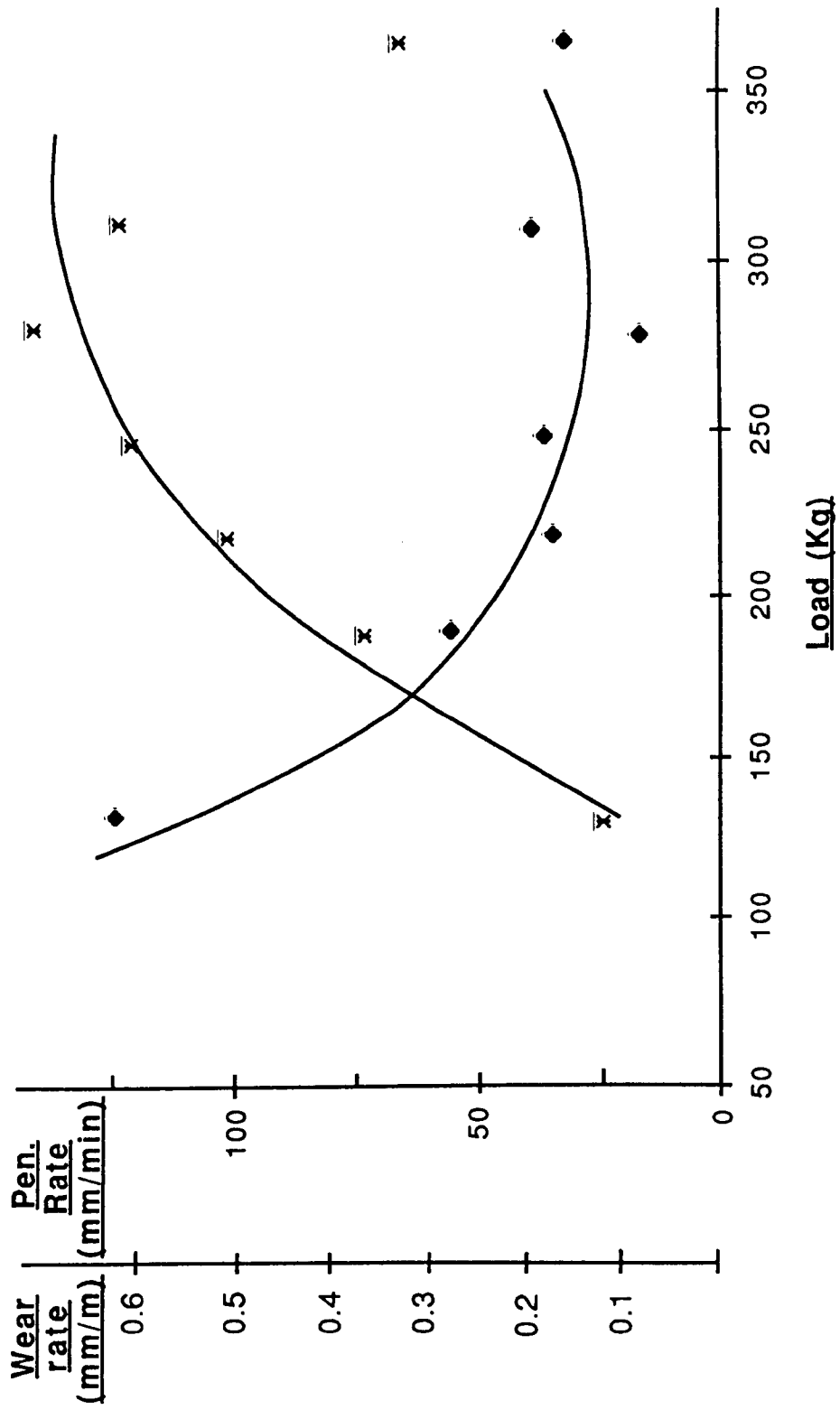


TABLE 4.8  
Performance characteristics for core bit 'B' in Swedish Granite

Test	Speed (rpm)	Load (Kg)	Distance Drilled (m)	AVERAGE WEAR			Mean Wear (mm)	Wear Rate (mm/m)	Average Pen. Rate (mm/min)
				Outside (mm)	Middle (mm)	Inside (mm)			
B1	1500	145	0.09308	0.050	0.050	0.059	0.059	0.063	24.40
B2	1500	211	0.60414	0.279	0.076	0.152	0.169	0.280	70.57
B3	1500	231	1.10722	0.254	0.075	0.228	0.186	0.170	100.28
B4	1500	270	2.0672	0.457	0.228	0.483	0.389	0.190	122.00
B5	1500	303	4.0193		0.302		0.302	0.080	143.17
B6	1500	337	1.20947	0.203	0.178	0.330	0.237	0.200	123.20
B7	1500	397	1.02211	0.127	0.152	0.178	0.152	0.150	60.50

**Fig 4.11 Performance characteristic for core bit 'B'**  
in Swedish Granite





penetration rate. Tables 4.4, 4.5 and 4.6 show the average wear and the calculated wear characteristics. Figures 4.7, 4.8 and 4.9 illustrate in graphical form, the wear characteristics of the outside, middle and inside sections of the core bit. Table 4.7. contains data relating to the three different positions on the kerf which were plotted against cumulative distance drilled and are illustrated in Figure 4.10.

In addition to these drill tests, consideration was given to wear of the bit crown in relation to the flush slots escape area and these were periodically re-cut to maintain adequate clearances.

Due to the unavoidable decline in penetration rate, frequent resharpenering of the bit became necessary. This was carried out in the weak abrasive sandstone and could entail drilling up to 0.5 metres of rock before a satisfactory cutting condition was achieved. However, it should be noted that wear measurements were always conducted each time before and after this operation took place.

#### 4.17. Core Bit "B". (Granite)

The drilling data obtained with this core bit when coring the Swedish granite are contained in Table 4.8. and illustrated graphically in Figure 4.11. It can be

seen that the best cutting conditions were obtained from the following drilling parameters:

Rotational speed	1500 rev/min. (180 m/min).
Load on the bit	303 kg.
Water flush rate	11 l/min.

These parameters gave a mean penetration rate of 125 mm/min. and a wear rate of 0.12 mm/metre drilled.

#### 4.17.1. Core Bit "B". (Sandstone)

The results obtained with this core bit when coring the coarse grained abrasive sandstone are contained in Table 4.9. The results presented in Figure 4.12. show penetration rates and wear rates plotted against load on the bit for a constant speed (1500 rev/min/) and a flush rate of 11 l/min. It can be seen from this graph that with a load of 200 kg the penetration rate is 260 mm/min and the wear rate is 0.09 mm/metre drilled.

Figure 4.13. illustrates penetration rate and wear rate plotted against speed with a constant load of 145 kg. and a flush rate of 11 l/min.

#### 4.18. Discussion of Results.

##### 4.18.1. Core Bit "A"

The results obtained for core bit "A" indicate that the wear occurring at the measured positions across the kerf, show a similarity of form of increasing wear with distance drilled. (see Figures 4.7, 4.8 and 4.9). The instantaneous wear rate has the expected peaks and troughs and the cumulative wear rate, initially indicating a gradual rising trend, then stabilising and levelling off at some constant rate. The major difference being the magnitude of the changes in the wear characteristics at the three different positions and with distance drilled.

Until the first metre was drilled, wear measurements proved to be unstable. This instability appeared to decline as the natural formation of the bit profile developed, e.g. "from flat to semi-round". Thereafter, the middle section of the bit crown experiences the least amount of wear and is illustrated graphically in Figure 4.10.

The bit life appears to go through three distinct wear phases where in phase 1. up to approximately five metres of drilling, the wear rate of the crown remained relatively constant, (see Figure 4.10) at

this point, (phase 2.) both the inside and outside sections experience a significant increase in wear rate. This second phase continues up to about seven metres of drilling for the inside section and about six metres for the outside section. In phase 3. the rate of ascent of both the inside and outside sections show a reduction and continues as in phase 1.

The middle section of the bit indicates no marked alteration in the gradient of its cumulative wear graph with total distance drilled and appears to represent the normal wear rate of the bit. It should be noted, that at some time during phase 3. the wear rates of both the inside and outside sections adopt a similar wear rate to the middle section.

The effect of these changes in wear rate at different distances drilled on the bit profile is illustrated graphically in Figure 4.14. and shows that up to about 5 metres drilled the profile is basically symmetrical, thereafter, greater wear appears to generate on the inside section.

#### 4.18.2. Core Bit "B".

At the outset of the drill trials with this core bit, it was envisaged that the test programme would follow the same format as with core bit "A" with only minor adjustments to the drilling parameters used. However

**Figure 4.12**

**Performance characteristic for core bit 'B' in sandstone at a constant rotational speed**

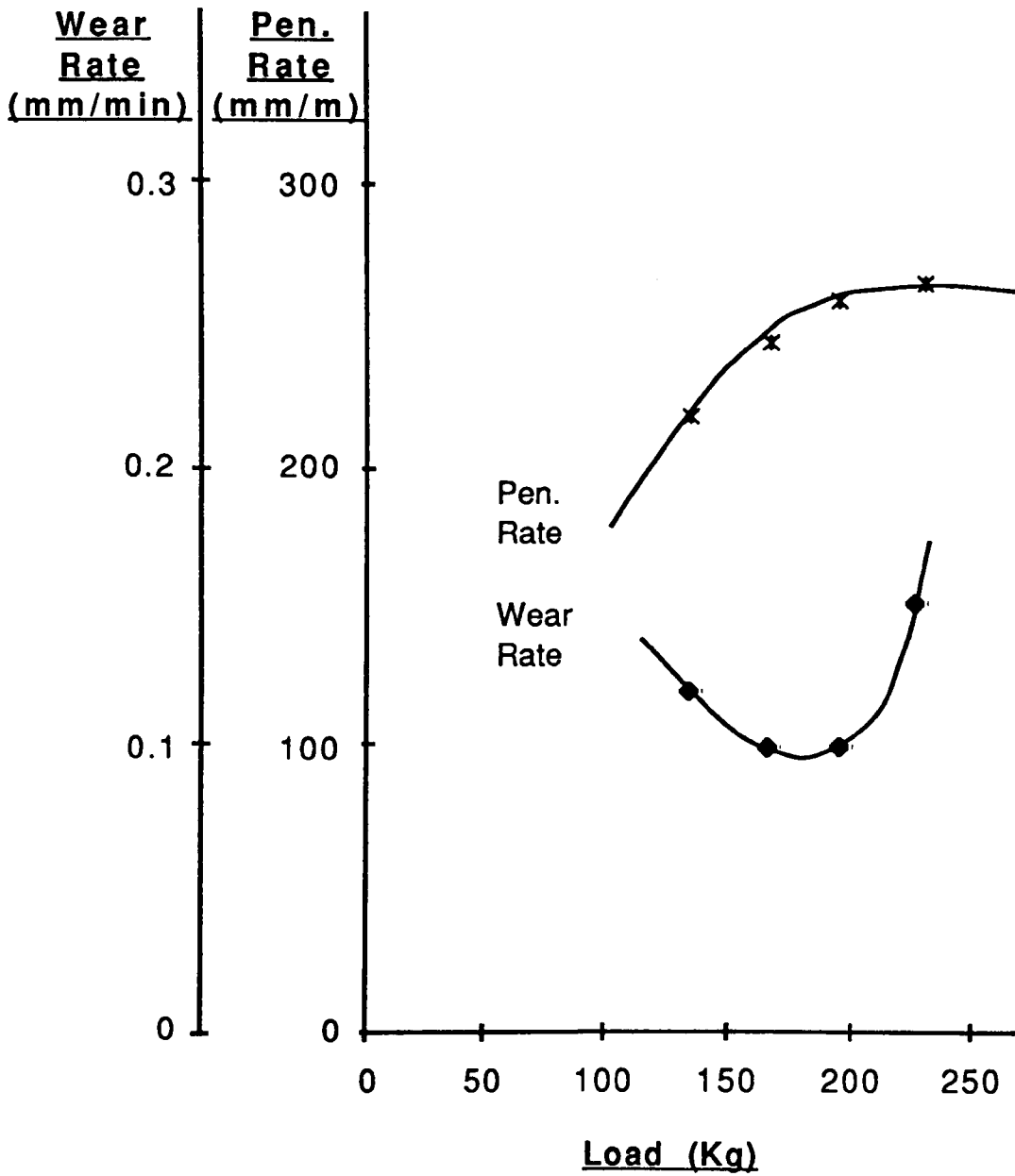
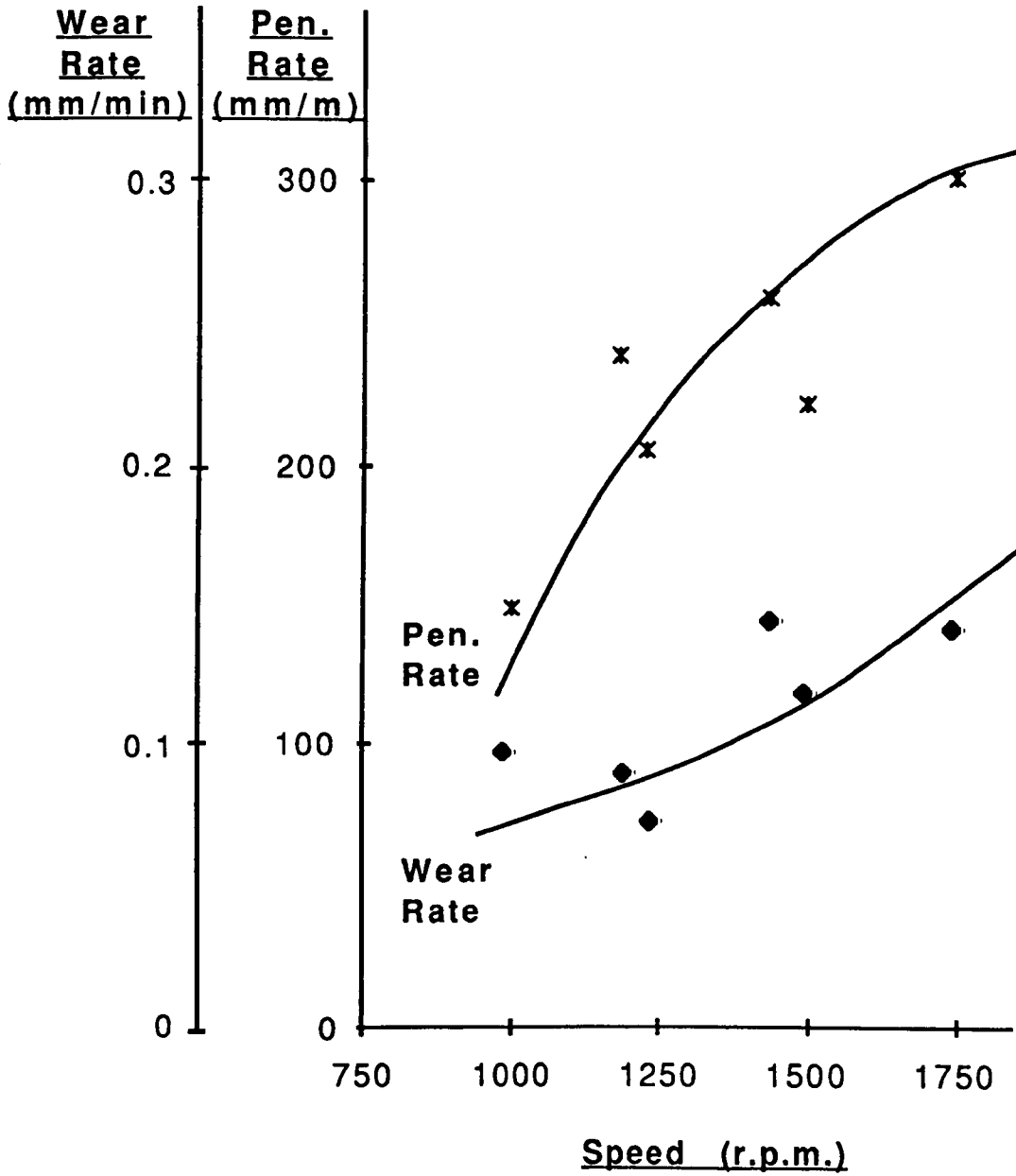


Figure 4.13

Performance characteristic for core bit 'B'  
in sandstone at a constant load on bit



difficulties were encountered in achieving a satisfactory drilling condition in the Swedish granite.

Subsequent inspection of the core bit under a microscope revealed certain defects, the nature of which appeared to result from the graphitization of the SDA100 diamonds. This was difficult to confirm with any degree of confidence as there was no evidence of overheating taking place during the core drilling process.

Therefore, in order to continue with the test programme, it was decided to resume the tests with this core bit in the sandstone. The subsequent test programme permitted an investigation of both load and rotational speed on cutting efficiency and as expected, the results show the marked influence these parameters have on drill bit performance and the rate of wear. These tests were proved to be satisfactory and it was possible to ascertain the best drilling parameters by altering the load on the bit whilst maintaining the rotational speed and water flush rate constant. Similarly, tests were carried out with speed and flush rates constant, with changes in bit load. The results obtained with this core bit when coring the coarse grained abrasive sandstone are shown in Figures 4.12 and 4.13. Figure 4.12. shows penetration rate and wear rate plotted against load on

the bit with a constant speed of 1500 rev/min and a flush rate of 11 l/min. It can be seen from this graph that the apparent best operating load at this speed is a load of 237 kg giving a penetration rate of 260 mm/min with a wear rate of 0.09 mm/metre drilled. Furthermore, with a constant speed of 1500 rev/min, and incrementally increasing the load up to about 200kg, penetration rates increase but with declining rates of bit wear. The deviation from this trend and could be attributed to some degree of recutting.

This trend however, did not hold when the load was held constant at 200kg. Figure 4.13. shows the trend to be a steady increase in wear rate with increasing speed, although up to about 1250 rev/min, it did appear to follow the same trend as with a constant load. This could be attributed to insufficient load or increased cutting velocities contributing to excessive abrasive wear.

Figure 4.13. illustrates penetration rate and wear rate plotted against speed with constant a load of 145 kg. and a flush rate of 11 l/min. From this graph it would appear that the best operating speed for this bit is 1500 rev/min.

During this test programme, a natural semi-round profile had been developed on the core bit and the condition of the bit appeared to be greatly improved. Consequently, at this stage it was considered



advantageous to resume tests in the Swedish granite and the results obtained are shown in Figure 4.11.

The tests proved to be satisfactory and it was possible to ascertain the best drilling parameters by altering the load on the bit whilst maintaining the rotational speed and water flush rate constant.

The results obtained when coring the Swedish granite are shown in Figure 4.11. and illustrates penetration rate and wear rate plotted against load on the bit with a constant speed of 1500 rev/min and a flush rate of 11 l/min. It can be seen from this graph that the apparent best operating load at this speed is 200 kg giving a penetration rate of 75 mm/min with a wear rate of 0.35mm/metre drilled.

#### 4.19. Conclusions.

The objectives of the investigation was to determine performance and wear characteristics of the two coring bits in hard rock i.e. Swedish granite and a moderately strong, highly abrasive rock. The two core bits were essentially identical apart from their diamond concentration, core bit "A" being 40 concentration and core bit "B" 45 concentration.

The planned test programme for drill bit "A" was carried out without any significant deviation and the results obtained have been noted.

The test programme for drill bit "B" however, received a severe setback due to the extraordinary characteristics of the apparent damage to the hard indenters, which appeared to result from graphitization. This damage or degradation was manifested by severe pitting and with some plucking on the inside section of the core bit. Under microscopic examination, there was no indication of the characteristic wear flats normally associated with these types of core bits.

The problem however, was particularly disturbing in view of the fact that this type of damage is normally associated with overheating and could not be traced to the actual coring process. This being supported by the test programme while changing the load on the bit, which appeared to discount the possibility of over loading. This was further supported by the fact that similar parameters were used when coring 50 mm diameter specimens used to determine the physical properties of the Swedish granite. This core bit was manufactured from the same grade of polycrystalline material i.e. SDA100 with a 50 concentration.

Both "A" and "B" core bits appeared to be greatly influenced by the naturally generated profile and not withstanding the degradation to the indenters, this phenomenon must be regarded as an important contributory factor with the cutting efficiency of the

core bit. There was a clear indication that as this profile developed from flat to semi-round both penetration rate and the rate of tool wear improved significantly.

The condition and physical properties of the rock material can significantly affect drilling performance and it was clear that the lower diamond concentration of core bit (A) was much more efficient in the Swedish granite than core bit (B). The rate of penetration therefore, appears to be greatly influenced by both hardness and physical strength whereas the abrasiveness of the rock affects cutting efficiency as a result of abrading the matrix material and thus ensuring a constant rate of new diamond exposure. It can be seen in Table 4.1. that the abrasiveness of the two rock samples were relatively similar, e.g. 3.9 for the Swedish granite and 3.6 for the sandstone. It would appear therefore, that the two rocks employed for the test programme, while similar in relative abrasiveness were markedly different in physical strength and hardness. Consequently, tool bit design must have regard to these physical properties and consideration given to both diamond concentration and matrix hardness that will ensure an economical compromise between penetration rate and wear rate.

It should be noted however, that any attempt to assess the quality of a new core bit design, requires a large

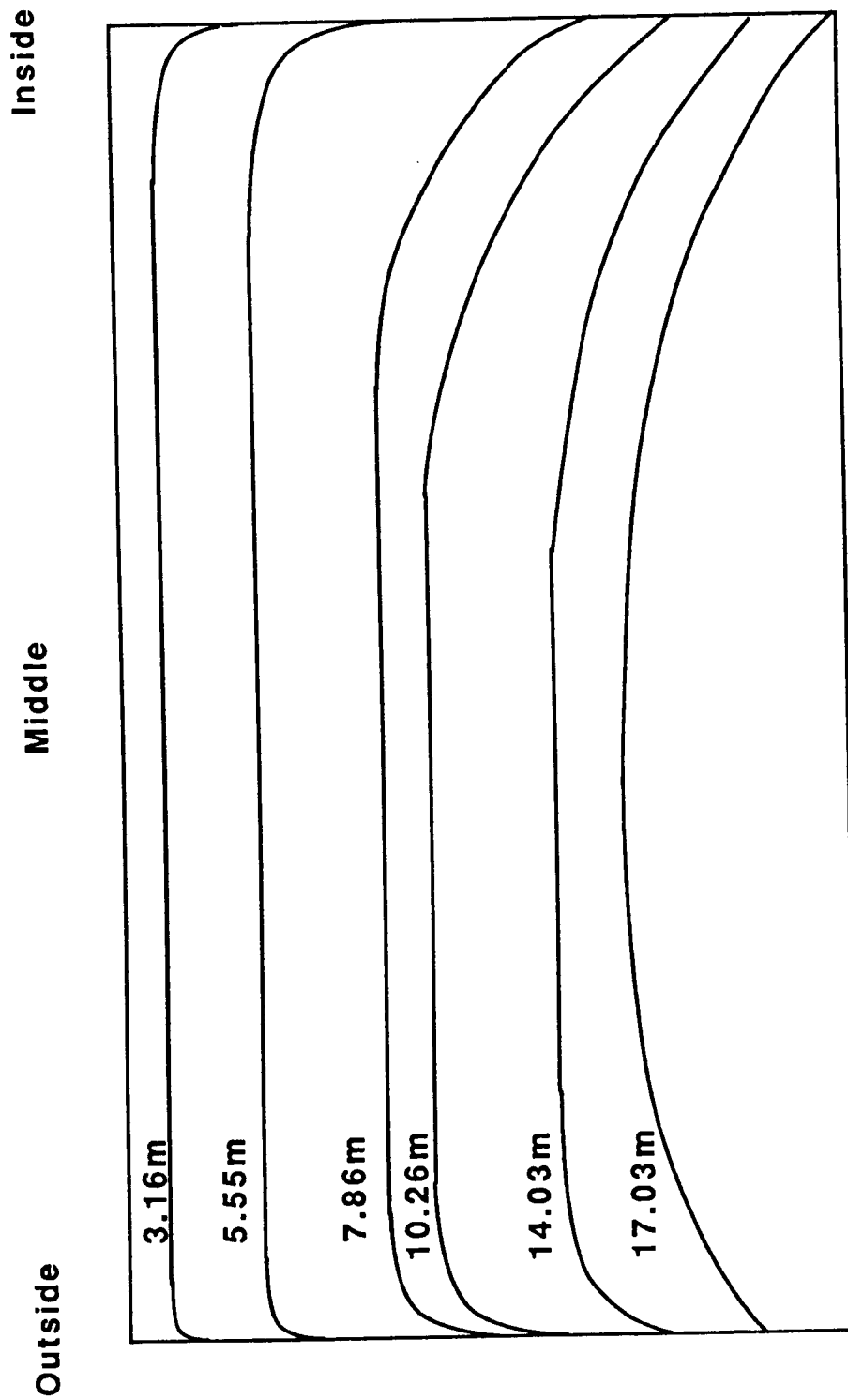


**Fig 4.14 Variation in bit profile with distance drilled**

# UNIVERSITY OF NOTTINGHAM

## DEPARTMENT OF MINING ENGINEERING

### DRILL BIT TEST REPORT: CA1

DATE OF TEST.....5/2/87  
MANUFACTURER.....CRAELIUS  
BIT TYPE.....IMP  
BIT SIZE.....38/22  
DIAMOND.....SDA100  
CONCENTRATION.....45  
MATRIX.....X99  
FLUSH MEDIA.....WATER  
ROCK TYPE.....GNEISS

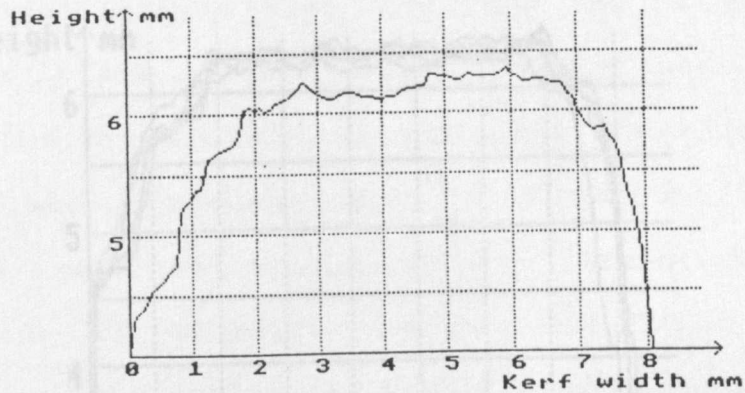
TIME	DISTANCE DRILLED	FLUSH RATE	TORQUE	SPEED	LOAD
sec	mm	l/min	Nm	rpm	kN
0.00	0.00	13.16	69.64	76.32	2624.00
30.00	40.75	11.69	42.85	2002.00	2591.20
60.00	83.62	11.69	44.15	2007.00	2607.60
90.00	124.05	12.88	40.86	2012.00	2591.20
120.00	162.66	12.79	40.86	2014.00	2607.60
150.00	208.62	11.26	42.86	2007.00	2607.60
180.00	233.80	13.07	43.16	2012.00	2607.60
187.00	233.80	12.50	2.45	104.94	2640.40
DATA LOGGING HELD					
188.00	233.96	10.82	1.16	391.14	2624.00
210.00	262.30	12.00	41.15	2012.00	2591.20
240.00	306.43	12.10	41.15	2011.00	2591.20
270.00	349.57	13.25	45.15	1997.00	2591.20
300.00	393.43	10.82	43.45	2000.00	2591.20
332.00	436.64	12.40	0.37	100.17	2591.20
DATA LOGGING HELD					
333.00	435.60	11.37	1.00	343.44	2624.00
360.00	469.68	10.71	42.44	2007.00	2591.20

TOTAL TIME OF TEST 372.00 seconds  
DISTANCE DRILLED DURING TEST = 483.57 mm  
AVERAGE PENETRATION RATE = 78.21 mm/min  
TOTAL DISTANCE DRILLED BY BIT = 2470.52 mm

Figure 4.15.

## PROFILE MEASUREMENT ANALYSIS CA1

DATE OF TEST.....5/2/87  
MANUFACTURER.....CRAELIUS  
BIT TYPE.....IMP  
BIT SIZE.....38/22  
DIAMOND.....SDA100  
CONCENTRATION.....45  
MATRIX.....X99  
FLUSH MEDIA.....WATER  
ROCK TYPE.....GNEISS



Test No 12

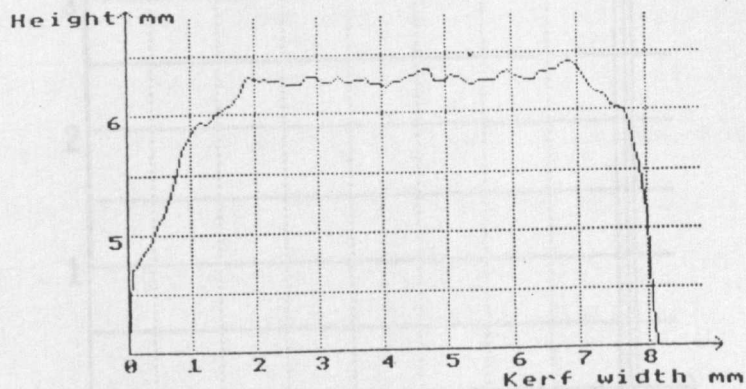


Figure 4.16.

## PROFILE MEASUREMENT ANALYSIS CA1

DATE OF TEST.....5/2/87  
MANUFACTURER.....CRAELIUS  
BIT TYPE.....IMP  
BIT SIZE.....38/22  
DIAMOND.....SDA100  
CONCENTRATION.....45  
MATRIX.....X99  
FLUSH MEDIA.....WATER  
ROCK TYPE.....GNEISS

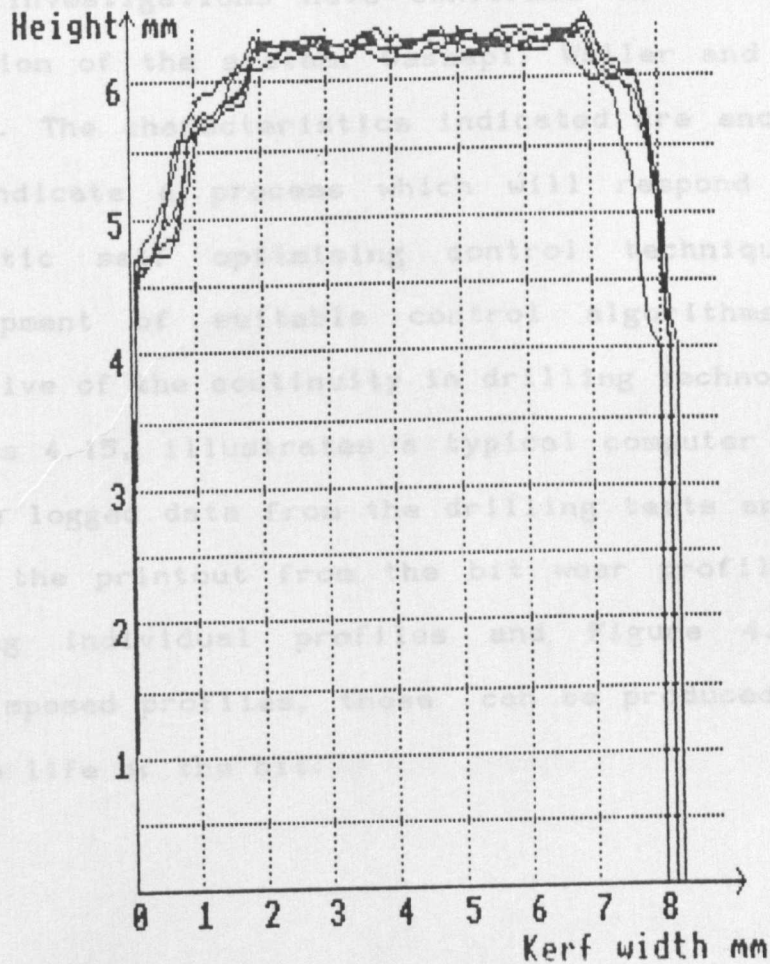


Figure 4.17.

number of tests with a variety of rock strata type together with an adequate number of sample bits.

The rig and monitoring system used to investigate the drilling performance of diamond impregnated core bits in differing rock types. The results obtained from these investigations have confirmed the satisfactory operation of the system. Cassapi, Waller and Ambrose. (1987). The characteristics indicated are encouraging and indicate a process which will respond well to automatic self optimising control techniques. The development of suitable control algorithms is an objective of the continuity in drilling technology.

Figures 4.15, illustrates a typical computer printout of the logged data from the drilling tests and Figure 4.16. the printout from the bit wear profile device showing individual profiles and Figure 4.17. the superimposed profiles, these can be produced for the entire life of the bit.



## **CHAPTER 5.**

### **FACTORS INFLUENCING THE SAWABILITY OF STONE.**

## CHAPTER 5.

### FACTORS INFLUENCING THE SAWABILITY OF STONE.

#### 5.1. Introduction.

The increasing demand for stone products has inevitably led to the opening of numerous new stone quarries all over the world. As a result of this expansion, the variety of stone type has increased and stones hitherto regarded as uneconomical to cut are now being more frequently exploited. This however, can present major problems when attempting to predetermine the correct diamond type and bond specifications for the diamond impregnated wheels used to cut these materials. Consequently, it has been difficult to make precise judgements on these parameters without the use of extensive machine trials in order to establish the sawability of any given stone type. Various attempts have been made to predetermine these factors, but this work has always involved costly and time consuming procedures.

This chapter describes the work carried out at the University of Nottingham to examine the relationship between the various rock properties and to attempt to

correlate these properties with actual sawing trial performances.

The practical sawing trials were carried out at the De Beers Industrial Diamond Division's Technical Services Centre at Charters, Sunninghill, Ascot, England.

The rock tests included a number of physical property tests and indices together with thin section petrological analysis of the rocks used.

The objective of this project was to suggest a more rapid and practical method for evaluating the sawability of stone.

#### **5.2. Sample Material Mineralogy and their Proportions.**

A selection of sample materials was supplied by De Beers and these comprised of seven Italian granites and one fine grained sedimentary sandstone. The granites being representative of the most difficult rock material to be sawn by stone cutting machines fitted with diamond impregnated wheels. The sandstone was chosen as an easily machinable rock and was used to show the degree of variation in cutting forces and wear rates when compared with the more difficult granite type of rock.

The rocks used for this experimental programme are listed as follows:

Sample No.	Mean Mohs hardness	Rock type	Quartz % Size (mm)	Plagioclase % Size (mm)	Orthoclase % Size (mm)	Other %
1	5.85	Grey Granite	15 1-4	40 1-5	35 3-10	10
2	6.05	Pink Granite	20 0.5-5	20 0.7-2	- -	50
3	5.63	Larvekite	- -	- -	80 4-7	20
4	6.05	Red Granite	30 3-8	13 1-6	50 1-1.5	7
5	4.76	Diorite	20 0.1-0.4	45 0.5-1.5	- -	35
6	6.38	Gabbro	- -	50 1-8	- -	50
7	6.32	Red Granite	25 0.5-3	20 1.5-5	55 2-6	-
8	5.9	Sandstone	70 0.125-0.25	(30% in cement)	- -	30

Table 5.1. : Mineralogy and Proportions

### Rock Sample.

- 1) Grey granite.
- 2) Pink granite.
- 3) Laurvekite.
- 4) Red granite.
- 5) Diorite.
- 6) Gabbro.
- 7) Red granite.
- 8) Sandstone.

In hand, all the sample material was found to be competent and in good condition, with no obvious evidence of weathering or chemical alteration.

In thin section, only those hard minerals mainly responsible for the problems associated with sawability were considered and these were determined as quartz and feldspars i.e. plagioclase and orthoclase, these minerals having a Moh's hardness of 7, 6.5 and 6 respectively.

Table 5.1. illustrates the main mineral constituents, their proportions and grain size. The mean Moh's hardness for the whole rock sample is also given.

### 5.3. Mechanical Tests.

In addition to petrological analysis of thin sections of each of the rock samples tested, a number of

GREGORI BRIDGE SAW.



Figure 5.1.

TABLE 5.2  
SUMMARY OF MECHANICAL PROPERTIES

Sample No	C <sub>2</sub> Specific Wear mm/m <sup>2</sup>	C <sub>15</sub> Cutting Force N	C <sub>3</sub> Shore Scleroscope Index	C <sub>4</sub> Cone Indenter	C <sub>5</sub> Cerchar Index	C <sub>6</sub> Compressive Strength MPa	C <sub>7</sub> Tensile Strength MPa
1	0.129	980	91.77	12.49	3.46	166.5	8.06
2	0.064	780	94.4	7.98	3.60	174.7	7.52
3	0.055	780	92.0	13.84	3.58	192.27	8.78
4	0.204	1075	98.90	16.04	2.84	158.88	6.87
5	0.030	700	81.08	9.89	3.75	194.77	11.89
6	0.085	830	82.00	14.04	3.32	211.80	12.51
7	0.124	915	97.1	12.43	3.98	190.06	10.89
8	0.019	300	42.5	2.77	2.12	83.68	4.52
Mean Values	0.08875	795	84.96	11.18	2.84	171.58	8.88

physical property tests were conducted and these consisted of the following tests:

- a) Uniaxial compressive strength.
- b) Tensile strength.
- c) Shore scleroscope hardness index tests.
- d) NCB cone indenter hardness index tests.
- e) Cerchar abrasive index tests.
- f) Specific wear tests on diamond impregnated saw blades.
- g) Cutting forces

Table 5.2. illustrates the results obtained from these mechanical tests.

#### 5.4. Sawing Trials.

The sawing trials were carried out on a Gregori bridge saw and is illustrated in Figure 5.1. The machine is powered by a 95 kW d.c. electric motor and is fitted with a thyristor variable speed control system with a variable range of speeds between 350 rev/min and 4350 rev/min.

This machine is capable of operating at a constant sawing rate or with a constant pre-set power level, 'which may result in a variable cutting rate'. The head traverse speed is variable between 0.3 mm/min and 14 mm/min. Throughout the test programme, the data on power, traverse speed and rotary speed were constantly



monitored on a potentiometric chart recorder. Cutting forces were measured on a specially designed force table attached to the main frame machine table.

### 5.5 Force Table.

The force table was mounted on the machine's main frame table, on flat ball bearings, placed between the force table and the vertical transducers to overcome frictional resistance and to enable the forces in the three mutually perpendicular directions to be measured.

The cutting forces were measured by means of sealed piezo-electric transducers mounted on the tool holder. The cutting forces were measured by means of sealed piezo-electric transducers mounted on the tool holder. The cutting forces were measured by means of sealed piezo-electric transducers mounted on the tool holder. The cutting forces were measured by means of sealed piezo-electric transducers mounted on the tool holder.

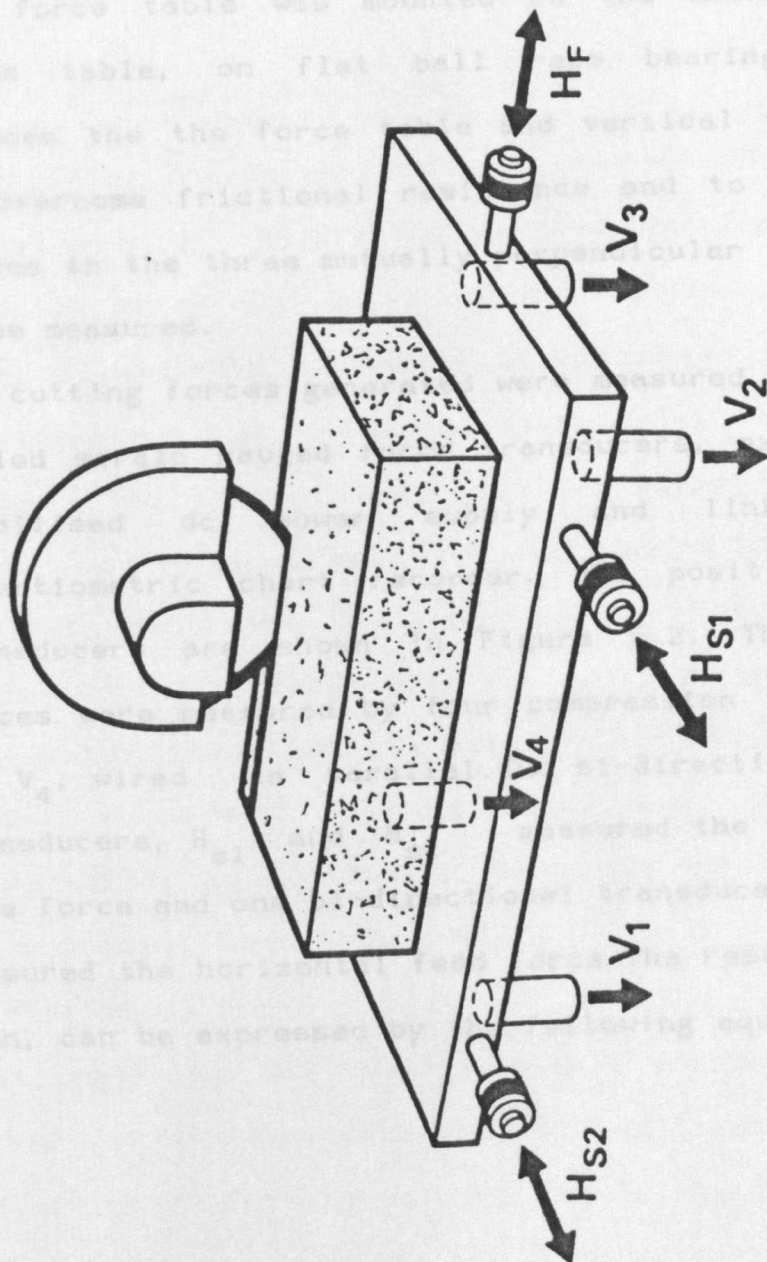


FIGURE 5.2

Arrangement of Load Cells

monitored on a potentiometric chart recorder. Cutting forces were measured on a specially designed force table attached to the main frame machine table.

#### 5.5. Force Table.

The force table was mounted on the machine's main frame table, on flat ball race bearings, placed between the the force table and vertical transducers  $\chi$  to overcome frictional resistance and to enable the forces in the three mutually perpendicular directions to be measured.

The cutting forces generated were measured by means of sealed strain gauged force transducers, excited by a stabilised dc power supply and linked to a potentiometric chart recorder. The position of the transducers are shown in Figure 5.2. The vertical forces were measured by four compression transducers,  $V_1 - V_4$ , wired in parallel. Two bi-directional transducers,  $H_{s1}$  and  $H_{s2}$  measured the horizontal side force and one bi-directional transducer,  $H_f$ , measured the horizontal feed force. The resultant force then, can be expressed by the following equation.

$$F_r = \sqrt{F_v^2 + F_h^2}$$

Where  $F_r$  = The resultant force.

and the direction of  $F_r$ , the angle  $\theta$ , as

$$\theta = \arctan \frac{F_v}{F_h}$$

(Eq 5.1)

### 5.6. Preliminary Investigations.

Preliminary investigations were carried out to assess the effects of cutting forces when varying the table traverse speed and depth of cut, while at the same time, maintaining a similar cutting rate in both the upcutting and downcutting directions.

However, it is of importance to study the cutting action and mode of wear on the diamond saw blade in order to determine the properties or functions which influence the efficiency of the cutting operation.

The German Industrial Standard DIN 8589, defines the sawing of natural rock or stone when using diamond bonded grit, as a slitting operation within the group of processes known as cutting with a geometrically indeterminate edge.

When analysing the cutting action and mode of wear, Buttner (1974), proposed that to facilitate a constant and efficient cutting action, the matrix material must wear at the same rate as the diamond grit. Thus, when the diamond cutting edge becomes worn, new grit will



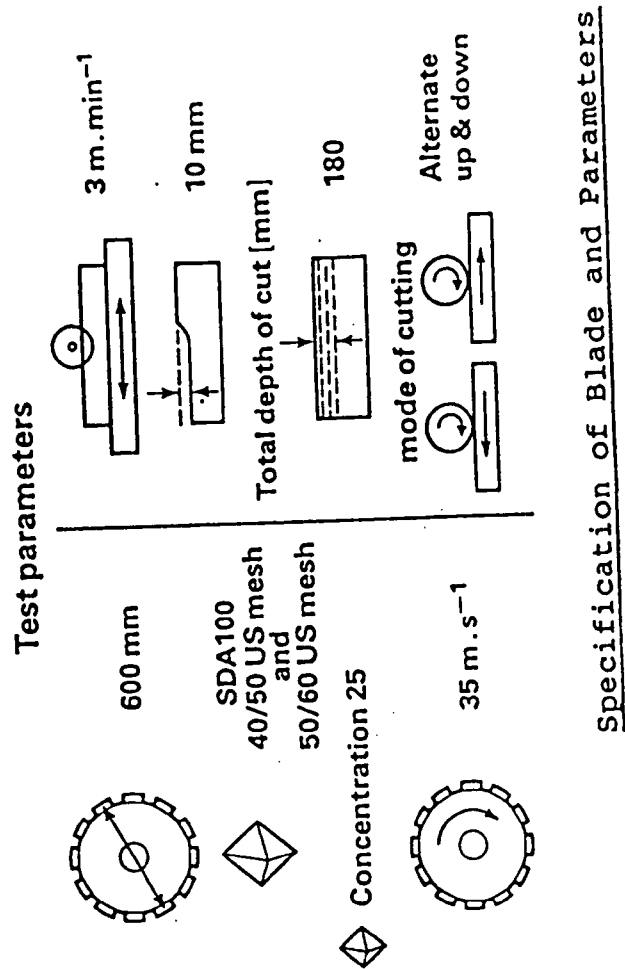


Figure 5.3

$v_s$ = Blade peripheral speed	mm/min
D = Diameter of blade	mm

### 5.7. Blade Specifications.

Based on the experience gained from previous work carried out at Charters, a blade of 600 mm diameter containing high quality synthetic diamonds was chosen. The diamonds (SDA100) were sized at 30-40 U.S. mesh with a 30 concentration, where a 100 concentration equals 4.4 carats of diamonds per cubic centimetre of matrix volume. These diamonds were chosen because of their high quality and strength, consequently, any variations due to the degradation of diamond specification could be ignored, thus permitting all the sample material to be sawn at the same cutting rate, 'even when sawing the hardest granite'. The linear peripheral cutting speed of the blade was 2100 m/min and the cutting rate was set at 300 cm/min, Thus permitting all the material to be sawn at the same cutting rate to enable a direct comparison of results to be made. The cutting rate was achieved by using a traverse rate of 3m/min and a depth of cut of 10mm. These parameters and blade specifications are illustrated in Figure 5.3.

TABLE 5.3.

Dependent and Independent Variables Used in  
Statistical Analysis.

Dependent Variables	Independent Variables	Symbols
Specific	Shore Scleroscope No.	C3
Wear	Cone Indenter No.	C4
Rate	Cerchar Index No.	C5
(C2)	UCS. MPa.	C6
	UTS. MPa.	C7
Cutting	Mean Moh's Hardness.	C8
Force	Mean Quartz Grain Size.	C9
(N)	Quartz Percentage.	C10
(C15)	Plagioclase Grain Size.	C11
	Plagioclase Percentage.	C12
	Orthoclase Grain Size.	C13
	Orthoclase Percentage.	C14

## **5.8. Presentation and Discussion of Results.**

The specific mean wear rates for the saw blade when cutting various rock types is governed by the physical, mineralogical and mechanical properties of rocks. Consequently, this section deals with the identification, interpretation and analysis of these factors. This was conducted to assess the sawability of rocks by the process of diamond sawing when using impregnated diamond wheels.

A laboratory test program was initiated to obtain basic data required for the statistical interpretation of the contributing factors. Table 5.1. shows the mineralogy and mean Moh's hardness of the various rocks selected and a summary of the index tests is presented in Table 5.2. These tests were considered to relate closely to those factors having the greatest influence on blade wear and the required cutting forces.

### **5.8.1. Statistical Analysis of the Data Base.**

In order to facilitate the analysis and interpretation of the results, it was useful to classify the data into independent and dependent variables. The observed wear rate and cutting forces were a function of rock petrology, mineralogy and the intrinsic mechanical properties of the rock. Table 5.3. Thus, factor



analysis was accomplished by correlating the specific wear rate values, referred to as 'dependent' variables. Petrological and index properties of rock are referred to as 'independent' variables. The data was then analysed using standard statistical routines in the following discrete steps.

- 1) Attempt to develop tentative relationships between observed wear rates and individual mineralogical and index properties of rock by statistical factor analysis.
- 2) Evaluate the combined effect of the most dominant individual mineralogical and index properties on the wear potential of saw blades by means of multiple regression analysis.
- 3) Isolation of the most important factors contributing to wear by further analysis of the multiple regression equation.

#### **5.8.2. Factor Analysis to Evaluate Specific Wear.**

As a preliminary step in the factor analysis, the data was analysed using the standard statistical program 'Minitab' developed by Penn State University (1981) for ICL 2900 series main frame computers. Data was analysed to calculate if individual rock parameters could be linearly correlated to a specific wear potential of rock and to determine the degree of

TABLE 5.4  
CORRELATION COEFFICIENTS BETWEEN SPECIFIC WEAR AND VARIOUS PARAMETERS

	C <sub>2</sub>	C <sub>3</sub>	C <sub>4</sub>	C <sub>5</sub>	C <sub>6</sub>	C <sub>7</sub>	C <sub>8</sub>	C <sub>9</sub>	C <sub>10</sub>	C <sub>11</sub>	C <sub>12</sub>	C <sub>13</sub>	C <sub>14</sub>
	Specific Wear	Shore Scleroscope	Cone Indenter Hardness	Cerchar Abrasivity Index	UCS Mpa	UTS Mpa	Moh's Hardness	Mean Quartz Grain Size mm	Quartz Percentage	Plagioclase Grain Size	Plagioclase Percentage	Orthoclase Grain Size	Orthoclase Percentage
Shore Scleroscope	0.641												
Cone Indenter Hardness	0.717	0.801											
Cerchar Abrasivity Index	0.064	0.737	0.457										
UCS	0.140	0.755	0.649	0.869									
UTS	-0.037	0.401	0.484	0.735	0.834								
Moh's Hardness	0.461	0.143	0.188	-0.150	-0.019	-0.132							
Mean Quartz Grain Size	0.841	0.530	0.374	-0.078	-0.060	-0.363	0.287						
Quartz Percentage	-0.170	-0.721	-0.741	-0.74	-0.916	-0.701	0.004	0.095					
Plagioclase Grain Size	0.723	0.475	0.637	0.213	0.410	0.447	0.574	0.412	-0.361				
Plagioclase Percentage	-0.219	-0.324	-0.181	-0.013	0.073	0.430	-0.145	-0.319	-0.006	0.367			
Orthoclase Grain Size	0.307	0.422	0.420	0.367	0.132	-0.007	0.063	0.060	-0.361	-0.033	-0.345		
Orthoclase Percentage	0.048	0.361	0.348	0.457	0.240	0.122	0.047	-0.212	-0.394	-0.182	-0.561	0.854	-

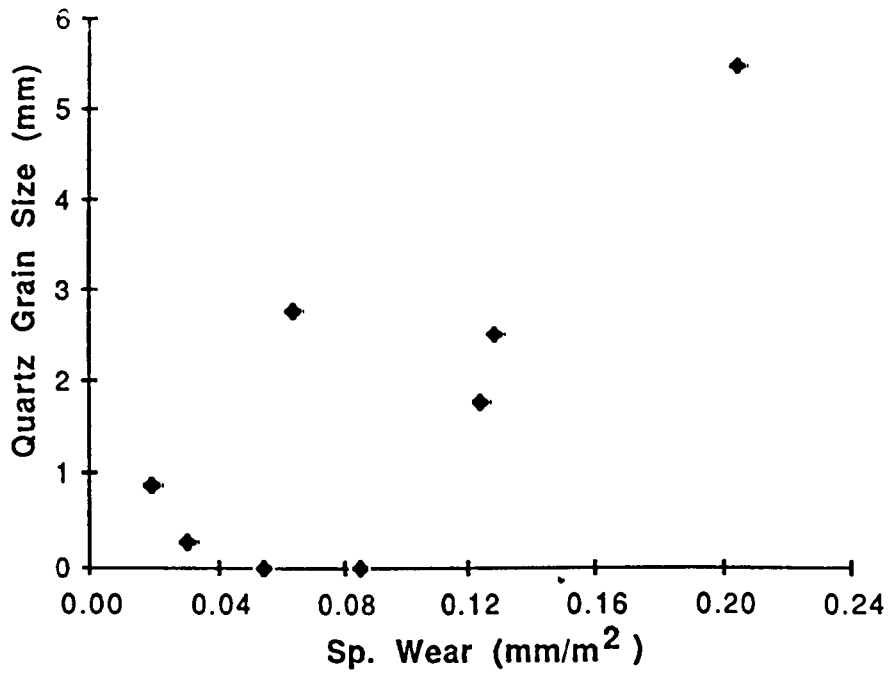
correlation. Table 5.4. show correlation coefficients between independent and dependent variables. It can be seen that there is a tentative linear correlation between specific wear rates (mm/m ) and quartz grain size, plagioclase grain size, mean Moh's hardness and NCB cone indenter and Shore scleroscope indices.

#### 5.8.3. Specific Wear Rates and Mineralogical Factors

The specific mean wear rates for the saw blade and associated relative mineralogical factors when cutting the various rock samples are presented in Tables 5.1. and 5.4.

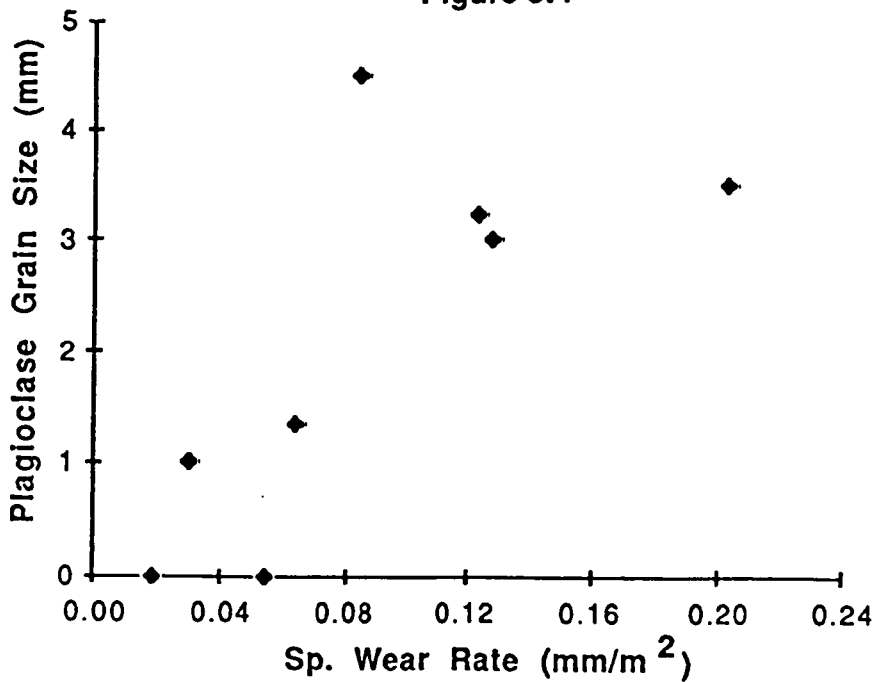
It can be seen that when cutting the hardest red granite (4), approximately 58% more wear over the next hardest rock i.e grey granite (1) was observed. The confidence limits indicated no significant difference between samples 1 and 7. Samples 2 and 3 were also found to be very similar. As anticipated, sample 8, the York sandstone, produced the least amount of wear, which was a significant 90% less than the red granite (4).

However, when examining these wear results with reference to the mineral composition presented in Tables 5.1 and 5.4. It is difficult to see any direct relationship between wear and the percentage of hard minerals present within the rock samples. Furthermore,



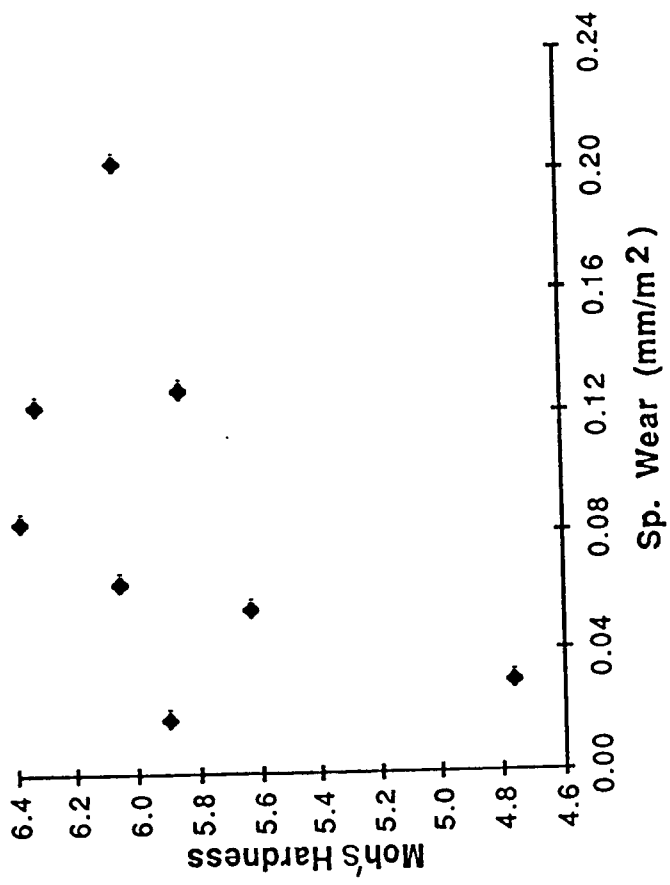
Scatter Plot Between Specific Wear Rate and Main Quartz Grain Size

Figure 5.4



Scatter Plot Between Specific Wear Rate and Main Plagioclase Grain Size

Figure 5.5



Scatter Plot Between Specific Wear and Moh Hardness

Figure 5.6

it is contrary to the established practice of the stone sawing industry to use percentage quartz content as a guideline to sawability. Figures 5.4 and 5.5. show a tentative correlation between quartz and plagioclase grain size with specific wear of the saw blade and it can be seen in Figure 5.6. that there is some correlation ( $R = 0.461$ ) between specific wear and the mean Moh's hardness number.

It would appear therefore, that when considering the various rock properties related to sawability, equal weight should be given to grain size and the mean Moh's hardness. For example, although the mean Moh's hardness for the granite samples 1,2,4 and 7. are all similar e.g. 5.85, 6.05, 6.05 and 6.32 respectively, the grain sizes are however, significantly different. These range from 1.0 - 4.0 mm, 0.5 - 5.0 mm, 3.0 - 8.0 mm, and 0.5 - 3.0 mm. Although this evidence is not conclusive, it can be seen that the rock samples which have a significantly larger range of grain sizes in the hard band of minerals. produce the higher rates of specific wear.

Furthermore, although the relationship between cutting force and grain size may not be a linear one, the same conclusions can also be drawn when considering cutting forces required, 'where there is a high percentage of large hard mineral grains present, the cutting force

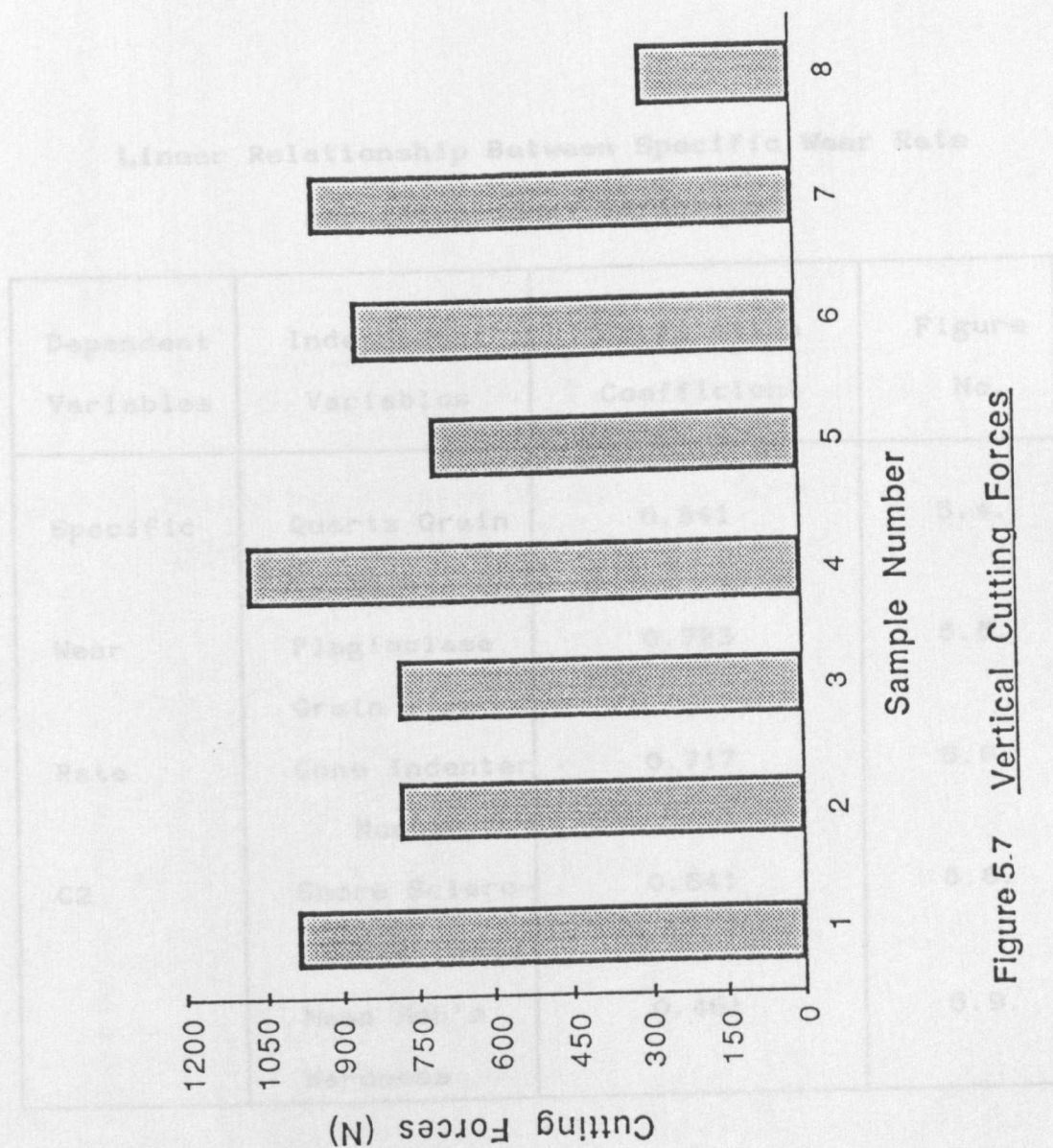


Figure 5.7 Vertical Cutting Forces

**TABLE 5.5.**

**Linear Relationship Between Specific Wear Rate  
And Independent Variables.**

Dependent Variables	Independent Variables	Correlation Coefficient	Figure No.
Specific Wear Rate C2	Quartz Grain Size	0.841	5.4.
	Plagioclase Grain Size	0.723	5.5.
	Cone Indenter Number	0.717	5.6.
	Shore Scleroscope Index	0.641	5.8.
	Mean Moh's Hardness	0.461	5.9.



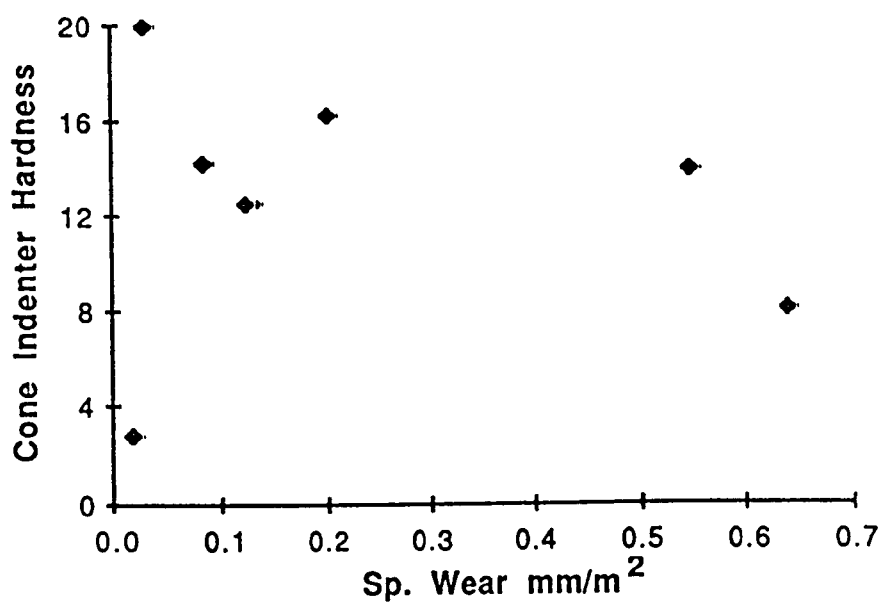


Figure 5.8 Scatter Plot Between Sp. Wear and Cone Indenter Hardness

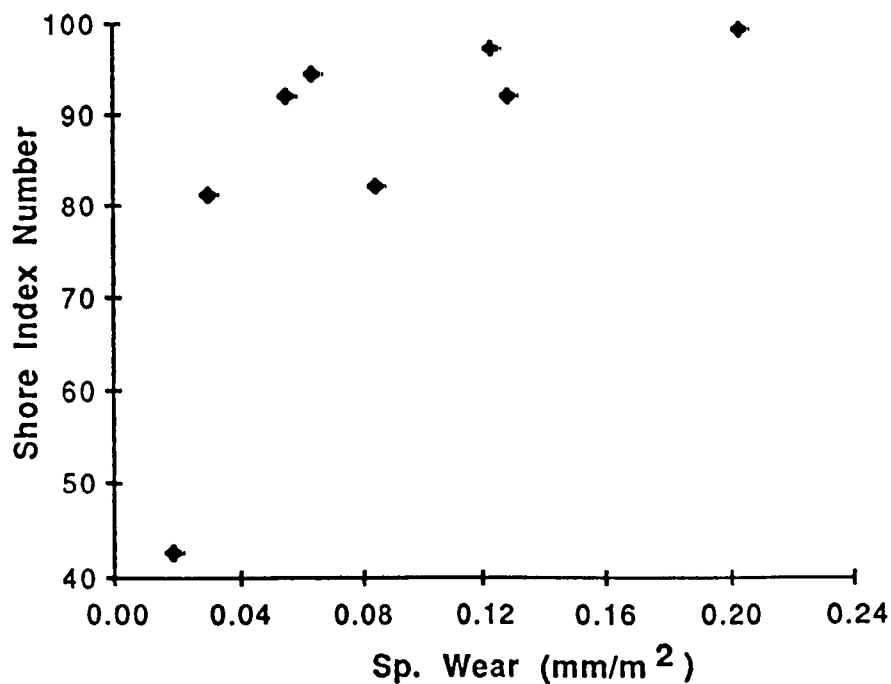


Figure 5.9 Scatter Plot Between Specific Wear and Shore Index Number

required is relatively higher'. This is illustrated in Figure 5.7.

#### 5.8.4. Specific Wear and Physical Properties of Rock.

A summary of the physical properties tests is presented in Table 5.2. These tests were carried out to determine any relationship between the actual cutting trials and the physical properties of the rock material being tested. The Table 5.5 shows only a marginal relationship between the NCB Cone Indenter hardness index number with blade wear (correlation coefficient 0.717) (Fig 5.6.) The relationship between the NCB Cone Indenter and the Shore Scleroscope hardness tests were also tentative ( $R = 0.801$ ) This could be attributed to the large grain sizes, where the Cone Indenter ( $R = 0.717$ ) appears to perform slightly better than the Shore Scleroscope. ( $R = 0.641$ ). Figures 5.8. and 5.9. illustrate scatter plots between specific wear and the NCB Cone Indenter and Shore Scleroscope hardness index number. Physical strength parameters do appear to have some bearing on the cutting forces required and the rate of blade wear, but has no correlation with either UCS or UTS (Table 5.4.) It can be seen that the three strongest rocks produce the highest wear rates and the highest demands on cutting forces, while the sandstone, the

weakest of the rocks tested, falls into the lowest category of consequential wear rates and power demands. The same conclusions can also be said of the tensile strength parameters which exhibited a good correlation with compressive strength. ( $R = 0.834$ ).

The Shore Scleroscope results appear to correlate well with specific wear. A contradiction to this statement could be put forward in consideration of rock samples 6 and 1. The reason for this contradiction could be explained by the major difference in the mineral particle grain size, where the grain size for the Gabbro ranges from 1-8mm of quartz (Moh's hardness 7) for 50% of the rock and the grain size for grey granite is 1-4mm of quartz for 15% and 1-5mm for 40% plagioclase feldspar (Moh's hardness 6-6.5).

#### **5.8.5. Specific Wear and Abrasiveness.**

The results shown in Table 5.4. indicate no correlation between the Cerchar abrasive index and specific wear. Based on the author's experience, it has been found that the Cerchar abrasive index when used with large grained material, tends to reflect the hardness of individual mineral grains, rather than the whole rock abrasiveness. This appears to be a function of the relatively short travel of the stylus (10mm)

TABLE 5.6  
CORRELATION COEFFICIENTS BETWEEN CUTTING FORCES AND VARIOUS PARAMETERS

Factors	Cutting Force N	Specific Wear $\frac{\text{mm}^2}{\text{mm}}$	Shore Hardness	Cone Indenter Hardness	Cerchar Index	Uniaxial Compressive Strength MPa	Uniaxial Tensile Strength MPa	Mohr Hardness	Quartz Grain Size mm	$\psi$ %
Cutting Force N	-	0.846	-	-	-	-	-	-	-	-
Shore Hardness	0.921	0.641	-	-	-	-	-	-	-	-
Cone Indenter Hardness	0.889	0.717	0.801	-	-	-	-	-	-	-
Cerchar Index	0.532	0.064	0.737	0.457	-	-	-	-	-	-
UCS MPa	0.608	0.140	0.755	0.649	0.869	-	-	-	-	-
UTS MPa	0.347	-0.037	0.401	0.484	0.735	0.834	-	-	-	-
Mohr Hardness	0.252	0.461	0.143	0.188	-0.150	-0.019	-0.132	-	-	-
Quartz Grain Size	0.645	0.843	0.536	0.374	-0.078	-0.060	-0.363	0.287	-	-
Quartz %	-0.629	-0.176	-0.721	-0.741	-0.748	-0.916	-0.701	0.004	0.095	-
Palioclase Grain Size	0.703	0.723	0.425	0.637	0.213	0.410	0.447	0.574	0.412	-0.36

TABLE 5.7.

**Linear Relationship between Cutting Force  
and Index Properties of Rock.**

Dependent Variables	Independent Variables	Correlation Coefficient	Figure No.
Cutting Force (N) (C15)	Shore Hardness Number.	0.921	5.10
	Cone Indenter Number.	0.889	5.11
	Plagioclase Grain Size	0.703	5.12
	Quartz Grain Size	0.645	5.13
	Uniaxial Compressive Strength	0.608	5.14
	Cerchar Abrasive Index	0.532	5.15

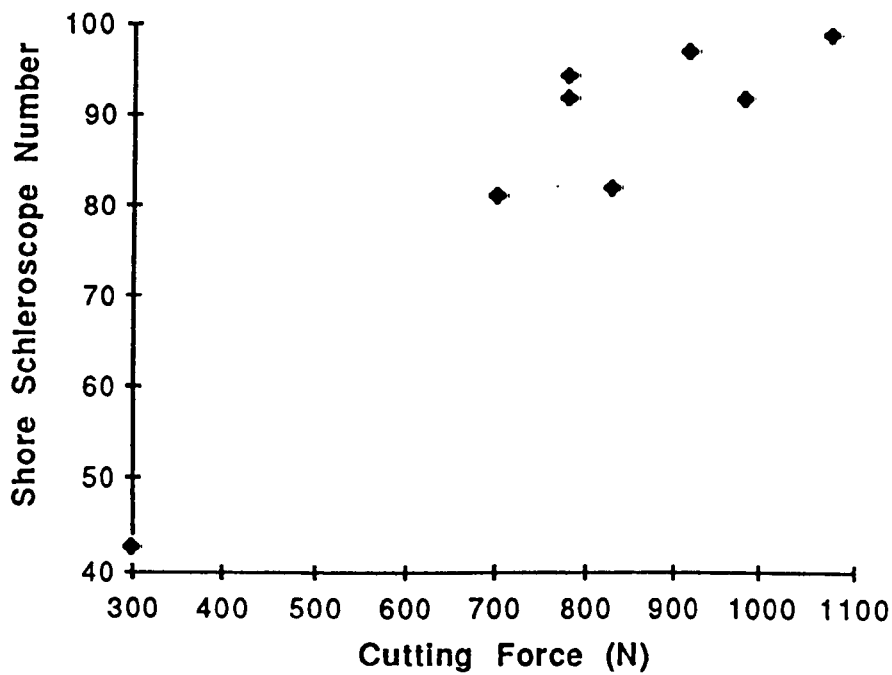


Fig. 5.10 Relationship Between Cutting Force and Shore Hardness Number

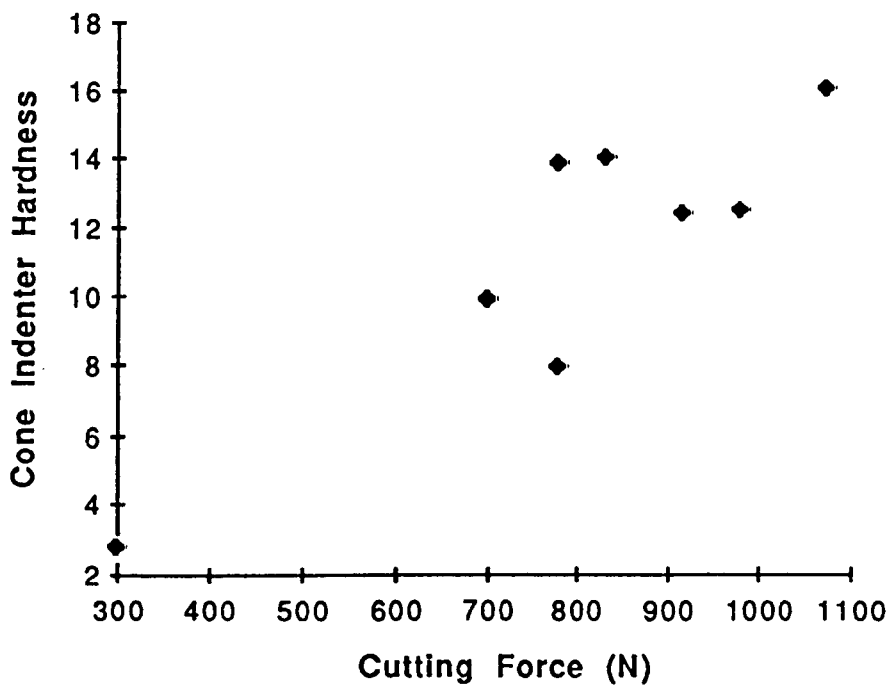


Fig. 5.11 Relationship Between Cutting Force and Cone Indenter Hardness

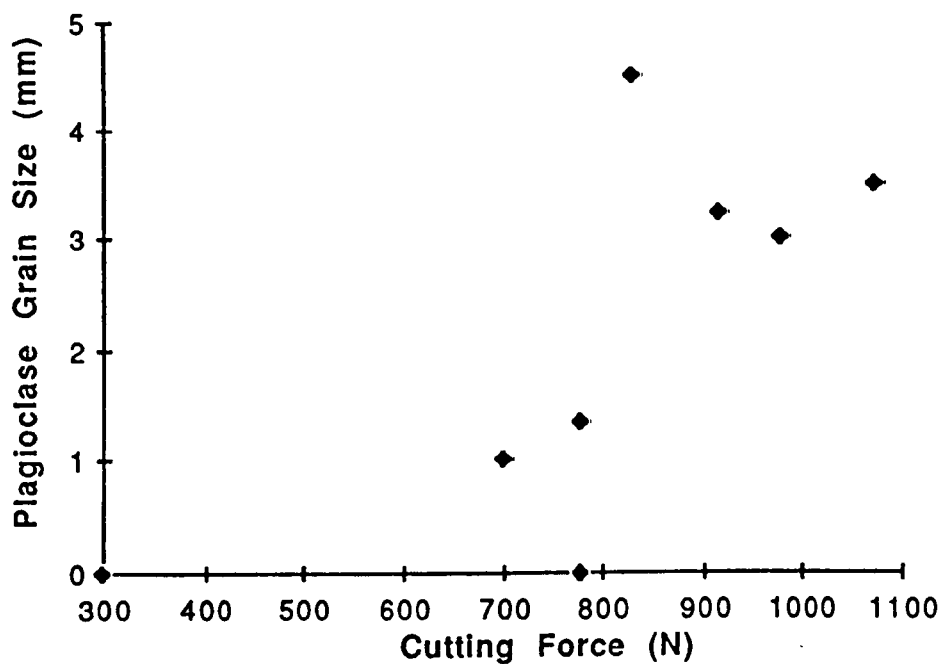


Fig. 5.12 Relationship Between Cutting Force and Plagioclase Grain Size

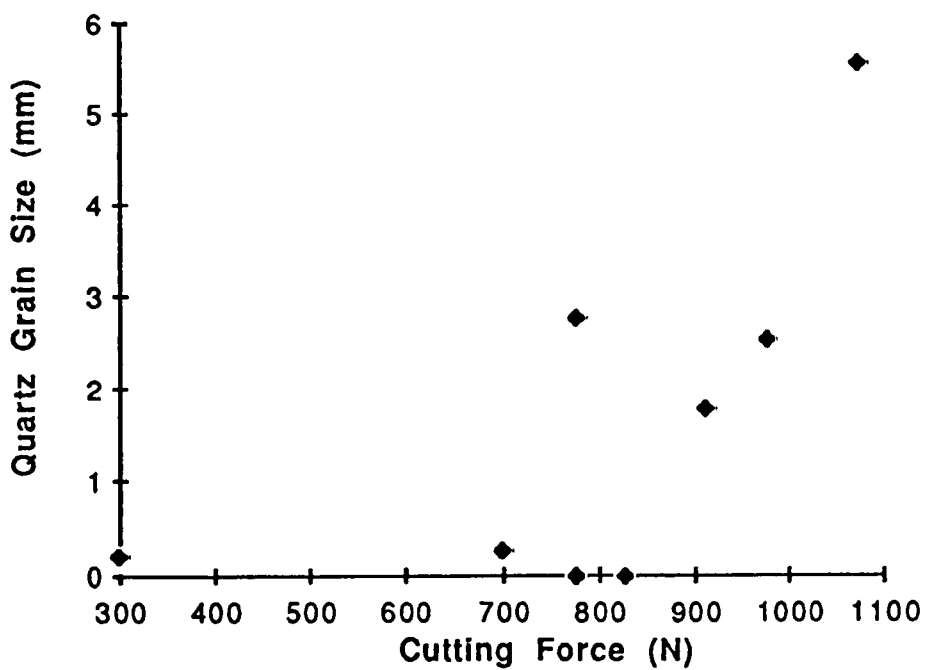


Fig. 5.13 Relationship between Cutting Force and Quartz Grain Size

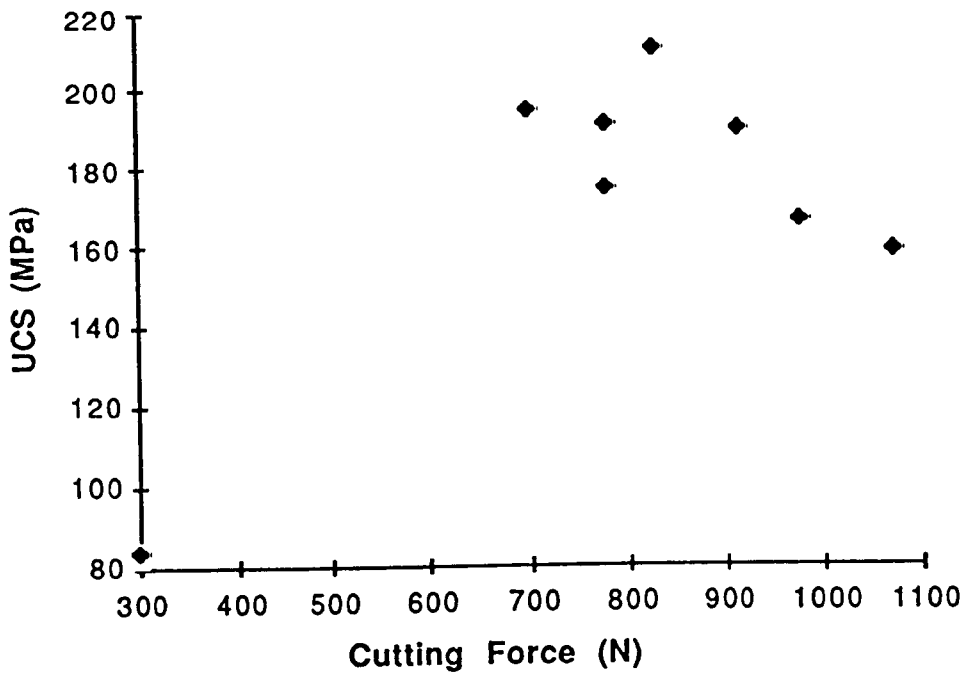


Figure 5.14 Relationship Between Cutting Force and Uniaxial Compressive Strength

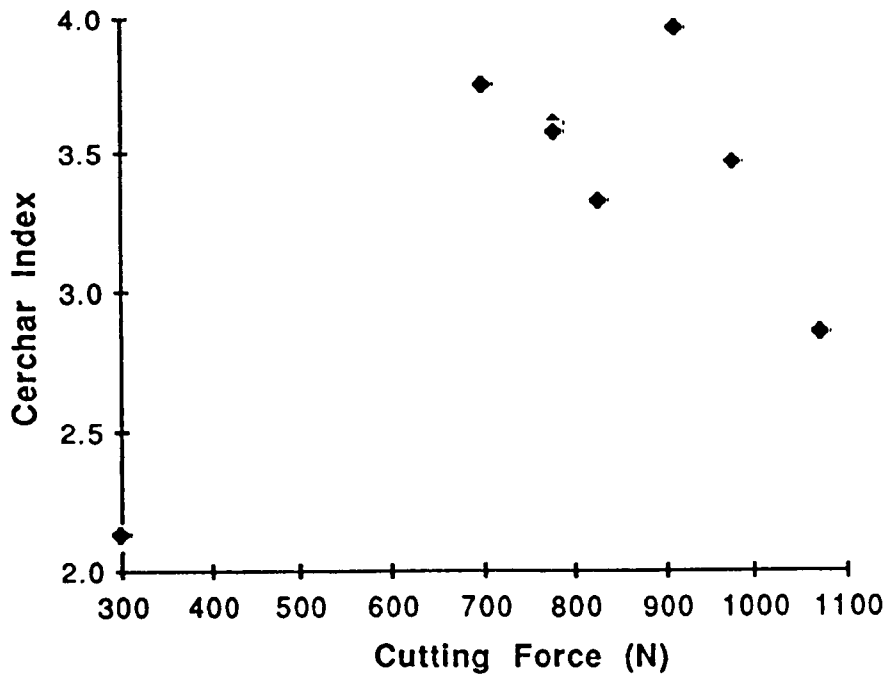


Figure 5.15 Relationship Between Cutting Force and Cerchar Index



Sample No.	% Category					
	Good	Wear flat	Rough	Cleaved	Shallow hole	Deep hole
1	17.5	25.1	19.8	8.0	15.8	13.8
2	19.2	27.7	15.6	7.7	16.9	12.8
3	18.5	27.3	18.5	8.2	15.3	12.2
4	14.2	30.1	22.1	9.3	11.4	12.8
5	23.1	33.1	9.7	5.4	12.6	16.1
6	30.9	21.4	12.9	9.4	11.7	13.7
7	22.2	26.3	17.1	6.7	17.1	10.6
8	30.0	35.7	5.1	3.4	13.3	12.5

Table 5.8 : Analysis of Diamond Particles after Sawing

over the surface of the rock and often this distance can be less than the actual grain size of certain rock mineral constituents. A summary of the Cerchar abrasive results are shown in the Table 5.2. and it can be seen that the results are all very similar for the hard granite rock types, ranging from 2.8 to 3.98. This differential is not sufficiently large enough to be able to apply the index with any degree of confidence.

#### **5.8.6. Factors Affecting Cutting Force for Sawing.**

Table 5.6. shows the linear correlation coefficient between the cutting force (N) and the various independent variables. It can be shown that there is a tentative linear relationship between cutting force (N) and hardness index numbers, the Cerchar abrasive index, plagioclase grain size and quartz grain size. The results are summarised in the Table 5.7. and in Figures 5.10 to 5.15.

#### **5.9. Analysis of Diamond Particles after Sawing.**

After each test on the various rock samples, an analysis of individual diamond particles was carried out and Table 5.8. indicates a category of the breakdown of the percentage degradation with each rock sample tested.

It can be seen, the percentage of good diamonds with sample 8 (sandstone) is 30% whereas the percentage of good diamonds when cutting the granite 4 is only 14%. Also, the percentage of rough diamonds is over 4 times higher when cutting the granite 4, and where the two granites such as 1 and 7, or 2 and 3 were found to be similar in terms of wear, the diamond particle analysis was also found to be similar.

#### **5.10. Multiple Regression Analysis and Prediction of Sawability of Rocks.**

##### **5.10.1. Prediction of Specific Wear.**

A multiple regression analysis was carried out to determine the relationship between 13 independent variables associated with specific wear of diamond saw blades. However, a linear factor analysis assisted in isolating most of the important independent variables to be used in the analysis as follows:

- 1) The Shore Scleroscope Hardness Index
- 2) The NCB Cone Indenter Hardness Index
- 3) Quartz Grain Size
- 4) Plagioclase Grain Size
- 5) Moh's Mean Hardness

Because both uniaxial and tensile strength parameters could be correlated with the Shore Scleroscope and NCB Cone Indenter hardness indices they were omitted from

the analysis.

The predictive equation as derived from multiple regression analysis is given below:

$$Y = - 0.059 - 0.008X_1 + 0.0077X_2 + 0.0138X_3 + 0.0212X_4 + 0.0054X_5 \quad (\text{Eq 5.3.})$$

Where  $X_1$  = Shore Scleroscope Hardness Index Number

$X_2$  = NCB Cone Indenter Hardness Index Number

$X_3$  = Moh's Mean Hardness Number

$X_4$  = Quartz Grain Size (mm)

$X_5$  = Plagioclase Grain Size (mm)

The correlation coefficient for the multiple regression analysis is given as: 0.980.

In the equation 5.3.  $X_1$ ,  $X_2$ ,  $X_3$ , are a function of rock hardness and can be correlated to each other. A modified predictive equation is presented in:

$$Y = + 0.0248 - 0.0018X_1 + 0.0098 X_2 + 0.024 X_3 \quad (\text{Eq 5.4.})$$

The correlation coefficient of the above equation is:

$$0.967$$

Where  $Y$  = Predicted rate of specific wear  $\text{mm/m}^2$

$X_1$  = NCB Cone Indenter hardness number

$X_2$  = Quartz grain size. mm

$X_3$  = Plagioclase grain size. mm

The equation (5.4) has the additional advantage of predicting the rate of wear from only 3 independent

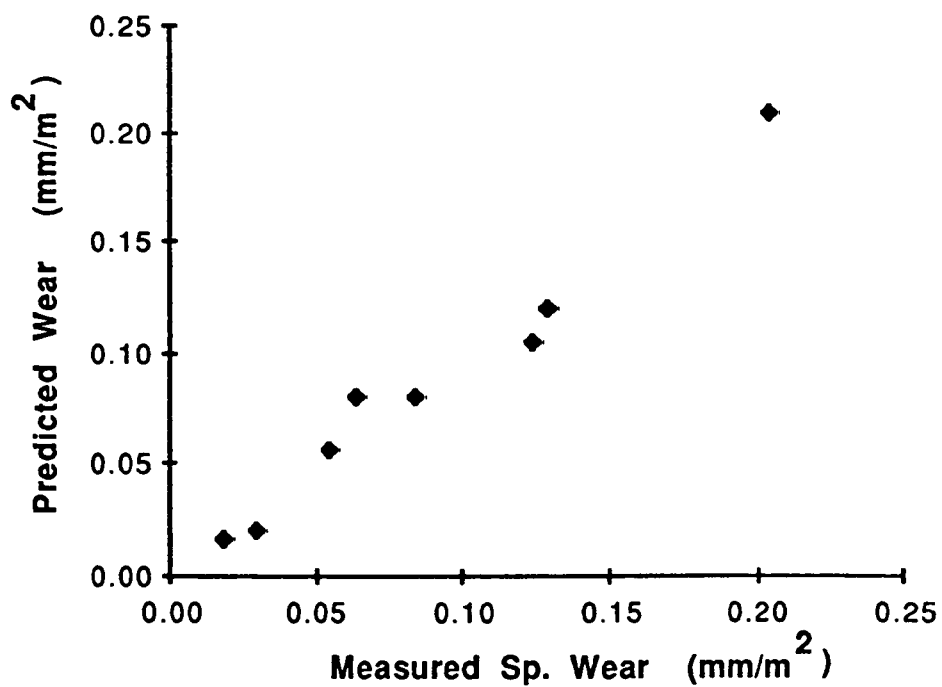


**Figure 5.16 Relationship Between measured and Predicted Wear Using Equation 5.3**

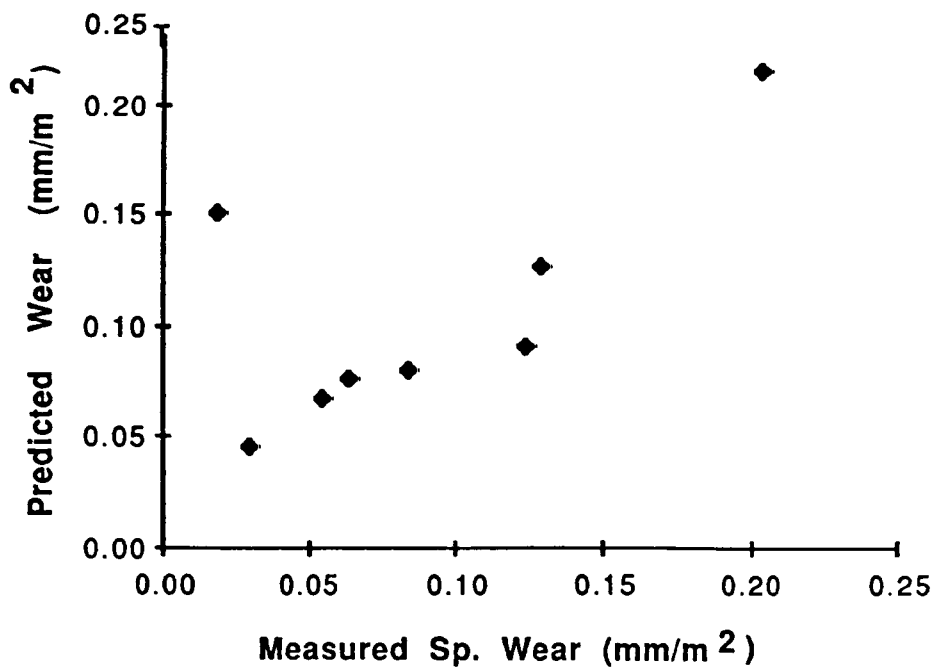


**Fig. 5.17 Relationship Between Measured and Predicted Wear Using Equation 5.4**

variables.

Figures 5.16. and 5.17 show the relationship between measured and predicted specific wear of the saw blade using the equation (5.3.) and equation (5.4.) respectively.

#### 5.10.2. Prediction of Cutting Force Requirements.

The factor analysis described in section 5.8.6. indicate that the cutting forces required to saw rock does not depend on any single factor, but on the combined effect of several factors. Thus factor analysis has been used to assist in the isolation of the most dominant factors which can be used to predict the required cutting forces for sawing rock by the use of diamond impregnated saws. These factors are listed in the following order:

- 1) The Shore Scleroscope Hardness Index Number
- 2) The NCB Cone Indenter Hardness Index Number
- 3) Quartz Grain Size
- 4) Uniaxial Compressive Strength
- 5) Cerchar Abrasive Index Number

The predictive equations using multiple regression analysis are presented as follows:

$$N = 211 + 8.86X_1 + 10.2X_2 - 1.93X_3 + 11.4X_4 - 2.12X_5 + 38.3X_6$$

(Eq 5.5.)

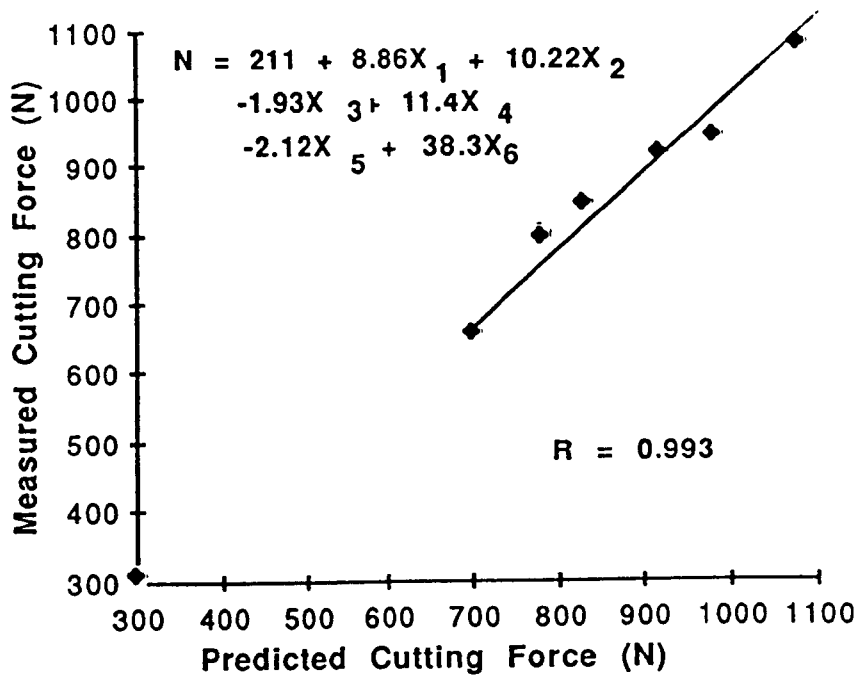


Figure 5.18 Correlation Between Predicted and Measured Cutting Forces

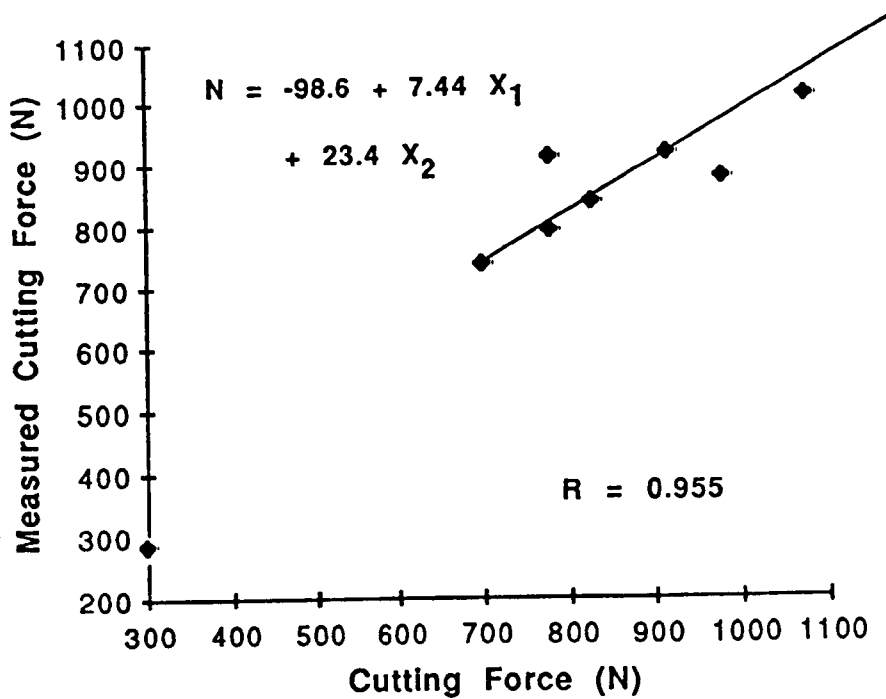


Fig. 5.19 Correlation Between Measured and Predicted Cutting Forces

Where N = Cutting Force Required. (Newtons)

$X_1$  = Shore Hardness Number (Dimensionless)

$X_2$  = Cone Indenter Number (Dimensionless)

$X_3$  = UCS (MPa)

$X_4$  = Mean Quartz Grain Size (mm)

$X_5$  = Quartz Percentage (%)

$X_6$  = Plagioclase Grain Size (mm)

The correlation coefficient for the above equation (5.5) was 0.993 and the relationship between the measured cutting forces and the predicted cutting forces is presented graphically in Figure 5.18.

The following predictive equation (5.6.) illustrates how the cutting forces (N) can be calculated from only two independent variables:

$$N = -98.6 + 7.44X_1 + 23.4X_2$$

(Eq 5.6)

Where  $X_1$  = Shore Scleroscope Hardness Number

$X_2$  = Cone Indenter Hardness Number

The correlation coefficient for the above equation (5.6) is 0.955 and Figure 5.19 illustrates graphically the relationship between measured and predicted cutting forces



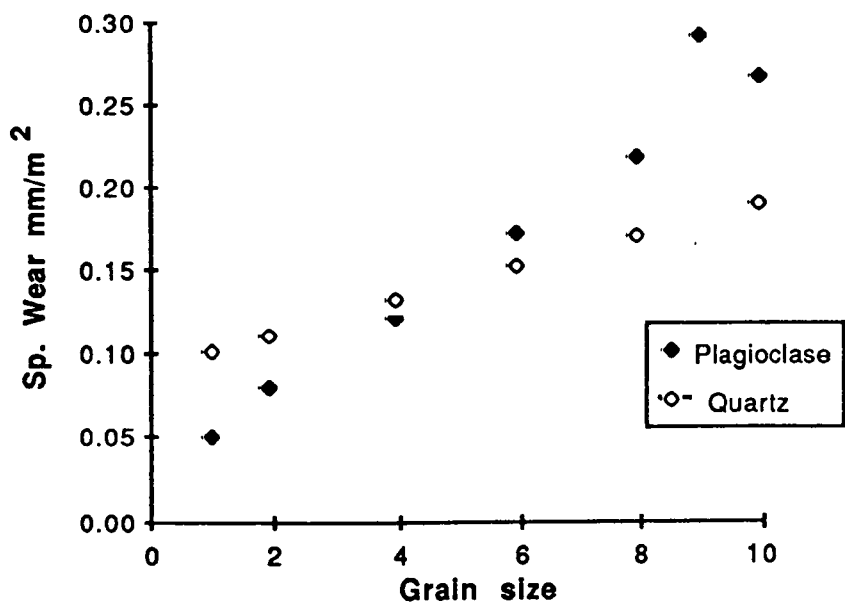


Figure 5.20 Effect of Grain Size on Sp. Wear

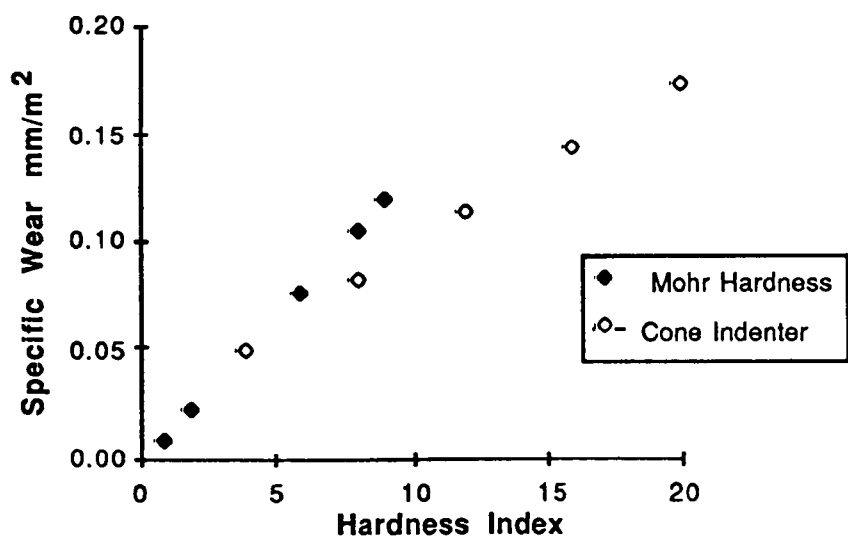


Figure 5.21 Effect of hardness on Specific Wear Rates of a Saw Blade

TABLE 5.9.

Assessment of Factors Affecting the Sawability of  
Rocks.

Predictive Index	Influencing Factors	Predictive Equation
Specific Wear Rate  (mm/m )	Quartz Grain Size (mm)	$Y = 0.0214X_4 + 0.211$
	Plagioclase Grain Size (mm)	$Y = 0.0054X_5 + 0.085$
	Moh's Hardness Index	$Y = 0.0013X_3 + 0.0059$
	Shore Sclero- scope Index	$Y = 0.0008X_1 + 0.174$
	Cone Indenter Index	$Y = 0.0077X_2 + 0.0197$

TABLE 5.10.

Assessment of Factors Affecting Wear Rates

Predictive Index	Influencing Factors	Predictive Equation
Specific Wear Rate  (mm/m )	Cone indenter. $X_1$ Index	$- 0.0018X_1 + 0.125$
	Quartz Grain Size. $X_2$	$0.0098X_2 + 0.092$
	Plagioclase Grain $X_3$ Size	$+ 0.024X_3 + 0.0260$

TABLE 5.11.

Assessment of Factors Affecting Cutting Force  
Requirements for Diamond Sawing.

Using Equation 5.3.

Predictive Parameter	Influencing Factors	Predictive Equation
Cutting  Force  (N)	Shore Scleroscope Index	$8.86X_1 + 81$
	Cone Indenter Index	$10.2X_1 + 470$
	UCS	$-1.93X_3 + 915$
	Quarz Grain Size	$11.4X_4 + 329.97$
	Quartz Percentage	$-2.12X_5 + 329.97$
	Plagioclase Grain Size	$38.6X_6 + 833.76$

**TABLE 5.12.**

**Assessment of Factors Affecting Force Requirements.  
For Diamond Sawing.**

**Using Equation 5.4.**

Prediction Parameter	Influencing Factors	Predictive Equation
Cutting  Force  (N)	Shore Scleroscope Index	$7.44X_1 + 163.0$
	Cone Indenter Index	$23.4X_2 + 533.5$

### **5.11. Analysis of Important Variables and their Interrelation with Sawability of Rocks.**

#### **5.11.1. Method of Analysis.**

The effect of different variables were analysed by changing the predictive equations 5.3. to 5.6. to be dependent upon one factor only, by assigning other parameters their mean average values. The derived equations are summarised in Tables 5.9. to 5.12. These equations provide an important method of investigating the effects of individual factors in assessing sawability of rocks.

#### **5.11.2. Factors Affecting Specific Wear Rates.**

The rate of wear of diamond impregnated saw blades appears to be influenced by the grain size of the predominantly hard mineral constituents of the rock. e.g. Quartz (Moh's 7) and Plagioclase feldspar (Moh's 6.0-6.5). Other related factors include, the average hardness of coarse mineral grains and the overall hardness of the whole rock. Thus specific wear rate will increase with overall hardness and with increased hard constituent mineral grain size. This is indicated by Figure 5.20. The effect of the average Moh's hardness, defined by thin section microscopy and the overall rock hardness defined by the NCB Cone Indenter is illustrated in Figure 5.21. Similar trends would

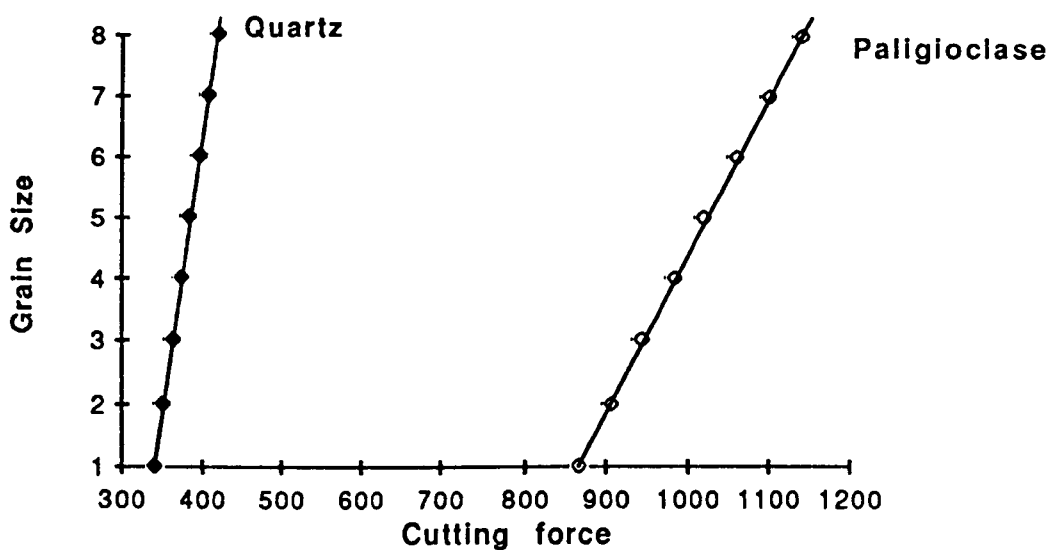


Figure 5.22 Effect of Grain Size on Cutting Force

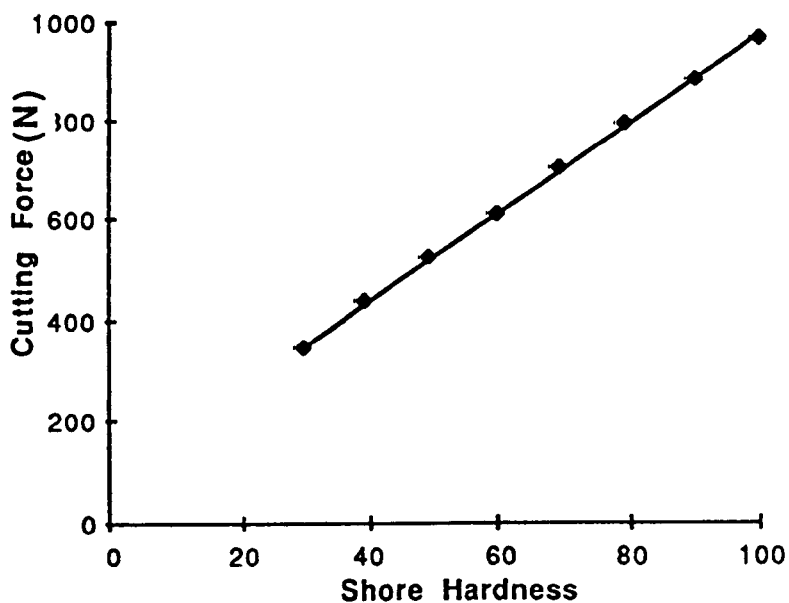


Figure 5.23 Effect of Shore Hardness on Cutting Force Requirements

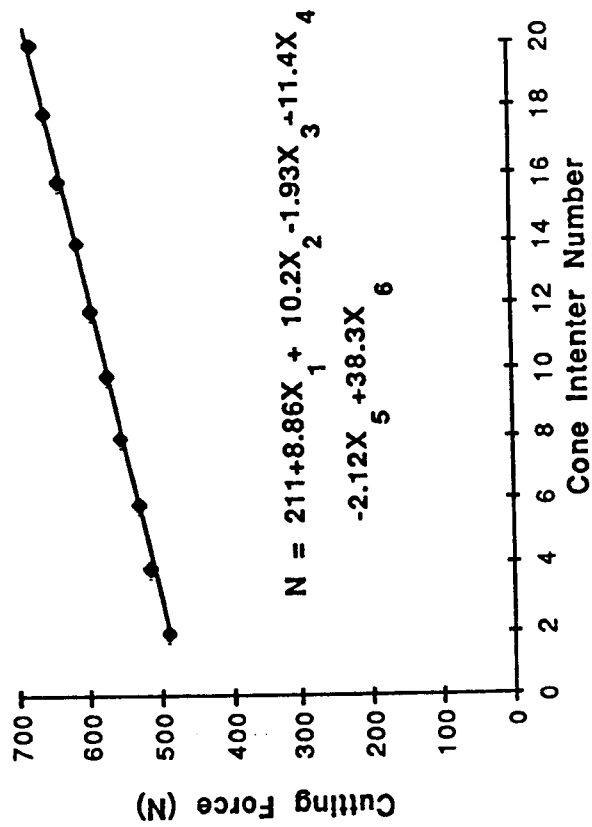


Figure 2.24 Effect of Cone Indenter Hardness to Cutting Force Requirements

be expected for rocks with a wider range of Shore Scleroscope hardness numbers.

#### **5.11.3. Factors Affecting Cutting Force Requirements.**

Factor analysis has indicated that the forces required to saw rock depends upon overall rock hardness, as indicated by the Shore Scleroscope and NCB Cone Indenter, the grain size of the hard constituent minerals present and uniaxial compressive strength. Figure 5.22 Shows the effect of grain size on cutting force. The indication is, that cutting force requirement is increased tentatively by approximately 23% - 30% when grain size show an increase from 1 mm to 8 mm. Similarly, Figures 5.23. and 5.24. show that cutting force requirement increases with overall hardness of rocks. The effects of quartz grain size and constituent quartz mineral percentage is at present, difficult to assess by this analysis.

#### **5.12. Discussion of Results.**

##### **5.12.1. The Need For Multiple Tests.**

After analysing all the data on specific wear, cutting forces, mineralogy and the various mechanical physical property tests, it is evident that, at this time, no single indicator exists for determination of the sawability of natural rock material.



The actual sawing process is a complex operation which involves the interaction of many interdependent factors. The important factors to be considered with the sawability of natural rock material appear to be those concerned with hardness, abrasiveness and the constituent mineralogy. This includes grain size and whole rock hardness. The latter can be derived from the various laboratory tests previously described in this work.

When testing most fine to medium grained sedimentary rock types, The shore Scleroscope and NCB Cone Indenter hardness tests have proven to be, reliable laboratory index tests. These tests also exhibit very good correlation with UCS and UTS.

Although the Shore scleroscope for instance, gave a slightly inferior indication of hardness than the NCB Cone Indenter with the rock types investigated, this could be attributed to the generally large grain sizes encountered with some of the rocks tested. It has also been found, that the Cerchar abrasive index does not perform as well when testing rocks consisting of large mineral grains. Therefore, the abrasiveness of these rock types would be better determined by tests that take account of these factors or they should relate more accurately to the rock breakage processes involved with diamond sawing. Following on with this work, two new abrasion tests will be discussed in a

subsequent chapter.

Physical strength parameters did not have a significant effect on the results obtained. This could be explained by the fact that there was no significant difference in the strength values of the seven granites and only one sandstone was tested. The sandstone being used as a standard comparative material only.

#### 5.12.2. Statistical Analysis.

Statistical analysis of the results obtained, appears to provide a promising solution to the predictability of likely tool wear and it has been shown that good correlation exists between the relevant factors studied. The most important of these being the apparent relationship between grain size and rock hardness. This is particularly important when one considers the major difference between the hard rocks tested was reduced to that of mineral grain size. Here, the diamond cutting process is predominantly one of attritional wear, causing gradual degradation of the diamonds. It can be seen that, the larger the mineral grain size, the greater the effect on wear and force. Conversely, with the sedimentary sandstone, it is the matrix material binding the diamonds which

erodes. thus unsupporting the diamonds which results in premature loss of hard indenter material.

#### 5.12.3. Rationalisation of Tests.

It is clear that some form of rationalisation of tests and their procedures should be followed. This is particularly important when specimen material is in limited supply. Furthermore, the identification of the problem and the adopted methods of testing in order to find a solution, should always be given careful consideration. e.g. Choice of compatible tests, non-destructive tests followed by destructive tests etc. Although useful data was acquired from the Cerchar abrasive index tests, new abrasive wear tests related to the diamond sawing processes are considered essential to the integrity of the results obtained. Mechanical and intrinsic property tests are well established and can provide useful data.

#### 5.12.4. Futher Scope for Development.

The test program described in this chapter was concerned with trials conducted on a single set blade, using predetermined cutting parameters on eight different rocks.

Scope exists therefore, for considerable work to be

carried out in the following areas:

- 1) The developement of new tests specifically related to the diamond sawing processes.
- 2) The effects of the interaction of independent cutting parameters on tool wear, cutting rates and specific energy.
- 3) The design of saw blade segment composition. e.g. Diamond type, size and concentration. The matrices type and hardness related to rock type and condition.

#### 5.13. Conclusions.

It is apparent that the sawability of rocks depends upon a number of factors and these include the following important areas:

- 1) Mineralogy. This includes the percentage of hard mineral constituents present, their grain size and shape and in some cases the degree of competence in which these grains are cemented.
- 2) Mechanical properties such as physical strength, hardness and abrasiveness.

##### 5.13.1. Sawability.

Sawability therefore, has been assessed by the use of the two principle parameters:

- 1) Cutting force requirements.
- 2) Specific wear of the saw blade indenter

material.

After all the available data had been collated, a number of important points emerged:

- 1) Statistical analysis gave an indication to the most important factors necessary to predict the sawability of rock.
- 2) Statistical analysis of the available data has indicated that cutting forces and specific wear can be predicted by the use of a set of multi-regression equations.
- 3) The scope of this method should be increased in the first instance, by extending the data base in the following manner:
  - a) A greater variety of rock types.
  - b) The inclusion of additional sawability parameters, such as:
    - Cutting speeds
    - Depth of cut
    - Rate of Sawing
    - Diamond type and concentration
    - Matrix material.
  - 3c) Increased data acquisition by continuous updating to establish a large data base and thus, enable the production of improved prediction equations.

The author considers that comprehensive laboratory sawing trials, together with physical and intrinsic

property testing, combined with statistical analysis, could provide an acceptable solution to the prediction of tool wear and optimum cutting conditions in diamond sawing.

## **CHAPTER 6.**

### **CASE HISTORIES.**

## CHAPTER 6.

### CASE STUDIES.

#### 6.1. Introduction.

Historical events have exposed many paradoxes as shown with the following case studies. For example, blast hole drilling operations are sometimes considered a good indicator of diggability, yet the Cuddalore Sandstone at Neyveli in India, probably one of the most abrasive materials to be excavated on a commercial scale by Bucket Wheel Excavators (BWE), exhibited high penetration rates with little bit wear during drilling. This could be attributed to the extremely weak and friable nature of the rock material, matched to the most suitable drilling equipment, while employing the best drilling parameters. This was not the case with the teeth on the buckets of the BWE's, which wore out at an alarming rate. This could be attributed to a different mechanism e.g. sliding and impact abrasion in contact with the extremely hostile mineralogy of the sandstone overburden. Conversely, in some weak non-abrasive limestones, penetration rates when drilling with impregnated diamond coring bits may be low, simply



because the abrasiveness of the rock is low and does not keep the bit sharp by failing to abrade the matrix material and thus expose fresh diamond.

The choice and method of operation can significantly affect the rate of wear incurred in various machines, tools and other auxiliary equipment and the following case studies highlight some of the problems encountered. The importance of the subsequent tests conducted in an attempt to provide reliable indicators have been discussed and recommendations proffered.

This Chapter outlines a number of case histories to identify the abrasive wear potential of rocks associated with certain rock excavation and rock cutting mechanisms, these include the following:

- a) Crawler mounted, underwater trenching machine operation.
- b) Bucket Wheel Excavator operations in unconsolidated sandstone.
- c) Bucket Wheel Excavator operations in weathered and coarse grained sandstones.
- d) A truck and shovel operation in uranium ore overburden.
- e) Diamond core drilling in hard rock formations.

WORN AND DAMAGED PICKS.

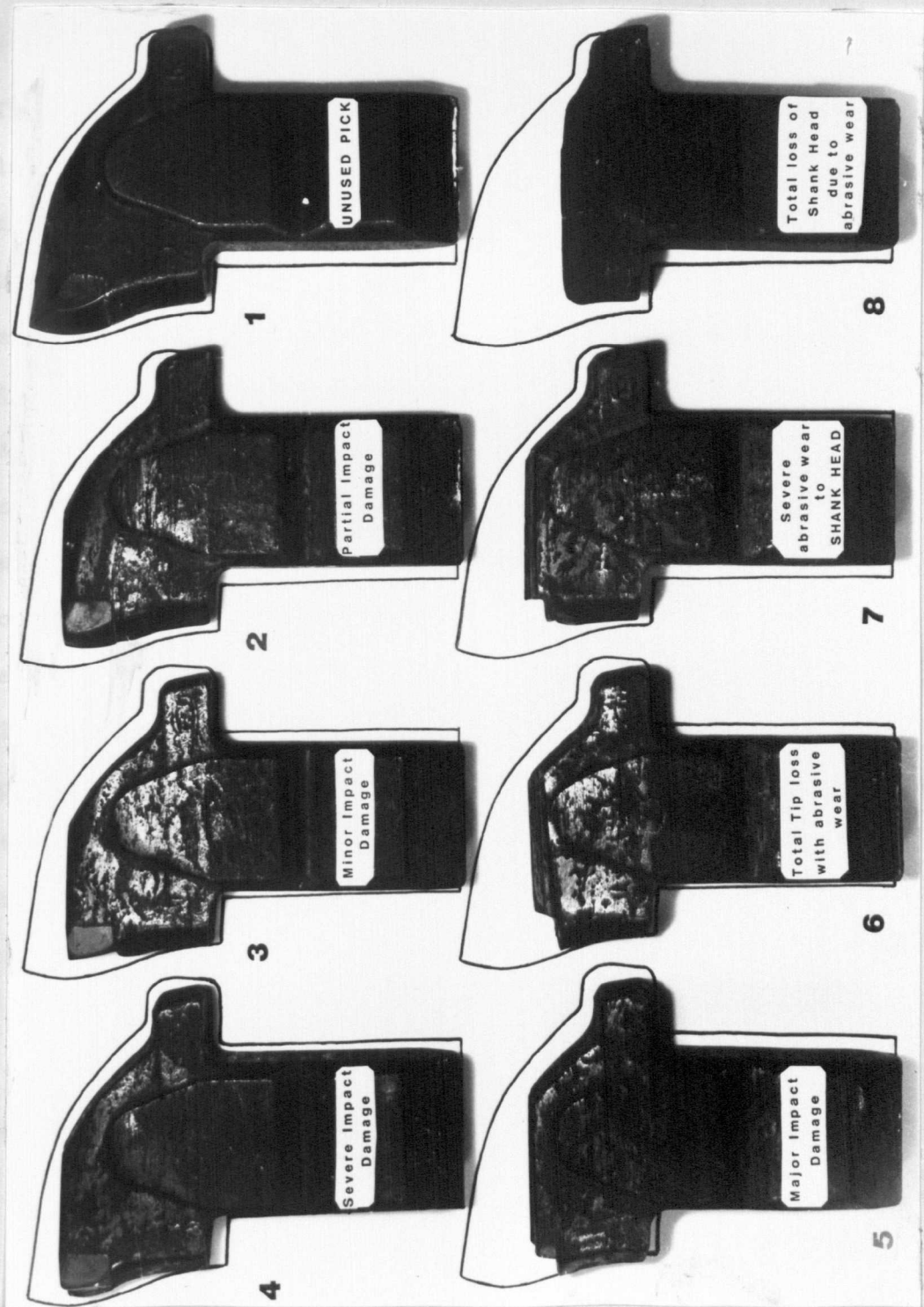


Figure 6.1.

## 6.2. UNDERSEA TRENCHING OPERATION.

### 6.2.1. Introduction.

This project involved an undersea trenching operation in the English Channel which was required for cross channel electric power cables to be layed on the sea bed. The operation was carried out by a crawler mounted, under-water trenching machine; controlled through umbilical cables from a sea-going vessel.

Acute wear problems and impact damage occurred while cutting through an off-shore section of green sandstone sediments. Moreover, large flint boulders caused substantial impact damage to the foreward attack picks normally used for this operation.

The purpose of this study was to investigate the physical properties of representative rock samples and their relevant contribution to both abrasive wear and impact damage. Figure 6.1. Illustrates the type of picks used and the extent of both abrasive wear and impact damage.

### 6.2.2. Rock Sample Material.

A total of 13 representative rock samples were received from the site of the trenching operation.

These were first examined as in-hand specimens and the following conclusions formed:

- a) Scratch tests revealed most of the material had a Moh's hardness ranging from 3.0 to 3.5.
- b) Some chemical change had taken place, which was evident from the discolouration caused by the presence of the green mineral identified as glauconite.
- c) All the samples were of a highly competent nature with no obvious signs of fracture spacing, Sample 6. appeared to be less well cemented than the other samples.

#### **6.2.3. Petrographic Analysis.**

Six of the total samples recieved were selected and prepared for thin section petrographic analysis and a brief description of these are given as follows.

- 1) Rock Sample 1: (KP44590) was a coarse grained quartzitic sandstone composed of silica, in which large quartz grains were embedded in a finer quartz matrix. The rock also contained some grains of glauconite in minor proportions.
- 2) Rock Sample 2: (KP44611) This sample was slightly tarnished on the surface and was identified as a dirty ironstone, grey to reddish black in colour. The rock had a high density, low porosity and a less pronounced metallic lustre.
- 3) Rock Sample 3: (KP41617) The rock appeared to be a

**TABLE 6.1.**

**Percentage Mineral Proportions.**

<b>Sample Number</b>	<b>Quartz</b>	<b>Glauc nite</b>	<b>Shell</b>	<b>Mud CO-3</b>	<b>Cement</b>
KP44590	18.9	0.5	8.7	-	71.9
KP44611	37.0	-	-	-	63.0
KP41617	46.1	3.5	8.1	5.7	36.3
KP41690	62.4	0.9	-	-	36.7
KP44611	54.1	6.6	-	-	39.3
KP44590	38.0	9.3	3.2	-	49.5

fine grained quartzitic sandstone with some quartz grains of glauconite and some remnants of shell fragment material. The rock was compact with medium density and low porosity.

- 4) Rock Sample 4: (KP41690) An indurated sediment with a high silica content. Traces of glauconite were present and the rock was very well cemented with medium density and low porosity.
- 5) Rock Sample 5: (KP44611) A sandstone with a quartz mineralogy and glauconite compacted and cemented together. The density was low with high porosity.
- 6) Sample 6: (KP44590) This was a coarse grained quartzitic sandstone, poorly cemented with low density and high porosity. The rock had traces of glauconite and shell fragments.

A detailed description of the rocks mineralogy and their proportions are given in Table 6.1.

#### 6.2.4. Summary of Petrographic Analysis.

The rock is a green sandstone, i.e. a sandstone which contains proportions of the mineral glauconite.

When the rock was deposited it probably consisted of shell material, quartz sand, glauconite and carbonate sand and mud. Subsequently, much of the sand and mud have gone into solution and has been reprecipitated to bind the sand into sandstone, 'an abrasive material'.

The original distribution of these components seem to have been variable, leading to patchy distribution of the different cements and varying concentrations of quartz grains, e.g. In Sample 3: (KP41617) the quartz is so abundant that most of the grains are in contact and the rock is grain supporting, whilst in Sample 6 (KP44590) The quartz is widely disseminated and floats in the cement.

The grain sizes range from 0.026 to 0.773 mm in diameter and is classified as a fine grained sedimentary sandstone rock. The grain shapes range from sub-angular to angular and can be regarded as hostile to cutting elements.

#### **6.3.5. Mechanical Pyhsical Property Tests.**

In addition to the petrological examination and study of thin sections of the sample rocks, a number of mechanical property tests were carried out. These included the following tests:

- 1) Point Load Index.
- 2) Protodyakinov Index.
- 3) Unconfined Compressive Strength.
- 4) Indirect Tensile Strength.
- 5) Youngs Modulus and Poisson's Ratio.
- 6) Bulk Density and Porosity.
- 7) Shore Scleroscope Hardness Index.

Table 6.2

Summary of Rock Test Results - CFCB Rock Trenching Machine - RTH III Project

Specimen Code	Rock Type	Point Load Index $P_{50}$ MPa	Mean Protodykanov Number	Uniaxial Compressive Strength $\sigma_c$ MPa	Uniaxial Tensile $\sigma_t$ MPa	Young's Modulus $E$ GPa	Poisson's Ratio $\nu$	Bulk Density $\gamma/m^3$	Porosity %	Saturation Moisture %	Cerchar Abrasivity Index	Toughness Index $T_1$
KP44590	Green Sandstone	2.98±0.5	7.66	83.05	8.30	10.06	0.095	2.54	2.21	0.87	4.25	34.3
KP44611	Maematlic Sandstone	3.92±1.49	10.35	115.67	7.56	41.69	0.12	3.01	3.85	1.286	3.32	16.05
KP44617	Sandstone	3.65±0.66	2.43	73.89	6.21	55.29	-	2.61	1.40	0.538	4.16	5.77
KP44690	Sandstone	2.28±3.41	6.41	67.84	6.32	58.95	-	2.505	2.38	1.396	2.48	3.70
KP44611	Porous Sandstone	2.40±0.66	6.03	30.91	6.14	9.47	0.035	1.933	12.46	6.39	4.25	5.04
KP44590	Sandstone	2.43±0.87	3.89	25.51	5.60	5.78	0.099	2.57	3.32	1.38	4.03	5.47

Table 6.3

Sample No	Quartz	Glauconite	Shell	Co <sub>3</sub> Mud	Cement	Total
KP44590	18.9	0.5	8.7	-	71.9	100
KP44611	37.0	-	-	-	63.0	100
KP44617	46.1	3.5	8.1	5.7	36.3	100
KP44690	62.4	0.9	-	-	36.7	100
KP44611	54.1	6.6	-	-	39.3	100
KP44590	38.0	9.3	3.2	-	49.5	100



8) NCB Cone Indenter Hardness Index.

9) Cerchar Abrasive Index.

A summary of the rock property mechanical tests are displayed in Tables 6.2. and 6.3.

#### 6.2.6. Discussion of Results.

The summary of the rock property results and the main conclusions regarding these and the rock petrology are as follows:

Rock Sample 1. (KP44590) The rock was a green sandstone which contained 18.9% quartz embedded in 71.9% cement. The rock density was  $2.54 \text{ t/m}^3$  and the porosity was 2.21. Its uniaxial compressive strength is 83.05 MPa and exhibits a very high toughness index of 34.3. It should be recalled that rock materials with a toughness index of more than 27.0 are normally regarded as difficult to cut by machines unless the rock mass possesses pronounced planes of discontinuities. This rock also exhibited a high Cerchar abrasive index of 4.25 and can be classified as a highly abrasive material and difficult to cut.

Rock Sample 2. (PK44611) This rock was a ferruginous sandstone containing 37.0% quartz embedded in 63.0% haematite rich cement. The rock had a bulk density of  $3.10 \text{ t/m}^3$  and the porosity was 3.85% with a compressive

strength value of 115 MPa. The toughness index for this rock was 16.05 and the Cerchar abrasive index was 3.32. Therefore, this rock can be regarded as an abrasive, medium strength material of high density and will have a high wear potential with the forward attack picks used to cut this material.

Rock Sample 3. (KP41617. A sandstone consisting of 46.10% quartz, 3.50% glauconite, 8.10% calcite and 5.70% carbonate embedded in 36.0% cement. The rock has a medium bulk density  $2.6 \text{ t/m}^{-3}$ , low porosity 1.40% and its uniaxial compressive strength was 74.0 MPa. The toughness index was 5.77 and the Cerchar abrasive index was 4.16. This is classified as a competent rock of medium strength with a high abrasive potential. Consequential interaction with cutting tools is likely to produce high rates of abrasive wear.

Rock Sample 4. (KP41690) The rock sample was a poorly cemented green sandstone containing 62.40% quartz, 0.90% glauconite and 36.60% cement. Its bulk density was  $2.5 \text{ t/m}^{-3}$ , the porosity was 2.38% and the toughness index was 3.39. With a Cerchar index of 2.48 and a compressive strength of 67.84 MPa, this material could be classified as of medium strength, but potentially abrasive material.

Rock Sample 5. (KP44611) A porous sandstone with a bulk density of  $1.93 \text{ t/m}^{-3}$ , the porosity was 12.50% and its compressive strength was 30.91 MPa. The rock consists of 54.10% quartz, 6.60% glauconite and 39.30% cement. Although the uniaxial compressive strength of this rock measured only 30.91 MPa, the Cerchar abrasive index was 4.25 and consequently, must be regarded as highly abrasive rock material.

Rock Sample 6. (KP44590) This rock sample contained 38.0% quartz, 9.30% glauconite embedded in 49.50% cement. The rock density was  $2.5 \text{ t/m}^{-3}$ , and the porosity was 3.32%. Its uniaxial compressive strength was 25.51 MPa. Like Rock Sample 5. this was a low strength rock material but with a high Cerchar abrasive index of 4.03, this must be regarded as a highly abrasive material.

#### 6.2.7. Conclusions.

The rock sample material therefore, was a green sandstone of low Cretaceous origin, containing a range of quartz and glauconite grains. Rock density, porosity and uniaxial compressive strength vary widely due to changes in characteristics and percentage of mineral cementing material. Generally, the rock varies

from abrasive to highly abrasive and this would be a major factor with wear. The impact damage could be attributed to the large flint boulders and/or the influence of the very high toughness index found in Rock Sample 1.

To summarise therefore, all the rock samples were potentially, highly abrasive. Furthermore, Rock Sample 1. also indicated a very high toughness index of 34.4. Consequently, the tools required to cut this rock material, must have a high wear resistance, which implies that a hard grade of tungsten carbide must be used. While this would help to solve the problems associated with abrasive wear, it would also serve to aggravate the problems of impact damage caused by the flint boulders. It would appear therefore, that a compromise between hardness and toughness of the insert material might be the best temporary solution, but in the long term, consideration to tip geometry should be seriously considered, this could include the use of point attack picks. Unfortunately, this would almost certainly involve major re-design of pick boxes and pick configuration.

### 6.3. BUCKET WHEEL OPERATIONS IN WEATHERED SANDSTONES.

#### 6.3.1. Introduction.

This section reviews the possibility of using Bucket Wheel Excavators (BWE's) at a surface coal mine that might be developed at Pentland in Northern Queensland. The Pentland Project is located in Northern Queensland and it is proposed to work the coal deposit using strip mining methods. The overburden depth however, exceeds 60 m. (the maximum economic depth for dragline stripping) and it was proposed to strip the overburden using a BWE with a around-the-pit belt conveyor system.

The upper overburden has been subjected to tropical weathering down to the LOX line (limit of oxidation). The overburden materials are severely weathered sandstones and are generally considered diggable by a BWE.

The depth of the LOX line is however, notoriously irregular and detailed strength and abrasivity studies were required to determine the suitability of the rock for excavation by BWE.

Data and rock samples were received from the client in the form of six sealed samples as follows, and the

more important elements of this data are also included.

#### 6.3.2. Core Sample Material.

Six core samples sealed and packed in wax and tin foil were received from Pentland and these samples were designated as follows:

Sample No.	Base Depth (m)	Thickness (m)
01	11.51	0.17
02	14.85	0.13
03	23.45	0.20
05	39.10	0.24
06	46.17	0.18
08	78.48	0.20

It should be noted that these samples all came from the upper overburden above the Pentland seams, lying above an apparently widespread mudstone horizon known as the gamma marker. The upper overburden materials are coarse grained sediments, sandstones and conglomerates, known as the Warang Sandstone (Triassic). Tertiary sandstones and conglomerates may also be present, (inferred from some sections supplied) but are not readily distinguished on the geotechnical logs.

### 6.3.3. Initial Inspection of Core Samples.

The sample material had not been opened or interfered with in transit and were received as intact sticks of cored material. The samples were logged for strength using the tactile tests outlined in the COGEO manual. Differences were immediately apparent on comparing our strength classifications with those in the printout listings for borehole PE 208G which was as follows:

Sample No.	COGEO estimated strength.	Estimated Strength of samples.
01	Weakly cemented soil G4	Weak to moderately weak rock. (2-3)
02	G4	Weak rock (R1)
03	G4	Very weak rock (R1)
05	G4	Weakly cemented soil (G4)
06	Compact soil (G3)	Very weak rock (R2)
08	Moderately weak rock (R3)	Moderately weak rock (R3)

On the basis of experience, the following preliminary and subjective assessments were then made:

TABLE 6.4  
BOWEN BASIN OVERBURDEN

Mineral Proportions (appx)								
Minerals Present:	PET 01	PET 02	PET 03	PET 05	PET 06	PET 08		
Quartz (+ quartzite)	80	85	80	75	80	80		
Geothite	10	5	15	15	10	<1		
Opal / Chalcedony	5	5	4	8	10	5		
Clay minerals (Kaolinite + illite)	4	5	1	<1	<1	10		
Muscovite (SS)	<1	<1	<1	<1	<1	5		
Orthoclase	<1	<1	<1	<1	<1	<1		
Biotite	<1	<1	<1	<1	<1	<1		
Chlorite	<1	<1	<1	<1	<1	<1		



TABLE 6.5  
BOWEN BASIN OVERBURDEN

Minerals Present:	Sizes (mm)							
	PET 01	PET 02	PET 03	PET 05	PET 06	PET 08		
Quartz (+ quartzite)	<1.5	<4.0	<2.0	<3.0	<3.0	<3.0		
Geothite	<0.1	<0.1	<0.1	<0.1	<0.1	<0.1		
Opal / Chalcedony	<0.2	<0.2	<0.2	<0.2	<0.2	<0.2		
Clay minerals (Kaolinite + illite)	<0.1	<0.1	<0.1	<0.1	<0.1	<0.1		
Muscovite (SS)	<0.2	<0.2	<0.2	<0.2	<0.2	<2.0		
Orthoclase	1-0.2	1-0.2	1.5-0.2	1.2-0.2	1.5-0.2	1.5-0.5		
Biotite	<0.2	<0.2	<0.2	<0.2	<0.2	<0.2		
Chlorite	<0.2	<0.2	<0.2	<0.2	<0.2	<0.2		

Sample No.	Diggability assessment.
01	Not economically wheelable.
02	Marginally wheelable.
03	Marginally wheelable.
05	Wheelable.
06	Marginally wheelable.
08	Not economically wheelable.

The samples were subsequently split and resealed prior to further testing and detailed examination.

#### 6.3.4. Mineralogical Examination.

Thin sections were prepared from the six samples and X-Ray diffraction (XRD) analysis undertaken. The mineralogical analysis from thin sections, using standard spot counting techniques permitted approximate estimates to be made of the following details:

- 1) Percentage of mineral proportions present.
- 2) Mineral grain/crystal sizes.
- 3) Mineral grain/crystal shapes.

A summary of the results obtained from the petrological examinations of these thin sections are illustrated in Tables 6.4 and 6.5. and a detailed description of these are given as follows:

Rock Sample 01: Most of the quartz grains are optically continuous, although some quartz aggregates (quartzite) were present. The quartz grain shape ranged from angular to subrounded and the larger grains contained subhedral inclusions of green biotite, muscovite and zircon ( $<0.2$  mm). Smaller quartz crystals ( $<0.2$  mm) made up a large proportion of the matrix. Some fragments of green biotite also occurred in the matrix. Clay minerals (probably kaolinite) and geothite were present as a matrix between the quartz grains. Later opal/chalcedony was present in fractures in the matrix and as growths around some quartz grains. The opal/chalcedony was often brown due to iron staining. Minor orthoclase was present but showed extensive alteration to kaolinite and consequently was cloudy.

Rock Sample 02: This rock material closely resembled rock sample 01, except the quartz grains were slightly coarser. The rock also contained far less geotite but with more clay minerals and secondary opal/chalcedony. Some green chloritoid was present in the matrix, and pyrite and muscovite crystals occurred as inclusions in the quartz.

Rock Sample 03: Similar to rock sample 01 with the exception that the geotite forms a larger proportion

of the rock and opal/chalcedony fills fractures (often has a banded structure).

Rock Sample 05: This rock material also resembled sample 01 with the exception that the geotite, again forms a high proportion of the matrix and some of the large quartz grains were intergrown with muscavite.

Rock Sample 06: This sample was similar to sample 05 but much of the quartz exhibited wavy extinction (pressure) and is slightly more rounded, but with somewhat less geotite.

Rock Sample 08: Similar to rock sample 06 but with larger amounts of kaolinite and clay minerals (mainly illite and kaolinite) Most of the muscavite is in the form of subhedral laths, which show no alteration (well crystallised illite) Some subangular rutile grains in matrix are also present (<0.1 mm).

#### 6.3.5. Conclusions.

The rocks are coarse grained sandstone/grits, their main component is subangular to subrounded quartz grains which have a broad span of particle size ranging from < 0.1 mm to 4 mm. The rock matrix material also contains clay minerals and micas,

although where the rock is oxidised, these have altered mainly to goethite with some limonite. Voids in the rock have been infilled by later opal/chalcedony, an amorphous silica, and this also coats some of the quartz grains.

The mineral proportions are shown in Table 6.4. and it can be seen that the quartz is the dominant mineral comprising 75% to 85% in all the samples. Approximately 15% of the cementing material appears in thin section as goethite and chalcedony i.e. hydrated oxides of iron and silicon. Clay minerals and related silicates were also present in the matrix and apparently comprised about 5% of the sample as determined by thin section. XRD analysis generally confirms these proportions. The review of mineral grain and crystal sizes is presented in Table 6.5. and serves to emphasise the importance of quartz grains/crystals with a range up to 3 to 4 mm. These and a significant proportion of finer grained quartz are present in the matrix. The quartz grains were predominantly angular to subangular with some smaller proportions of rounded grains. Based on the comparison with other rocks, including sandstones, all the samples appear to have a relatively high abrasive potential. This is however, a subjective assessment and should be considered in the context of other index tests.

The general conclusions are that the overburden is too abrasive to be excavated by BWE's and that in view of the depth of the overburden, tandem dragline stripping would have been preferred.

Medium powder ratio blasting will be required to assist the dragline operation. The drag bucket, the drag chains and the ends of the drag ropes will be subjected to greatly increased wear since they contact the overburden material during the digging cycle, e.g. about 25% of the digging time, thus involving both sliding and impact abrasion.

To account for this, the availability of draglines was reduced by 5% from 85% to 80% for scheduling purposes, and the operating costs increased by 12.5% for cost appraisal. These figures are based on relevant experience from other operations.

#### 6.4.BUCKET WHEEL OPERATION IN FINE GRAIN SANDSTONE.

##### 6.4.1. Introduction.

The Oaklands Project which is located in the south west corner of New South Wales (N.S.W), close to the Victoria border. It represents one of Australia's major energy reserves with in excess of 500 million tonnes in situ of sub-bituminous coal. It is strategically placed between N.S.W, Victoria and South Australia, one of Australia's most heavily populated and industrialised areas.

The overburden consists mainly of coarse grained sandstone and the stripping ratios appear to favour the use of BWE's in conjunction with around-the-pit belt conveyor transport for overburden stripping.

There appeared however, to be potential problems in digging the sandstone with BWE's and consequently a number of rock property tests were conducted on site sample material to determine the abrasive potential of the overburden.

#### **6.4.2. Rock Sample Material.**

Five rock samples were recieved and these were immediately unpacked weighed and in-hand inspection carried out.

The rock was securely packed and appeared to travel well with no obvious signs of deterioration. This could be attributed to the excellent method of packaging in cling film, polyurethane sheet and plastic tubing which afforded adequate protection against moisture loss and possible damage during transit.

The samples and their respective weights are listed as follows:

##### **Sample 1.**

Clayey Gravelly Sandstone. (PKA), (NOK 218).

76.05 - 76.26 m.

2.86 kg.

##### **Sample 2.**

Carbonaceous Siltstone. (NOK 224).

64.27 65.04 m.

5.708 kg.

##### **Sample 3.**

Sandstone. (3b).

81.1 - 81.53 m.

2.906 kg.



**Sample 4.**

Fine Grain Sandstone. (NOK 218).

55.85 - 56.12 m.

3.766 kg.

**Sample 5.**

Sandstone/Kaolin. (NOK 218).

48.66 - 48.83 m.

3.674 kg.

In-hand, all the sample material appeared to be of a particularly weak and friable nature and contained a high inherent moisture content. This condition precluded the possibility of normal Cerchar and penetrometer tests to determine hardness and abrasive ness. Therefore, 100g of each sample was retained for moisture content determination and the remainder oven dried for subsequent hardness and abrasive tests.

**6.4.3. Test procedure.**

A minimum number of tests are normally conducted to determine the hardness and abrasive potential of rock material, these are listed as follows:

- 1) Uniaxial compressive strength.
- 2) Indirect tensile strength.
- 3) Toughness index.
- 4) Shore Scleroscope Hardness index.
- 5) NCB Cone Indenter Hardness index.
- 6) Cerchar abrasive index.
- 7) Particle dynamic impact abrasive test.
- 8) Petrological analysis.
- 10) Moisture content.

#### 6.4.4. Summary of Test Results.

All the sample material was tested to determine the percentage moisture content and the following results were obtained from 100 grammes of each sample.

Sample Material.	% Moisture.
Sample 1.	7.8
Sample 2.	9.8
Sample 3.	8.5
Sample 4.	13.04
Sample 5.	14.63

It should be noted that moisture content reflects the specific density of rocks and can significantly reduce their strength properties by as much as 60% - 70%

Consequently, all subsequent tests were conducted with dried sample material.

#### 6.4.5. NCB Cone Indenter.

The following results were obtained from each of the samples tested.

Sample Material. Index.	Standard NCB Hardness
Sample 1.	Too friable to test.
Sample 2.	1.0-1.2. (Spurious result).
Sample 3.	1.0. (Spurious result).
Sample 4.	1,194. (Acceptable).
Sample 5.	0.802. (Acceptable).

Because of the extreme friability of the sample material at least 3 of the samples tested must be regarded as unacceptable.

#### 6.4.6. The Shore Scleroscope Hardness Test.

The Shore Scleroscope determines hardness as a function of the materials elastic properties and is essentially dependent on the quality of the surface finish presented. This can affect the integrity of the results and in this case, most of the material

tested proved to be difficult to produce the degree of surface finish normally acceptable for this test.

The results obtained therefore, must be viewed with some degree of subjectivity and with due regard to the petrological analysis.

Sample Material.	Shore Scleroscope Index.
Sample 1.	Spurious result.
Sample 2.	15.
Sample 3.	12.
Sample 4.	16.9.
Sample 5.	12.38.

#### 6.4.7. The Cerchar Abrasive Index.

It may be recalled that because this test relies on minimum penetration to avoid side wall support of the steel stylus, it is not ideally suitable for the abrasive determination of certain unconsolidated material. The results obtained therefore, must be viewed with some doubt and the author considers that only Sample 1. to be of acceptable integrity. However, the tests were attempted and the results obtained shown as follows:

Sample Material.	Cerchar Abrasive Index.
Sample 1.	4.2. (acceptable).
Sample 2.	1.0-1.2 (Not reliable)
Sample 3.	1.0. (Not reliable)
Sample 4.	0.8-0.9 (Not reliable)
Sample 5.	Not tested.

#### 6.4.8. Dynamic Impact Abrasive Test.

This abrasive index is based on the weight loss sustained by a thin metallic strip contained in a semi-circular rectangular duct after having been impacted by 1000g of specially sized material at a predetermined velocity. The index reference material is an artificial corundum (Baux 60) Moh's hardness 9. and is normally employed as an abrasive medium for grinding wheels. This reference material is given an index of 10, for a specific weight loss and all other materials are expressed relative to this.

Futher details of this test are given later in Chapter 7. of this thesis.

The results obtained from this test show all the material to be of an abrasive to highly abrasive nature and the results obtained are as follows:

Sample Material.	Dynamic Impact Index.
Sample 1.	11.9
Sample 2.	8.1
Sample 3.	10.6
Sample 4.	10.84
Sample 5.	9.9

#### 6.4.9. Petrological Analysis.

Petrological analysis of thin sections of rock was conducted to determine the mineral constituents, their proportions, grain size and shape. This analysis was then used to support the results obtained from standard mechanical tests. Resin impregnated sections were produced from all the sample material and the following descriptions ascertained.

##### Sample 1.

Description: Loose gravel embedded in matrix rich sandy and clay particles.

In hand, both the specimen and thin section exhibited quartz pebbles, the largest reaching up to 10 mm. The matrix material composing of rock fragments, plus sandy grains of quartz and quartzite appeared to be cemented and surrounded by clay and some small amounts of gypsum was also evident. It was very poorly sorted

and angular in shape, the large pebbles were all sub-rounded. These however, could produce very sharp angular material if broken.

#### Sample 2.

Description: Silty Clay. The rock sample material exhibited extensive lamination with fine lamina bands alternating with fine grain quartz or clay rich bands. The rock is not very well cemented and all the grains appear as angular.

#### Sample 3.

Description: Sandstone. This rock sample was rich in opaque phases, the grains are well sorted and sub-rounded. There are some strong bands which exists where the clay reach bands alternate with the sandy reach bands. The cementing material was clay/kaolinite.

#### Sample 4.

Description: Loose fine to medium silt. The rock was poorly sorted and the grains appear to be sub-rounded. The maximum grain size extends up to 1.0 mm. With over 50% of fine grain silicate minerals, Moh's hardness 7, This material could be particularly hostile to the mining operation

TABLE 6.6

## OAKLANDS PROJECT

## Mineral Proportions %

Rock Sample Description	SiO <sub>2</sub> Quartz (7)	SiO <sub>2</sub> Chert (7)	Quartzite + rock fragments (7)	Gypsum CaSO <sub>4</sub>	Clay/ Kaolinite AL <sub>2</sub> O <sub>3</sub> SiO <sub>2</sub> ·H <sub>2</sub> O	Mica KAT <sub>3</sub> Si <sub>0</sub> 10(OH) <sub>2</sub>	Feldspar NaAlSi <sub>3</sub> O <sub>8</sub> - CaAl <sub>2</sub> Si <sub>2</sub> O <sub>8</sub> (5.5 - 6.5)	Carbonate Ca CO <sub>3</sub> (2.5 - 3)	Opaque minerals (6 - 7)
1 Gravelling Sandstone	50	2	20	1	27	-	-	-	-
2 Silty Clay	20	-	10	-	60	10	-	-	-
3 Sandstone	25	-	10	-	52	3	-	-	10
4 Fine to Medium Silt	40	4	4	-	46	<1	2	3	-
5 Coarse loose slit to fine loose sandstone	63	-	5	-	20	<1	1	10	-

NOTE:- Numbers in brackets indicate Moh's Hardness



### Sample 5.

Description: Coarse loose silt to fine loose sandstone. The matrix was a mixture of clay carbonates and very fine quartz and the grains appear sub-rounded and sorted. The quartz however, appear more angular than the rock fragments, the rock fragments being mostly quartzite. It is probable that the quartz and quartzite came from two different geological origins. A summary of the mineral constituents and their proportions is given in Table 6.6.

### 6.4.9. Conclusions.

All the material was extremely weak, friable and unconsolidated which would place it approximately R1 (weak rock) or G4 (cemented soil) on the IGS scale. The material contained high quantities of residual moisture which varied from 7.8% to 14.63%. This moisture content could significantly reduce the shear and compressive strength of the material by as much as 60% to 70%.

Because of the aforementioned condition of the material, standard laboratory tests such as the Cerchar abrasive test, the NCB Cone Indenter and Shore Scleroscope were not possible, without first drying the moisture out of the material. However, it was

apparent that even though these tests were made possible by the effects of drying out the moisture, the clay matrix binding the mineral constituents was not sufficiently competent to permit specimen preparation of the acceptable standard finish, normally required for these tests.

The Cerchar abrasive index for example, is a very useful and simple laboratory test to perform and the results obtained from competent fine to medium grain rock have been shown to be completely reliable with good correlation with picks and cutter replacements in road headers and full face tunnelling machines.etc. The principal weakness with this test however, lies in the fact that the stylus sinks too deeply into this type of unconsolidated material, thus gaining support for the point on the sides of the stylus. This action results in a much smaller wear flat which almost certainly indicates a lower Cerchar index number than expected.

The Shore Scleroscope relies on surface finish for accuracy with the results obtained. Because this quality of surface finish was not possible, the results obtained reflect this deficiency with a high degree of scattered high and low readings, thus leading to spurious and unreliable results.

The NCB cone indenter gives very good results with fine to medium grain competent rock material of almost

any strength and excellent correlation has been found with uniaxial compressive strength. However, because even under the lowest adjusted normal load, mineral particle displacement occurred thus leading to unreliable hardness indices. Consequently, the results obtained from these three mechanical tests, must be viewed with some scepticism.

However, the Dynamic Impact Abrasive Index Test can be viewed with some degree of confidence and the results obtained can be supported by the petrographic analysis of the resin impregnated thin sections.

This test shows all the material to possess a moderate to very high abrasive potential.

Sample 1. which is described as a "gravelly sandstone" contains a high proportion of hard angular minerals (Moh's hardness 7) weakly cemented in a clay matrix. The majority size range of these minerals was below 2.0 mm. and of these, about 80% were below 0.5 mm. These small mineral grains can under certain circumstances, prove to be extremely abrasive, further, depending on the operation, if the pebbles and larger material are broken down, these can present many new sharp edges which could significantly increase the abrasive potential of the material. The index was 11.9 which indicates a very high abrasive potential.

Sample 2. Described as a "silty clay" and with about 52% clay/kaolinite matrix material, the majority of the hard minerals was made up from approximately 30% fine quartz (<350  $\mu\text{m}$ ) and quartzite plus rock fragments (<150  $\mu\text{m}$ ) this is still an abrasive material. Though not as abrasive as Sample 1. an abrasive index of 8.1. indicates an abrasive material.

Sample 3. Described as a "sandstone". The material is made up from 35% quartz and quartzite plus fine rock fragments the remainder being made up from approximately 10% opaque minerals and some small amounts of white mica. The size range of these mineral grains was screened out at plus 210  $\mu\text{m}$  to minus 350  $\mu\text{m}$  and this size range has proven to be the most abrasive range with the dynamic impact test. This most probably accounts for the high abrasive index. An abrasive index of 10.6 indicates a highly abrasive material.

Sample 4. "A loose fine to medium silt". With 48% fine angular quartz grains, all of which were in the most abrasive size range. This material must be regarded as potentially, a highly abrasive material which is borne out by the abrasive index of 10.84.

Sample 5. "Coarse loose silt to fine loose sand". With 58% quartz and quartzite material present, the abrasive index might have been expected to be higher. However, it has been found that grain partical shape can significantly affect the abrasiveness of certain rock forming minerals. The sub-rounded material in this sample can be put forward as the reason for this marginally lower than expected abrasive index.

An abrasive index 9.9 is still a potentially high abrasive material.

Because it was easily possible to break down the cementing material in water, all the impact abrasive tests were conducted on wet screened and unaltered mineral constituents. This has an added advantage over normally crushed competent rock material, where some alteration in the natural size and shape of the minerals is unavoidable. Thus the integrity of the results obtained from this type of sample material will only be enhanced.

## 6.5. URANIUM MINING OPERATION.

### 6.5.1. Introduction.

A large South African Uranium surface mining operation presented major abrasive wear problems during the excavation of the overburden.

The mine was a conventional open pit mine, excavating about 5 million tonnes per year worked by the following systems:

- a) Drill and blast using 356 mm diameter blast holes and dense ANFO explosives.
- b) Large Circa 14 cubic metre rope shovels.
- c) Large Circa 180 t. rear dump trucks.

The rock has distinctive jointing patterns and tends to break out in block formations approximately 1.5 cubic metres in size. Consequently, high powder factors were required to reduce these block sizes.

The major problems encountered in this operation were due to the following causes:

- a) Abrasion.
- b) Fatigue failure of the shovel dipper sticks and booms.

- c) Choking of the primary gyratory crushers due to excessive fines caused by the high powder ratios.

To reduce these problems therefore, a better understanding of the abrasive properties of the overburden rocks and their structure was required. The structural aspects have not been considered in this thesis, although, there had been major metamorphism of the area and distinctive steeply dipping joints and bedding planes were evident.

#### 6.5.2. Rock Sample Material.

A total of nine rocks were received from Rossing Uranium Mine through Mr Fenwick, the Assistant General Manager and these are designated in the following order:

##### Sample No.

- 1) px-hb Gneiss
- 2) px-gt Gneiss
- 3) Amphibolite
- 4) px-gt Gneiss
- 5) bi-amph Schist
- 6) Marble
- 7) Bi-cord Gneiss
- 8) Pegmatic Granite
- 9) Granite

TABLE 6.7

NO.	ROCK SAMPLE	ROCK HARDNESS INDEX						ROCK ABRASIVE INDEX		COMPRESSIVE STRENGTH MPa			
		NO. OF TESTS	SHORE SCLEROSCOPE	NO. OF TESTS	NCB CONE INDENTER	NO. OF TESTS	CERCHAR INDEX	NO. OF TESTS	STANDARD H/D RATIO = 2:1	DERIVED UCS VALUE			
											MEAN		S.D.
		MEAN	S.D.	MEAN	S.D.	MEAN	S.D.	MEAN	S.D.	MEAN	S.D.	MEAN	S.D.
1	Pyroxene-Hornblende Gneiss	80	81.7	9.05	30	10.34 m	4.68	10	4.65	0.26	-	-	173.2
2	Pyroxene-Garnet Gneiss	80	95.7	4.15	30	11.96 m	5.02	10	3.46	0.031	-	-	202.8
3	Amphibolite	80	63.16	6.6	30	9.71 m	2.99	10	4.48	0.11	-	-	133.8
4	Pyroxene-Garnet Gneiss	80	84.75	7.2	30	6.23 m	1.72	10	4.01	0.15	-	-	179.6
5	Biotite-Amphibole Schist	80	43.9	10.4	30	4.18 s	2.07	10	3.6	0.314	-	-	103.6
6	Marble	80	46.97	9.2	24	3.78 s	1.39	10	4.17	0.26	-	-	99.5
7	Biotite-Cordierite Gneiss	80	72.9	11.8		5.69 s	2.24	10	4.56	0.3	-	-	154.5
8	Pegmatic Granite	80	94.26	13.0		9.50 s	7.7		4.69	0.23	-	-	199.8



These rocks were tested to determine the following parameters:

- 1) Uniaxial Compressive Strength.
- 2) Shore Scleroscope Hardness.
- 3) NCB Cone Indenter Hardness.
- 4) Cerchar Abrasive Index.
- 5) Petrological analysis.

Visual in-hand examination of the sample material revealed that all the material was of a highly competent nature and scratch tests indicated a Moh's hardness of 6 to about 7.5. Based on this test alone, this material could be regarded as a hard and highly abrasive rock. Unfortunately, insufficient material was supplied to carry out conventional uniaxial compressive strength tests and this parameter was subsequently derived from the Shore Scleroscope and NCB cone indenter hardness tests.

A summary of the physical property test results are given in Table 6.7.

#### 6.5.3. Rock Description.

Thin sections of all the rock material were prepared and subsequently analysed under a petrological microscope to determine the texture, the mineral constituents and their proportions.

**Sample No 1. Pyroxene-Hornblende Gneiss.**

A granoblastic texture consisting mainly of pyroxene and plagioclase feldspar with some quartz. Minor grains of zircon and apatite were present as inclusions in pyroxene and feldspar. Opaque minerals were present interstitially to the feldspar and pyroxene. In some places carbonate had been introduced (secondary) and was associated with the alteration of pyroxene to chlorite and feldspar to sericite.

**Sample No 2. Pyroxene-Garnet Gneiss.**

A granoblastic texture of slightly altered plagioclase feldspar, quartz and pyroxene. Abundant granular zircon was present as was minor apatite and opaques. Some interangular carbonate were also present and seemed to be associated with the alteration of some pyroxenes.

**Sample No 3. Amphibolite.**

A granoblastic texture of hornblende brownish green, (slightly poikiloblastic) and plagioclase.

**Sample No 4. Pyroxene-Garnet Gneiss.**

A granoblastic texture of green pyroxene, plagioclase and quartz. The clear pyroxene (diopside) seemed to be forming small metacrysts. Some biotite was present and

showed slight alteration to chlorite. Granular apatite, zircon and opaques were also present.

**Sample No 5. Biotite-Amphibole Schist.**

A decussate texture of hornblende, biotite and plagioclase which showed slight sericitisation. Hornblende and biotite were present in schistose layers.

**Sample No 6. Marble.**

A granoblastic texture of carbonate, diopside and forsterite, much of which showed alteration to serpentine. Some platy muscovite was also present.

**Sample No 7. Biotite-Cordierite Gneiss.**

A schistose groundmass of biotite laths, plagioclase and quartz. Some quartz porphyroblasts were present and contained poikiloblastic inclusions of feldspar.

**Sample No 8. Pegmatitic Granite.**

This rock consisted of feldspar (microcline and plagioclase) and quartz with large laths which showed alteration to chlorite with associated carbonates. The microcline and quartz often occurred in graphic intergrowths. Minor muscovite and zircon were also present. Epidote was present as inclusions in biotite.

#### Sample No 9. Granite.

An equigranular mass of quartz and feldspar.

#### 6.5.4. Conclusions.

The silica content present as quartz was low in all the samples with the exception of Sample No 8. Pegmatitic Granite, which was 37.5%. However other hard minerals were present and these could cause high levels of abrasion due to their hardness and crystal shape. Some of the rocks had a wide range of hardness e.g. Schist. This can cause increased abrasion as when being excavated, passing through transfer points, and pipelines, etc. where new abrasive surfaces are continually being presented to abrade the confining media.

Free silica, generally quartz, have irregular grain shapes that may range from very angular through sub-angular to rounded. All have a high abrasive potential but the more angular grains will obviously be more abrasive initially.

Sample No 1. px-hb Gneiss. Although this sample had only 8.5% angular quartz grains  $SiO_2$  (chain structure), Mh7 (Moh's hardness 7,) it contained 63.5% feldspar,  $SiO_3$  Mh6 and 24.5% pyroxene  $SiO_2$  Mh5-6. The feldspar and pyroxene have cleavage planes

at approximately 90°. The Cerchar abrasive index was 4.65 (mean). This rock therefore, must be regarded as a very highly abrasive material.

Sample No 2. px-gt Gneiss. This rock was similar in composition to Sample No 1. but the Cerchar abrasive index was lower at 3.46 (mean). However it must still be regarded as an abrasive rock material.

Sample No 3. Amphibole. With 67% hornblende and 32.5% feldspar taken together with a Cerchar abrasive index of 4.48 (mean), this is a highly abrasive rock material.

Sample No 4. px-gt Gneiss. This rock contained 69.5% feldspar and 15.5% pyroxene. With a Cerchar abrasive index of 4.01 (mean) this rock will have a high abrasive potential.

Sample No 5. bi-amph Schist. This rock is also a highly abrasive rock.

Sample No 6. Marble. Despite the high carbonate content of some 49.5% and the relatively low hardness of these minerals, it contained 44.5% diopside Mh5-6 and 4.5% forsterite Mh6-7. It was not surprising therefore, that the Cerchar index for this material

was as high as 4.16 (mean). Thus, this rock must be classified as a highly abrasive material.

Sample No 7. bi-cord Gneiss with 10% quartz Mh7, 47.5% feldspar, 12% cordierite, Mh7-7.5. and 5% garnet Mh6.5-7.5. this rock must be regarded as a highly abrasive material. The cordierite has orthorombic and short pseudo hexagonal crystals. Garnet has rhombdodecahedron and trapezohedron crystals. Although less angular than quartz they present many hard, structurally strong, sharp surfaces to severely abrade the confining media. Furthermore, as the material degrades when passing through transfer points, it presents additional abrading surfaces. Finally, with a Cerchar abrasive index of 4.56 (mean) this must be regarded as an extremely abrasive rock material.

Sample No 8. Pegmatitic Granite. This rock material contained 37.5% of fine grained angular quartz Mh7 and 62.5% feldspar Mh6-6.5. The Cerchar abrasive index was the highest at 4.96 (mean) and was classified as an extremely high abrasive rock material.

Sample No 9. Granite. With 18% quartz Mh7 and 82% feldspar Mh6-6.5. This rock has a very high abrasive potential.

**TABLE 6.8**  
**Mineral Proportions**

Rock	Quartz	Feldspar	Pyroxene	Hornblende	Biotite	Diopside	Forsterite	Cordierite	Garnet	Carbonate	Zircon	Opaque
1. px - hb gneiss	8.5	63.5	24.5	-	-	-	-	-	-	-	0.5	3.0
2. px - gt gneiss	7.5	64.0	25.0	-	-	-	-	-	-	-	3.5	-
3. Amphibolite	0.5	32.0	-	65	-	-	-	-	-	-	-	-
4. px - gt gneiss	6.5	69.5	15.5	-	1	-	-	-	-	-	-	-
5. Bi-amph Schist	4.0	22.0	-	72	2	6	-	-	-	-	0.5	1.0
6. Marble	-	-	-	-	Muscovite	44.5	4.5	-	-	49.5	-	-
7. Bio-cordierite gneiss	10.0	47.5	-	-	25	-	-	12	5	-	-	-
8. Pegmatitic granite	37.5	62.5	-	-	-	-	-	-	-	-	-	-
9. Granite	18.0	82.0	-	-	-	-	-	-	-	-	-	-

TABLE 6.9  
Mineral Sizes (mm)

Rock	Quartz	Feldspar	Pyroxene	Hornblende	Biotite	Diopside	Forsterite	Cordierite	Garnet	Carbonate	Zircon	Opaque
1. px - hb gneiss	<0.5	<0.7	<0.4	-	-	-	-	-	-	-	<0.1	<0.2
2. px - gt gneiss	<0.5	<1.0	<0.5	-	-	-	-	-	-	-	<0.2	-
3. Amphibolite	<0.5	<0.5	-	<2	-	-	-	-	-	-	-	-
4. px - gt gneiss	<0.5	<0.5	<0.4	-	<0.5	<0.4	-	-	-	-	<0.1	<0.1
5. Bi-amph Schist	<0.3	<0.3	-	<0.4	<0.4	-	-	-	-	-	-	-
6. Marble	-	-	-	-	Muscovite <0.3	<0.4	<0.3	-	-	<5	-	-
7. Bio-corderite gneiss	<0.5	<0.5	-	-	<0.5	-	-	<0.7	<0.7	-	-	<0.1
8. Pegmatitic granite	<4.0	<5.0	-	-	-	-	-	-	-	-	-	-
9. Granite	<4.0	<5.0	-	-	-	-	-	-	-	-	-	-



A summary of the mineral proportions and mineral grain sizes is given in Table 6.8. and 6.9.

To reduce block size and reduce the production of fines, the following measures were taken:

- a) A closer blast hole grid was used,
- b) Smaller diameter blast holes were drilled, thus reducing the size of charge, resulting in reduced fines.
- c) Bottom initiation was adopted using detonating cord to a cannister primer. The detonating fuse is not strong enough to detonate the heavy ANFO.

The use of decked charges was considered, but because of charging problems and the presence of ground water, it was decided that smaller blast holes were more practical.

The shovel abrasion problems remained but conveyor idler bearing failures were much reduced and the choking problem was completely eliminated.

## 6.6.BWE. OPERATION IN WEAK UNCONSOLIDATED SANDSTONE.

### 6.6.1. Introduction.

This study was concerned with the surface mining operations of lignite where the overburden removal of unconsolidated sandstone presented major problems caused by severe abrasive wear.

The Neyveli Lignite Mine is located in the State of Madras, South India, approximately 180 miles south of Madras. The overburden is of Tertiary age and consists mainly of clays, marls and weak sandstones and the major bed is the Cuddalore sandstone. The mine was planned for an initial lignite output of 3.5 million tonnes per year and the lignite and overburden was mined using Terrace Mining techniques with BWE excavation and belt conveyor transport. Extremely severe abrasive wear problems occurred from the start of mining.

This section covers a number of tests made on the overburden i.e. 'Cuddalore Sandstone' to ascertain hardness and abrasiveness with particular reference to BWE operations.

SAMPLE MATERIAL SET IN CONCRETE.



Figure 6.2.

SPECIMEN MATERIAL PRODUCED.

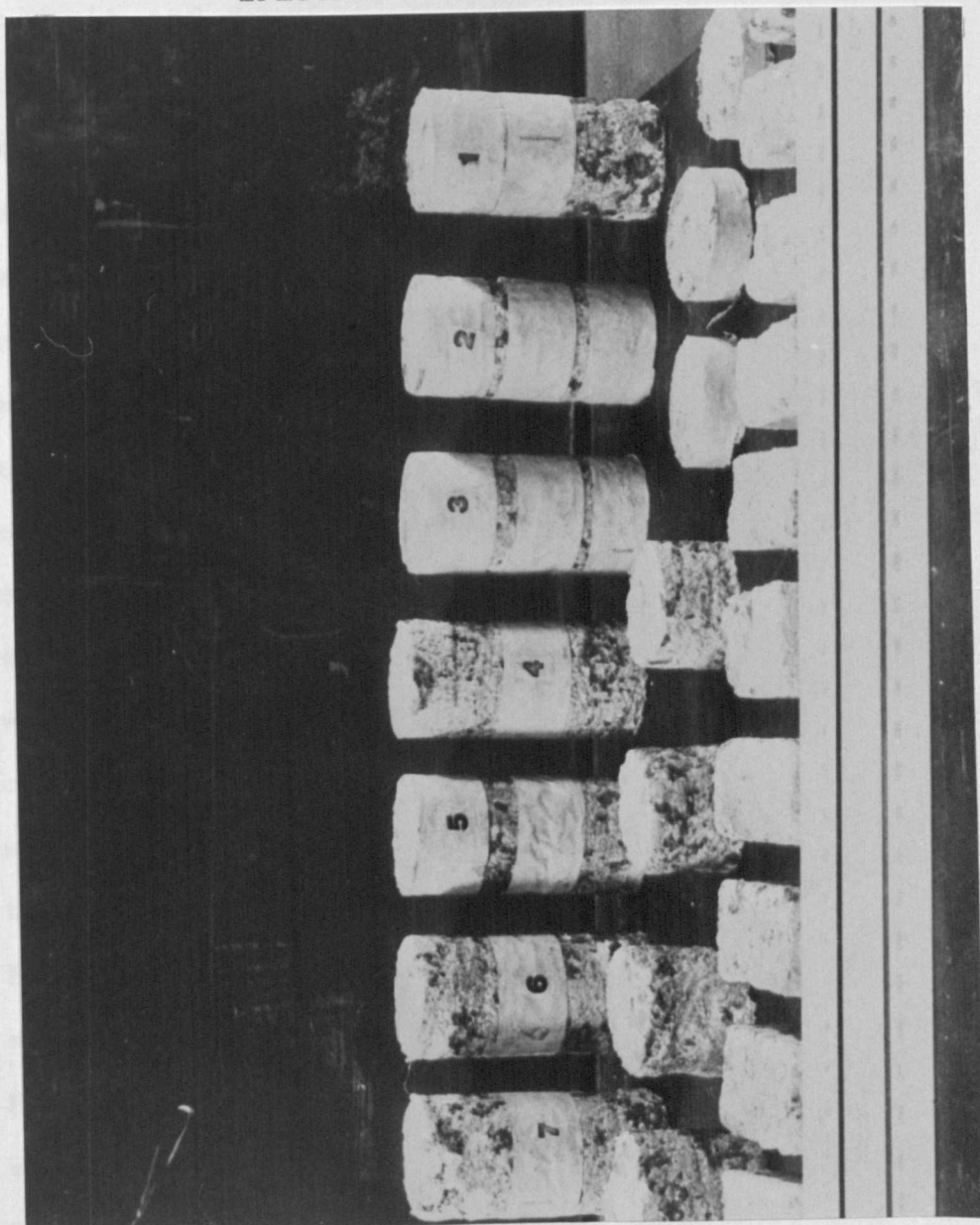


Figure 6.3.

#### 6.6.2. Sample Material.

A total of 9.3 kg of sample material carefully packed in polyurethane was supplied in bulk. However, there was evidence of some degree of dehydration during transit and immediately upon receipt, the sample was treated with polyurethane varnish to retard further moisture loss. Owing to the relatively small amount of material available for testing, the sample was later set in a concrete cast to facilitate maximum core and other specimen recovery. This technique of setting sample material in concrete, enables accurate orientation while presenting the maximum area of sample material for coring, at the same time, allowing stress free coring to be carried out.

A total of seven cores 38 mm diameter by 76 mm long were produced together with a number of discs and cuboid blocks. Five cores were used to determine the uniaxial compressive strength and the remainder used to determine hardness and abrasiveness.

Figure 6.2. shows the sample material set in concrete and the core specimens produced.

Figure 6.3. Shows the total amount of specimen material produced.

Subsequently, five established tests were conducted as follows:

TABLE 6.10.

## SHORE SCLEROSCOPE HARDNESS TEST

Rock Material: Cuddalore Sandstone

Site of Origin:

Specimen Number 5		Specimen Number 6		Specimen Number 7		Specimen Number	
8	7	8	6	14	9		
13	7	9	10	14	8		
8	8	9	10	7	10		
9	10	12	10	7	9		
8	8	10	9	8	10		
12	10	10	9	10	9		
9	8	10	10	8	9		
10	10	11	11	6	8		
8	13	10	9	8	10		
10	11	9	6	11	8		
9	9	9	7	9	7		
11	9	11	9	8	8		
7	14	11	8	14	11		
7	11	9	7	6	9		
7	8	10	9	9	12		
12	10	8	7	6	7		
9	10	7	9	10	8		
13	12	11	10	7	10		
9	7	11	9	7	9		
11	8	8	12	10	10		
$\bar{x}$	9.55	$\bar{x}$	9.52	$\bar{x}$	9.00	$\bar{x}$	
SD		SD		SD		SD	
<u>Remarks</u>							

TABLE 6.11.

SHORE SCLEROSCOPE HARDNESS TEST

Rock Material: Cuddalore Sandstone

Site of Origin:

Specimen Number 1		Specimen Number 2		Specimen Number 3		Specimen Number 4	
10	7	7	10	15	8	10	7
10	9	9	10	13	8	8	10
8	9	9	10	8	8	8	14
10	12	11	8	11	8	7	10
9	10	8	8	9	9	8	10
10	7	10	7	7	9	8	12
11	11	8	7	9	9	8	10
6	9	9	8	7	15	9	7
8	6	8	11	8	8	9	9
8	10	12	11	12	14	8	10
8	12	10	7	8	10	8	12
10	8	9	8	10	7	10	12
8	10	9	10	9	7	12	12
9	8	9	9	7	8	7	9
8	7	8	12	10	12	6	9
9	10	10	12	13	7	9	10
9	9	5	10	10	9	9	10
11	11	5	10	10	10	6	9
12	7	12	11	10	8	10	10
11	8	11	10	10	8	11	9
$\bar{x}$	9.05	$\bar{x}$	9.2	$\bar{x}$	9.8	$\bar{x}$	9.3
SD		SD		SD		SD	

RemarksMean of 7 specimens = 9.345  $\pm$  0.101

- 1) Uniaxial Compressive Strength.
- 2) NCB Cone Indenter Hardness Test.
- 3) Shore Scleroscope Hardness Test.
- 4) Cerchar Abrasive Index.
- 5) Thin Section Petrological Analysis.

#### 6.6.3. Test Results.

Rock hardness was determined by both the NCB Cone Indenter and the Shore Scleroscope. Forty test readings were made on each of the seven test specimens and used to determine the Shore hardness values and Tables 6.10. and 6.11 show the results obtained. It can be seen that these range from 9 to 9.8 with a mean Shore hardness determination of 9.345 from 280 measurements.

The NCB Cone Indenter hardness index was determined from 7 discs and used to supplement the hardness index obtained from the Shore Scleroscope tests. Normally at least 20 indices can be measured from each face on a specimen, however, because of the extremely friable nature of the sample rock material, the cone penetration even under the lowest recommended force (12 N) was considerably deep and consequently, any attempt to take measurements in close proximity to each other caused the rock to fail at the point of contact, thus only 5 tests were possible on each





specimen disc. Table 6.12. illustrates the results determined from 35 measurements obtained from 7 discs. The hardness index is defined as for weak rocks and the normal load used for this test was 12 N. The mean resultant NCB Cone Indenter hardness index was 1.711.

Abrasiveness was determined by the Cerchar abrasive index and the results were derived from 40 determinations. The resultant index therefore, was 1.358. However, because of the extremely weak nature of this rock material, the stylus tends to sink deeper into the rock thus redistributing the load of 7 kg onto the sides of the cone and away from the point, consequently, indicating a lower index than might be anticipated. This index therefore, must be regarded with some degree of scepticism.

Subsequent dynamic impact tests conducted on remnants of this rock material after the report was completed, substantiated the highly abrasive nature of the material.

Petrological analysis of thin sections showed that the material consisted of angular quartz grains <0.5 mm that show undoluse extinction (pressure twinning). The quartz is set in a ground mass of cryptocrystalline silica (chalcedony) and fine grained clay minerals. Some small quantities of zircon <0.1 mm and geothite were also present. The grain shapes were

almost all angular to very angular with practically no sub-angular or rounded grains.

Because of the simple composition of this material XRD tests were not considered necessary. The principal mineral proportions are given as follows:

Quartz	Crypto Silica	Clay Minerals
58%	31%	11%

A summary of the test results are given in the following list:

Shore Scleroscope Hardness Index	9.375.
NCB Cone Indenter Hardness Index	1.711.
Cerchar Abrasive Index	1.358.
Uniaxial Compressive Strength	1.585 MPa.

#### 6.6.4. Soak Tests.

Aqueous soak tests were conducted on three test specimens of equal mass (23 - 24g) to investigate the possibility of material breakdown with water infusion. The specimens were immersed in water and stored at an ambient room temperature of 20°C in an undisturbed environment. The water was adjusted to three pH values of pH 7, pH 4 and pH 10.

The tests showed immediate reaction taking place when the rock was immersed and minor cracks appeared within

the first few minutes. Disintegration began within the next 24 hours with almost total disintegration after 72 hours. It was significant however, that reaction to acidity pH 4 was marginally greater than the other two. Water infusion would probably not be successful as the rock breaks down slowly, mainly due to its relatively low permeability caused by the clay matrix material.

#### 6.6.5. Conclusions.

The Cuddalore sandstone is a weak and friable rock material about R1 (weak rock) or G4 (cemented soil) of the GS scale. On strength parameters alone, this material would normally be considered as "marginally wheelable" for digging with specially designed bucket wheel excavators, without the necessity for prior ground preparation by blasting.

Although the material, based on the results obtained from the Cerchar test was 'not' found to be highly abrasive, petrological analysis indicated the abrasiveness to be extremely high and was considered to be more accurate in this case. A photomicrograph of a thin section of the Cuddalore Sandstone, clearly illustrated the severe angularity of the hard quartz constituent mineral grains. (see Figure 2.2.)

The existing operation using light blasting with soft explosives reported teeth life of 350 hours (originally 2.5 to 3.5 hours) before a complete change of teeth was necessary. Modifications included large tungsten carbide inserts on the teeth with the parent metal being protected by hard facing with tungsten carbide granules in a cobalt alloy metal deposited on a buffer layer. All the welding was done in the workshop and quick fixing devices were employed to facilitate fast changes of bucket and cutting bow assemblies. Down time for a tooth change took approximately 9 hours.

The tests indicate that the material is not suitable for excavation by BWE's. The digging action of the BWE continually forces the bucket wheel and cutting bow teeth into contact with fresh ground. The presence of a high percentage of highly angular quartz grains can result in major abrasive wear problems to the teeth and their supports. One method of reducing this wear is to obtain a high degree of loosening of the rock material before digging. This could be achieved by the use of horizontal blast holes which, with a low specific explosive charge produces better fragmentation. This form of blasting however, is more difficult to schedule as it must be carried out just ahead of the excavation and there must be a clear bench above for a safe distance.

Conventional excavation using crowd shovels after blasting, loading onto a mobile crusher before loading onto a conveyor belt system, would probably greatly reduce abrasive wear problems associated with BWE teeth. Crusher wear could be overcome by the use of MMD type crushers.

## 6.7.CORE DRILLING IN BANDED IRONSTONE.

### 6.7.1.Introduction.

The investigation was concerned with problems associated with the difficulties encountered when core drilling banded ironstone in Australia.

This section describes tests conducted on banded ironstone rock samples supplied by Craelius AB. in Sweden. The objectives of the project were to evaluate certain rock properties in order to assist in the choice of the most suitable bit design with special regard to the matrix material, diamond type and concentration.

The following tests were subsequently carried out:

- 1) Uniaxial compressive strength. (UCS).
- 2) Shore Scleroscope hardness tests.
- 3) NCB Cone Indenter hardness tests.

- 4) Cerchar abrasive tests.
- 5) Petrographic analysis.

#### 6.7.2. Rock Sample Material.

The rock sample material consisted of eight pieces of rock made up from the following:

Sample 1. Described as Australian banded ironstone.

This rock sample comprised a short length of cored material 35 mm diameter by 150 mm long which was cored at 25° to the bedding. Figure 6.5.

Sample 2. Comprised six small fragments of rock similar to Sample 1. illustrated in Figure 6.6.

Sample 3. A short length of cored material 35 mm diameter by 60 mm long which appeared to have broken away from Sample 1.

#### 6.7.3. Specimen Preparation.

In-hand inspection of the rock samples showed all the material to be of a highly competent nature with no obvious signs of faulting or jointing. The material was measured and weighed to establish volume and density. Subsequently, thin slices were cut along the length of Sample 1. and eight thin sections were prepared for petrographic analysis. Further slices

were cut along the opposite face of the core to provide material for the NCB Cone Indenter hardness test, the Shore Scleroscope hardness test and Cerchar abrasive test. In addition, one slice was cut from one of the remaining rock samples for thin section petrographic analysis. Because of the opaque nature of some of the thin section specimens, duplicate specimens were made in the form of polished mounts and examined under a standard petrographic microscope using reflected light.

Unfortunately, insufficient material was made available for standard uniaxial compressive strength tests and consequently, this important parameter was derived from the hardness tests.

#### 6.7.4. Discussion of Results.

---

The eight rocks were examined and tested and the following conclusions ascertained. The specimens were identified under the following designations:

0/M27 - 7/M34, 7A/M35 and 0/M36.

All the rock samples were of the same origin and are described as an ironstone formation of Pre-Cambrian age and located in Australia.

The rock is characterised by an interlaminated succession of disseminated bands of stratified iron oxides together with microcrystalline silica. Three



TABLE 6.13.

% MINERAL PROPORTIONS

Sample No.	$\text{Fe}_3\text{O}_4$ Magnetite	$\text{Fe}_2\text{O}_3$ Hematite	$\text{SiO}_2$ Quartz	$\text{FeS}_2$ Pyrite	$\text{CaCO}_3$ Carbonate	$\text{Si}_4\text{O}_{10}$ Mica
0/M27	44	10	45	<.5	<.5	<.5
1/M28	10	24	65	<.5	<.5	<.5
2/M29	40	20	39	<.5	<.5	<.5
3/M30	50	<1	45	<.5	<.5	<.5
4/M31	45	5	46	<.5	<.5	<.5
5/M32	55	14	30	<.5	<.5	<.5
6/M33	40	<5	55	<.5	<.5	<.5
7/M34	40	15	45	<.5	<.5	<.5
7A/M35	36	3	60	<.5	<.5	<.5
0/M36	-	95	4	<.5	<.5	-

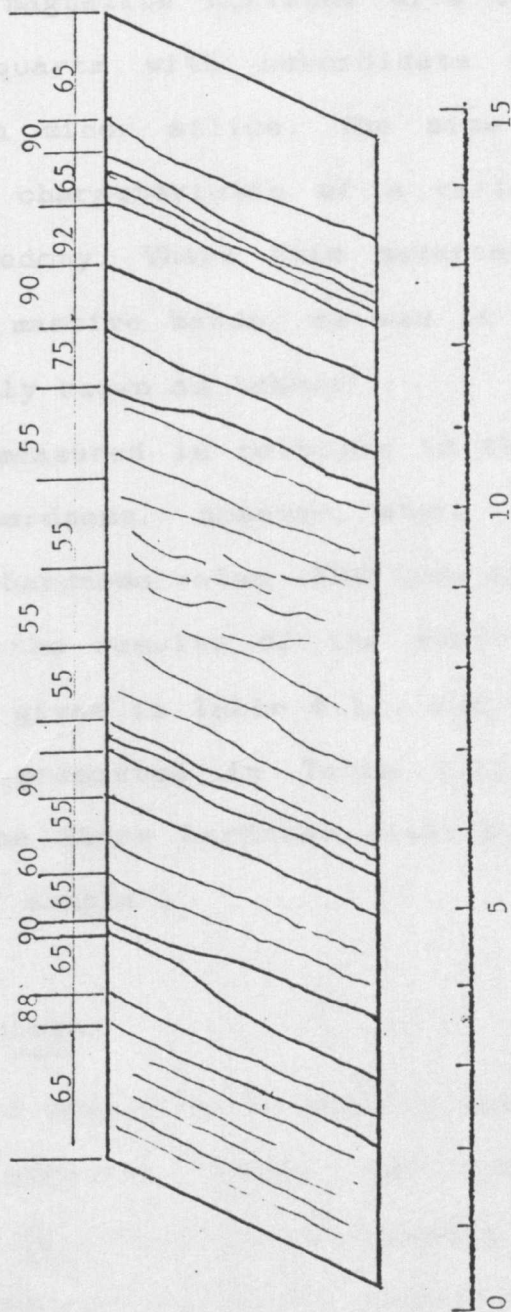
TABLE 6.14.

LABORATORY INDEX TESTS

ROCK SAMPLE	ROCK HARDNESS INDEX					ABRASIVE INDEX			STRENGTH PROPERTIES	
	NO. OF TESTS	SHORE SCLEROSCOPE		NO. OF TESTS	NCB CONE INDENTOR	NO. OF TESTS*	CERCHAR INDEX		DERIVED UCS MPa	
		MEAN	SD				MEAN	SD		
1 O/M27 - 7/M34	30	81.65	11.62	20	6.86	10	3.28	0.304	171.52	
2 7A/35	20	86.15	13.26	20	7.24	10	3.14	0.134	181.06	
3 O/M36	20	84.3	7.03	20	7.08	10	4.2	0.245	177.136	

# AUSTRALIAN BANDED IRONSTONE

Shore Scleroscope Hardness Distribution.



main types of banding occurred in most of the sections analysed, the first being coarsely crystalline, predominantly magnetite horizons with the second and third being quartz with subordinate haematite and haematite with minor silica. The size and textures observed were characteristic of a variety of silica known as chaledony. Where this material occurred as stratified or massive bands, as was in this case, it is more commonly known as 'chert'.

Hardness was measured in relation to the Moh's scale of mineral hardness, however, where appropriate a Vickers micro-hardness value (VHN) was also applied.

A summary of the results of the tests on the three main rocks is given in Table 6.13. and the laboratory test results presented in Table 6.14. Figure 6.5. illustrates the Shore hardness distribution over the full length of sample 1.

#### 6.7.5. Conclusions.

Samples 1 and 2 appear to be equally abrasive and with a Cerchar abrasive index of 3.28 and 3.14 respectively, this rock would normally be classified as an abrasive rock material. Sample 3. had a higher Cerchar abrasive index of 4.2 which could be classified as a highly abrasive rock. The hardness and derived physical strength parameters were very similar

for all the specimen material and is clearly substantiated by the petrological analysis where all the principal minerals were in the range 5.5 - 7 on the Mohs hardness scale and 593 - 1038 on the Vickers hardness scale.

The physical strength parameters were calculated from the Shore hardness and NCB cone indenter index values. Physical strength properties have been shown to be a function of the degree of cementation in addition to the mineral constituents present. In this case, the cementing material was made up from very fine and tightly interlocking grains of haematite. The quartz bands are massive fine grained material 0.05 - 0.1 mm. In Sample 3. very little cementing material was present and the rock acquired its strength from minute interlocking anhedral grains. Where the oxide was in contact with the gangue, (non-metalliferous minerals) finely inter-penetrating thin tabular crystal terminations 0.01 - 0.02 mm maximum were observed.

It was evident that the drilling of this material by the diamond coring process would prove to be very difficult. This was attributed to the high strength and hardness properties of the rock formation and although the abrasiveness of the material was considered high for most rock breakage processes, the cuttings generated at the interface between the bit and the rock, did not sufficiently abrade the matrix

material of core bit to allow for the provision of fresh indenters.

A compromise between bit wear and penetration rate could be achieved by the choice of a core bit with a thin kerf such as a 'T' or 'TT' series core barrel. This could be set with a lower concentration of good quality small artificial diamond indenters, e.g. a 30 - 35 concentration of SDA 100. polycrystalline diamonds and with low wear resistance matrix material. This configuration would allow worn and polished diamonds to be released earlier and although the nominal penetration per metre drilled per bit would be lower, this would be more than compensated for by the down time saved by tripping and the reduced capital costs per bit.

Drill operator experience would also be essential when coring this type of rock formation. The chosen drilling parameters such as rotational cutting speed, load on the bit, (a constant rate of feed would be better in these circumstances) and flush flow rate would require expert control to ensure the most efficient use of the down hole drilling equipment.

## **CHAPTER 7.**

### **DEVELOPMENT OF DYNAMIC TESTS FOR THE EVALUATION OF ABRASIVITY AND HARDNESS OF ROCK.**

## CHAPTER 7.

### Development of Dynamic Tests for The Evalution of Abrasivity and Hardness of Rock.

#### 7.1. Introduction.

The action of the two specific wear mechanisms, commonly known as attritional wear and dynamic impact wear can be related to many processes involved with the comminution or transport of particulate rock material.

Attritional wear for instance, can be directly related to the action of a cutting tool used with road headers or coal cutting machines etc. This mechanism can be defined as function of a continual interaction of a mechanical device under a specific a specific force (N) over a predetermined distance (m). Wear being generated by the frictional resistance of the interacting media. Dynamic impact abrasion can be related to the action of fine particulate material being transported in pipes and its effect on the transport confining media, in addition to the effect it may have on impellers and other mechanical components of associated pumping equipment. The mechanism being one of continual impaction by rock particles at a velocity (m/sec) and quantity (kg). This mechanism produces surface micro-fracturing with subsequent material loss or degradation.

In the past, the Cerchar abrasive test has been commonly exploited to determine a classification for abrasiveness of



rocks. However, this test has been found to be inapplicable for a number of rock types and rock breakage processes. Consequently, it became apparent that a limited number of new tests which could provide an assessment of abrasiveness of both consolidated and unconsolidated rocks was necessary. Moreover, these new tests should bear some relation to both dynamic impact and attritional wear mechanisms.

## 7.2. Research Objectives.

The objectives pursued in this area of research was to investigate and attempt to find a solution to the following problems:

- a) To determine the abrasiveness of weak and friable rock material. This type of rock material is normally regarded as untestable by the Cerchar method.
- b) To determine the abrasiveness of unconsolidated rock material.
- c) To determine the abrasiveness of strong competent rock material, where the grain sizes extend beyond the normal stroke of the Cerhars stylus. (10 mm)
- d) To design a test or tests to simulate both impact and attritional wear mechanisms.
- e) To correlate any new test concept with actual field data or laboratory trials with mechanical and or intrinsic properties of rocks.

- f) The new tests should have regard for basic economics and limited supply of sample material without loss of integrity.

### 7.3. Dynamic Particle Impact Abrasive Test.

Work on drilling and sawing of rocks, previously described in Chapters 4 and 5 of this thesis, exposed the limitations of the available tests to relate to the rock disintegration processes involved. Therefore, the impact abrasion test was designed to simulate those processes involving various dynamic impact mechanisms of fine rock particles associated with sawing and drilling (with diamond tools). This test involves the production of very fine particulate rock material at very high cutting velocities (80-100 m/sec.). Although it should be noted that in the latter example, it is the saw that interacts with the rock rather than the rock interacting with the mechanical device. In drilling operations, wear occurs at the interface between the bit and the rock, thus resulting in attritional wear of the diamond indenters and matrix materials of the crown. Impact and attritional abrasive wear problems associated with down the hole equipment occur as a result of high up-hole velocities of the debris carrying flush media. The test can also be associated with transport systems in pipes, impaction of broken rock material unloading from conveyors onto the walls of chutes and transfer points etc.

### **7.3.1. Description of Test Equipment.**

The Impact Abrasive Test comprises a semi-circular, square sectioned steel duct manufactured from EN 24 alloy steel. The duct has a 75 mm radius and its effective section is 6 mm x 6 mm providing a cross sectional area of 36 mm squared. A square to round pipe adaptor is attached to each open end of the duct to facilitate the attachment of feed and return pipes. The duct is manufactured from two separate components:

#### **1) The Open Duct Section.**

This section has an accurately machined 6 mm x 6 mm square sectioned groove turned to 150 mm diameter in a 25 mm wide circular disc. A 12.5 mm wide recess by 0.1 mm deep is machined into the outer periphery of the duct to locate an inter-changable thin metallic wear strip. This wear strip is employed to determine the abrasive potential of the rock material. After the disc had been machined, the disc was cut to provide a 180 degree semi circle.

#### **2) The Duct Cover Cap.**

The duct cover cap was manufactured from the same material as the duct and was turned from a disc 200 mm diameter by 25 mm wide. 3 holes were drilled on a pitch circle around the periphery to accomodate 3 caphead screws used to locate and secure the cover cap and wear strip. These screws were off set to avoid interference with the wear strip.

#### **3) Wear Strip.**

The wear strip is manufactured from 0.1 mm thick shim

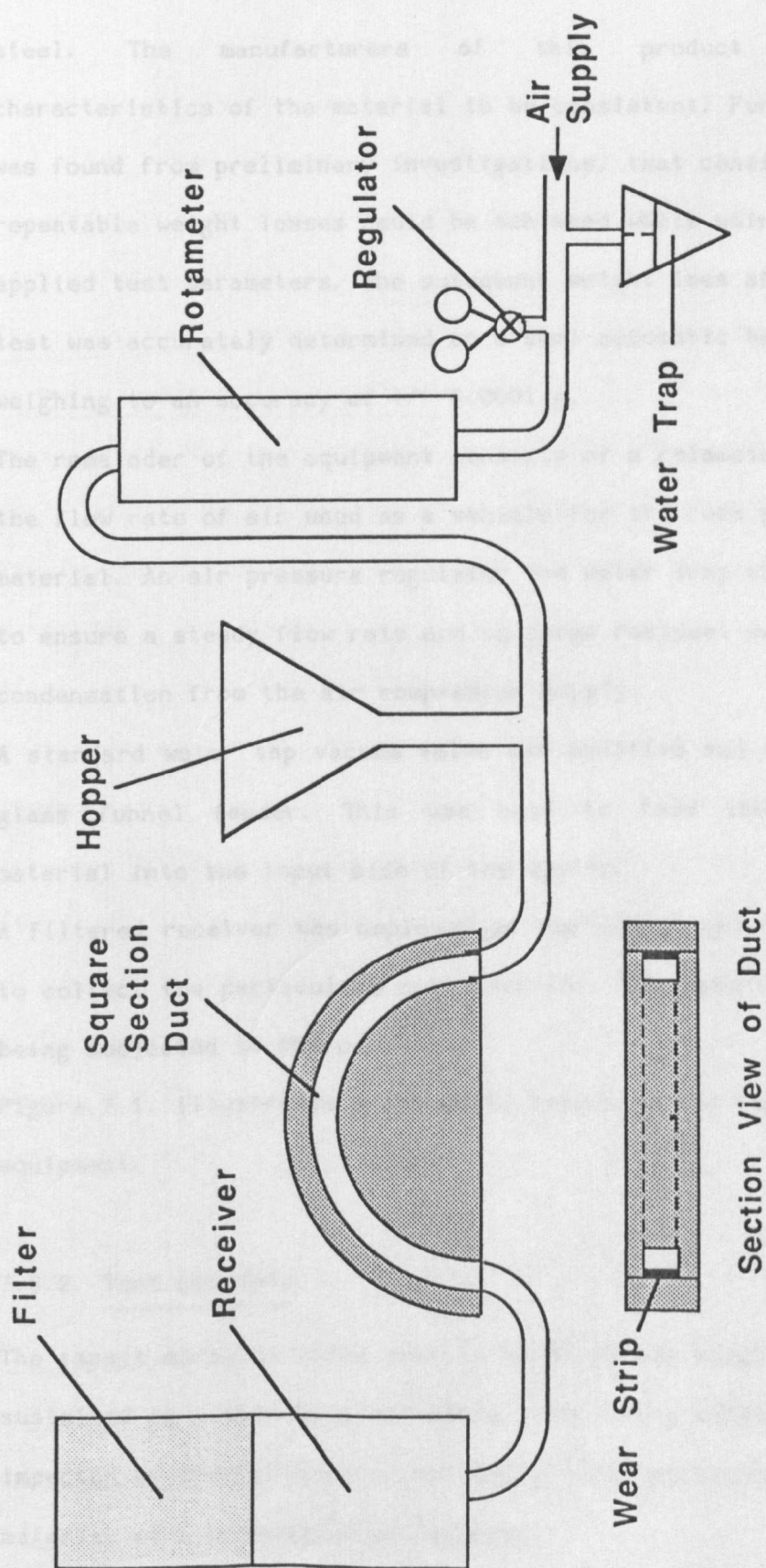


Figure 7.1. Schematic View of Impact Abrasive Test Equipment

steel. The manufacturers of this product claim the characteristics of the material to be consistent. Furthermore, it was found from preliminary investigations, that consistently repeatable weight losses could be achieved while using similar applied test parameters. The subsequent weight loss after each test was accurately determined on a semi-automatic balance weighing to an accuracy of  $\pm 0.0001$  g.

The remainder of the equipment consists of a rotameter to measure the flow rate of air used as a vehicle for the rock particulate material. An air pressure regulator and water trap was employed to ensure a steady flow rate and to purge residual water condensation from the air compressor supply.

A standard water tap vacuum valve was modified and attached to a glass funnel feeder. This was used to feed the particulate material into the input side of the system.

A filtered receiver was employed at the output end of the system to collect the particulate rock material. The material under test being subjected to one pass only.

Figure 7.1. illustrates a schematic layout of the impact abrasive equipment.

#### 7.3.2. Test Concepts.

The impact abrasive index test is based on the weight loss sustained to a thin metallic strip after being tangentially impacted by 1000 grammes of specially sized particulate rock material at a predetermined velocity.

The strip, contained in the semi-circular duct is weighed before and after each test and the subsequent weight loss is expressed numerically as a function of the abrasive potential of the whole rock material.

The index base material is an artificial corundum "Baux 60" normally employed as a grinding abrasive for grinding wheels. The material is of a consistently regulated hardness (9 on the Moh's scale of hardness) and is of a regular blocky particle shape. This permitted accurate control of the original test program to establish a base index of 10 on the scale.

After extensive trials with various material particle sizes, quantity and transport velocity, a maximum weight loss for a predetermined quantity and velocity was established from which a constant (K) based on these trials was established.

The index scale for this test was established from 1000 grammes of "Baux" abrasive sized at +210 $\mu$  to -350 $\mu$ . A weight loss of 0.1223 grammes occurred when impacted at a velocity of 63.8 m/s

Where  $Q = AV$

$$V = Q/A$$

$$\text{Area of Duct} = 36^2 \text{ mm}$$

$$\text{Rate of Flow} = 138 \text{ l/min. (ignoring frictional losses and turbulent flow)}$$

$$V = \frac{138 \times 1000 \times 10^3}{36} = \text{l/min}$$

$$= \frac{138 \times 10^6}{36 \times 60} = \text{l/s}$$

$$= 0.0639 \times 10^3 = \text{m/s}$$

$$= 63.8 \quad \text{m/s}$$

(Eq 7.1.)

The value for K is derived from :

$$\frac{1000}{0.1223} = 100K = 8176.6$$

$$\text{Therefore } K = \frac{8176.6}{100} = 81.766$$

(Eq 7.2.)

and this is used to define the numerical value of 10 on the scale.

Values for other materials in the same size range, velocity and quantity are calculated by multiplying their respective weight losses by the constant K.

$$K = 81.766.$$

### 7.3.3. Impact Tests on Unconsolidated Rock Material.

A major advantage with the Dynamic Particle Impact Abrasive Test is, that it can be used to determine the abrasiveness of those rocks that cannot be found by the more popular Cerchar method.

These include the following:

- a) Unconsolidated rock material.
- b) Weak and friable rocks.
- c) Crushed and sized rock particles from competent rock material.
- d) Engineering soils. (Although the testing of soils has been outside the scope of this thesis).

#### **7.4. Abrasive Wear Tests on Consolidated Material.**

##### **7.4.1. Continuous Abrasive Test.**

This new test can be used to assess the abrasive potential of competent rock material where attritional or sliding wear problems exist. The test is non-destructive and employs standard rock cores of a quality normally acceptable for physical property tests. Therefore, both physical property and abrasive index testing can be conducted on the same rock specimen material.

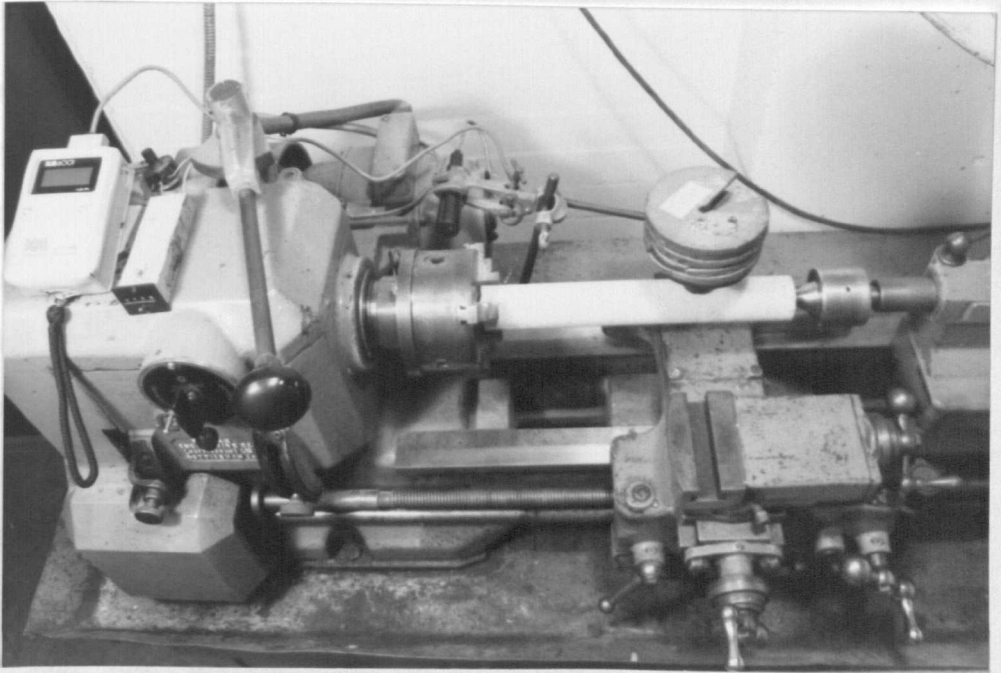
##### **7.4.2. Description of Test Equipment.**

The test equipment consists of a standard workshop centre lathe, fitted with a three-jaw self centering chuck and rotating tailstock centre. The rock core specimen is held in the three-jaw chuck and trued up to rotate concentrically about its horizontal axis. A standard travelling steady, (normally employed for turning and screw cutting duties on long slim diameter shafts) was slightly modified to accept the spindle of a deadweight carrier plate. This was used to support a mass of 2.3kg placed vertically and diametrically central over the top of the rock specimen.

An electromagnetic trip switch and digital counter was fitted to count the number of revolutions per test and a phototachometer was used to measure the speed of rotation, (rev/min). Because the lathe was fitted with an adjustable conical belt drive system, this permitted infinitely variable speeds within the permissible range.

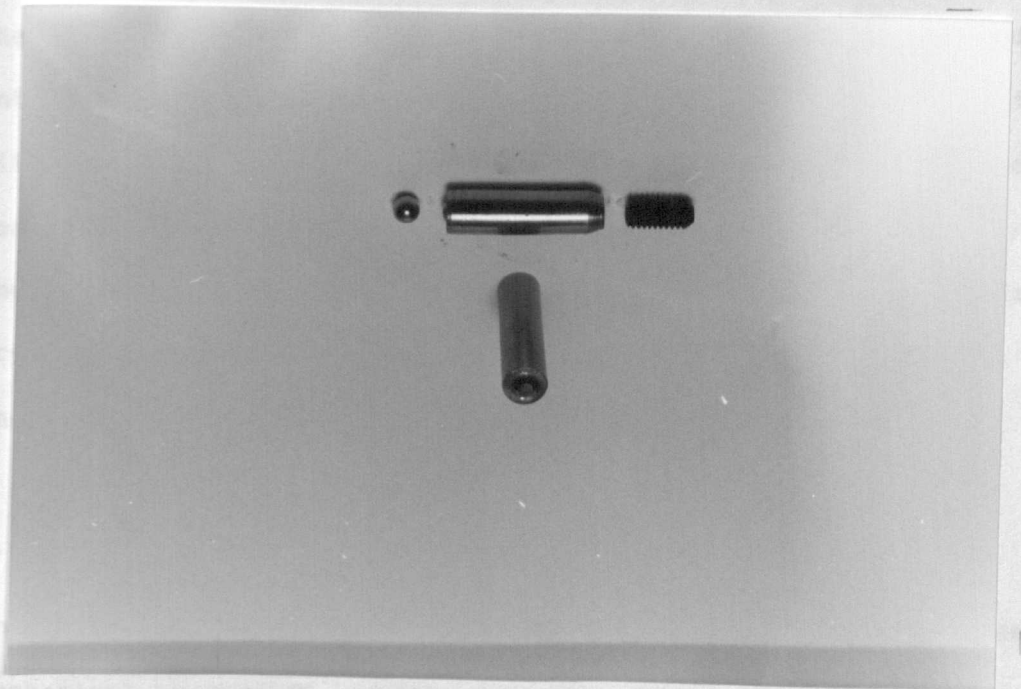


## CONTINUOUS ABRASIVE TEST EQUIPMENT



### CENTRE LATHE.

Showing Test Specimen, Tachometer, Counter and Dead Weight Carrier.



Tube and Ball Assembly

Figure 7.2.

The abrasive index is derived from the resultant wear flat generated on the surface of a standard 4 mm diameter ball bearing. These ball bearings are manufactured by a well known UK ball bearing manufacturer from EN25 alloy steel and are accurately hardened, ground and lapped to precise mechanical engineering limits. In addition, the hardness of each ball is rechecked on the Shore Sleroscope, and only those balls that fall within the range 92 - 94 Shore hardness are used for the test. This hardness range results in the minimum percentage of rejects and this amounts to approximately 15% - 20% of the balls purchased. (Current purchase price of balls = £4.00 per 100.)

The ball is held captive in a steel tube by an allen grub screw in such a way that approximately one third of the ball protrudes through the open end of the tube. The tube and captive ball is then inserted into a specially manufactured bronze bush fitted into the travelling steady, so that the ball comes into contact with the rock core specimen and is then loaded with the deadweight and carrier plate.

The subsequent wear flat generated on the ball after the test, is accurately measured by means of a travelling microscope.

The test equipment is illustrated in Figure 7.2.

#### 7.4.3. Test Concepts.

The continuous abrasion test was designed to simulate those mechanical processes which involve attritional or sliding abrasive actions. These mechanisms can be associated with low

stress abrasive problems, e.g. continual scratching or the erosion of surfaces of chutes and hoppers etc. It can be related to wear of various mechanical components of transport systems, in addition to the gradual erosion of insert tip material of rock cutting tools, diamond core drilling and diamond sawing.

The continuous abrasion test index is therefore, derived from the resultant wear flat generated on the surface of a hardened ball bearing which has been subjected to a continuous rubbing action.

The parameters were established after a number of trials at various applied loads, distances and velocities. The final choice of the predetermined parameters used, was based on the diameter of generated wear flat, which should be sufficiently large enough to accurately measure, (even with very low abrasive rocks). The amount of frictional heat generated is minimal, to avoid degradation of the ball bearing. Although it was found that increased loads gave appreciable increased generated wear flats, a compromise between rock strength, hardness and heat generation had to be made. Increased velocities did not give the same proportional increased wear flat, but the heat generation was proportionally high. The best variable with the predetermined applied load and velocity was 'distance travelled'. The only restriction to this being the length and diameter of core specimen permissible. Therefore, the test parameters established for the continuous abrasion test are as follows.

Linear Speed = 10 m/min.

Load. (Mass) = 2.38 kg.

Linear distanced travelled = 10 metres.

The abrasive index is given as the same numerical value as the diameter of the resultant wear flat in mm. e.g. a wear flat of 1.8 mm is given an abrasive index 1.8 (Very abrasive)

#### **7.5.Characteristics of Unconsolidated Rock Material.**

##### **7.5.1.Rock Sample Description.**

The unconsolidated rock material used for these tests was obtained from an opencast prospect in New South Wales, Australia, and the samples comprised of the following unconsolidated sediments:

**i) Gravelly Sandstone:**

This material contained a high proportion of hard angular quartz grains (Moh's Hardness 7.) weakly cemented in a clay matrix. The majority size range was below 2.0 mm and of these 80% were wet screened out to -500 $\mu$ . These small mineral grains can significantly influence the abrasiveness of the rock. Further more, depending on the operation, the large grains or pebbles, can if broken down, produce many sharp edges to increase the abrasive potential of the material.

**ii) Silty Clay.**

This rock contained 60% clay/kaolinite cementing material. The majority of the hard minerals were made up from approximately 30% fine grained quartz -150 $\mu$  reaching up to +350 $\mu$ . Some quartzite rock fragments was also present.

**iii) Sandstone.**

The Sandstone was made up from 44% quartzite plus some fine rock fragments. The remainder being approximately 12.5% opaque minerals and some small amounts of white mica. The size range of these minerals was wet screened to +210 $\mu$  to - 350 $\mu$ .

iv) **Silt.**

This material was described as loose fine grained medium silt. It contained 72% fine angular quartz -420 $\mu$  to + 150 $\mu$ . This size range has proven to be the most abrasive range with the impact abrasive test.

v) **Loose Sand.**

The loose sand was described as "coarse loose silt to fine loose sand". It contained 58% Quartz and quartzite material and all the grains were sub-rounded,

All the material was extremely weak, friable and unconsolidated, this would place it approximately R1 (weak rock) or G4 (cemented soil on the IGS scale. The material contained high quantities of residual moisture which varied from 7.8% to 14.63%. This amount of moisture could significantly reduce the shear and compressive strength of the material by as much as 60% to 70%.

#### 7.5.2. Difficulties Encountered With Conventional Tests.

Difficulties were encountered with conventional index tests when testing unconsolidated materials of the kind previously described. This was because the high moisture content prevented adequate specimen preparation to the standard normally required

for index testing. Neither the Cerchar abrasive test, the NCB Cone Indenter or Shore Scleroscope hardness tests could be carried out without first drying out the sample material. However, it was apparent that even though the tests were made possible by the effects of drying out the moisture, the clay matrix binding the minerals was not sufficiently competent to permit specimen preparation of the minimum standard of surface finish normally acceptable. The Cerchar abrasive test for example, is a very useful and easily conducted laboratory test. Furthermore, the results obtained from competent fine grained rock material have been shown to be reliable and have provided good correlation with the rate of disc cutter replacement on full face tunnelling machines. Des Lauriers and Broennimann, (1979). The principle weakness with this test, lies in the fact that the stylus sinks far too deep into unconsolidated and weak rocks. This action results in support to point on the sides of cone, consequently, giving way to a much smaller representative wear flat. "Often, the shape of the resultant wear, assumes a spheroidal form rather than the easily measurable wear flat". The Shore Scleroscope gives extremely good results with most competent rock types and correlates well with other hardness tests and physical strength properties also. However, because the integrity of the results obtained rely on a surface finish not normally possible with weak and unconsolidated rock, tests conducted on this type of material must be regarded with some degree of caution.

The NCB Cone Indenter also gives very good results with competent material and shows good correlation with other tests. However,

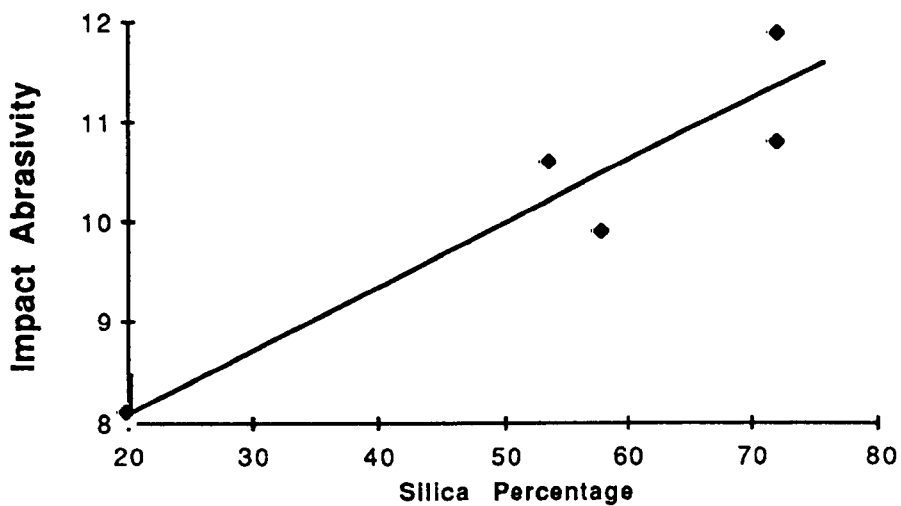


**Figure 7.3 (a) Correlation between Impact Abrasivity and Silica Percentage**

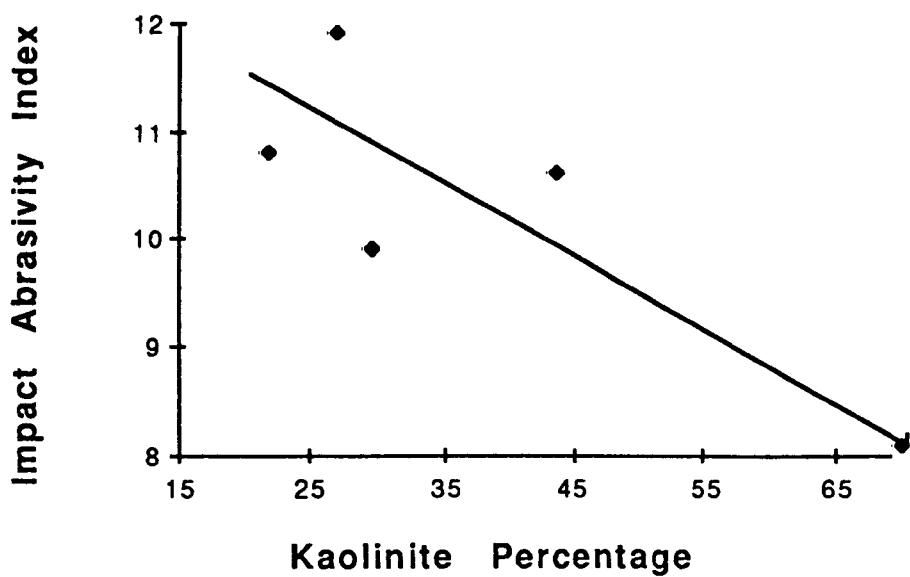


**Figure 7.3 b Correlation Between Impact Abrasivity Index and kaolinite Percentage**

TABLE 7.1.

Impact Abrasive Wear Index and Petrological Properties of Unconsolidated Rock Material

Rock Sample Description	Impact Abrasive Wear	$\text{SiO}_2$ Quartz	$\text{SiO}_2$ Chert	Quartzite + rock fragments	Gypsum $\text{CaSO}_4$	Clay/ Kaolinite $\text{Al}_2\text{O}_3\text{SiO}_2\text{H}_2\text{O}$	Mica $\text{KAlSi}_3\text{O}_{10}(\text{OH})_2$	Feldspar $\text{NaAlSi}_3\text{O}_8$ - $\text{CaAl}_2\text{Si}_2\text{O}_8$	Carbonate $\text{CaCO}_3$	Opaque minerals	Grain Size
1 Gravelly Sandstone	11.9	50	2	20	1	27	-	-	-	-	0.5 to 2mm 80% <0.5mm
2 Silty Clay	8.1	20	-	10	-	60	10	-	-	-	150 to 350 $\mu\text{m}$
3 Sandstone	10.6	31.25	-	12.5	-	40	3.75	-	-	12.5	210 to 350 $\mu\text{m}$
4 Fine to Medium Silt	10.8	64	4	4	-	22	<1	2	3	-	0.2 to 0.5 $\mu\text{m}$
5 Coarse Loose Silt to Fine Loose Sandstone	9.9	53	-	5	-	30	<1	1	10	-	0.5 to 1 mm

NOTE: Numbers in brackets indicate Mohr's Hardness.



when testing weak and unconsolidated rock material, even with the minimum loading of 12 N, the excessive depth of cone penetration causes displacement of mineral constituents. Thus the integrity of the results obtained must be regarded doubtfully.

It is clear therefore, that the reliability of each of these three tests is unsatisfactory when employed with unconsolidated rock material.

#### 7.5.3. Dynamic Impact Abrasive Results.

All the rocks described in section 7.5.1. have been tested using the dynamic abrasive index test and a summary of the results obtained is illustrated in Table 7.1. It can be seen that impact abrasiveness of rocks depends upon the percentage of hard mineral constituents. Figure 7.3.a. shows the effect of the total quartz percentage on abrasiveness. This indicates increased abrasive potential with increased total silica content. Grain size cannot be considered here, because all the material has been discretely sized. However, when the sizing of material has been obtained from a crushing or grinding process. this process can produce very sharp angular mineral particles. Figure 7.3.b. shows the effect of Kaoline percentage and indicates that as Kaoline percentage increases, abrasivity decreases. These results serve to confirm the experiences with the impact dynamic abrasive test and statistical analysis can be viewed with some degree of confidence. Furthermore, because it was possible to break down the cementing material in water, all the impact abrasive tests

were conducted on wet screened and unaltered mineral constituent material. This had the added advantage over the normally crushed competent rocks, where some alteration in the natural size and shape of the minerals is unavoidable. Thus, the integrity of the test results obtained from this type of unconsolidated rock material is enhanced.

## **7.6. Assessment of Abrasivness of Consolidated Rocks.**

### **7.6.1. Preliminary Tests.**

Tests to determine the abrasivness of a range of rock materials which included a selection from igneous, metamorphic and sedimentary origins were carried out. The purpose of this preliminary study was to determine by laboratory methods, strength and deformation parameters, petrology and index properties of rock and to attempt to correlated these with various abrasivity indices. The selected rocks therefore are itemised as follows:

#### **i) Fine Grain Siltstone.**

Sedimentary origin, high strength, very stiff, quasi-elastic fine grained low abrasive rock.

#### **ii) Granite.**

An igneous rock, very stiff, quasi-elastic very high strength, coarse grained abrasive rock.

#### **iii) Limestone**

Sedimentary origin, very stiff, quasi-elastic, fine grained very low abrasive rock.

	ROCK TYPE							MEAN
	Fine Grained Sandstone	Granite	Limestone	Pennant Sandstone	Darley Dale Sandstone	Mudstone	Gneiss	
Uniaxial Compressive Strength (MPa)	216.00	202.00	168.00	123.00	72.60	52.00	180.00	144.8
Young's Modulus E (GPa)	18.7	17.7	18.0	10.1	7.90	5.7	-	
Toughness Index	124.0	115.0	76.4	75.0	33.0	23.0	-	
Internal Friction Angle (degrees)	52.0	39.0	34.0	46.0	43.0	38.5	-	
Shear Strength Intercept (Cohesion) [(C) MPa]	36.9	54.5	43.9	29.2	20.6	14.5	-	
Tensile Strength $T_o$ (MPa)	14.2	6.86	7.02	10.29	4.01	4.08	10.46	
Range of Shear Strength (Confining Pressure 0-10) (MPa)	-	47-70	68-77	37-74	22-55	18-35	-	
Shore Scleroscope Hardness Index	62.4	84.5	53.6	63.7	46.2	29.8	83.6	60.54
NCB Cone Indenter Hardness Index	5.6	18.6	5.32	5.3	3.5	2.3	12.45	7.58
Impact Abrasiveness Index	6.3	12.9	0.3	6.4	8.4	2.8	11.6	6.95
Cerchar Abrasiveness Index	1.75	3.55	1.92	3.2	2.8	1.65	4.13	4.84
Continuous Abrasion Test	1.52	1.18	0.64	1.67	2.00	-	1.08	1.147
Average Grain Size ( $\mu\text{m}$ )	0.3	2.75	0.03	0.3	-	0.055	1.5	0.747
Silica and Feldspar (%)	97	95	-	90	-	30	95	98.85

Table 7.2. Laboratory Index Properties and Petrographic Analysis and Abrasivity Index of Rocks.

iv) **Pennant Sandstone.**

Sedimentary origin, stiff, semi-elastic, high strength medium grained abrasive rock.

v) **Darley Dale Sandstone.**

Sedimentary origin, semi-stiff, semi-elastic, weak medium grained abrasive rock.

vi) **Mudstone.**

Sedimentary origin, medium stiffness, semi-elastic, weak fine grained low abrasive rock.

vii) **Gneiss.**

Metamorphic origin, high strength, high stiffness, coarse grained abrasive rock.

Three different types of abrasive tests were conducted on these rocks, these were as follows:

- 1) The Cerchar Abrasive Index Test.
- 2) The Dynamic Impact Abrasive Test.
- 3) The Continuous Abrasive Test.

Table 7.2. summarises strength and deformation properties together with hardness indices, abrasive indices and petrographic properties of the rocks.

In order to better understand the interrelation of these various rock properties, a statistical analysis of this data was carried out using the Minitab statistical computer program. Table 7.3. presents a summary of the correlation coefficients between the various abrasive indices and twelve other rock properties.

TABLE 7.3.(a)

Correlation Between Mechanical Properties, Petrological Parameter, Index Tests and Abrasivity Tests

Tests	Uniaxial Compressive Strength MPa C <sub>2</sub>	Young's Modulus GPa C <sub>3</sub>	Toughness Index C <sub>4</sub>	Internal Angle of Friction ø C <sub>5</sub>	Cohesive Strength C C <sub>6</sub>	Tensile Strength σ <sub>t</sub> MPa C <sub>7</sub>	Shear Strength τ C <sub>8</sub>
E (GPa)	0.969	-	-	-	-	-	-
Toughness Index	0.978	0.897	-	-	-	-	-
ø	0.243	0.067	0.381	-	-	-	-
C Cohesion	0.886	0.900	0.833	0.160	-	-	-
σ <sub>t</sub> MPa	0.712	0.595	0.778	0.740	0.352	-	-
τ MPa	0.021	0.125	-0.062	0.736	0.428	-0.392	-
Shore Sclerscope	0.805	0.708	0.851	0.188	0.866	0.471	0.289
Cone Indenter	0.618	0.555	0.641	-0.154	0.822	0.068	0.347
Impact Abrasive Number	0.273	0.123	0.387	0.308	0.353	0.044	-0.043
Cerchar Abrasivity Number	0.125	0.017	0.215	0.003	0.376	-0.099	0.495
Continuous Abrasivity Number	0.204	0.106	0.282	0.625	0.096	0.353	-0.094
Average Grain Size (mm)	0.472	0.397	0.516	-0.135	0.688	-0.052	0.272
% of Hard Rock forming Minerals	0.904	0.887	0.879	0.151	0.853	0.705	0.306

TABLE 7.3.(b)

Correlation Between Mechanical Properties, Petrological Parameter, Index Tests and Abrasivity Tests

Tests	Shore Sclerscope Number	Cone Indenter Number	Impact Abrasive Number	Cerchar Index	Continuous Abrasivity Number	Average Grain Size	SiO and Feldspar %
	C <sub>9</sub>	C <sub>10</sub>	C <sub>11</sub>	C <sub>12</sub>	C <sub>13</sub>	C <sub>14</sub>	C <sub>15</sub>
E (GPa)	-	-	-	-	-	-	-
Toughness Index	-	-	-	-	-	-	-
Ø	-	-	-	-	-	-	-
C Cohesion	-	-	-	-	-	-	-
$\sigma_t$ MPa	-	-	-	-	-	-	-
$\tau$ MPa	-	-	-	-	-	-	-
Shore Sclerscope	-	-	-	-	-	-	-
Cone Indenter	0.861	-	-	-	-	-	-
Impact Abrasive Number	0.680	0.733	-	-	-	-	-
Cerchar Abrasivity Number	0.686	0.660	0.790	-	-	-	-
Continuous Abrasivity Number	0.445	0.103	0.566	0.551	-	-	-
Average Grain Size (mm)	0.781	0.978	0.820	0.698	0.118	-	-
% of Hard Rock forming Minerals	0.795	0.499	0.118	0.241	0.266	0.319	-

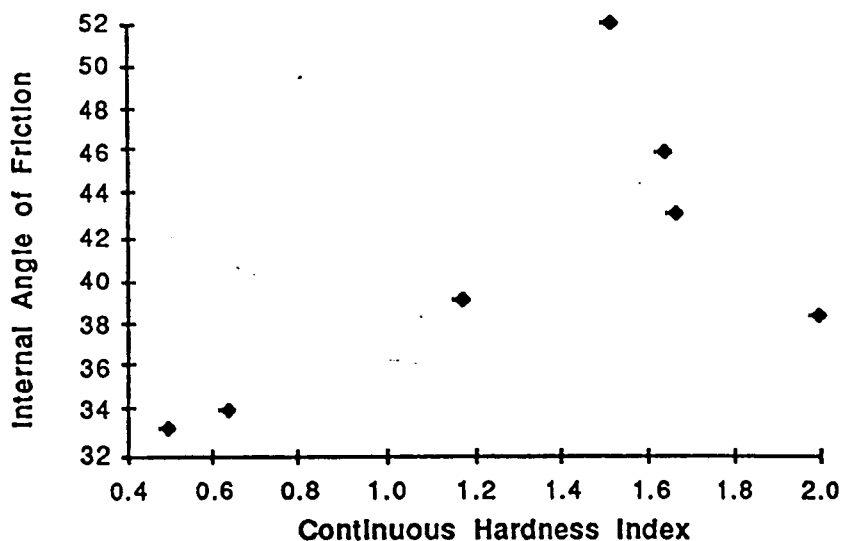


**Figure 7.4 Correlation of Internal Angle of Friction and Continuous Abrasivity Index**

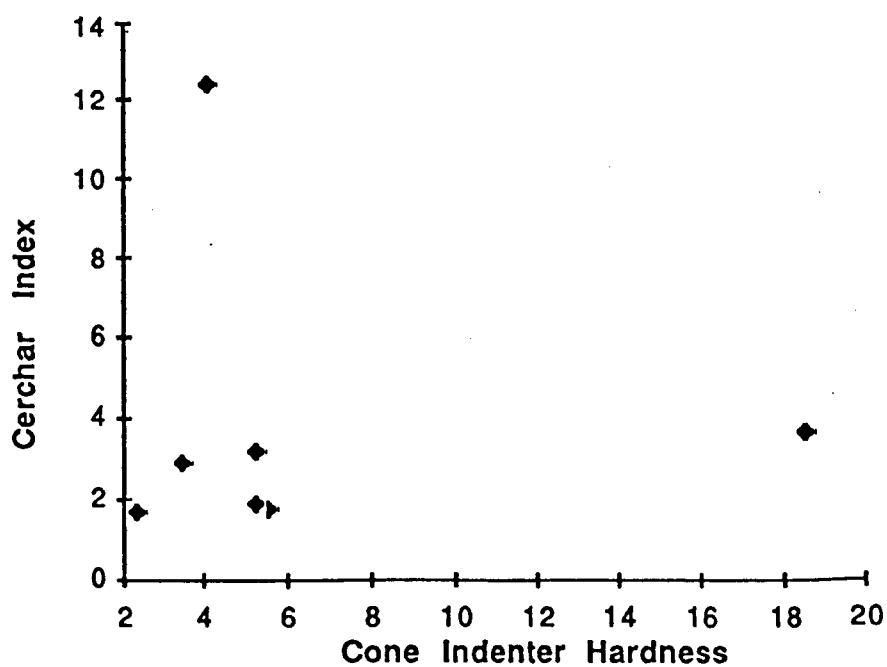


**Figure 7.5 Cerchar abrasivity and cone indenter hardness**

## **7.7. Discussion of Preliminary Test Results.**

### **7.7.1. The Effects of Strength and Deformation Properties.**

#### **of Rock on Various abrasivity Indices.**

It can be seen in Table 7.3. that the effect of strength and deformation properties of rock on the various abrasivity indices, indicate no apparent correlation between the mechanical properties of the rock and the Cerchar or Impact abrasive indices. However, the results do indicate some relationship between the internal angle of friction and the results obtained from the Continuous abrasive test ( $R = 0.625$ ) Figure 7.4. Moreover, the results indicate that nothing is gained from the determination of mechanical properties when attempting to assess the abrasiveness of rocks.

### **7.7.2. The Effects of Hardness and Petrographic Properties**

#### **on the Abrasivity of Rocks.**

The effects of hardness and mineralogy on abrasiveness was studied and was established by the results obtained from the NCB Cone Indenter and the Shore scleroscope hardness indices. It can be seen that these two hardness tests can be correlated to each other ( $R = 0.861$ ). Table 7.3. also shows that the Shore scleroscope number can be correlated to the average grain size of the hard mineral constituents, ( $R = 0.795$ ). Similarly, the NCB Cone Indenter number can be correlated with the average grain size ( $R = .978$ ). The correlation between the Cone Indenter and



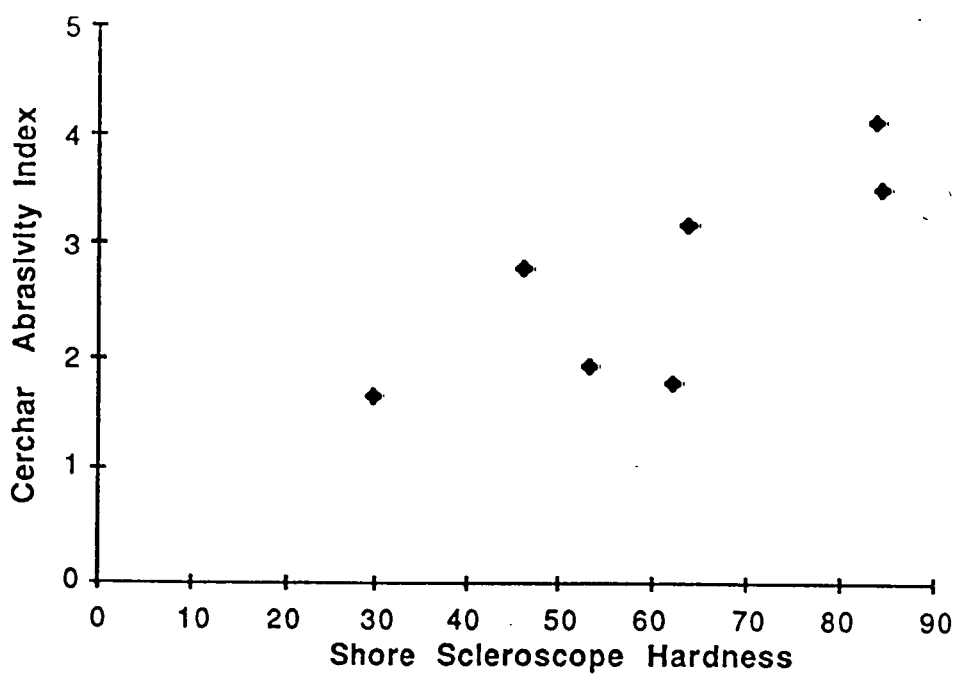


**Figure 7.6 Cerchar Abrasivity and Shore Scleroscope Hardness Number**

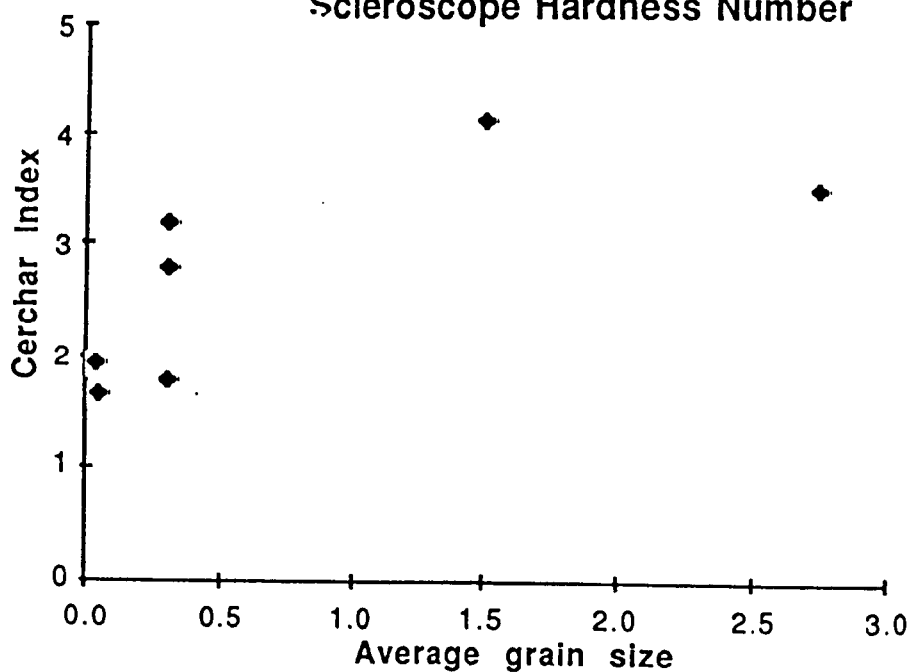


**Figure 7.7 Effect of Grain Size on Shore Scleroscope Hardness Number**

percentage grain size of the hard mineral constituents was ( $R = 0.5$ ).

Further analysis indicates the impact abrasiveness correlates with the Cone Indenter hardness number ( $R = 0.773$ ), Shore scleroscope hardness number ( $R = 0.680$ ) and average grain size in mm. ( $R = 0.978$ ).

A multiple regression equation which incorporates these aforementioned hardness and mineralogy parameters is given below:

$$Y = 1.26 + 0.26X_1 - 2.93X_2 + 16.0X_3$$

(Eq 7.3.)

Where  $Y$  = Impact Abrasive Index.

$X_1$  = Shore Hardness Index Number.

$X_2$  = Cone Indenter Hardness Index Number.

$X_3$  = Average Grain Size (mm)

The correlation coefficient for the above equation was:

0.994.

It can further be seen that the Cerchar abrasive index can be correlated to the Shore Scleroscope hardness number, ( $R = 0.686$ ) in addition to the NCB Cone Indenter hardness number ( $R = 0.660$ ) and average grain size ( $R = 0.820$ ) and is illustrated graphically in Figures 7.5 to 7.7.

Conversely, the Continuous abrasive test index appears to depend more on the internal angle of friction of rocks where ( $R = 0.625$ ) and the Shore hardness number ( $R = 0.44$ ) and does not appear to be influenced by the petrology of rock.

### 7.7.3. Interaction of Impact Abrasivity, Cerchar Index

#### and the Continuous abrasive Index.

The statistical analysis presented in Table 7.3. indicates that the Impact abrasive index can be nominally correlated with the Cerchar abrasive index, ( $R = 0.790$ ). The correlation coefficient between the Cerchar index and Continuous abrasive index is given as ( $R = 0.551$ ). Similarly, the correlation between the Continuous abrasive index and the Impact abrasive index is ( $R = 0.556$ ). Thus it can be seen, there is a poor correlation between these three indices. This is not unexpected when considering the mechanisms involved represent completely different interactions. However, it can be shown that various abrasivity tests, petrographic properties and hardness indices can be interrelated and Table 7.4. presents the interrelation of these various indices of abrasiveness, hardness and grain sizes of the rocks tested.

Table 7.4.

The Influence of the Cerchar Abrasive Index, Continuous Abrasive Index, and Hardness Indices on Impact Abrasiveness.

Dependent Variable	Independent Variables	Correlation Coefficient
Impact Abrasive Index	Average Grain Size	0.820
	Cone Indenter Index	0.733
	Shore Hardness Index	0.680
	Cerchar Abrasive Index	0.790
	Con't Abrasive Index	0.566

The equation 7.4. presents an empirical relationship between the Impact abrasive index and the Shore hardness index, NCB Cone indenter hardness index and Continuous abrasive index:

$$Y = 6.00 - 0.231X_1 + 1.09X_2 + 5.03X_3$$

Eq 7.4.

Where Y = Impact abrasive index

$X_1$  = Shore hardness index (C9)

$X_2$  = Cone indenter hardness index (C10)

$X_3$  = Continuous abrasive index (C11)

The correlation coefficient for the equation 7.4. is 0.95.

The equation 7.5. correlates the Impact abrasive index to the Cerchar abrasive index, Continuous abrasive index and average constituent grain size of the hard rock forming minerals:

$$Y = 1.05 - 0.103X_1 + 2.88X_2 + 3.24X_3$$

Eq 7.5.

Where Y = Impact abrasive index

$X_1$  = Cerchar abrasive index

$X_2$  = Continuous abrasive index

$X_3$  = Average grain size

The correlation coefficient for equation 7.5. is 0.946.

Further analysis has indicated that by the use of a multiple regression equation, the Impact abrasive index can be correlated to the Cone indenter hardness index and Continuous abrasive index as follows:

$$Y = 2.08 + 0.412X_1 + 1.10X_2 + 2.36X_3$$

Eq 7.6.

Where Y = Impact abrasive index

$X_1$  = Cone indenter index

$X_2$  = Cerchar abrasive index

$X_3$  = Continuous abrasive index

The correlation coefficient for the above equation is 0.89.

Therefore, from the analysis outlined in this section, the following tentative conclusions can be assumed:

- i) The various abrasive indices cannot be correlated to the mechanical properties of rocks.
- ii) Abrasive indices can be directly correlated to hardness indices and petrographic properties such as grain size and the percentage of hard mineral constituents.
- iii) Individual abrasive indices cannot be easily interrelated to each other.
- iv) It is however, possible to interrelate various abrasive indices with each other together with hardness and petrological properties.

#### 7.7.4. Toughness Index of Rock and its Interrelation to Rock Abrasiveness.

The toughness index is a derived second order parameter which reflects the ease in which the cutting or disintegration of rocks can be carried out. This index represents the magnitude of elastic energy required to deform rock by means of some

TABLE 7.5.

Rock Sample Material	Uniaxial Comp Strength $\sigma_c$ (MPa)	Youngs Modulus E (GPa)	Toughness Index $T_I$	Strength Classification
1. Granite	202	17.7	115.0	Very High Strength
2. Siltstone	216	18.7	124.0	
3. Limestone	168	18.0	76.0	High Strength
4. Pennant Sandstone	123	10.1	75.0	
5. Darley Dale Sandstone	72.6	7.9	33.0	Medium Strength
6. Mudstone	52.0	5.7	52.0	Low Strength

TABLE 7.6.

Dependent Variable	Independent Variables	Correlation Coefficient
Toughness	Uniaxial Compressive Strength $\sigma_c$	0.978
Index	Youngs Modulus E	0.897
$T_I$	Percentage Hard Minerals ( $-16 + 1.19C_{15}$ )	0.879
	Cohesive Strength	0.833
	Uniaxial Tensile Strength $\sigma_t$	0.788
	Shore Hardness Index ( $Y_4 = 33.4 + 1.9C_9$ )	0.851
	Cone Indenter Hardness	0.641
	Mineral Grain Size	0.561
	Impact Abrasive Index	0.387
	Cerchar Abrasive Index	0.215
	Continuous Abrasive Index	0.286

mechanical or chemical interaction and can be derived from the stress-strain curve. The toughness index is one of the most important second order parameters used for the evaluation of cuttability or rippability of intact and massive rock and is extensively used by equipment manufacturers to determine power and weight ratios for excavating machinery, e.g. the higher the toughness index, more powerful and robust heavy duty machinery will be required.

The toughness is derived from the area under the stress-strain curve in the elastic range and is given by the following equation:

$$T_1 = \frac{\frac{1}{2} \sigma_c^2}{E} \quad \text{Eq 7.7.}$$

Where  $T_1$  = Toughness Index

$\sigma_c$  = Uniaxial Compressive Strength

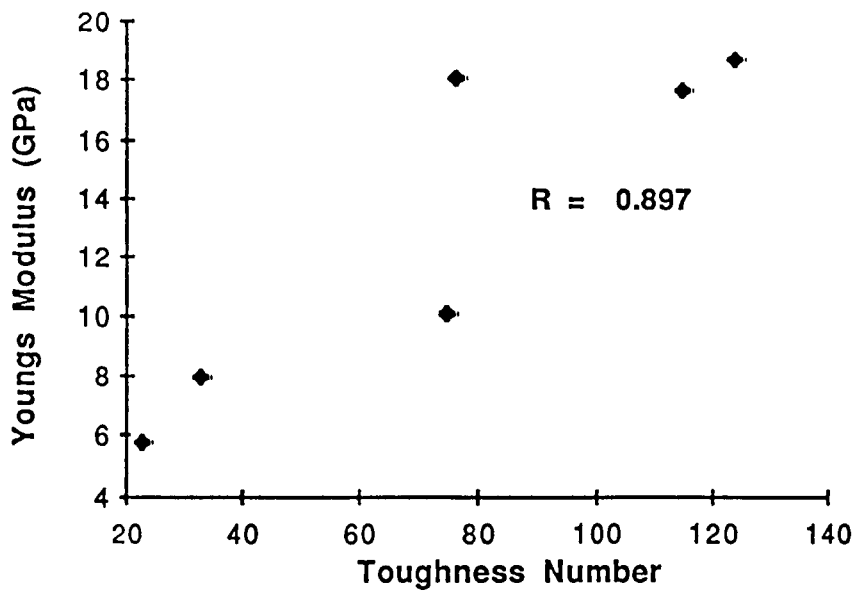
E = Youngs Modulus of Elasticity

Table 7.5. presents the toughness index of the various rock samples tested, together with their strength classifications. It can be seen that the selected range of rocks in the test program was from low to very high strength.

The toughness index of rocks can be correlated to various rock strength and deformation properties in addition to other index properties and petrology. This is summarised in Table 7.6.

It can be seen that the toughness index can be highly correlated with uniaxial compressive strength, uniaxial tensile strength, Youngs Modulus and cohesive strength. It should also be noted that the toughness index is a linear function of the percentage





**Figure 7.8 Correlation of Toughness Index and Youngs Modulus**

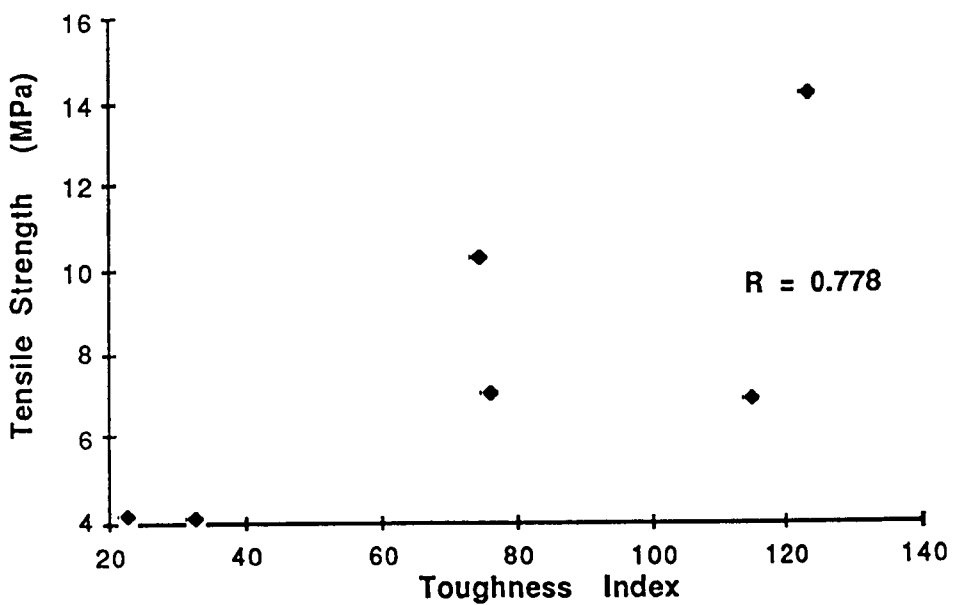


**Figure 7.9 Correlation of Toughness Index and Tensile Strength**

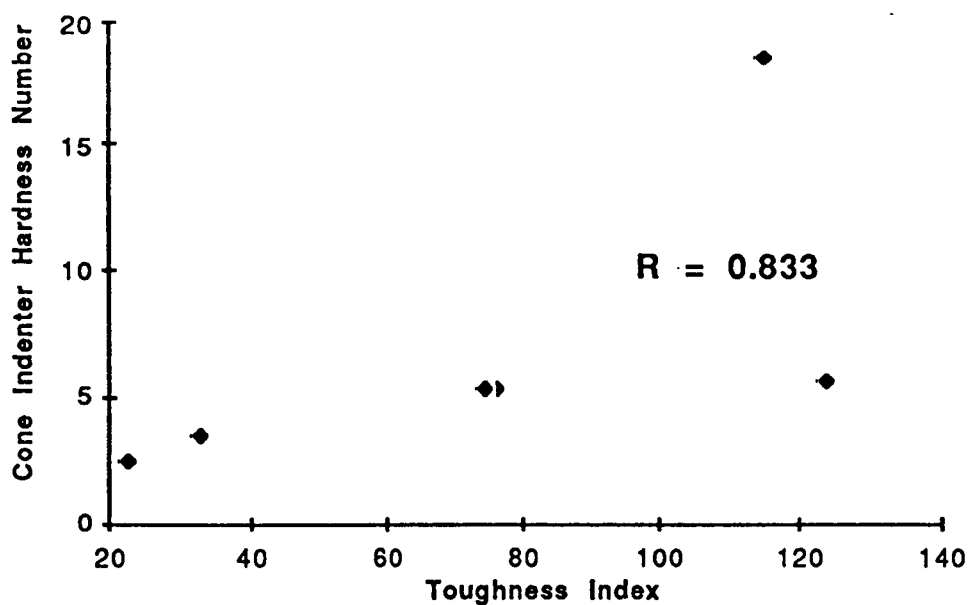


**Figure 7.10 Correlation Between Toughness Index and  
Cone Indenter Hardness Number**

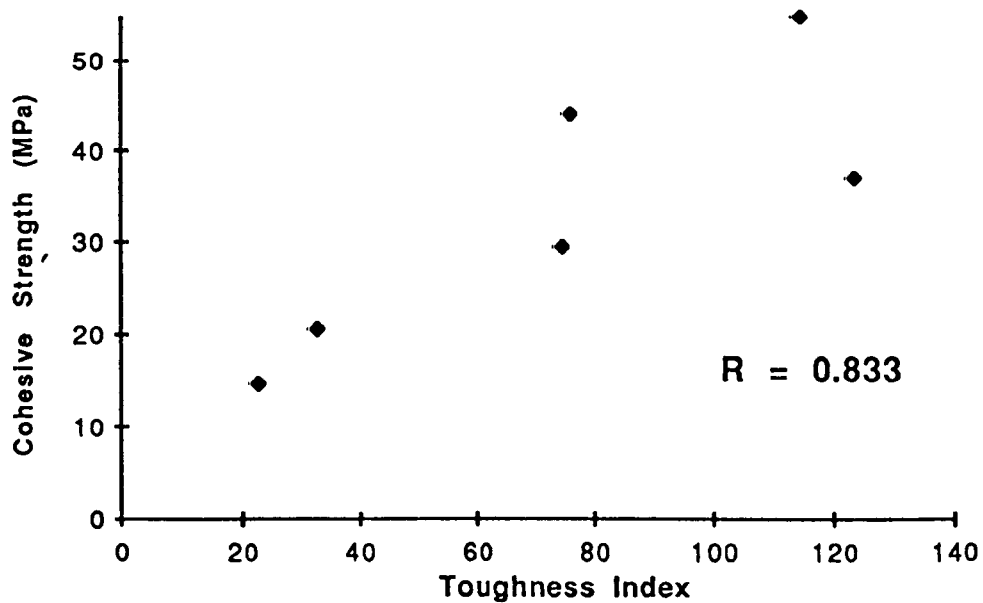


**Figure 7.11 Correlation Between Toughness Index and  
Cohesive Strength**

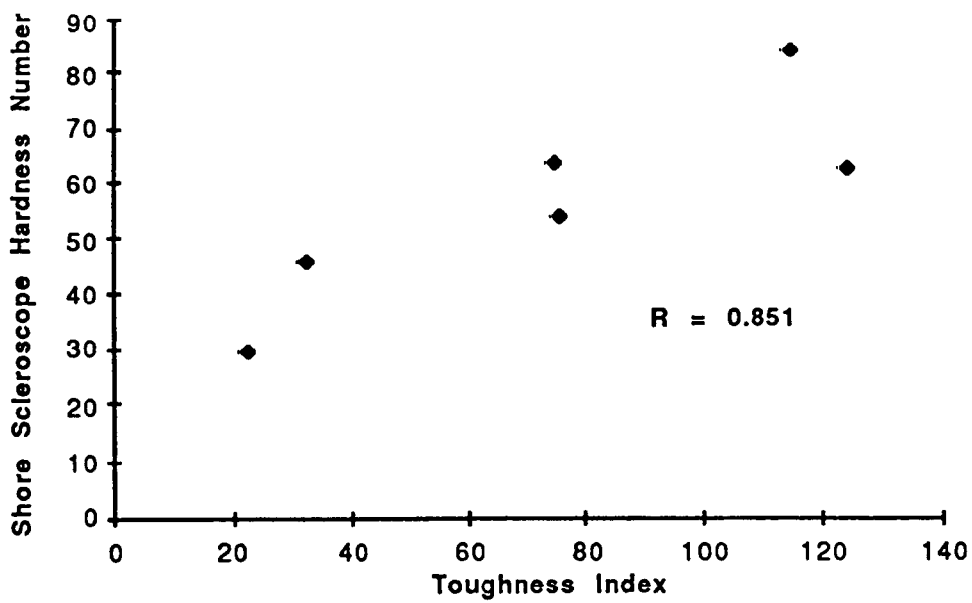


**Figure 7.12 Correlation Between Toughness Index and Shore Scleroscope Hardness Number**

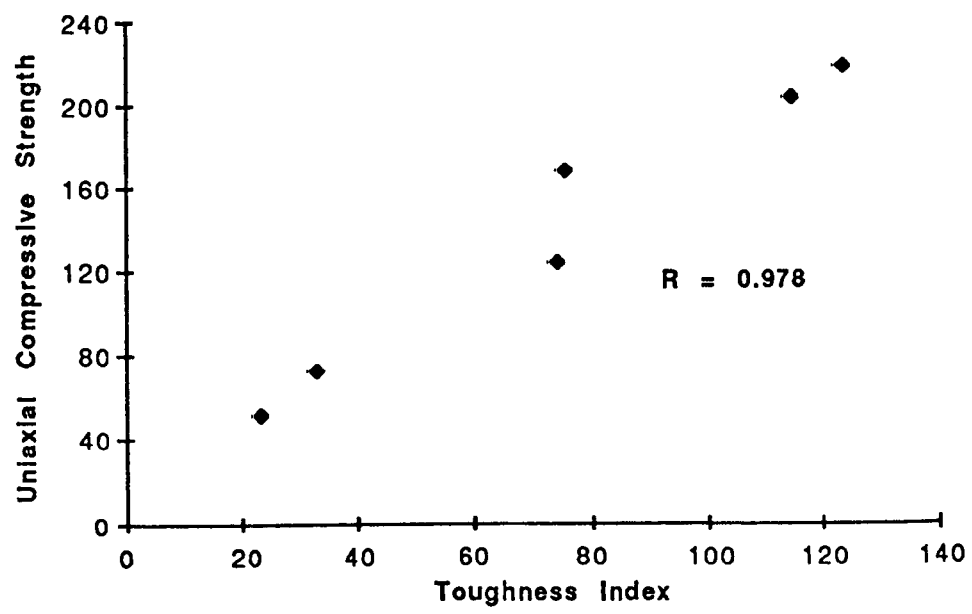


**Figure 7.13 Correlation Between Toughness Index and Uniaxial Compressive Strength**

	UCS MPa	Tensile Strength MPa	Shore Sclerscope	Cone Indenter Hardness	Impact Abravity	Cerchar Abravity	Continuous Abrasion	Average Grain Size	S10 <sub>2</sub> %
1 Grey Granite	166.5	8.06	91.77	12.49	11.06	3.46	1.50	2.5	15
2 Pink Granite	174.7	7.52	94.4	7.98	10.07	3.60	1.42	2.75	20
3 Larvekite	192.88	8.78	92.0	13.84	12.59	3.58	1.08	5.5	-
4 Red Granite	158.88	6.87	98.90	16.04	12.19	3.84	1.25	5.5	30
5 Diorite	194.77	11.89	81.08	9.89	8.87	3.75	1.13	0.25	20
6 Gabbro	211.8	12.51	82.00	14.04	10.23	3.32	0.98	3.5	0.0
7 Red Granite	190.06	10.89	97.1	12.43	11.69	3.98	1.37	1.75	25
8 Sandstone	83.68	4.52	42.5	2.77	7.74	3.12	2.10	3.30	70
9 Siltstone	216.00	14.2	62.4	5.6	6.3	1.75	1.52	0.3	97
10 Granite	202.00	6.86	84.5	18.6	12.9	3.55	1.18	2.75	95
11 Limestone	168.00	7.02	53.6	5.32	0.3	1.92	0.64	0.03	0.0
12 Pennant S.S.	123.00	10.29	63.7	5.30	6.4	3.20	1.67	0.3	90
13 Darley Dale Sandstone	72.60	4.01	46.2	3.5	8.4	2.80	2.0	0.3	45
14 Mudstone	52.00	4.08	29.8	2.30	2.8	1.65	-	0.055	30
15 Gneiss	180.00	10.46	83.6	12.45	11.6	4.13	1.08	1.05	95

Table 7.7. Abrasivity Results on 15 Rock Types together with Hardness and Petrographic Properties.

	UCS MPa C <sub>2</sub>	UTS C <sub>7</sub>	Shore Sclerscope C <sub>9</sub>	Cone Indenter C <sub>10</sub>	Impact Abravity C <sub>11</sub>	Cerchar C <sub>12</sub>	Continuous Abravity C <sub>13</sub>	Grain Size C <sub>14</sub>	% Hard Mineral C <sub>15</sub>
Shore Sclerscope C <sub>9</sub>	0.750	0.453	-	-	-	-	-	-	-
Cone Indenter C <sub>10</sub>	0.694	0.307	0.846	-	-	-	-	-	-
Impact Abravity C <sub>11</sub>	0.444	0.792	0.794	-	-	-	-	-	-
Cerchar C <sub>12</sub>	0.373	0.187	0.787	0.688	0.855	-	-	-	-
Continuous Abravity C <sub>13</sub>	-0.061	0.010	0.093	-0.101	0.344	0.319	-	-	-
Grain Size C <sub>14</sub>	0.260	-0.096	0.573	0.621	0.667	0.517	0.134	-	-
% Hard Minerals C <sub>15</sub>	-0.046	0.009	-0.252	-0.252	-0.381	-0.325	0.129	-0.480	-0.046

Table 7.8. Correlation between Abravity Indices, Hardness Numbers and Petrological Properties.

of hard constituent minerals, rock hardness indices and to a lesser extent the mean grain size. However, the results do not indicated any direct relationship between toughness and the various abrasive indices. Figures 7.4. to 7.13. show the correlation of the toughness index with various strength and deformation properties and rock hardnesses.

A multiple regression equation predicting the toughness index from the various other rock property indices is presented as follows :

$$Y_4 = 34.5 + 0.923C_9 + 0.743C_{15}$$

(Eq 7.8.)

Where  $Y_4$  = Toughness Index

$C_9$  = Shore hardness index

$C_{15}$  = Percentage quartz and feldspar

The correlation coefficient for the above equation is 0.91.

## 7.8. Presentation and Analysis of Results.

Cerchar, Impact and Continuous abrasive tests were determined for 15 rock types. These represent a wide range of rock material and Table 7.7. illustrates the various abrasive indices together with, the Shore and NCB Cone indenter hardnesses and relevant petrological properties.

### 7.8.1. Factors Affecting Abrasivity of Rocks.

A statistical analysis of the data has been carried out and the results are summarised in Table 7.8. The statistical analysis

also indicate that the impact abrasive index of rocks can be linearly correlated to the Cerchar abrasive index, average grain size, Shore hardness and NCB Cone indenter hardness. However, as expected, the Impact abrasive test shows poor correlation with uniaxial strength and no direct correlation with the Continuous abrasive test results. These results are summarised in Table 7.9. The results presented in Table 7.8. also indicate that the Cerchar abrasive index can be correlated to the Impact abrasive index ( $R = 0.855$ ), NCB Cone indenter ( $R = 0.688$ ) and to a lesser degree, the mean grain size ( $R = 0.517$ ). The Continuous abrasive index however, can only be marginally correlated to the internal angle of friction and cannot be directly correlated to any of the other rock properties examined.

#### **7.8.2. Multiple Regression Analysis and Prediction** **of Various Abrasive Properties.**

A multiple regression analysis was carried out to correlate various rock abrasive, hardness and petrological properties. These relationships can be used to predict various abrasive indices.

#### **7.8.3. Prediction of Cerchar Abrasivity.**

##### **1) Cerchar Abrasivity and other Abrasive Indices.**

The following equation 7.9. presents the empirical relationship between the Cerchar abrasive index, Impact abrasive index and the Continuous abrasive index.

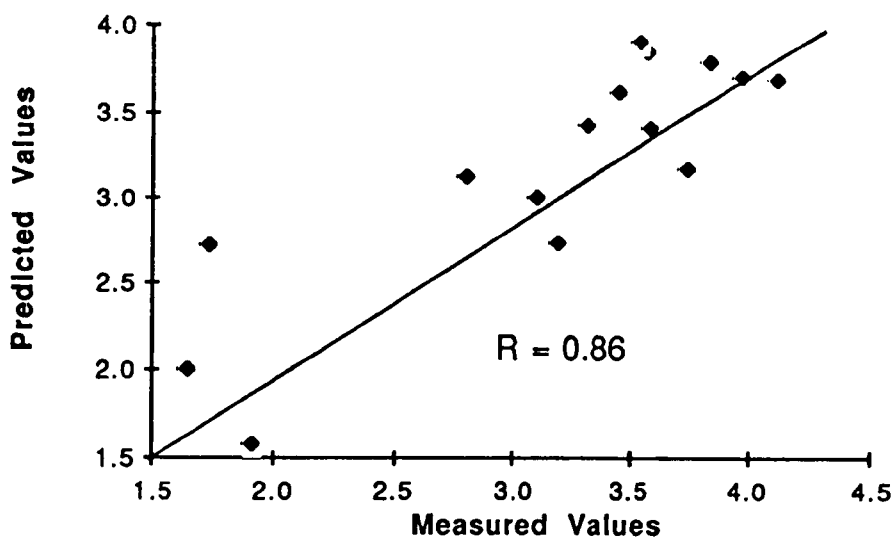


**Figure 7.14 Correlation Between Predicted and Measured Cerchar Abrasivity**

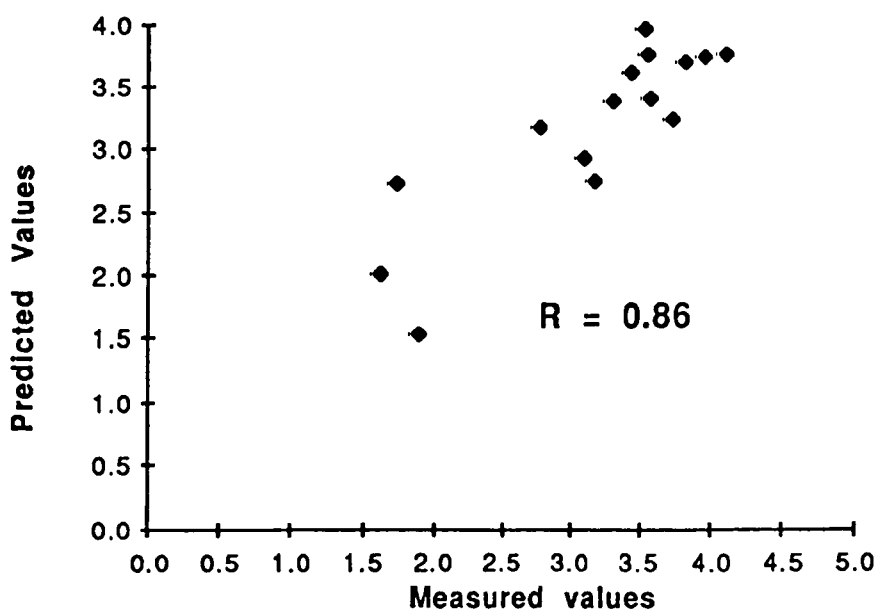


**Figure 7.15 Correlation Between Measured and Predicted Cerchar Index**



$$Y_C = 11.48 + 0.185C_{11} + 0.0423C_{13}$$

(Eq 7.9.)

Where  $Y_C$  = Cerchar abrasive index  
 $C_{11}$  = Impact abrasive index  
 $C_{13}$  = Continuous abrasive index

The correlation coefficient of the equation 7.9. is 0.86. and Figure 7.14 shows the relationship between the measured Cerchar index with the predicted values, thus indicating the validity of the predictive equation.

#### ii) Relationship between Cerchar and other Abrasive Indices and Grain Size.

An empirical relationship between the Cerchar abrasive index with other abrasivity indices and average grain size is given in the following equation:

$$Y_C = 1.45 + 0.199C_{11} + 0.0266C_{13} - 0.039C_{14}$$

(Eq 7.10.)

The correlation coefficient of the above equation is 0.86 and Figure 7.15 indicates the relationship between the measured and predicted Cerchar abrasive index.

#### 7.8.4. Prediction of Impact Abrasivity.

The impact abrasiveness of rocks can be predicted by using various multiple regression equations incorporating a combination of rock properties. These are listed as follows:

- 1) Shore and Cone indenter hardness indices.
- 2) Hardness and grain size.

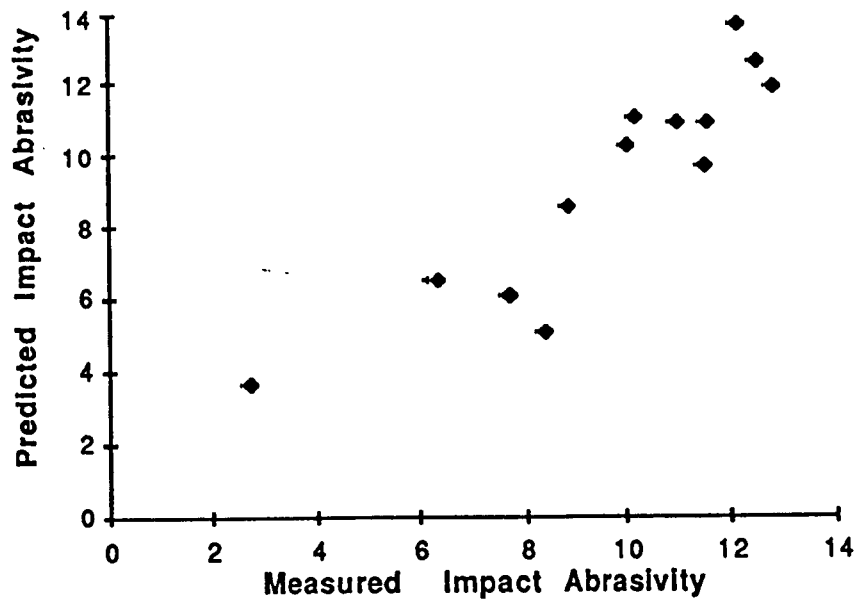


**Figure 7.16      Correlation Between Predicted and Measured Impact Abrasivity**

Figure 7.17

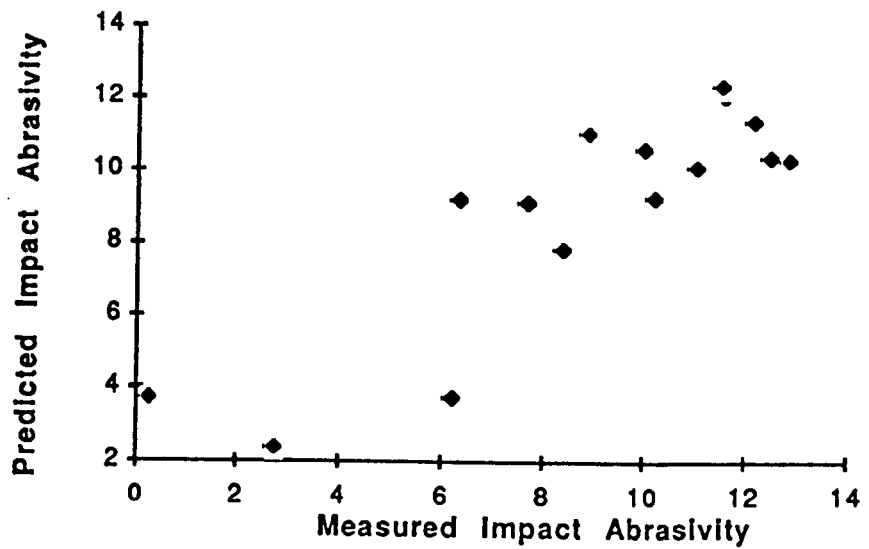


**Figure 7.17      Correlation Between Predicted and Measured Impact Abrasivity**

- 3) Cerchar and Continuous abrasive indices.
- 4) Cone indenter hardness and other abrasive indices.
- 5) Shore hardness and other abrasive indices.
- 6) Cerchar abrasiveness and rock hardness indices (C9 and C10).
- 7) Continuous abrasiveness and rock hardness (C9 and C10).
- 8) Grain size and other abrasive indices.

The practical advantage of using these various equations is to eliminate the time consuming and protracted impact abrasivity tests.

#### 7.8.4.1. Using Hardness and Grain Size.

An empirical equation relating the abrasive index to various hardness indices and grain size is given below:

$$Y = 1.25 + 0.26X_1 - 2.933X_2 + 16.0X_3 \quad (\text{Eq 7.11})$$

Where  $Y$  = Impact Abrasiveness

$X_1$  = Shore Scleroscope Index (C9)

$X_2$  = Cone Indenter Index (C10)

$X$  = Grain Size (mm) (C14)

The correlation coefficient for the above equation was 0.994 and Figure 7.16 illustrates graphically the correlation between predicted and measured Impact abrasiveness.

#### 7.8.4.2. Prediction of Impact Abrasivity by using other abrasive Abrasive Indices.

The following equation 7.12. presents an empirical equation between Impact abrasiveness and other abrasive indices:

$$Y_I = -3.92 + 33.8C_{12} + 0.569C_{13} \quad (\text{Eq.12})$$

Where  $Y_I$  = Estimated Impact Abrasiveness

$C_{12}$  = Cerchar Abrasive Index

$C_{13}$  = Continuous Abrasive Index

The correlation coefficient for the equation 7.12. is 0.86 and Figure 7.17. shows the relationship between predicted and measured Impact abrasiveness. Furthermore, by using rock hardness indices with abrasive indices, the correlation coefficient can be improved as discussed in the following section.

#### 7.8.4.3. Prediction of Impact Abrasiveness by Cone Indenter and other Abrasive Indices.

The prediction of Impact abrasiveness by the NCB Cone Indenter and other abrasive indices can be shown by using the equation 7.13. This equation presents a multi-linear relationship between predicted impact abrasiveness and the measured Cone indenter hardness index, Cerchar abrasive index and the Continuous abrasive index.

$$Y_I = -2.94 + 0.397C_{10} + 1.74C_{12} + 1.99C_{13}$$

(Eq 7.13)

Where  $Y_I$  = Estimated Impact Abrasive Index

$C_{10}$  = Cone Indenter Index

$C_{13}$  = Continuous Abrasive Index

The correlation coefficient of the above equation is 0.93 Figure 7.18. shows the predicted Impact abrasive index in relation to the measured values.

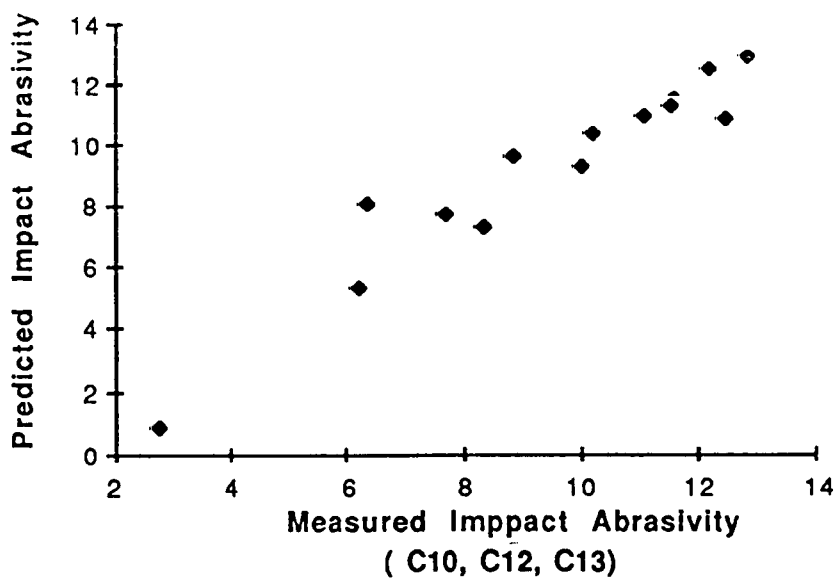


**Figure 7.18 Predicted and Measured Impact Abrasivity Based on C10, C11, C13**

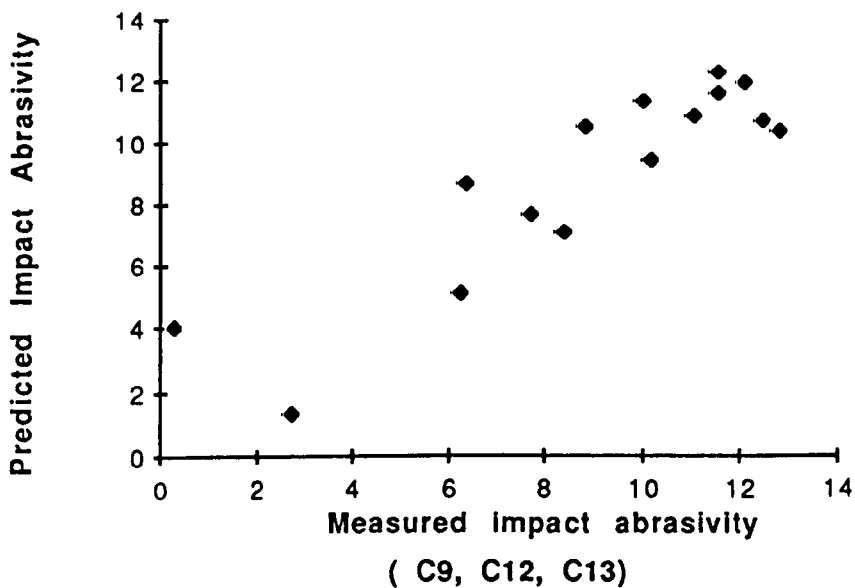


**Figure 7.19 Predicted and Measured Impact Abrasivity Based on C9, C12 and C13**

#### 7.8.4.4. Impact Abrasivity in Relation to Shore Hardness

##### and other Abrasive Indices

An empirical equation for the prediction of the Impact abrasive index based on the measured values of Shore hardness, Cerchar abrasive index and Continuous abrasive index is given as follows:

$$Y_I = - 4.47 + 0.0615C_9 + 2.37C_{12} + 1.03C_{13}$$

(Eq 7.14)

Where  $Y_I$  = Estimated Impact Abrasive Index.

$C_9$  = Measured Shore Hardness

$C_{12}$  = Cerchar Abrasive Index

$C_{13}$  = Continuous Abrasive Index

The correlation coefficient for this equation is 0.89. and Figure 7.19. shows a plot of the predicted Impact abrasive index against the measured index.

#### 7.8.4.5. Prediction of Impact Abrasivity using Shore

##### and NCB Cone Indenter hardness and Cerchar Abrasive Indices.

The following empirical equation permits the prediction of the Impact abrasive index based on the Shore scleroscope and NCB Cone Indenter hardness indices and the Cerchar abrasive index:

$$Y_I = -2.28C_9 - 0.0002C + 0.28C_{10} + 2.69C_{12}$$

(Eq 7.15.)

Where  $Y_I$  = Impact Abrasive Index

$C_9$  = Measured Shore Hardness Index

$C_{10}$  = NCB Cone Indenter Hardness Index

$C$  = Cerchar Abrasive Index

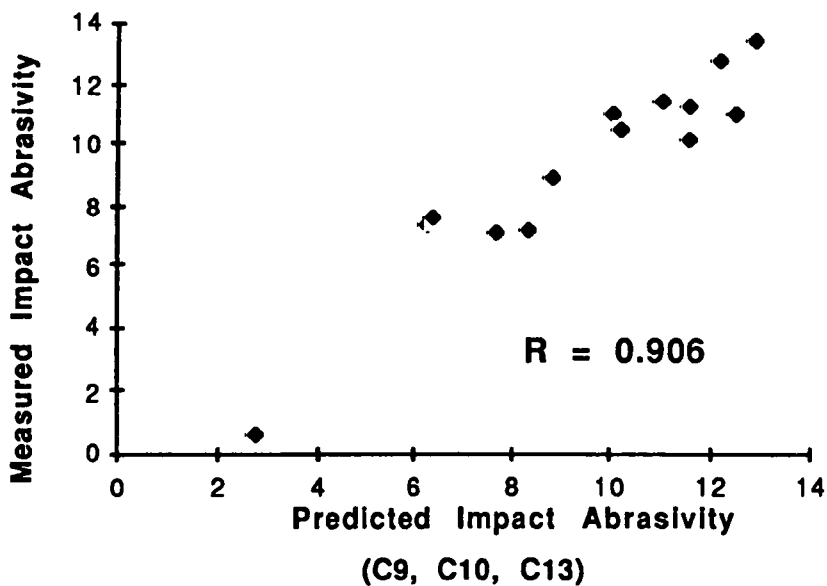


**Figure 7.20 Measured and Predicted Impact Abrasivity Based on C9, C10 and C13**

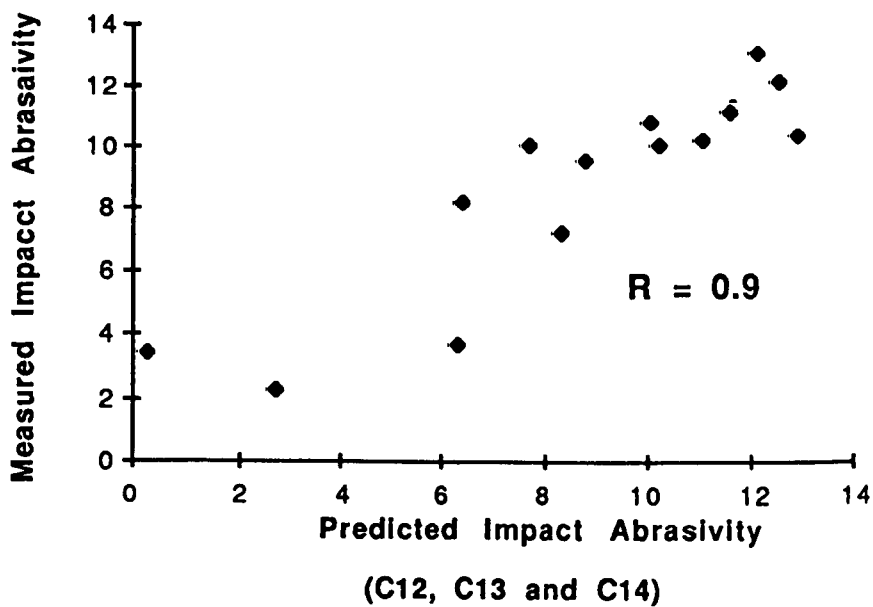


**Figure 7.21 Predicted and Measured Impact Abrasivity Based on C12, C13 and C14**

The correlation coefficient for the equation 7.15 is 0.89.

#### 7.8.4.6. Prediction of Impact Abrasivity From Continuous

##### Abrasivity and Rock Hardness.

Equation 7.16. presents a predictive equation for the estimation of Impact abrasiveness based on the Shore and NCB Cone Indenter hardness indices and the Continuous abrasive index:

$$Y_I = -1.42 + 0.0284C_9 + 0.49C_{10} + 2.83C_{13} \quad (\text{Eq 7.16.})$$

Where  $Y_I$  = Estimated Impact Abrasive Index

$C_9$  = Shore Hardness Index

$C_{10}$  = NCB Cone Indenter hardness Index

$C_{13}$  = Continuous Abrasive Index

The above equation 7.16. has a correlation coefficient of 0.91 and has been plotted in Figure 7.20.

#### 7.8.4.7. Predictive Equation for Impact Abrasivity, Based

##### on Measured Values for Grain Size and other Abrasive Indices.

This multiple regression equation was based on the Cerchar and Continuous abrasive indices and mineral grain size. The correlation coefficient for the equation is given as 0.9 and the Impact abrasive index is estimated from the following:

$$Y_I = -2.83 + 3.05C_{12} + 0.644C_{13} + 0.621C_{14} \quad (\text{Eq 7.17.})$$



Where  $Y_I$  = Estimated Impact Abrasive Index

$C_{12}$  = Cerchar Abrasive Index

$C_{13}$  = Continuous Abrasive Index

$C_{14}$  = Average Mineral Grain Size

The results based on the above equation is presented in Figure 7.21.

#### **7.8.5. Prediction of Continuous Abrasive Indices.**

##### **7.8.5.1. Continuous Abrasivity and Internal Angle of Friction**

###### **With Measured Shore Scleroscope Hardness Indices.**

The results obtained from the statistical analysis indicate a tentative relationship between the Shore Scleroscope hardness index and the internal angle of friction with the Continuous abrasive index measurements. This is shown in the following equation 7.18:

$$C_{13} = -2.34 + 0.065C_5 + 0.0136C_9 \quad (\text{Eq 7.18.})$$

Where  $C_{13}$  = Continuous Abrasive Index

$C_5$  = Internal Angle of Friction of Rock

$C_9$  = Shore Scleroscope Hardness Index

The correlation coefficient for the above equation is 0.72.

##### **7.8.5.2. Relationship Between Continuous Abrasivity and Cerchar and Impact Abrasive Indices.**

A tentative relationship can also be found between the Continuous

abrasive index and other abrasive indices by incorporating the multiple regression analysis method as follows:

$$C_{13} = -3.58 + 0.08C_5 - 0.035C_{11} + 0.65C_{12}$$

(Eq 7.19.)

Where  $C_{13}$  = Continuous Abrasive Index

$C_5$  = Internal Angle of Friction of Rock

$C_{11}$  = Impact Abrasive Index

$C_{12}$  = Cerchar Abrasive Index

The Correlation coefficient for this equation is 0.90.

#### 7.9. Discussion of Results.

The results so far, indicate the two new tests designed to evaluate the abrasiveness of rocks have been successfully developed. These new tests offer the advantage of testing material which cannot be tested by the normally accepted Cerchar abrasive test equipment for the following reasons:

- i) The Cerchar test is not amenable to unconsolidated or weak and friable rock material.
- ii) Erroneous results are obtained when testing rocks with large constituent mineral grain sizes.
- iii) The Cerchar abrasive test, fails to represent the more dynamic mechanisms involved with many of the rock breakage processes.

It has been suggested by West (1981) Atkinson and Cassapi (1984) McFeat-Smith and Fowell (1977) et al. that the abrasiveness of rock depends on the percentage and hardness of the mineral

constituents in addition to their grain size and angularity. It has further been suggested that the cementing material binding the mineral grains in sedimentary rocks, can also greatly affect abrasiveness in addition to physical strength properties.

This study indicates that there is a strong correlation between hardness as indicated by the Shore scleroscope and NCB Cone Indenter and the petrology of rocks to the various abrasive indices. There is also an indication that various abrasive indices can be tentatively correlated to each other. Thus, it is now possible to conduct tests on a range of materials and estimate their hardness and abrasiveness. Figures 7.22 to 7.23. show correlations between Cerchar and Impact abrasive indices and Impact and Continuous abrasive indices. Therefore, it is possible to classify rocks according to abrasiveness and estimate various other properties from a suite of index tests.

## 7.10 Conclusions.

### 7.10.1. Limitations of The Cerchar Abrasive Test.

(1) With the exception of special purpose abrasive tests, the Cerchar abrasive index has assumed the most popular mechanical method of assessing the abrasive potential of rock material. Although it is true to state, the Cerchar abrasive index gives good results when correlated to other indices, this test has serious limitations when applied under the following conditions:

- 1) The Cerchar test cannot be used to determine the abrasiveness of unconsolidated rock or soils. This is

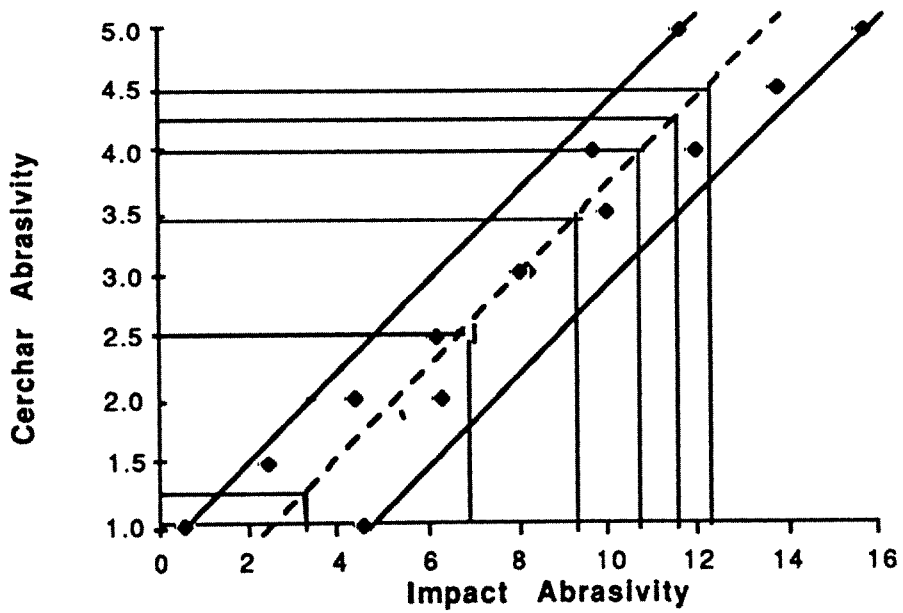


Figure 7.22 Correlation between Cerchar and Impact Abrasivity

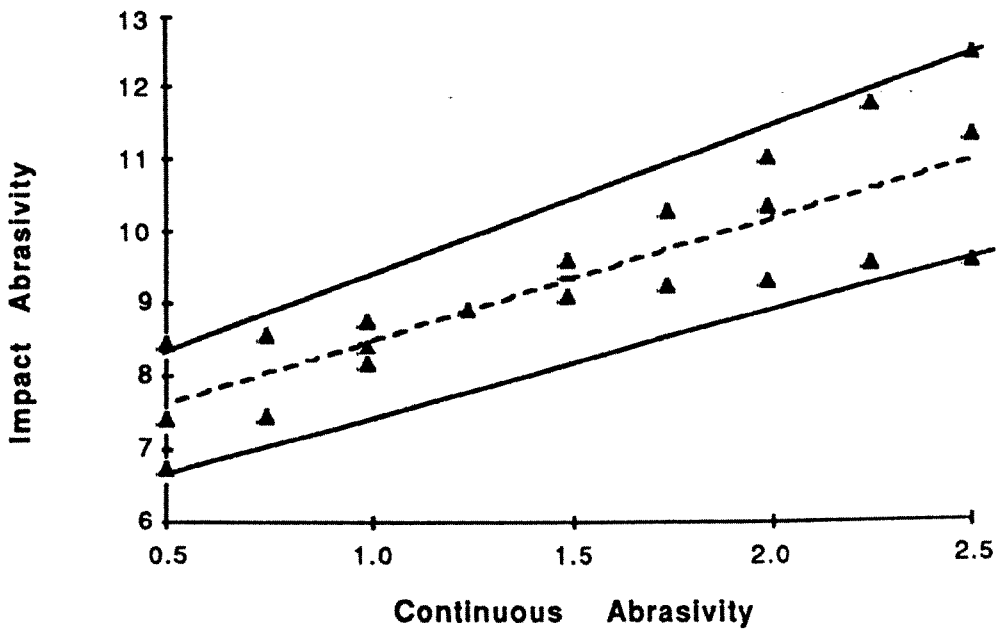


Figure 7.23 Correlation between Impact and Continuous Abrasivity

because the stylus penetrates to deeply into the rock material, thus gaining support for the point on the sides of the conical stylus, resulting in a much smaller generated wear flat. The results therefore, cannot be regarded with any degree of confidence.

ii) The results obtained from rock materials containing large constituent mineral grains, may be spurious because the average constituent grain size may exceed the travel of the stylus. (10 mm).

iii) The Cerchar abrasive index does not represent mechanisms involving more dynamic abrasive processes.

(2) The two new tests; e.g. the Impact abrasive test and the Continuous abrasive test, have been developed and successfully tested on 15 different rock types. These tests now present a method of evaluating the abrasive potential of rock material which cannot be assessed by the Cerchar method.

(3) A statistical analysis of the results has indicated that the abrasive indices of rock cannot be directly correlated to strength and deformation properties of rock.

(4) It has been shown that the hardness of rock determined by the Shore scleroscope and NCB Cone indenter, together with average grain size and the percentage of hard constituent minerals, can be used to predict the abrasive potential of rock by the use of multiple regression analysis.

(5) Because of the different mechanisms employed with each of the tests exploited with this test program, it was not anticipated

that it would be possible to directly correlate the various abrasive indices with each other. However, a classification system for each of the abrasive index tests has been established and is presented in Table 7.9.

TABLE 7.9.

Classification	Cerchar Abrasive Index	Impact Abrasive Index	Continuous Abrasive Index
Extremely Abrasive	>4.5	>12.5	>2.0
Highly Abrasive	4.25-4.5	11.5-12.5	1.9-2.0
Abrasive	4.0 -4.25	10.5-11.5	1.7-1.9
Mod Abrasive	3.5 -4.0	9.5-10.5	1.5-1.7
Med Abrasive	2.5 -3.5	7.0- 9.5	1.3-1.5
Low Abrasive	1.25-2.5	3.5- 7.0	1.1-1.3
V.Low Abrasive	<1.25	<3.5	<1.0

## **CHAPTER 8.**

### **GENERAL CONCLUSIONS AND RECOMMENDATIONS FOR FUTHER STUDY.**

## CHAPTER 8.

### GENERAL CONCLUSIONS AND RECOMMENDATIONS FOR FURTHER STUDY.

#### 8.1. General Conclusions.

Wear of mechanical equipment associated with the excavation and processing of rock forming minerals has been shown to be very costly. Indeed the cost has been estimated at £500,000,000 per annum incurred in the UK mineral extractive industry alone. Tribology in Mineral Extraction. (1984) Case histories show the urgent need to accurately define the causes and modes of wear and to take steps to reduce and control this major problem. Much research has already been carried out in this area and the problems associated with abrasion have been discussed in conference at both national and international level. The subjects related to abrasion have been wide ranging and varied involving many interrelated disciplines. These include the Material Sciences, devoted to the discovery of new and improved wear and corrosive resistant materials, Machine and Machine Tool Design Engineering to improve cutting efficiency to reduce tool wear and damage by improved tool geometry. Improvements in bearing seals to prevent



abrasive wear, damage and corrosion caused by the ingress of fine particulate abrasive rock material and contamination by corrosive liquids, These combined with the development of new and improved lubricants are just some of the areas currently undergoing continued rigorous investigation.

It has been stated that the mining engineer should be aware of the abrasive potential of the rock material being excavated or processed. This is vitally important, if production losses caused by down time due to and worn and damaged machinery is to be brought under control. Consequently, the need to conduct tests to determine the abrasive potential of rock material must be regarded as of major importance. It has further been shown that single index testing to determine the abrasiveness of rock material can lead to erroneous results and therefore, a suite of tests related to the processes involved are to be recommended.

A number of the tests to determine the abrasiveness of rocks have been discussed, however, the major problem with many of these tests is that they have been designed for special purpose applications and cannot be used for general purpose testing of all rock materials. Furthermore, they may often require costly proprietary test equipment and or the involvement of protracted time consuming test procedures.

The basis of this work has been to determine hardness and abrasiveness of rock material by the use of a limited number of tests and attempt to find some relationship between the results obtained from all the tests conducted with each other and actual machining trials where possible.

These tests have been listed under the following headings:

- a) Index Tests to determine the hardness and abrasiveness of rocks.
- b) Physical property tests to determine strength and deformation properties.
- c) Petrological analysis to determine the proportion, size and shape of the hard mineral constituents of rocks.
- d) The use of both factor analysis and statistical regression analysis to provide predictive equations for wear rates and required cutting forces.
- e) The rationalisation of test procedures to enable the most fruitful yield of test data from often, minimal supply of sample material.

Chapter 4 of this thesis demonstrates work conducted on a drilling program designed to study the mode of wear with diamond impregnated core bits of a new design concept. This chapter has outlined the interfacing of a radial arm workshop drilling machine, (modified for laboratory rock drilling duties) with a micro-computer

in order to monitor and record the drilling parameters and penetration rates. In addition, a computerised drill bit profile measuring device has been designed and developed to accurately measure changes in profile shape with distance drilled. The results obtained from this test program gave good indications to both the mode of wear with the bits tested and the limitations of the test drill rig with regard to the required torque necessary to comprehensively conduct the intended test program

Chapter 5. of this work describes a collaborative test program designed to determine the wear rates of diamond saws used in the stone quarrying industry. All the sawing trials for this work were conducted at the DeBeers research establishment at Charters near Ascot, Berks. The sawing trials were carried out on a specially modified Gregori Circular Saw and the test results were accurately monitored by the use of an interfaced micro-computer. The program for the determination of the relevant rock properties and the analysis of the all the test results (including the results obtained from DeBeers) was carried out at the University of Nottingham.

It can be seen that a number of important statistical relationships between the rock properties and the actual sawing trials have been established. The investigation has served to show which of the various

parameters obtained from the rock test results, predominantly affect sawability. Subsequently, these results have permitted an alternative method to the prediction of both tool wear and the cutting forces required to saw rock..

A number of case histories have been discussed which illustrate a variety of problems associated with the various processes involved with both mine excavation machinery and drilling in hard rock formations. In each case, the common denominator has been the effect of the rock properties and mineral constituents on each of the individual processes discussed. It has been shown that contrary to general opinion, rock strength properties are of lesser importance when considering wear, and the percentage of hard mineral constituents of the rock, together with their size and shape assumes greater importance.

Two new abrasive tests have been introduced in Chapter 7. These tests were designed to represent problems associated with dynamic impact and attritional wear mechanisms. The Impact Abrasive Test has been tried and developed to provide a method of determining the abrasiveness of rock as a direct result of impact wear caused by the interaction of rock particles. In addition, it can effectively be used to determine the abrasiveness of unconsolidated rocks. The Continuous Abrasive Test was designed to simulate wear mechanisms

associated with attritional wear problems.

A total of 15 different tests were conducted on a variety of rock types and the results correlated by the use of multiple regression analysis. Because of the different mechanisms involved with each of the abrasive tests, it was not unexpected that some difficulty existed with the correlation of each of the individual abrasive tests with each other. It was possible however, to establish a classification system for the Cerchar, Impact and Continuous abrasive index tests.

To summarise therefore, it is difficult to foresee any immediate solution to the problems associated with abrasive wear in the mineral extractive industry. The envisaged objective in this work was concerned with an attempt to identify the cause by detailed investigation of the rock materials being machined or processed. This has involved the use of a variety of rock tests and the rationalisation of these tests to avoid the necessity of conducting unnecessary protracted and costly test procedures. A number of important factors have emerged as a result of these investigations:

- i) Abrasion can be directly related to rock hardness.
- ii) Abrasion can be directly related to mineralogy, including grain size and shape.
- iii) There are tentative relationships between mineralogy, rock hardness and other physical and intrinsic properties of rock.

iv) Combined with the use of multiple regression analysis, the determination of the aforementioned rock properties can be used to produce reliable predictive equations to determine specific abrasive wear rates and cutting forces.

#### 8.2. Recommendations for Further Study.

The most important area of future study with the continuation of the work described in this thesis, must be concerned with the acquisition of reliable field and laboratory data to build up a substantial data bank. This approach would permit a much greater degree of confidence and reliability in the method of determination of the potential abrasiveness of rock material.

The many other areas of research concerned with abrasion, together with the design of machines and machine tools are far beyond the scope of any one individual. Idealistically, if one half of one percent of the total losses incurred in the mineral extractive industries alone, was allocated to a collaborative research group, working under one umbrella, it could, if expertly directed, provide much valuable information which could be used to bring about a marked reduction in down time due to worn and damaged equipment.

## LIST OF REFERENCES.

1. Atinoluk, S.  
Investigations into the Effects of Geometry on the Durability of Rock Excavation Tools.  
Ph.D Thesis, University of Newcastle upon Tyne, 1981.
2. Atkinson, T. and Cassapi, V.B.  
The Prediction and Reduction of Abrasive Wear in Mine Excavation Machinery.  
Tribology in Mineral Extraction.  
C341/84. I.Mec.E. International Conference.  
University of Nottingham, 17-19 Sept 1984.  
pp 165-174.
3. Atkinson, T. and Cassapi, V.B.  
The Preparation of Laboratory Cored Specimens from Friable Rock.  
The Mining Engineer, 1983.
4. Atkinson, T. Cassapi, V.B. and Denby, B.  
Properties Associated with Rock Material in Surface Mining Equipment Selection.  
Mining Equipment Selection Symposium.  
Calgary, Alberta, Canada. 7-8 Nov 1985.
5. Atkinson, T, Cassapi, V.B. and Denby, B.  
Properties Associated with Rock Material in Surface Mining Equipment Selection.  
Trans. Instn. Min. Metall. (Section A. Min. Industry) 1985.

6. Barr, M.V.  
Downhole Instrumentation, "A Review  
for Tunnelling  
Ground Investigation".  
CIRIA, Technical Note No 90. London 1977.  
Construction Industry Research and Information  
Association.
7. Buttner, A.  
Diamond Tools and Stone.  
Industrial Diamond Review.  
March 1974. pp 89-93.
8. Brown, E.T. and Phillips, H.R.  
Recording Drilling Performance for Tunnelling  
Site Investigations.  
CIRIA, Technical Note 81. London, 1977.  
Construction Industry Research and Information  
Association.
9. Berry, N.S.M. and Brown, J.G.W.  
Performance of Full Facers on Kielder Tunnels  
Tunnels and Tunnelling, 9 (4) pp 35-39, 1977.
10. Cassapi, V.B.  
Aspects of Laboratory Cored Specimens from  
Friable Coal Measures.  
Conference of Mechanics of Mining Ground.  
Banaras Hindu University, India, 19-24 Feb, 1983.
11. Cassapi, V.B. Waller, M.D. and Ambrose, D.  
Performance and Wear Characteristics in Diamond  
Drilling.  
Institution of Mining and Metallurgy, Conference,  
Drillex 87. 7-10 April 1987.
12. Cassapi, V.B. and Wright D.N.  
Factors Influencing the Sawability of Stone.  
Le Mausolee. Paris. Feb 1985. vol 52, No 528,  
pp 246-257.



13. Des Lauriers and Broennimann.  
The Midi/Mini Full Facers - North American Experience.  
Proceedings of the Rapid Excavation and Tunnelling Conference, Atlanta. 1979.  
pp 309-332.
14. Deere, D.V. and Miller, R.P.  
Classification and Index Properties for Intact Rock.  
Report A.F.W.L. - TR-65-116, Air Force Special Weapons Centre, Kirkland AFB. New Mexico, USA. 1977.
15. Fowell, R.J. and McFeat-Smith, I.  
Factors Influencing the Cutting Performance of Selective Tunnelling Machines.  
Tunnelling 1976. (London), IMM, 1976.
16. International Society of Rock Mechanics. (ISRM).  
Commission on Standardisation of Laboratory and Field Tests. Suggested Methods for Determining Hardness and Abrasiveness of Rock.  
Int. Jour. Rock Mech. and Min. Sciences, Vol 15.  
pp 89-97. (1978).
17. Kenny, P. and Johnson, S.N.  
Non-Blunting Tool for Cutting Coal and Rock.  
M.R.D.E. Bretby, pp760-763.
18. Kasturi, T.S.  
Tribology - Its Effectiveness to the Operation and Maintenance Problems in the Conveyor Systems of the Neyveli Lignite Mines.  
International Conference on Tribology in Mineral Extraction, I.Mech.E. Nottingham. 1984.
19. Montgomery, R.S.  
The Mechanism of Percussive Wear on Tungsten Carbide Composites.  
"Wear" Nov 1968, 12, 5 p, 309.

20. McFeat-Smith, I.  
Rock Property Testing for the Assessment of  
Tunnelling Machine Performance.  
Tunnels and Tunnelling.  
Vol 9, No 2, pp 29-33. (1972).
21. McKenzie, J.C. and Dodds, G.S.  
Mersey Kingsway Tunnel Construction.  
Proc. Instn. Civ. Engrs. Part 1-51, March, 1972.  
pp 503-533.
22. Muftuoglu, Y.V.  
A Study of Factors Affecting Diggability in  
British Surface Coal Mines.  
Unpublished Ph.D. Thesis, University of  
Nottingham, May, 1983.
23. Osbourne, H.J.  
Wear of Rock Cutting Tools.  
Powder Metallurgy, 1969, 12, No 24, pp 471-501.
24. Potts, E.L.J.  
Second Progress Report to the Wolfson Foundation.  
University of Newcastle upon Tyne. 1972.
25. Potts, E.L.J. and Roxborough, F.F.  
An Assessment of the Cuttability Characteristics  
of Selected Rock Specimens Recovered from the  
Proposed Route of the Tyne-Tees Aqueduct Tunnel.  
University of Newcastle upon Tyne. (1972).
26. Powers, M.C.  
A New Scale Roundness for Sedimentary Particles.  
Journal of Sedimentary Petrology. Vol.23. No 2.  
pp 117-119. (1973).
27. Poole, R.W. and Farmer, I.W.  
Consistency and Repeatability of Schmidt Hammer  
Rebound Data during Field Testing.  
International Journal of Rock Mechanics and  
Mineral Sciences, Vol 17. pp 167-171. (1980).

28. Rae, D.  
SMRE Research Report.  
No. 236. 1966.
29. Singh, R.N. Hassani, F.P. and Elkington, P.  
Application of Strength and Deformation Index  
Testing to the Stability Assessment of Coal  
Measures Excavations.  
24th US Symposium on Rock Mechanics, 1983.
30. Szlavín, J.  
Relationships Between some Physical Properties  
of Rocks Determined by Laboratory Tests.  
NCB, MRDE, Report No 19 1974.
31. Tarkoy, P.J and Hendron, A.J.  
Rock Hardness Index Properties and Geotechnical  
Parameters for Predicting Tunnel Boring Machine  
Performance.  
Report for the National Science Foundation,  
Research Grant GI-36468, Urbana, University of  
Illinois.
32. West, G.  
A Review of Rock Abrasiveness Testing for  
Tunnelling.  
Int.Soc. Rock Mech. Symp. On Weak Rock.  
Tokyo, pp 222-232. 1981.
33. Van Moppes IDP Ltd.  
Gouscester, UK.  
Drilling Handbook.
34. Valatin. A.  
Cerchar Tests for the Measurement of 'Durete'  
and 'Abrasure' of Rocks.  
Document 73-59, Centre of Study and Research of  
the French Coal Mining Industry. 1973.

35. Vickers, Das. B.  
Hardness Concept in the Light of Vickers  
Impression.  
Inst. J. Rock Mech. Min. Sci and Geo. Mech.  
Abstr. 11. pp 85-99. 1974.

## BIBLIOGRAPHY

Atkinson, T. Cassapi, V.B. and Singh, R.N.  
Assessment of Abrasive Wear Resistance Potential  
in Rock Excavation Machinery.  
International Journal of Mining and Geological  
Engineering.  
Vol 3, pp 151- 163. March 1986.

An Introduction to The Study of Minerals and Rocks  
Under the Microscope.  
Department of Earth Sciences.  
University of Leeds.

Geology for Engineers By  
Blyth F.G.H. and Freitas M.H.  
6th Edition. Edward Arnold (Publishers) Ltd.

Minerals and Rocks by  
Kirkaldy, J.F. D.Sc.  
Head of the Department of Geology,  
Queen Mary College,  
London.  
Published by Blandford Press Ltd. 1973.

Transactions.

Combating Wear in Bulk Solids.

Papers Read at the Headquarters of

The Institution of Mechanical Engineers.

Process Industries Division.

Minerals Engineering Society.

I Mech E. Tribology Group.

30 April 1986.

Transactions.

Drillex 87.

Papers presented at the Drillex Conference

organised by The Institution of Mining and Metallurgy

and the British Drilling Association,

Held in Stoneleigh, Warwickshire, England.

7-10 April 1987.

Transactions.

Mining Equipment Selection Symposium.

Faculty of Continuing Education,

University of Calgary and CANMET,

Canada Centre of Mineral and Energy Technology,

Calgary Coal Research Laboratory.

7-8 November 1985.

Minerals and How to Study Them. (Third Edition) by  
Dana, E.S.

John Wiley & Sons, Inc. New York. London & Sidney.

Oilwell Drilling Engineering.

Principles and Practice By

Rabia, H.

Graham and Trotman Ltd

London SW1V 1DE.

Sample Preparation and Equipment.

Precision and Versatility.

Logitec Ltd. (Scientific Consultants and Engineers)

Tecnology Manual for Thin Rock Section Production.

Old Kilpatrick, Dunbartonshire, Scotland. 1984.

Selection and Use of Engineering Materials by

Crane F.A.A. and Charles J.A.

Butterworths, Garden City Press Ltd.

1984.

Singh, R.N.

Laboratory Assessment of Mechanical Properties of  
Rock from Two Tunnelling Sites.

A Special Report to Robertsons Research International Ltd.

Department of Mining Engineering.

University of Nottingham. October 1984.

Strength of Materials by  
Ryder G.H.  
Principle Lecturer,  
Royal Military College of Science,  
Shrivenham, Third Edition, 1969.  
The MacMilan Press Ltd.

Singh, R.N.  
Laboratory Assessment of Mechanical Properties of  
Rock from Two Tunnelling Sites.  
A Special Report to Robertsons Research International Ltd.  
Department of Mining Engineering.  
University of Nottingham. October 1984.

Singh R.N. and Cassapi, V.B.  
Application of Predevelopment Mining Data to Mine  
Design in Remote Areas.  
Journal of Mines, Metals and Fuels.  
pp 165-172, April 1984.

Transactions.  
Tribology in Mineral Extraction.  
War On Wear.  
Papers Read at the International Conference held  
at the University of Nottingham.  
England on the 17-19 September 1984.



## ACKNOWLEDGMENTS.

The author would like to acknowledge with gratitude the contributions made by the following persons, without which, this thesis may not have been completed:

To Professor T Akinson, Head of the Department of Mining Engineering, for his inspiration with the initiation of the research project and thereafter, for his continued and invaluable advise and encouragement.

To Dr R.N Singh for much valuable advise and discussion during the various stages of the project.

Thanks are due to Mr Derek Wright of DeBeers, for providing the facilities and sawability data for the work described in Chapter 5. of this thesis.

Finally. the author would also like to acknowledge the important work carried out by Mrs Margaret Jackson, friend and neighbour, for her valued contribution as proof reader.